A Pd-Catalysed [4 + 2] Annulation Strategy to Densely Functionalised *N*-Heterocycles

Larry Hoteite

Doctoral thesis supervised by

Prof Enrique Gómez Bengoa & Prof Joseph P. Harrity

2021

Abstract

This thesis describes the synthesis of a library of novel sp^3-rich *N*-heterocycles containing orthogonal functionality *via* a palladium-catalysed allylation-condensation sequence. The employment of a readily available cyclic carbamate in the presence of a palladium catalyst generates a palladium-stabilised zwitterion, which reacts with a wide range of carbonyl substrates to provide the corresponding α-allylated compounds. These products can be further converted into six-membered *N*-heterocycles through a TFA-mediated deprotection-condensation step.

The scope of this methodology to 1-aryl-2-indanones, 1-aryl-2-tetralones, α-fluoro-β-ketoesters and α-trifluoromethylthio-ketones is discussed, and the potential of the final heterocyclic compounds to undergo further derivatisation is demonstrated. Furthermore, the application of this methodology towards the synthesis of lysergic acid is presented.

Resumen

Esta tesis describe la síntesis de una biblioteca de nuevos heterociclos nitrogenados ricos en carbonos sp3, que contienen funcionalidad ortogonal, introducida mediante una secuencia de alilación-condensación catalizada por paladio. El empleo de un carbamato cíclico fácilmente disponible, en presencia de un catalizador de paladio, genera un ion híbrido estabilizado por el metal, que reacciona con una amplia gama de sustratos de carbonilo para proporcionar los compuestos α-alilados correspondientes. Estos productos se pueden convertir adicionalmente en N-heterociclos de seis miembros, mediante una etapa de desprotección-condensación mediada por TFA.

Se discute el alcance de esta metodología para 1-aril-2-indanonas, 1-aril-2-tetralonas, α-fluoro-β-cetoésteres y α trifluorometiltiocetonas, y se analiza el potencial de los compuestos heterocíclicos finales para experimentar una derivación adicional. Además, se presenta la aplicación de esta metodología a la síntesis de ácido lisérgico.

Acknowledgements

I would like to thank Prof Joe Harrity for giving me the opportunity to work on this project and for his continuous support, guidance and encouragement throughout my time in his group. It has been an enriching journey on both a scientific and personal level, thank you. I would also like to thank Prof Enrique Gómez Bengoa for welcoming me into his group and for teaching me the intricacies of DFT which have broadened my theoretical understanding. My secondment in the Basque Country was great (apart the galernas), albeit short but sweet. I am immensely grateful for the funding supplied by the European Union's Horizon 2020 research and innovation programme which enabled me to carry out this research.

I would like to thank all the members of the Harrity and Gómez Bengoa groups, both present and past, but in particular, I would like to thank Matt, Chris, Kenji, Marie, Sophie, David, Fernando, Olivier and Lia. I have enjoyed your company as well as our stimulating scientific discussions, most of all those after a couple of Punk IPAs at Interval or Uni Arms.

Thank you to all the technical staff, particularly Sandra, Craig, Sharon and Rob, who made my research work run smoother.

Finally, I thank my family and friends, for their unwavering support, advice and encouragement over the last few years, particularly during the current pandemic.

Contents

List of Abbreviations

Ac	acetyl
Ar	aryl
Bz	benzoyl
Bn	benzyl
Boc	*tert*-butoxycarbonyl
^{n}Bu	*n-butyl*
^{t}Bu	*tert*-butyl
C	Celsius
Cbz	carboxybenzyl
Cp	cyclopentadienyl
Δ	Reflux
dba	dibenzylideneacetone
DCE	1,2-dichloroethane
DMAP	dimethylaminopyridine
DMF	*N*,*N*-dimethylformamide
DMSO	dimethylsulfoxide
d.r.	diastereoisomeric ratio
ee	Enantiomeric excess
EI	electron impact
eq.	equivalent(s)
ESI	electrospray Ionisation
Et	Ethyl
et al.	*et alia*
EWG	electron withdrawing group
FCC	flash column chromatography
FTIR	Fourier-transform infrared spectroscopy
h	hour(s)
Hz	Hertz
HRMS	high resolution mass spectrometry
L	generic ligand
L*	generic chiral ligand
MPA	3-mercaptopropionic acid
J	coupling constant
K	Kelvin
LA	Lewis acid
LG	leaving group
[M]	metal
M	molar
m	meta
Me	methyl
min	minutes
mol	moles
MS	molecular sieves
NMR	Nuclear magnetic resonance
Nu	generic nucleophile
Ph	phenyl
^{i}Pr	isopropyl
PTC	phase transfer catalyst
R	generic carbon-containing group
r.t.	room temperature
T	temperature
t	time
TFA	trifluoroacetic acid
THF	tetrahydrofuran
TMM	trimethylenemethane
Ts	4-methylbenzenesulfonyl

1. Introduction

1.1. Tsuji-Trost Allylic Alkylation Reaction

A core aim in organic synthesis is the development of novel synthetic methodologies for the generation of carbon-carbon and carbon-heteroatom bonds, which are fundamental transformations for the elaboration and extension of carbon frameworks. To this end, palladium-catalysed carbon-carbon and carbon-heteroatom bond-forming reactions have emerged as powerful synthetic processes, and are therefore extensively adopted by the synthetic community. The ability of palladium catalysts to generate palladium π-allyl cation species *via* oxidative addition of allylic electrophiles led to the development of the Tsuji-Trost allylic alkylation reaction, which has been widely incorporated to the synthetic chemist's repertoire. This Pd-catalysed process allows the smooth addition of allyl moieties to a large number of nucleophiles (Scheme 1).[1-4]

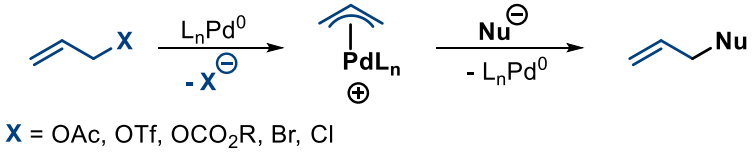

Scheme 1 *- Pd-catalysed allylic alkylation reaction*

It is established that the reaction first proceeds *via* coordination of the low valent palladium(0) to the alkene providing an η^2-π-complex, which undergoes oxidative addition and thereby generating an η^3-π-allylpalladium complex.[5] This intermediate

is then attacked by a nucleophile to deliver the allylated product and regenerate the palladium(0) catalyst (Figure 1).

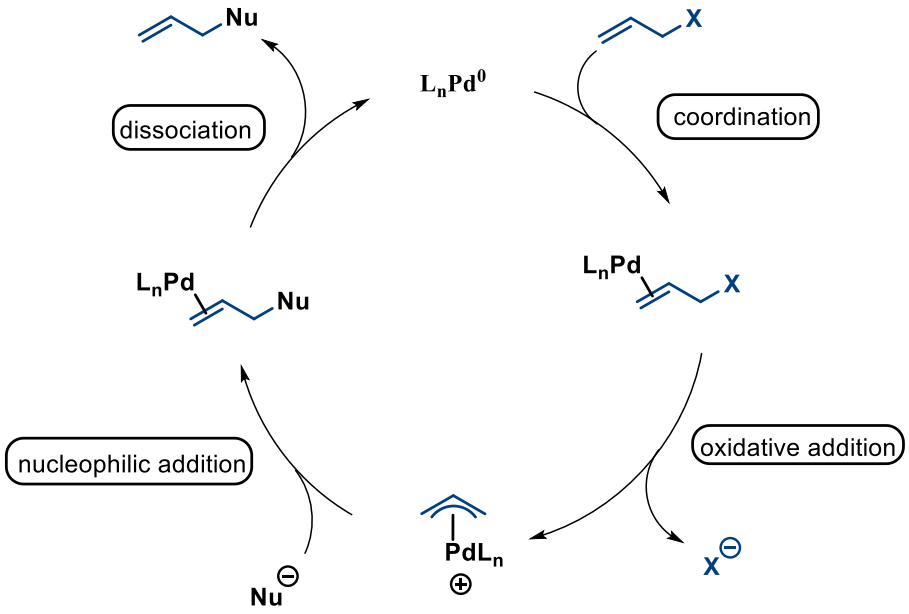

Figure 1 *- Tsuji-Trost allylic alkylation reaction's catalytic cycle*

Depending on the nature of the nucleophile, the attack could proceed *via* two distinct mechanistic pathways, outer-sphere or inner-sphere, resulting in different stereochemical outcomes (Figure 2).[4, 6, 7] "Soft" or stabilised nucleophiles, such as enolates and those that derive from conjugate acids with pKa's < 25, generally attack directly the π-allyl fragment outside the palladium's coordination sphere, and therefore result in net retention of configuration. In contrast, non-stabilised or "hard" nucleophiles (conjugate acids with pKa's > 25), attack first the palladium centre to form a neutral intermediate, followed by reductive elimination to deliver the organic product. This inner-sphere pathway delivers the allylated compound with an overall net inversion of stereochemistry.

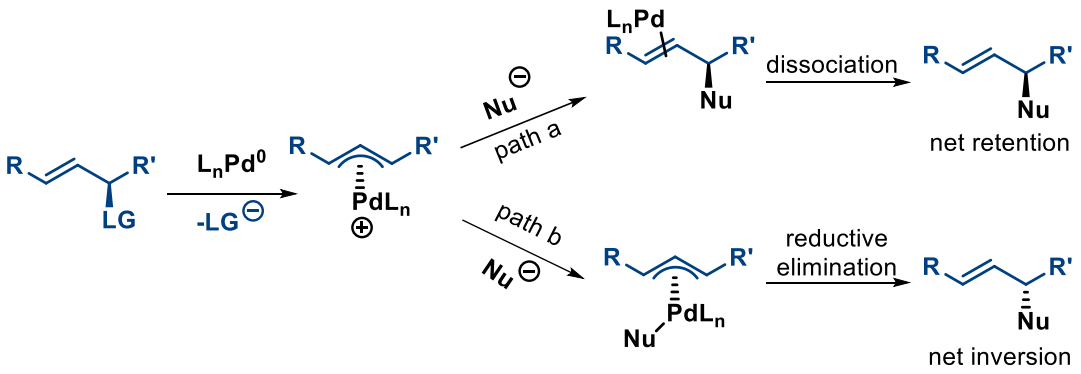

Figure 2 *- Stereochemical outcome for inner- and outer-sphere pathways*

1.2. Palladium-Stabilised Zwitterionic Species

Palladium catalysis offers an efficient method for the formation of dipolar intermediates, which enable rapid access to a variety of functionalised heterocycles *via* formal cycloaddition reactions.[8] These versatile zwitterionic reagents generally comprise an electrophilic palladium π-allyl complex and a nucleophilic stabilised anion, which could be carbon-, nitrogen-, or oxygen-centred. As the primary objective of this thesis is the formation of *N*-heterocycles, the following parts of this chapter will focus on the palladium-catalysed synthesis of nitrogen-containing compounds.

1.2.1. Palladium-Stabilised Zwitterions Containing a Carbanion

Almost forty years ago, Trost and Chan disclosed one of the important breakthroughs in ring-forming cycloaddition processes.[9] It was shown that palladium-trimethylenemethane (Pd-TMM), a zwitterionic intermediate, could be generated from 2-[(acetoxymethyl)allyl]trimethylsilane in the presence of a Pd(0) catalyst. This

palladium-stabilised zwitterion could then engage in a formal [3+2] cycloaddition process with alkene acceptors to deliver a range of *exo*-methylenecyclopentane adducts (Figure 3).

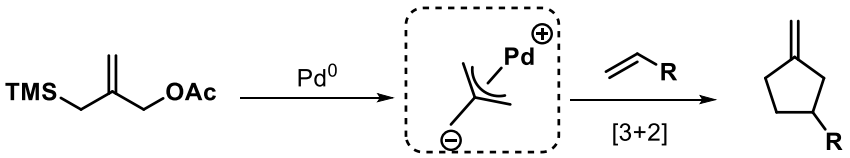

Figure 3 *- Generation and reactivity of Pd-TMM*

Since the initial disclosure of Pd-TMM cycloaddition processes, significant progress was achieved to explore and further expand the scope of this chemistry.[10-24] More related to the work presented in this thesis, Pd-TMM annulation reactions were also applied to the synthesis of saturated nitrogen heterocycles. In 1986, Jones and Kemmitt have initially demonstrated that allylic acetate **1** and mesylate **2** are able to undergo palladium mediated annulation with a narrow selection of imine acceptors to give substituted pyrrolidine products.[25] For example, phenyl imine **3** and dibenzylidenehydrazine **4** underwent [3+2] cycloaddition to provide the corresponding cycloadducts in moderate yields (Scheme 2).

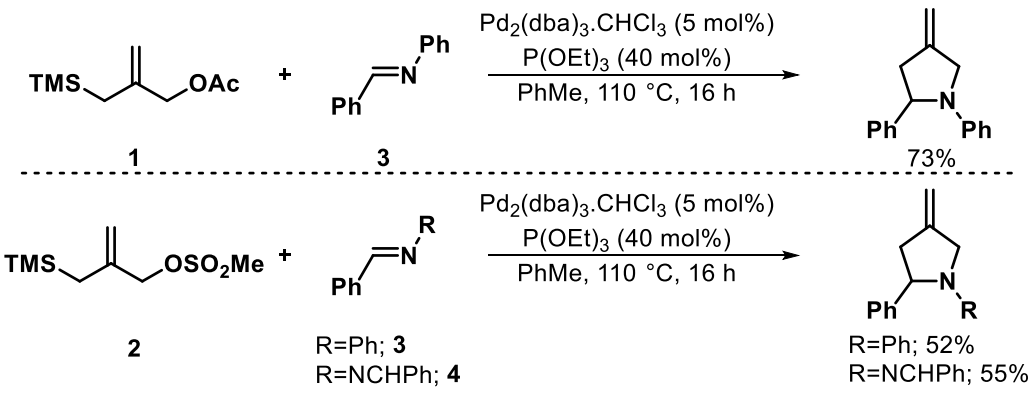

Scheme 2 *- [3+2] cycloaddition of Pd-TMM to aldimines*

A couple of years later, the scope was expanded by Trost and co-workers, who showed that this process could be further generalised to a wide range of imines. Their initial attempts to perform the palladium-catalysed annulation with unactivated aliphatic aldimines proved unsuccessful.[26] To address this limitation, the initial strategy was converted into a two-step process which involved the use of a synthetic equivalent of TMM, organostannane **5**, and a Lewis acid to activate the imine (Scheme 3). Subsequent addition of a Pd complex initiated the cyclisation and led to the corresponding pyrrolidines in high yields.[26]

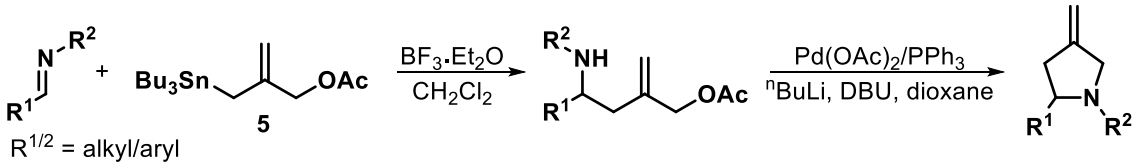

Scheme 3 *- Trost's two-step sequence towards pyrrolidines*

Although this strategy was applicable to a wide range of imines, the toxicity of organostannane compounds and the two-step sequence lured the authors to develop a one-step Pd-catalysed process. *N*-tosylimines, which exhibit enhanced electrophilicity, were therefore examined in the Pd-catalysed cycloaddition and found to readily react with TMM to provide an array of pyrrolidine compounds in excellent yields.[27] *N*-activated imines bearing electron-rich and electron-poor aromatics were both tolerated (Scheme 4). Additionally, the employment of allylic carbonate **6** as TMM precursor allowed the reaction to be achieved at lower temperatures.

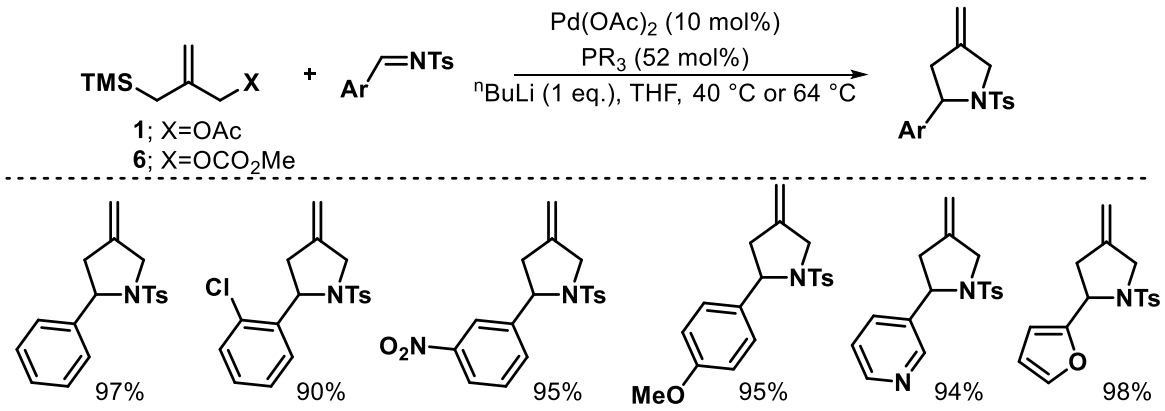

Scheme 4 *- Pd-catalysed [3+2] annulation with various aryl N-tosyl imines*

Interestingly, unsaturated substrates showed chemoselective cycloaddition at the imine rather than the alkene (Scheme 5). For instance, aldimine **7** derived from cinnamaldehyde reacted with Pd-TMM to give solely the pyrrolidine adduct. The conjugated aldimine **8** was also tolerated and gave the five-membered *N*-heterocycle in high yield, although as a mixture of diastereomers.

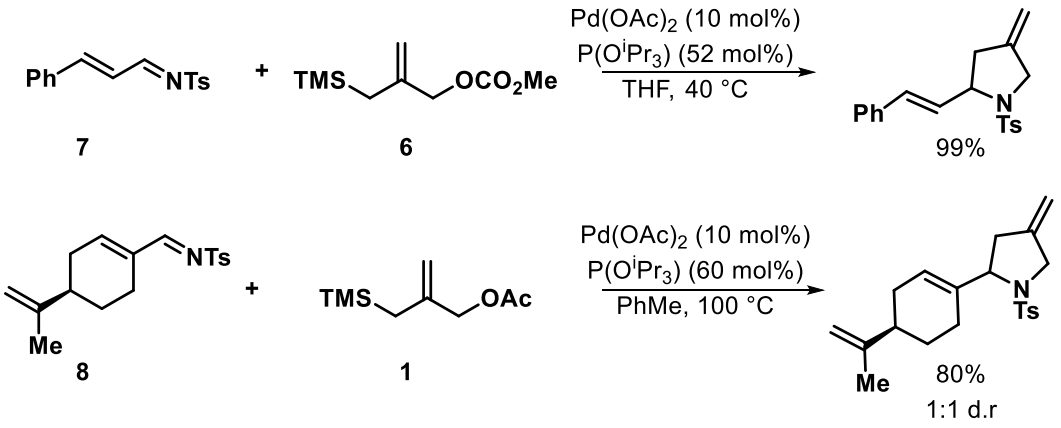

Scheme 5 *- Chemoselective [3+2] cycloaddition of conjugated aldimines*

Furthermore, various aliphatic *N*-activated aldimines underwent [3+2] cycloaddition with Pd-TMM, however sterically hindered substrates necessitated higher reaction temperatures (Scheme 6).[27] The lower yields obtained in some cases were attributed to substrate synthesis rather than the Pd-catalysed annulation process itself, since the aldimines were employed without prior purification.

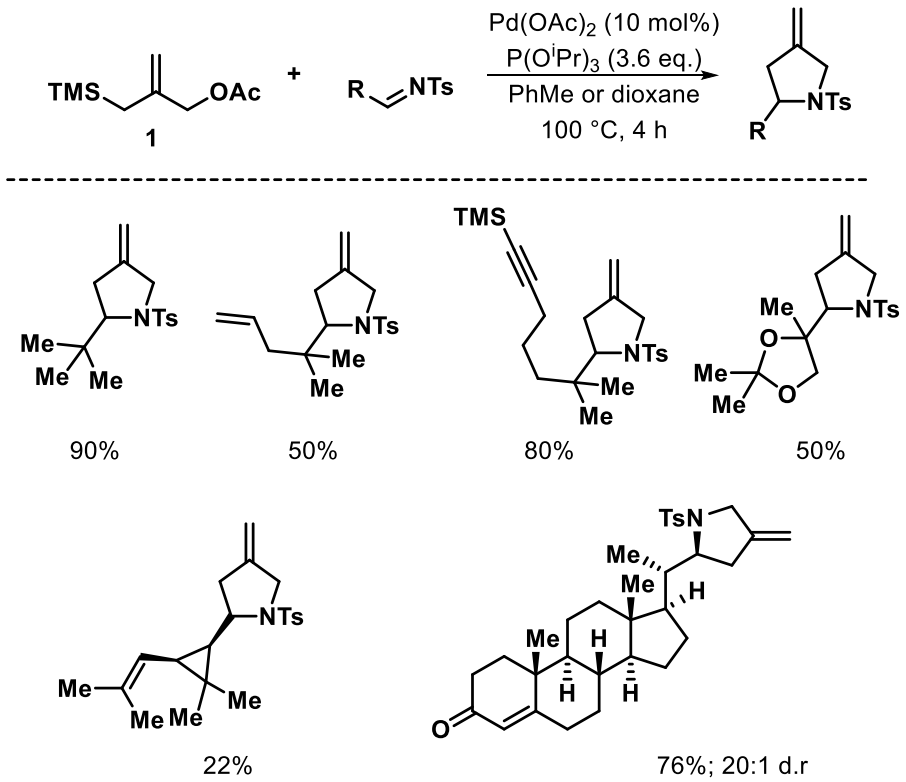

Scheme 6 *- Pd-catalysed cycloaddition with aliphatic N-activated aldimines*

Strained camphorsulfonic acid derived imine **9** and *α,β*-unsaturated ketimine **10** also performed well in the formal [3+2] cycloaddition (Scheme 7). Moreover, nitro-activated ketimines, such as nitrimines **11** and **12**, were also examined and found to undergo smooth cycloaddition with the Pd-stabilised zwitterion to provide the corresponding cycloadducts in good yields, and in the case of **11**, with a 17:1

diastereomeric ratio. However, unhindered nitrimines generated from cyclooctanone and 2-hexanone failed to participate in the cycloaddition reaction, a lack of reactivity that was ascribed to the greater likelihood of these activated ketimines to enolise.

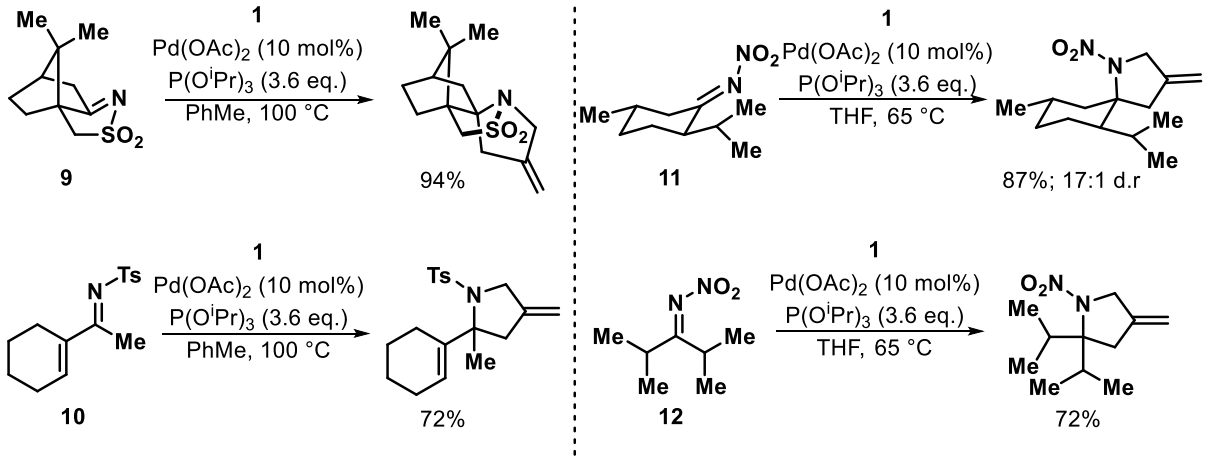

Scheme 7 *- Pd-catalysed cycloaddition with N-activated ketimines*

This transition metal-catalysed [3+2] annulation process allows rapid access to densely functionalised sp^3-rich heterocycles, therefore its potential prompted the authors to develop an asymmetric variant of this methodology. In 2007, Trost *et al.* reported the first enantioselective Pd-catalysed cycloaddition of trimethylenemethane with aldimines.[28] It was found that chiral phosphoramidite ligands were successful in promoting the reaction with high levels of enantiocontrol. Notably, the phosphoramidite ligand **L1** with a bis-2-naphtyl substituted pyrrolidine effectively catalysed the cycloaddition and provided the corresponding *N*-heterocycles in high yields and enantioselectivities. Interestingly, the reaction also performed well with *N*-Boc and *N*-aryl aldimines, which were found to be unreactive in the initial reaction conditions. This highlighted the increase in reactivity that these BINOL-derived

phosphoramidite ligands were able to provide to the palladium-stabilised zwitterion. Furthermore, the process demonstrated to be insensitive to the electronic nature of the aryl group on the nitrogen atom and proceeded efficiently in the presence of *N*-aryl imines bearing electron-rich or electron-poor aromatics. Heterocyclic-based imines were also tolerated and provided the corresponding cycloadducts in high enantiomeric ratios, although slightly lower yields were obtained (Scheme 8).

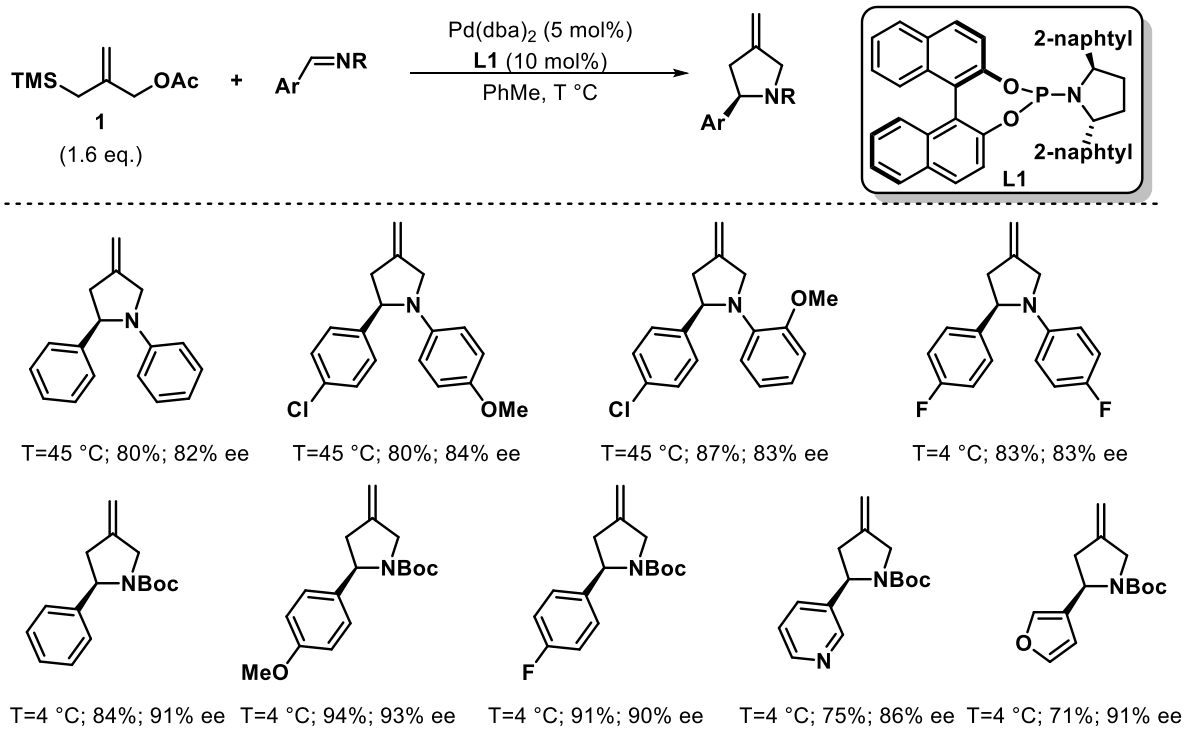

Scheme 8 *- Asymmetric Pd-catalysed cycloaddition of N-Boc and N-aryl aldimines. Adapted from ref. [8]*

Inspired by the success of this asymmetric methodology with aldimines, Trost *et al.* examined the palladium-catalysed asymmetric cycloaddition of cyano-TMM to the less reactive ketimines in order to generate highly substituted pyrrolidines.[29] *C*-aryl and *C*-alkyl substituted activated imines were demonstrated to react smoothly

leading to the desired pyrrolidines in high yields (Scheme 9). *N*-Boc imines proved to be inefficient in this case, presumably due to their tendency to isomerise to the enamine tautomer. However, *N*-tosyl imines were less susceptible to the tautomerisation issue. The reaction performed well in almost all cases, providing the desired product in high yield and selectivity.

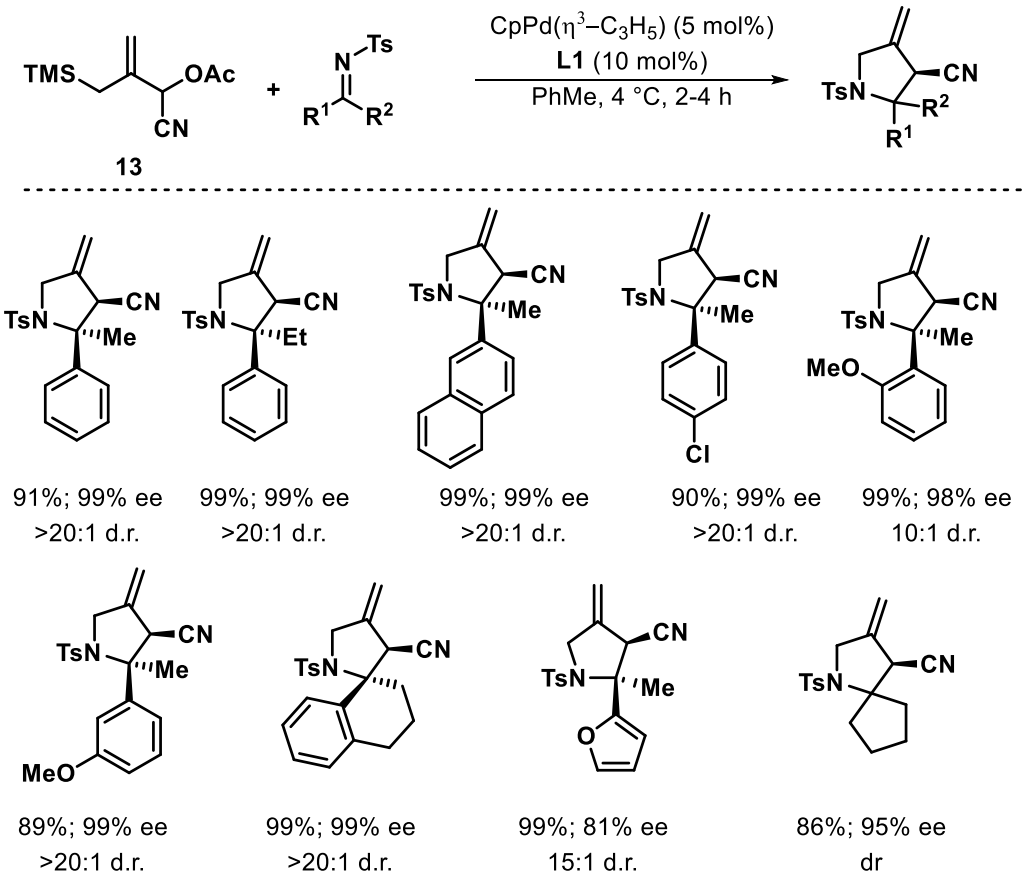

Scheme 9 *- Asymmetric Pd-catalysed [3+2] cyano-TMM cycloaddition to ketimines. Adapted from ref. [8] and [29]*

The proposed model for the cycloaddition's diastereoselectivity is shown in Figure 4 and was based on the imine geometry, which was revealed by NOE analysis.[29] It was proposed that the top conformer would lead to the observed diastereomer,

which appears to be the thermodynamically less favoured one based on theoretical calculations (by an energy difference of 1.09 kcal/mol relative to the other diastereomer), whereas the bottom conformer would lead to the second diastereomer, which would be disfavoured due to steric clash between the π-allyl system and the tosyl group.

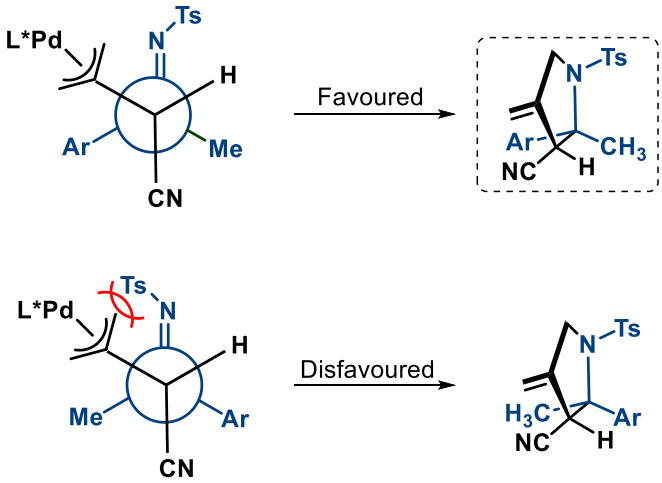

Figure 4 *- Proposed model for the diastereoselectivity of the reaction*

Unsymmetrical aliphatic ketimines proved to be challenging substrates for cycloaddition and suffered from a lack of selectivity when subjected to the standard reaction conditions in the presence of **L1**. However, further ligand optimisation led to the use of azetidine-based phosphoramidite ligand **L2**, which provided the desired products in high yields and with high levels of enantio- and diastereoselectivity (Scheme 10).

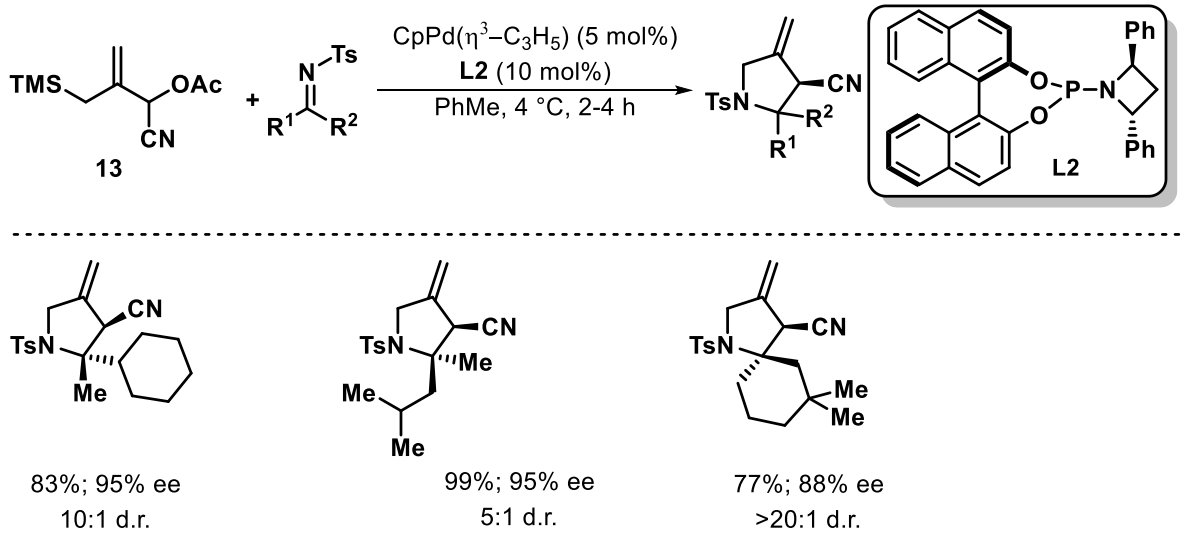

Scheme 10 *- Pd-catalysed [3+2] cyano-TMM cycloaddition to aliphatic imines*

The reactivity of palladium-trimethylenemethane is not limited to [4+2] annulation processes and was thereby exploited in various other cycloaddition reactions. For instance, Pd-TMM precursors have also been shown to undergo [3+3] cycloaddition reactions with a range of nitrogen-containing acceptors to provide six-membered *N*-heterocycles.[8] Hayashi and co-workers have disclosed the Pd-catalysed [3+3] cycloaddition process with azomethine imines to form hexahydropyridazine cycloadducts in high yields.[30] Substrates containing alkyl, electron-rich and electron-poor aromatics were all tolerated (Scheme 11). Although, when the azomethine imine bearing a sterically bulky *t-Bu* group was employed, a significant drop in the yield was observed. Substrates substituted with alkyl groups on the pyrazolidinone also performed well in the [3+3] reaction and gave the corresponding products in excellent yields.

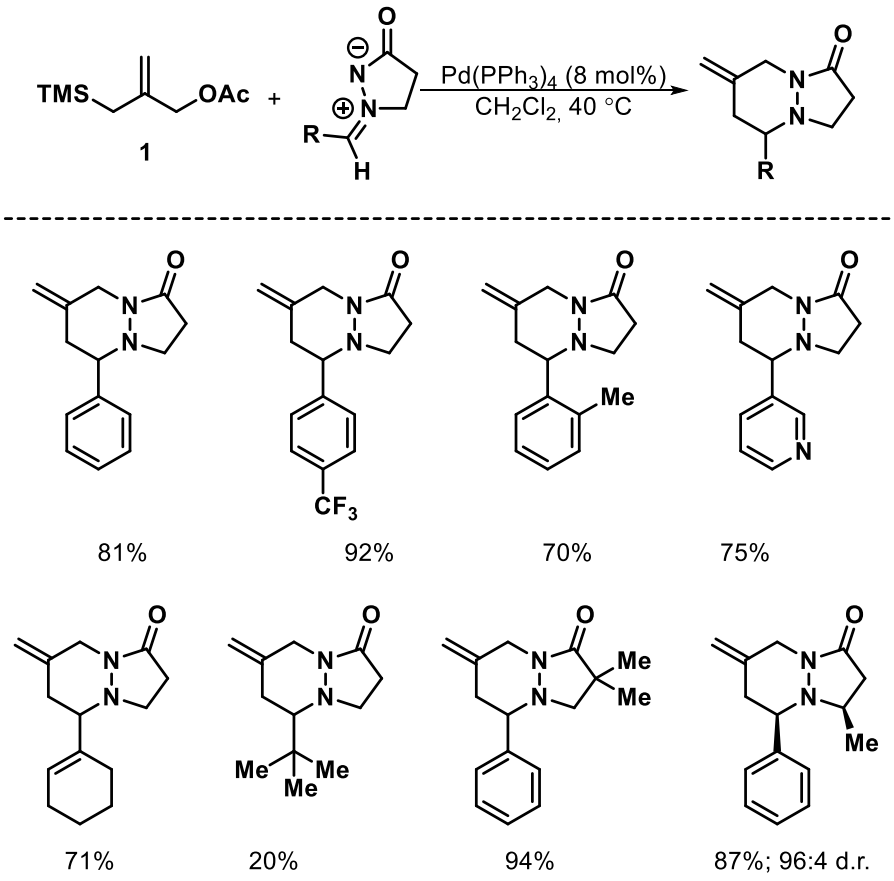

Scheme 11 *- Pd-TMM [3+3] cycloadditions with azomethine imines. Adapted from ref. [8] and [30]*

The authors also demonstrated that substituted trimethylenemethane precursors could undergo asymmetric palladium-catalysed [3+3] cycloaddition with nitrone substrates to produce tetrahydro-1,2-oxazine products as single regioisomers, with good diastereocontrol and high levels of enantioselectivity (Scheme 12).[31] However, a racemic mixture was obtained when unsubstituted TMM precursor **1** was employed, although the six-membered heterocycle was isolated in high yield.

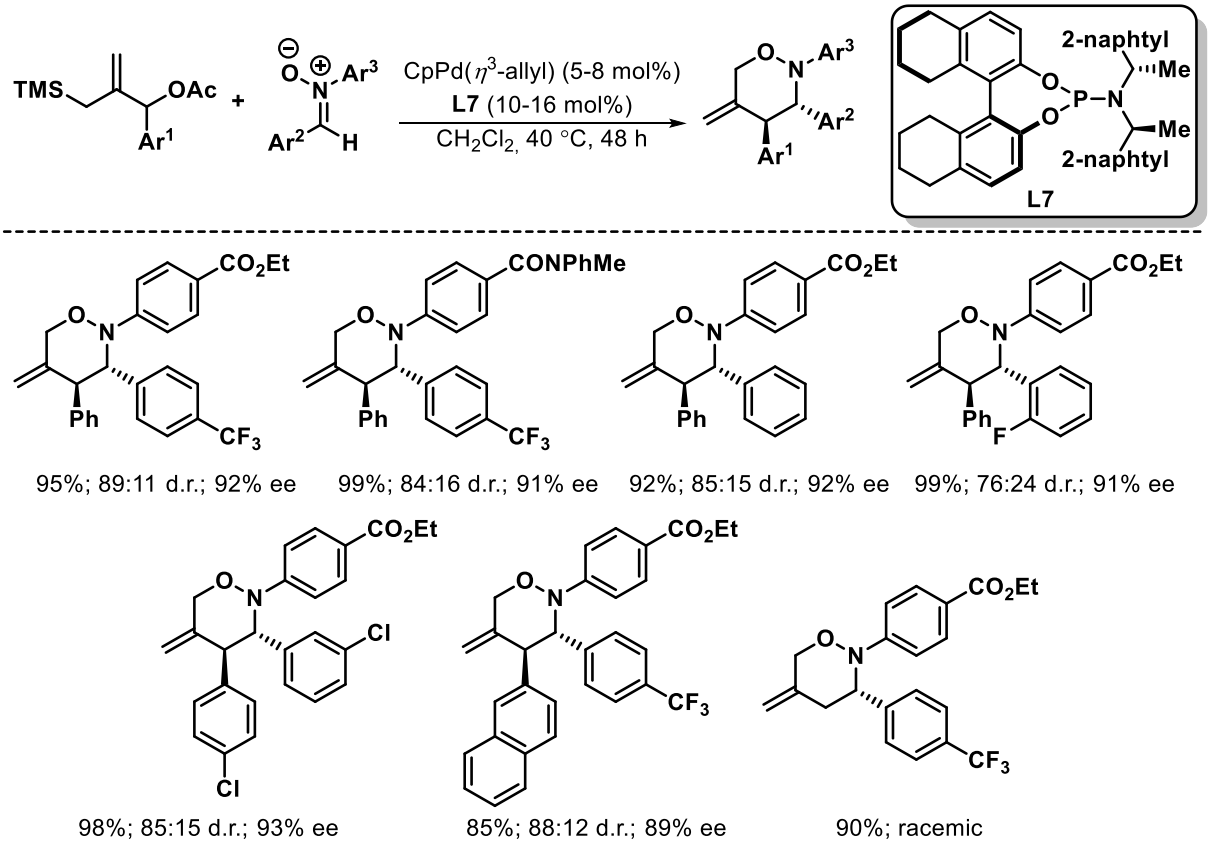

Scheme 12 *- Asymmetric Pd-TMM [3+3] cycloadditions with nitrones. Adapted from ref. [8] and [32]*

Furthermore, Kemmitt and co-workers reported the first Pd-catalysed [3+3] cycloaddition of trimethylenemethane with activated aziridines to produce piperidines (Scheme 13).[33] *N*-Tosyl and *N*-*p*-nitrobenzoate aziridines were both tolerated and gave the corresponding piperidines in good yields.

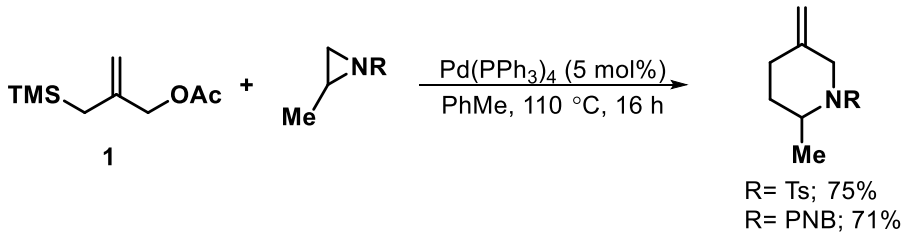

Scheme 13 *- Initial Pd-TMM [3+3] cycloaddition to activated aziridines*

Harrity *et al.* revisited this palladium-catalysed process and expanded its scope to a range of enantioenriched alkyl and aryl-substituted aziridines (Scheme 14).[34, 35] The cycloaddition showed excellent regioselectivity with the ring-cleavage occurring at the less hindered carbon of the three-membered heterocycle, with the exception of 2-phenylazirdine in which unsurprisingly ring-opening also occurred at the benzylic position, thereby leading to a mixture of regioisomeric compounds. Notably, the [3+3] cycloaddition reaction proved to be enantiospecific providing all the nitrogen-containing compounds with complete retention of stereochemistry. Aziridines bearing a silyl-protected alcohol or an allyl fragment were also tolerated in the process, providing a synthetic handle for further transformations.

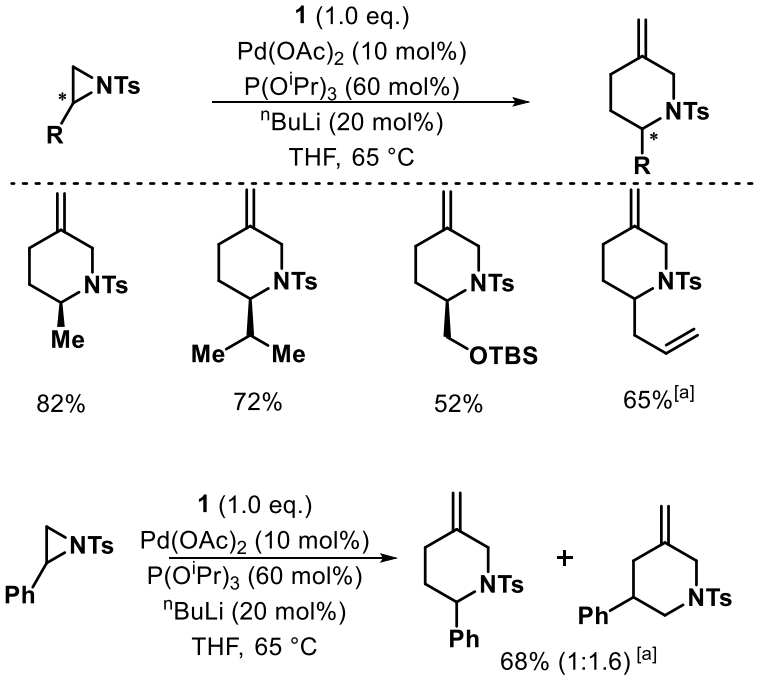

Scheme 14 *- Pd-TMM cycloaddition with 2-substituted aziridines. [a] Reaction performed on racemate. Adapted from ref. [34]*

Later, Harrity and co-workers showed that this process was also applicable to a variety of disubstituted aziridines.[35] For instance, 2,2-substituted aziridines were successfully employed and provided a range of spirocyclic piperidines (Scheme 15).

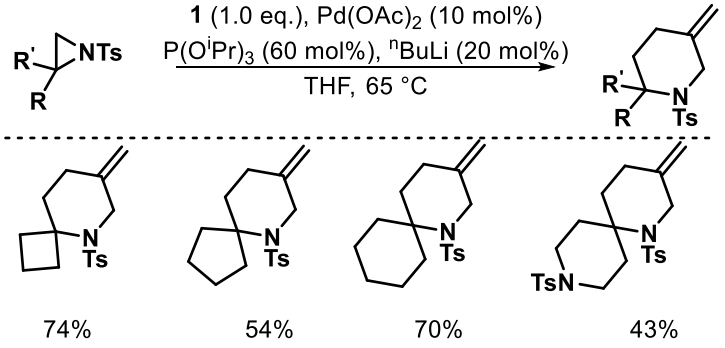

Scheme 15 - *Pd-TMM cycloaddition with 2,2-disubstituted aziridines.* Adapted from ref. [8] and [35]

The use of 2,3-disubstituted substrates led to the corresponding *trans*-fused bicyclic systems, although in low yields (Scheme 16). The poor reactivity of these substrates likely arises from the increased steric bulk at the electrophilic carbon of the aziridine, therefore limiting the nucleophilic addition of Pd-TMM.[35]

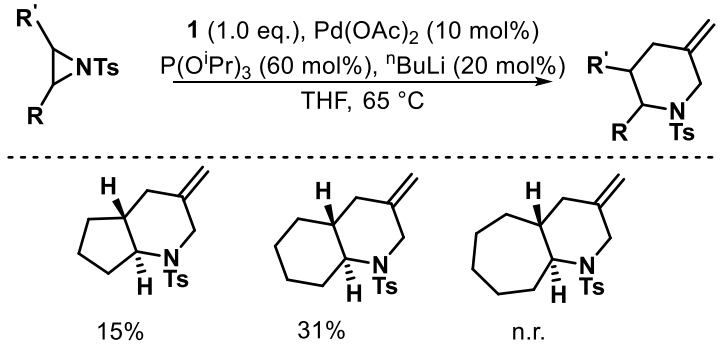

Scheme 16 - Pd-TMM cycloaddition with 2,3-disubstituted aziridines. Adapted from ref. [8] and [35]

Alternative palladium-stabilised zwitterionic species that contain a carbanion have also been shown to undergo palladium-catalysed cycloaddition reactions with various nitrogen-containing electrophilic partners.[8]

Tsuji *et al.* first described the palladium-catalysed [3+2] cycloaddition of activated vinylcyclopropanes with aryl isocyanate partners to provide a range of vinyl γ-lactam compounds (Scheme 17).[36] Several years later, Shi and co-workers expanded the scope to diazooxaindole substrates to give highly functionalised pyrazolidine products.[37, 38]

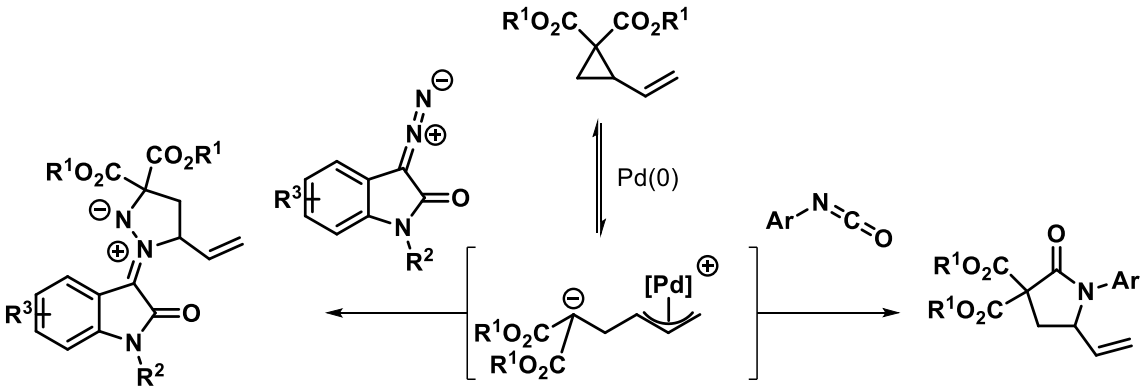

Scheme 17 *- Pd-catalysed [3+2] cycloaddition of vinylcyclopropanes to isocyanate and diazooxaindole acceptors*

Furthermore, Hayashi *et al.* disclosed a new palladium-catalysed cycloaddition process for the synthesis of *N*-heterocycles, which involves the employment of various γ-methylidene-δ-valerolactones. In the presence of a palladium(0) complex, these lactones generate a four-carbon zwitterionic intermediate, which was found to react with a number of acceptors, such as nitrones,[39] isocyanates,[32, 40] imines[41] and aziridines[42] to give a series of nitrogen-containing heterocycles (Scheme 18).

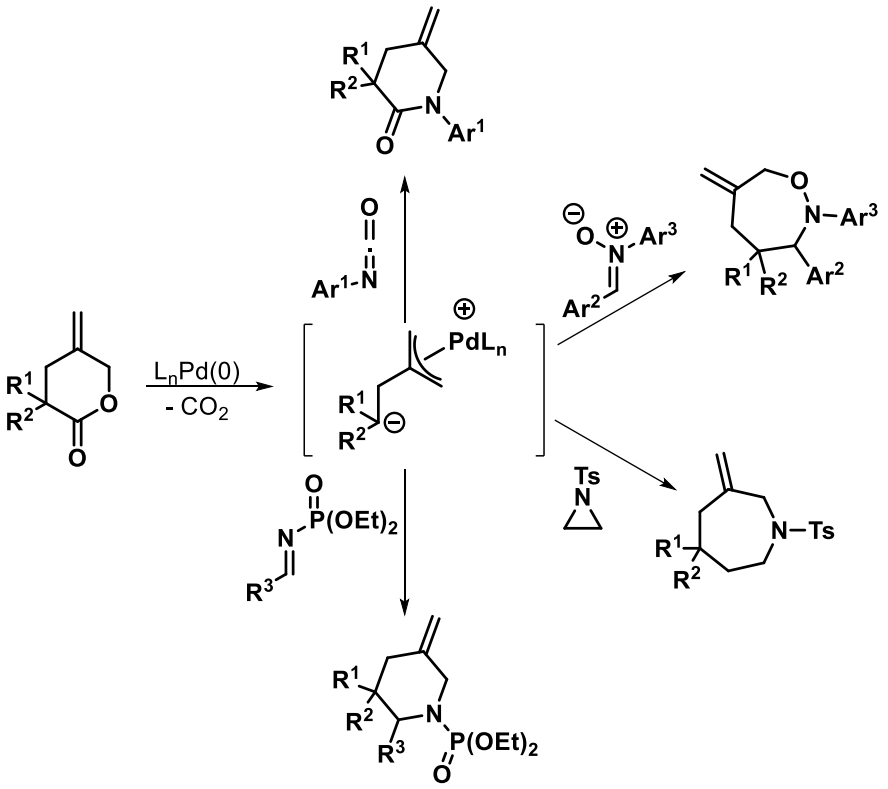

Scheme 18 *- Pd-catalysed cycloaddition of γ-methylidene-δ-valerolactones to various acceptors*

1.2.2. ***Palladium-Stabilised Zwitterions Containing a N-Centred Anion***

The utility of palladium-stabilised dipolar reagents containing a nitrogen-centred anion has also been investigated in the synthesis of *N*-heterocycles. The most common precursors used for the generation of amide zwitterions are vinylaziridines and vinyloxazolidinones. It was demonstrated that in the presence of catalytic palladium(0), these systems undergo ring opening to generate a N^1-1,3-dipole which could then be intercepted by an electrophile (Scheme 19).[8]

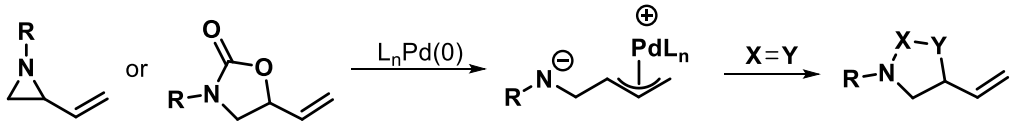

Scheme 19 *- Generation and cycloaddition of Pd π-allyl amide zwitterion*

Alper and co-workers reported the first Pd-catalysed [3+2] cycloaddition reaction of vinylaziridines with a number of heterocumulene substrates, such as isocyanates, isothiocyanates and carbodiimides, to provide the corresponding five-membered heterocycles (Scheme 20).[43] The methodology was further extended to the analogous vinylazetidine and vinylpyrrolidine substrates to give six- and seven-membered heterocycles, respectively.[44-47]

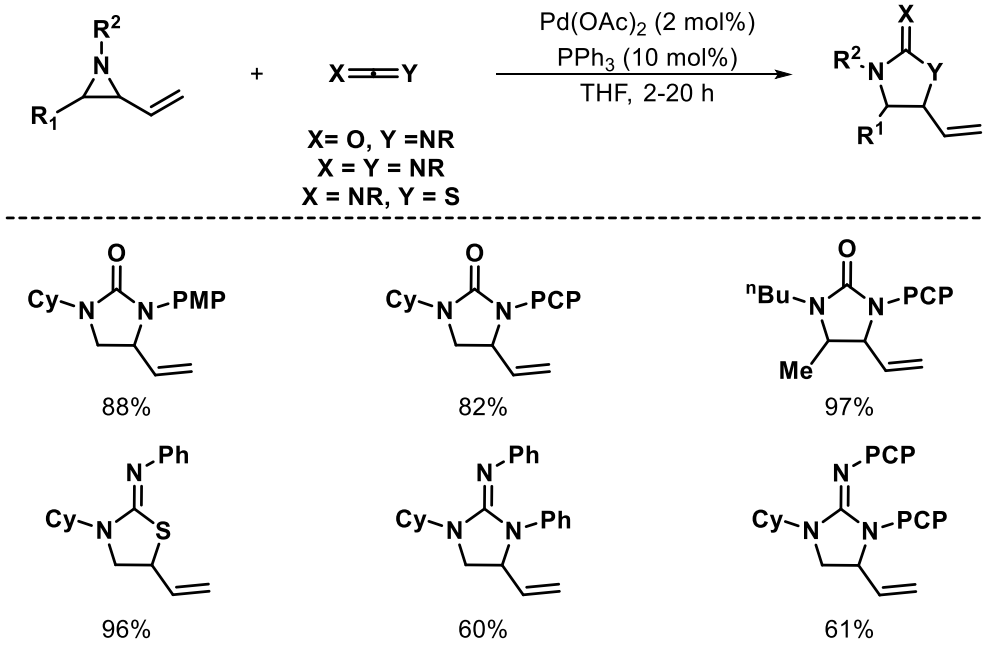

Scheme 20 *- Palladium-catalysed [3+2] annulation of vinylaziridines with heterocumulene acceptors. Adapted from ref. [8] and [43]*

Furthermore, the successful palladium-catalysed [3+2] cycloaddition reaction of isocyanates to vinylaziridines prompted Trost and co-workers to develop an enantioselective process. It was demonstrated that in the presence of **L8**, racemic vinylaziridines substrates could undergo dynamic kinetic asymmetric cycloaddition reaction with isocyanates to provide a range of enantioenriched imidazolidin-2-ones (Scheme 21).[48]

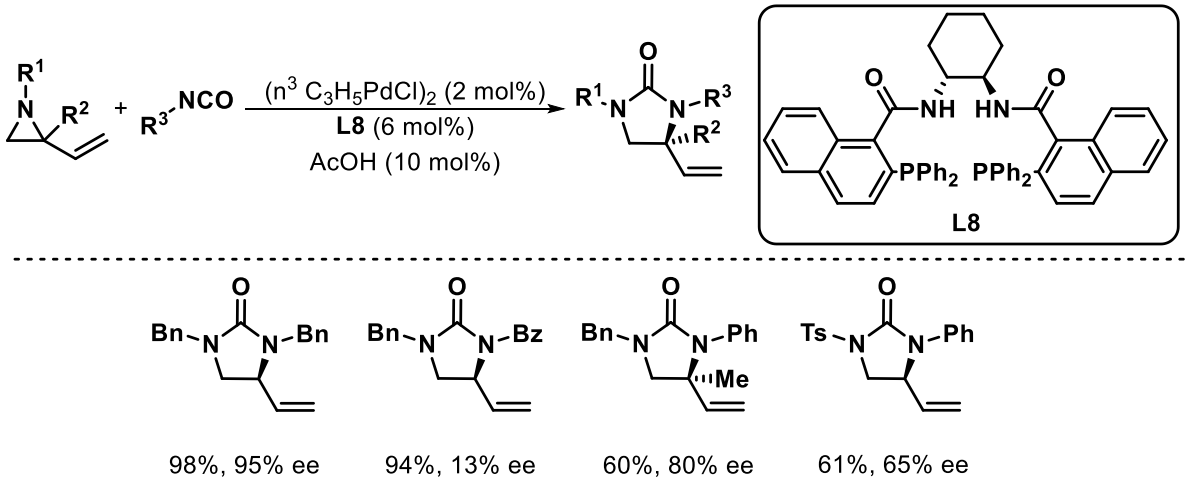

Scheme 21 *- Pd-catalysed dynamic kinetic asymmetric cycloaddition of vinylaziridines to isocyanates. Adapted from ref. [8]*

The synthesis of *N*-heterocycles using N^1-1,3-dipoles derived from vinylaziridines is not limited to heterocumulene cycloadditions. Yamamoto *et al.* disclosed the palladium-mediated annulation of vinylaziridines with a number of doubly activated alkenes to give the corresponding pyrrolidine products in high yields, albeit with low levels of diastereocontrol (Scheme 22).[49]

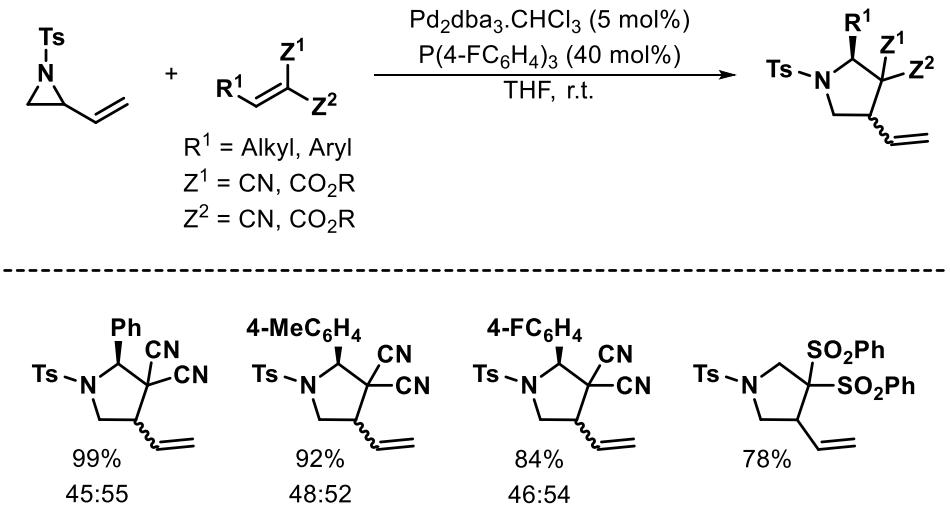

Scheme 22 *- Pd-catalysed [3+2] annulation of N-tosylvinylaziridine with highly activated alkenes. Adapted from ref. [8]*

Later, Knight *et al*. reported the Pd-catalysed decarboxylative [3+2] annulation of vinyloxazolidinones to highly activated olefins.[50] Yamamoto has previously demonstrated that in the presence of a palladium(0) complex, vinyloxazolidinone substrates could readily undergo decarboxylation to give the corresponding vinylaziridines.[51] Therefore, Knight reasoned that vinyloxazolidinones could be employed in place of aziridine derivatives to form a N^1-1,3-dipole which would then undergo a formal [3+2] cycloaddition reaction with activated alkenes to produce pyrrolidine compounds. Their initial investigation using Meldrum's acid benzylidene substrate provided the desired product, although in low yield. Further optimisation studies found the addition of halides to dramatically improve the yield of the reaction (Scheme 23).[52]

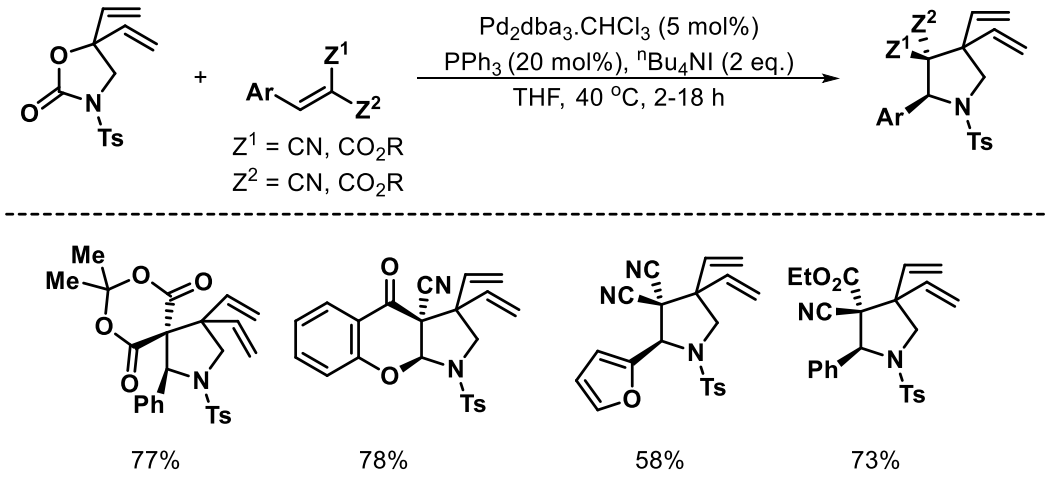

Scheme 23 *- Pd-catalysed decarboxylative annulation of vinyloxazolidinones with doubly activated Michael acceptors. Adapted from ref. [49]*

In related work, Aggarwal et al. demonstrated that singly activated Michael acceptors were also viable electrophiles. In 2011, the authors reported the Pd-catalysed annulation of enantioenriched vinylaziridines with methyl vinyl ketone and ethyl acrylate to provide substituted pyrrolidine compounds with high levels of diastereoselectivity.[53] However, as previously reported by Knight, the presence of halides additives proved critical to the success of the annulation reaction. The stabilisation of the *in situ* generated amide anion by the palladium complex may slow its nucleophilic addition to the electrophile. Halide additives could improve the nucleophilicity of the amide anion by disrupting its interaction with the Pd-π-allyl cation (Scheme 24).[8, 52, 53]

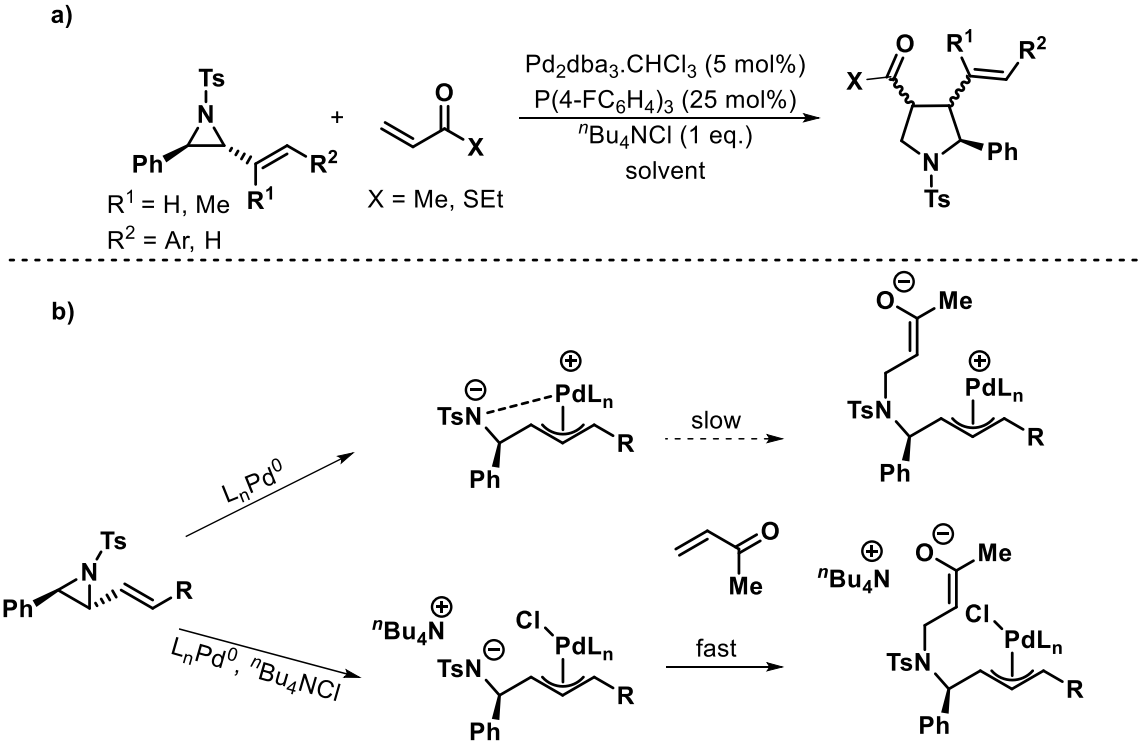

Scheme 24 *- a) Pd-catalysed annulation of vinylaziridines with methyl vinyl ketone and ethyl thioacrylate b) Rationalisation of the enhanced reactivity in the presence of halides*

Further examples of palladium-stabilised zwitterions containing a nitrogen-centred anion were reported by Tunge and co-workers.[54] The authors showed that 6-alkenyl-1,3-oxazinones could undergo decarboxylation in the presence of Pd^0 to form a N^1-1,4-dipole intermediate, which could then be intercepted by doubly activated alkenes to provide highly substituted piperidines in good yields and high levels of diastereoselectivity.

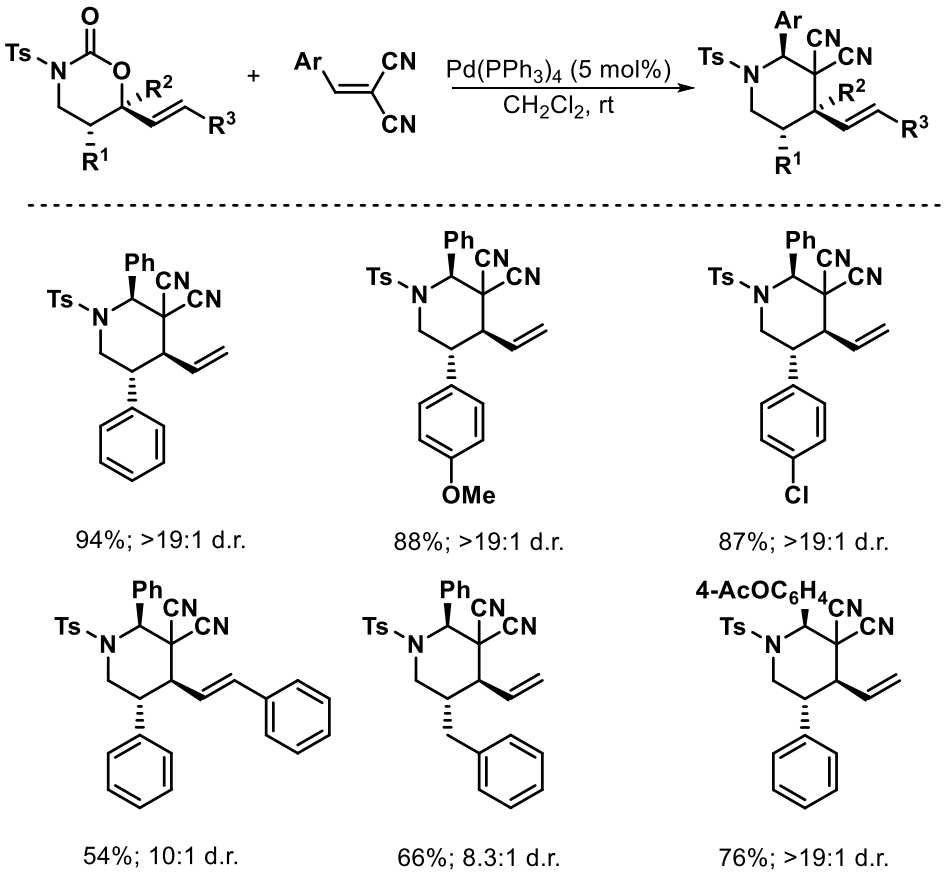

Scheme 25 *- Pd-mediated [4+2] cycloaddition of 6-vinyl oxazinones to highly activated Michael acceptors*

Furthermore, Tunge extended this annulation process to vinyl benzoxazinanone substrates.[55] In the presence of a Pd^0 catalyst and electron-deficient alkenes, a formal [4+2] cycloaddition reaction occurs to produce highly substituted hydroquinoline compounds (Scheme 26). The use of Trost's ligand **L9** allowed the reaction to perform with high levels of diastereo- and enantiocontrol. Benzoxazinanones bearing both electron-rich and electron-poor substituents were tolerated in the Pd-catalysed process.

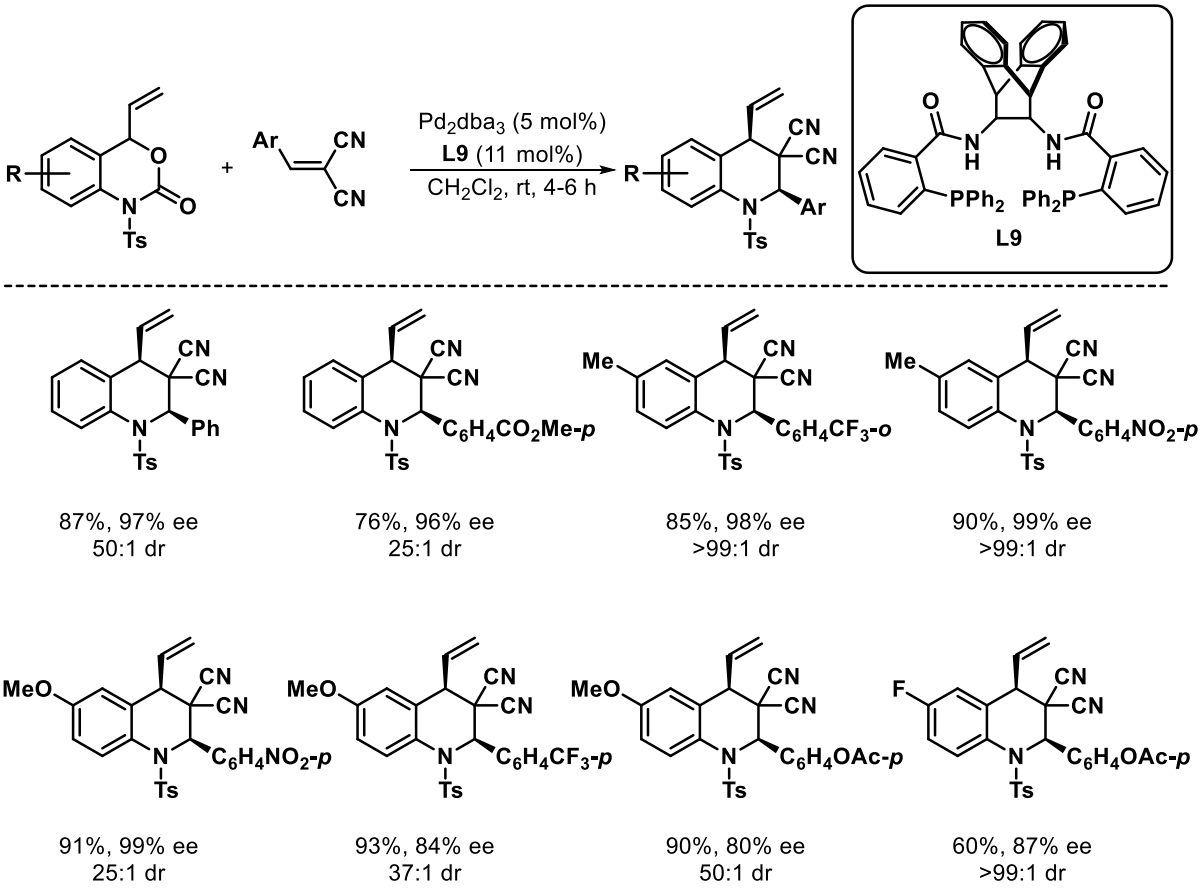

Scheme 26 *- Pd-catalysed [4+2] cycloaddition of vinyl benzoxazinanones to highly activated alkenes. Adapted from ref. [8] and [55]*

2. Functionalised Polycyclic Piperidines

2.1. Introduction

Nitrogen-containing molecules are valuable building blocks for pharmaceuticals and agrochemicals. Almost two-thirds of FDA-approved small-molecule drugs contain a nitrogen heterocycle, among which piperidine is the most commonly used.[56]

Over the past decade, molecules that are rich in sp^3 carbon atoms, particularly sp^3-rich heterocycles, received increasing interest from the drug discovery community. It was shown that the fraction of sp^3 hybridised carbon atoms (Fsp^3 = number of sp^3 carbon atoms/total carbon atom count) in drug candidates is correlated to important physical properties, such as solubility and melting point. Increasing the sp^3 character of the drug resulted in higher aqueous solubility and lower melting point. Furthermore, it has been demonstrated that sp^3-rich compounds are more likely to successfully progress through clinical trials. Additionally, the presence of stereogenic carbon atoms was found to positively impact the clinical progression of a drug-like molecule.[57, 58]

In this context, the Harrity group has developed a novel precursor to a dipolar reagent (Figure 5), which can react with readily available carbonyl compounds to give nitrogen heterocycles. These building blocks are able to undergo orthogonal

functionalisation with the potential to form sp^3-rich products in a stereocontrolled manner.

The dipolar intermediate can be generated *in situ* from a cyclic carbamate precursor in the presence of a palladium catalyst and a phosphoramidite ligand.

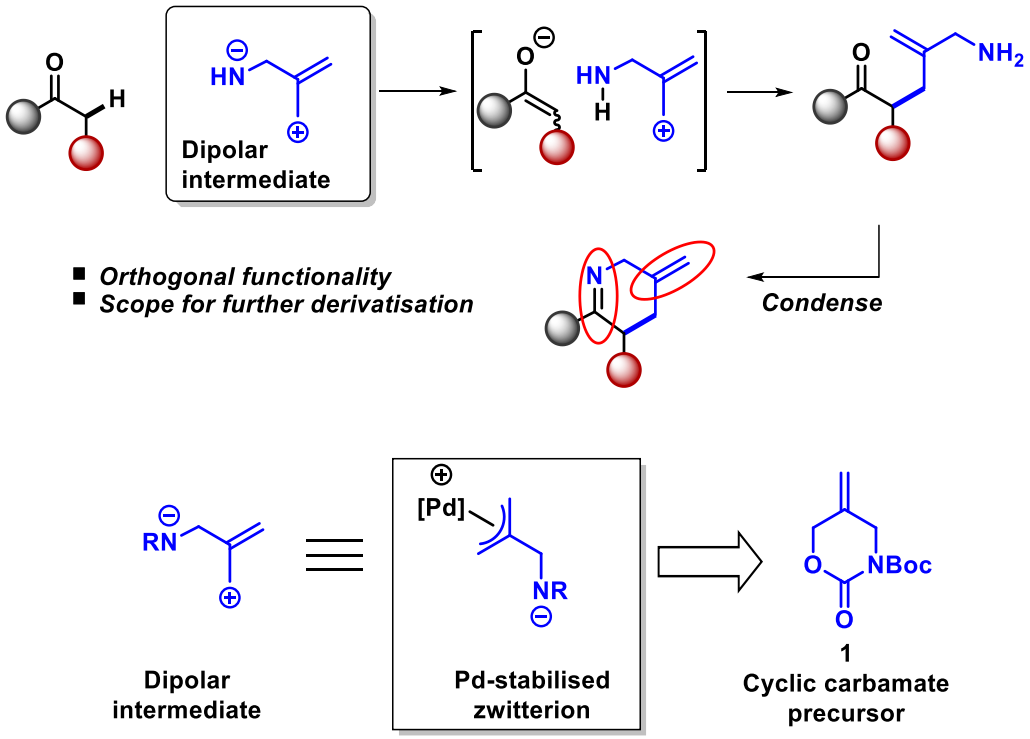

Figure 5 *- New strategy for the synthesis of highly functionalised N-heterocycles*

2.1.1. 1,3-Dicarbonyl Substrates

This palladium-stabilised zwitterion has been proven to react effectively with a range of 1,3-dicarbonyl substrates, such as 1,3-diketones, lactones, cyclic and acyclic β-

ketoesters, to give the corresponding allylated products in good to excellent yields (Scheme 27).[59]

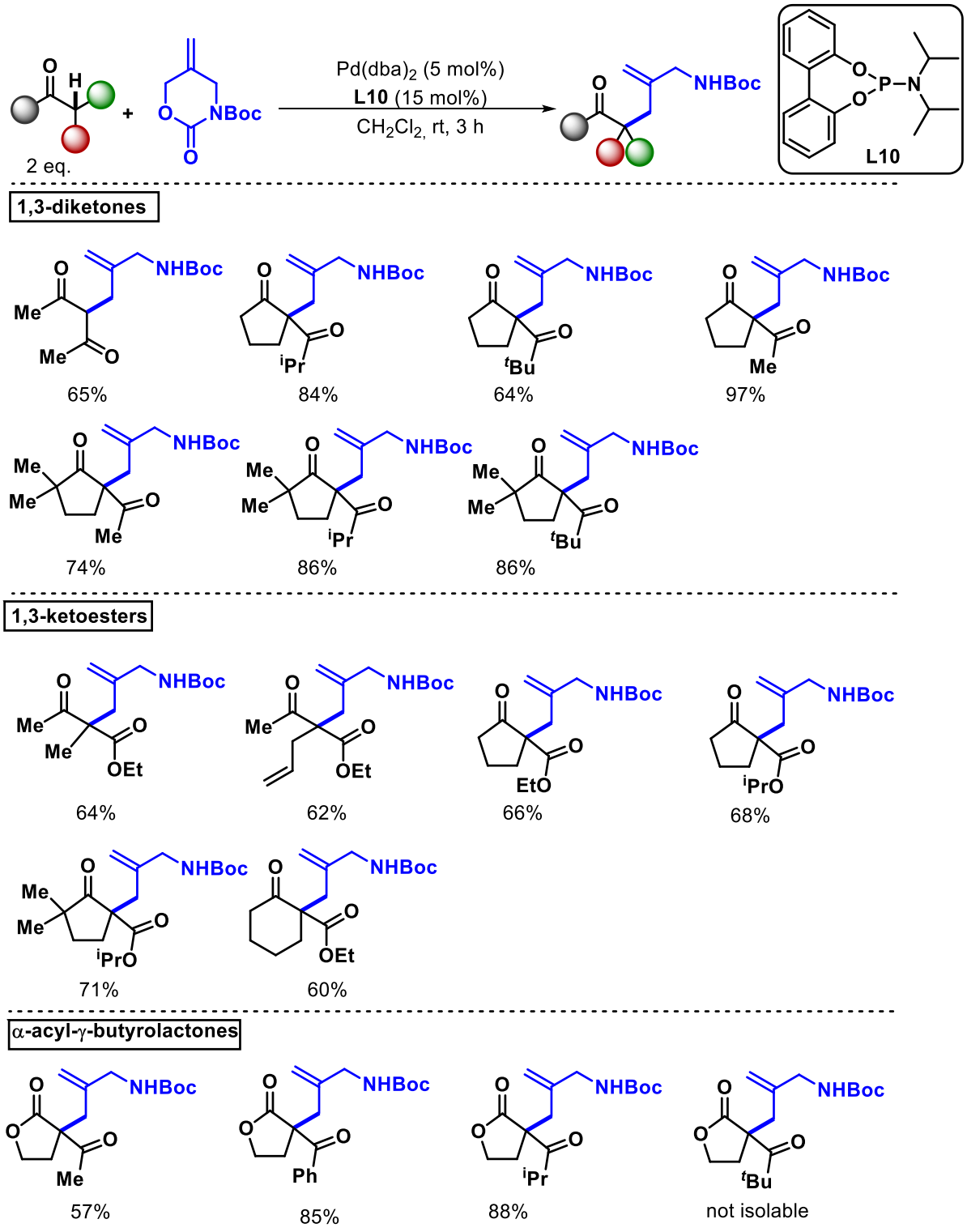

Scheme 27 *- Previous scope of Pd-catalysed 1,3-dicarbonyl allylation*

Treatment of these allylated substrates with TFA, allowed the deprotection of the *N*-Boc group and the condensation of the ketone with the amine, to give a wide range of piperidine derivatives (Scheme 28). Under these conditions, α-acyl-γ-butyrolactones gave only the spiro-piperidine products and 1,3-ketoesters gave the fused systems, whereas unsymmetrical 1,3-diketones raised a regioselectivity matter during the condensation step and led to a mixture of regioisomers (Scheme 28).[60]

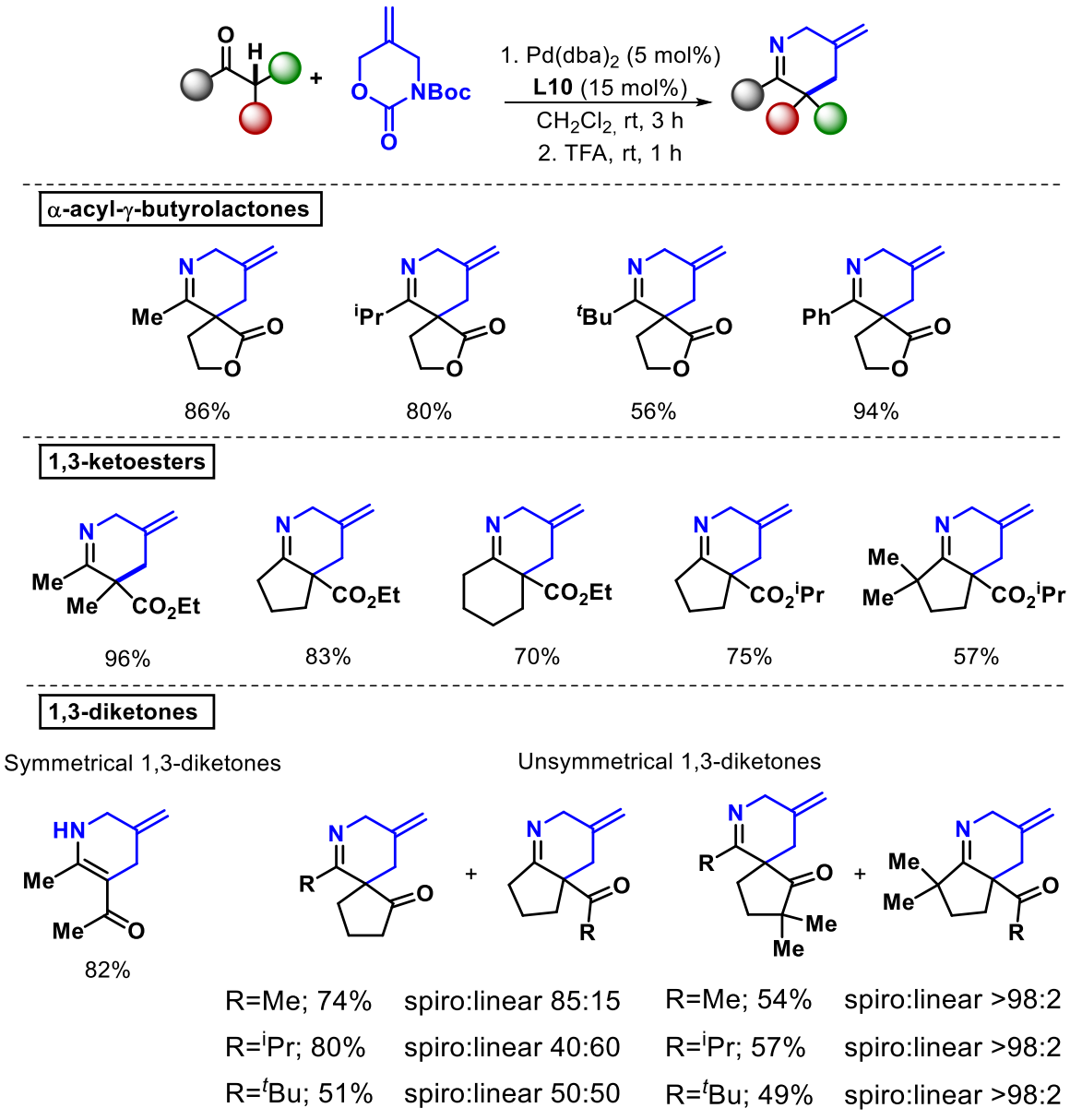

Scheme 28 *- Allylation-condensation to give a wide range of N-heterocycles*

2.1.2. ***Asymmetric Allylation: 1,3-Dicarbonyl Substrates***

A powerful development of this methodology would be to perform these reactions enantioselectively, and an asymmetric catalytic variant of this process was therefore considered. Based on Trost's work[61], a range of chiral phosphorous-based ligands was screened. It was found that chiral phosphoramidite ligands **L11**, **L12** and **L13** are able to induce enantioselectivity. Nevertheless, only a limited class of substrates gave the corresponding products with high enantiomeric excesses (Scheme 29).[59, 60]

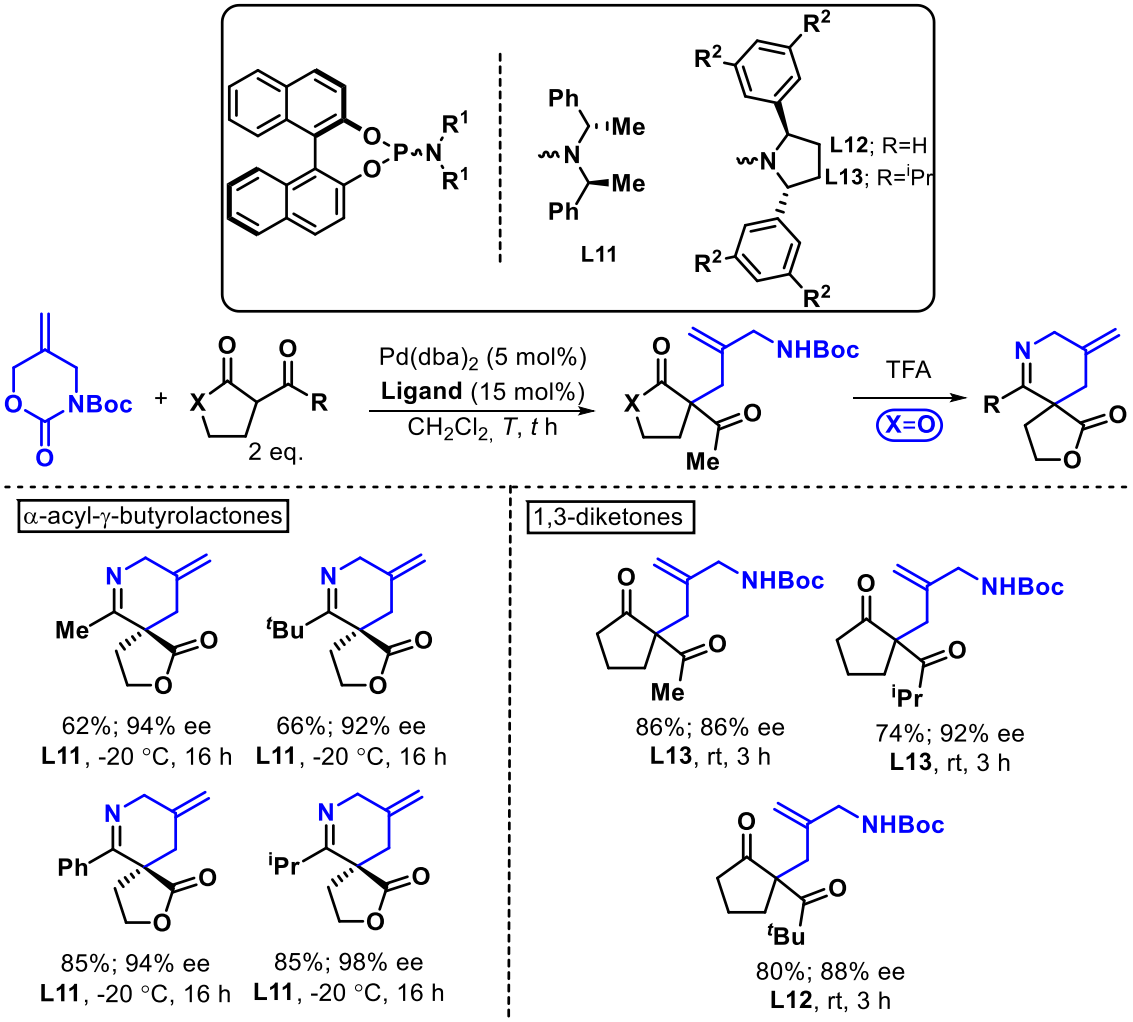

Scheme 29 *– Asymmetric allylation of α-acyl-γ-butyrolactones and 1,3-diketones*

2.1.3. Hypothetical Reaction Mechanism

It was proposed that the mechanism of this palladium-catalysed allylation reaction would first proceed with coordination of palladium to the alkene resulting in a three-coordinate complex (**I**) (Figure 6). The resulting catalyst-substrate complex **I** would then undergo an oxidative addition that could cleave the carbon-oxygen bond and result in an η^3-allyl complex (**II**).

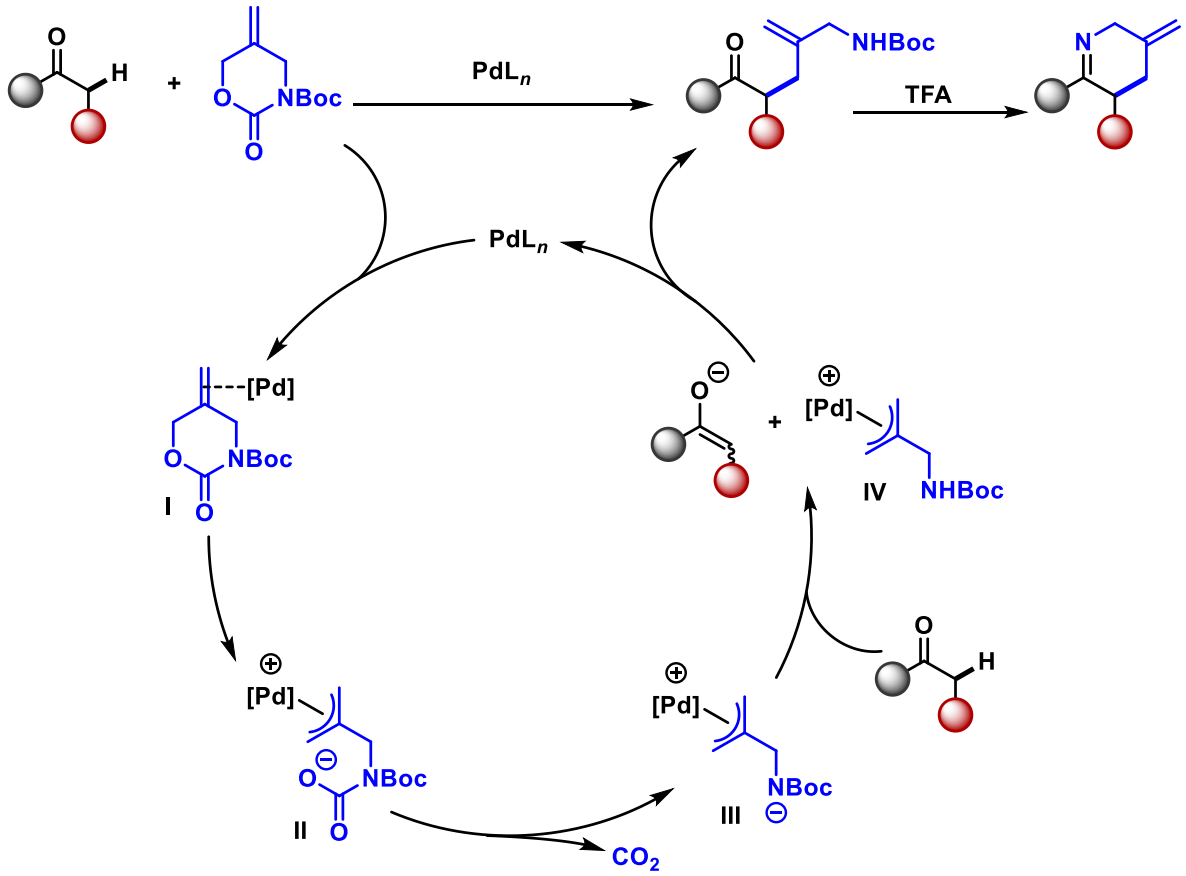

Figure 6 *- Proposed mechanism of the Pd-catalysed α-carbonyl allylation*

Subsequently, an irreversible decarboxylation could occur and lead to zwitterionic intermediate **III**. The resulting amide anion would then be able to deprotonate *α* to

the carbonyl to give the corresponding enolate. The mechanism would continue with nucleophilic attack of the enolate to the π-allyl complex, presumably through an outer-sphere pathway,[7] thereby leading to the allylated compound. Finally, a TFA-mediated deprotection-condensation step would provide the desired six-membered *N*-heterocycle.

2.1.4. 1-Substituted-2-Tetralone Substrates

Extension of this procedure to a range of 1-aryl-2-tetralone substrates (Scheme 30), delivered the corresponding allylated compounds in high yields and with the expected regioselectivity.[59] This methodology proved to be tolerant of a range of aryl groups, as well as alkyl and ester moieties.

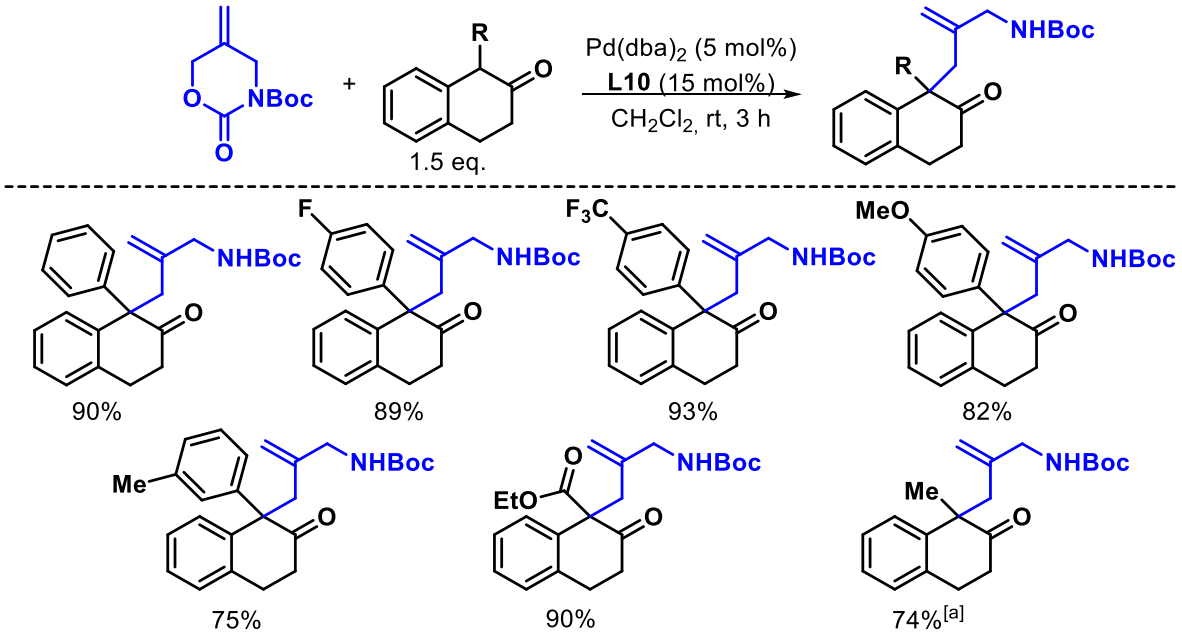

Scheme 30 *- Pd-catalysed α-functionalisation of 2-tetralone substrates. [a] Reflux*

A deprotection-condensation step in TFA followed by reduction of the cyclic imine with $NaBH_4$, allowed the formation of tricyclic piperidine products as single diastereomers (Scheme 31). However, their isolation proved difficult, leading to low isolated product yields. The *in situ* protection of the amine with a Cbz group prior to purification, improved the overall yield. The relative stereochemistry was assigned as *trans* by X-ray crystallography.

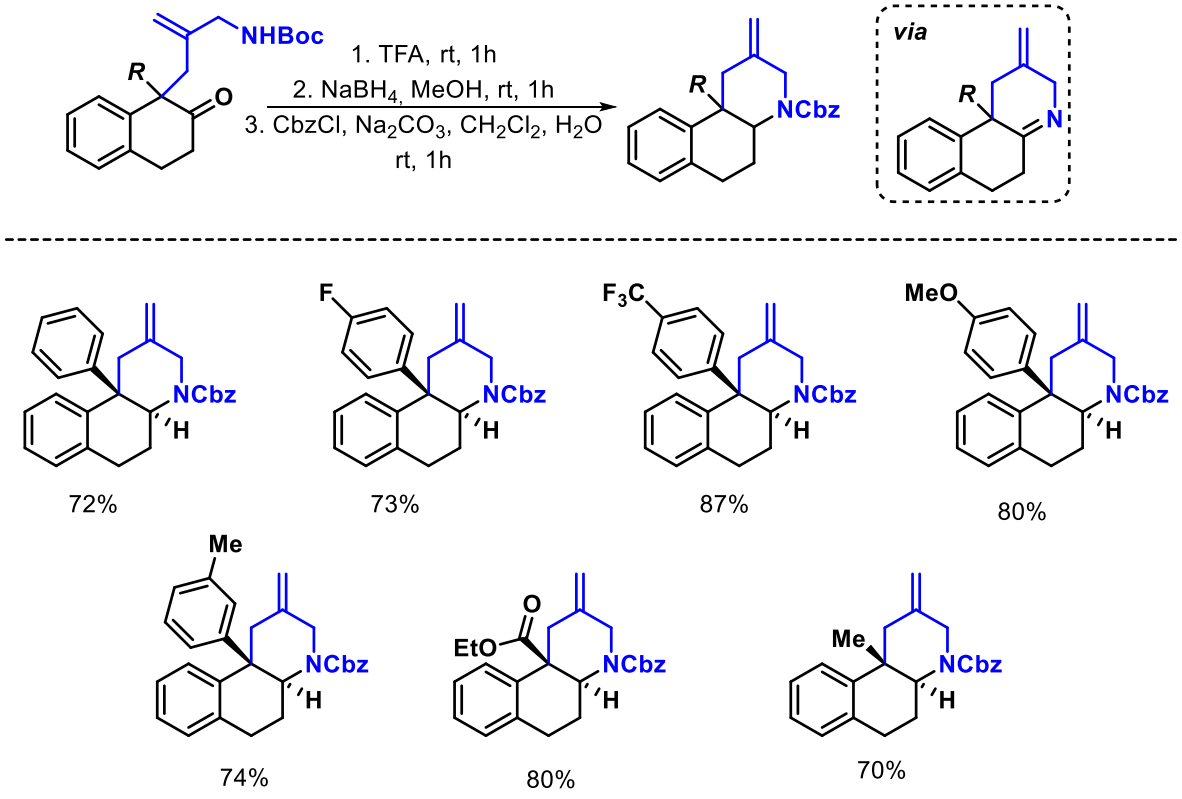

Scheme 31 - *Formation of Cbz-protected tricyclic piperidines*

Based on previous investigations that have been undertaken within the group, the aim of this work was to further develop the palladium-catalysed annulation strategy, initially by expanding its substrate scope and then by developing an enantioselective synthesis of functionalised piperidines. Furthermore, the diastereoselective

functionalisation reactions of these heterocyclic compounds would be studied in order to exhibit their utility, and the application of this methodology to the synthesis of a natural product would be investigated.

2.2. Results and Discussion

2.2.1. Pd-Stabilised Zwitterion Precursor Synthesis

The synthesis of Pd-stabilised zwitterion precursor **17** started with the desymmetrisation of 2-methylene-1,3-propanediol **14** through an Appel reaction. Exposure of **15** to AgOCN, delivered the cyclic carbamate **16**, which was then protected with a Boc group on the nitrogen atom to give the desired precursor (Scheme 32).[62]

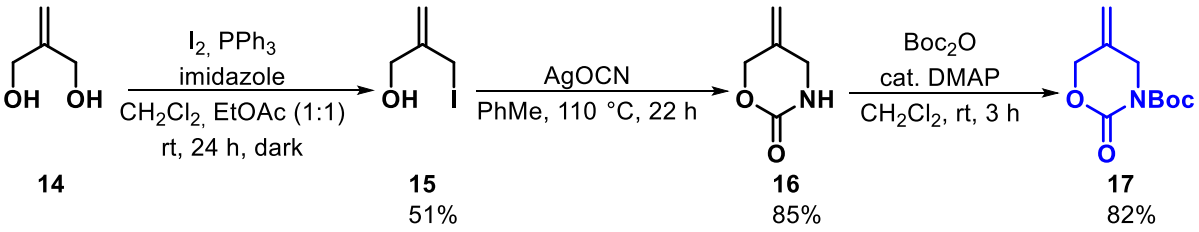

14 | **15** 51% | **16** 85% | **17** 82%

Scheme 32 *- Synthesis of the Pd-stabilised zwitterion precursor* ***17***

The first step proceeds in only modest yield as allyl iodide product **15** competes with starting material **14** in the Appel reaction, to form the diiodide as a by-product. Furthermore, allyl iodide **15** is unstable to light and decomposes slowly during chromatographic purification.

In an effort to improve the overall yield, it was reasoned that replacing the iodide with a tosylate might make the mono-functionalisation of **14** more controlled due to steric hindrance, and at the same time increase the stability of the product to light.

After subjection of diol **14** to classical tosylation conditions, in dichloromethane at room temperature, two compounds were isolated (Scheme 33). The first structure characterised proved to be the desired compound **19**, although the product was isolated in just 7% yield. The major product isolated from the reaction was monochlorinated compound **18**, which was obtained in 92% yield. Exposure of **18** to silver cyanate resulted in 88% conversion to cyclic carbamate **16** after six days.

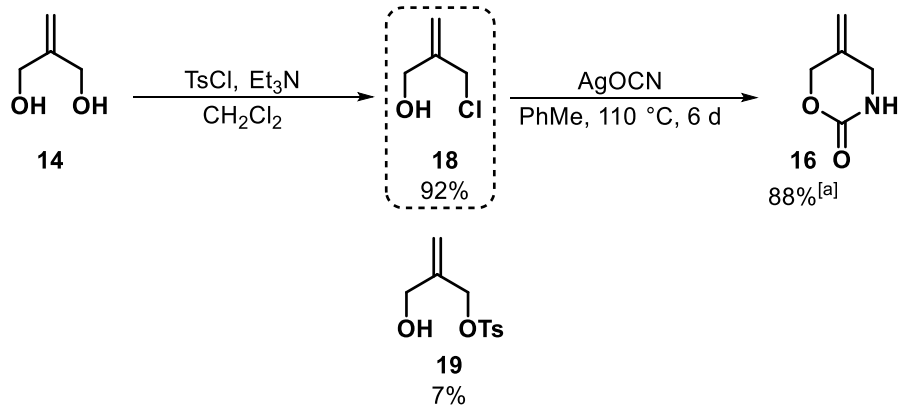

Scheme 33 *- Alternative route to precursor **17**. [a] % conversion determined by ^{1}H NMR spectroscopy*

Although this new approach to precursor **17** requires long reaction times by comparison, it may have some advantages in terms of atom economy and overall yield.

2.2.2. 1-Substituted-2-Indanone Substrates

In order to expand the substrate scope of the palladium-catalysed allylation process, a range of 1-substituted-2-indanone substrates was synthesised. These substrates were particularly interesting as the regioselectivity of enolate formation and hence its selective reaction with the Pd-stabilised zwitterion was not obvious.

1-Phenyl-2-indanone **22** was accessed through reaction of phenylmagnesium bromide with 1-indanone **20** followed by acid-promoted dehydration in HCl to give alkene **21** in 70% yield. The latter was oxidised to product **22** by using a mixture of Oxone® monopersulfate with $NaHCO_3$ (Scheme 34).[63]

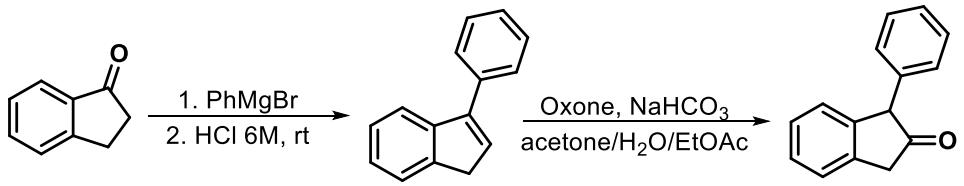

20 **21** 70% **22** 61%

Scheme 34 - *Synthesis of 1-phenyl-2-indanone* ***22***

However, this two-step procedure proved to be rather limited and substrates bearing substituted aryl groups were unsuccessful in this transformation. A longer route to the 1-aryl-2-indanone substrates was considered. Minehan and co-workers have previously reported a six-step process to a range of *para*-substituted 1-aryl-2-indanones (Scheme 35).[64]

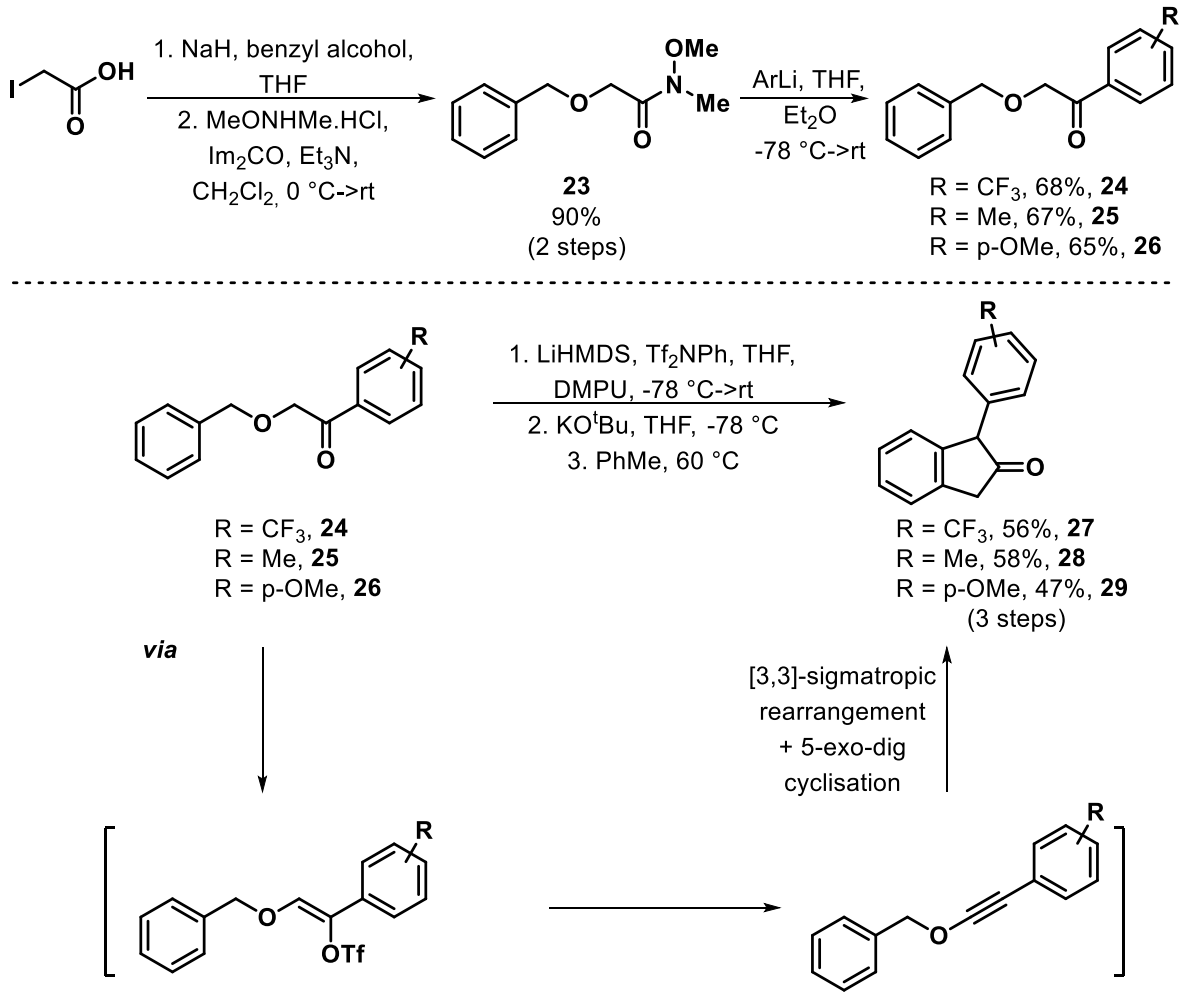

Scheme 35 *- Alternative synthesis to 1-aryl-2-indanones*

The six-step process began with treatment of commercially available iodoacetic acid with sodium hydride and benzyl alcohol, followed by a coupling reaction with *N*,*O*-dimethylhydroxylamine to provide Weinreb amide **23** in 90% yield. The addition of the appropriate aryllithium intermediate to Weinreb amide **23** provided α-alkoxy ketones **24** to **26** in good yields. Treatment of these substrates with LiHMDS at −78 °C, followed by addition of phenyl triflimide in THF/DMPU, led to the enol triflates. These were rapidly filtered through silica gel, then immediately treated with potassium *tert*-butoxide to give the corresponding benzyl alkynyl ethers. When these intermediates were heated to 60 °C in toluene, a [3,3]-sigmatropic rearrangement

followed by a 5-exo-dig cyclisation occurred to give the *para*-substituted 1-aryl-2-indanone products **27** to **29** in moderate overall yields. *Meta*-substituted 1-aryl-2-indanone **31** was synthesised in four steps (Scheme 36), using a procedure that was previously described by Baran and coworkers.[65] The Grignard addition of 3-methoxyphenylmagnesium bromide on to the commercially available 1-indanone, followed by acid-mediated dehydration with HCl, gave **30** in 90% yield. Dihydroxylation of indene **30** with OsO_4 and 4-methylmorpholine *N*-oxide followed by an acid-promoted pinacol rearrangement in toluene, provided indanone **31** in 59% yield over two steps.

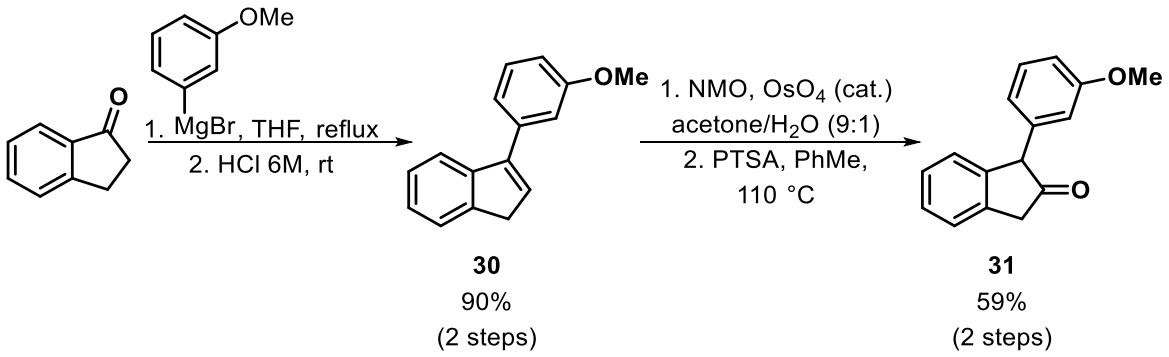

Scheme 36 - *Synthesis of 1-(3-methoxypheny)-2-indanone* ***31***

Alkyl-substituted 2-indanone **33** was synthesised in a slightly different fashion (Scheme 37). Treatment of 1-indanone with methylmagnesium bromide followed by acid-mediated dehydration gave indene **32** in 78% yield. Epoxidation of **32** with mCPBA followed by BF_3-promoted Meinwald rearrangement provided 1-methyl-2-indanone in 33% yield.

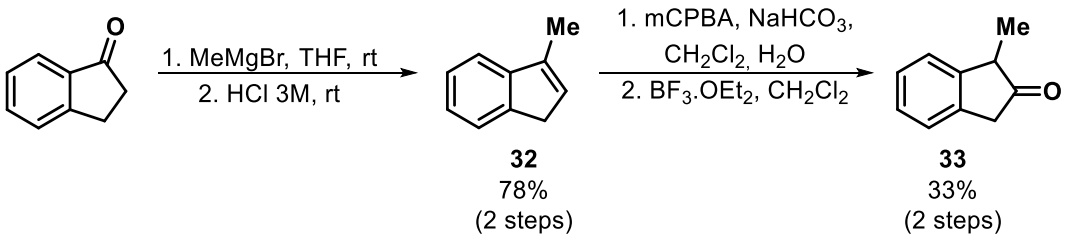

Scheme 37 - *Synthesis of 1-methyl-2-indanone* ***33***

1,3-Ketoester **34** was readily prepared in a one-step reaction (Scheme 38).[66] Treatment of 2-indanone with sodium hydride and diethyl carbonate gave compound **34** in 57% yield after two hours.

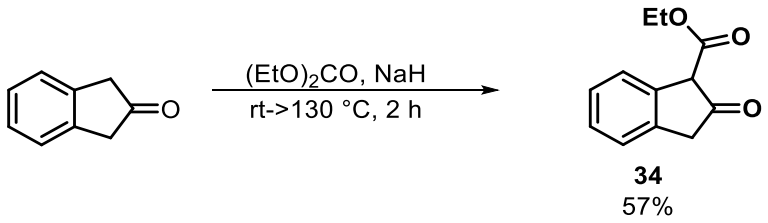

Scheme 38 - *Synthesis of 1-ester-2-indanone* ***34***

Having synthesised a range of 1-substituted-2-indanone substrates, their reactivity in the Pd-catalysed allylation process was investigated. Most of the substrates underwent the allylation reaction with carbamate **17** efficiently (Scheme 39). Allylated compounds **35** to **40** were isolated in good to excellent yields. However, 1-methyl-2-indanone **33** raised a selectivity issue and a mixture of two regioisomers was obtained (Scheme 40).

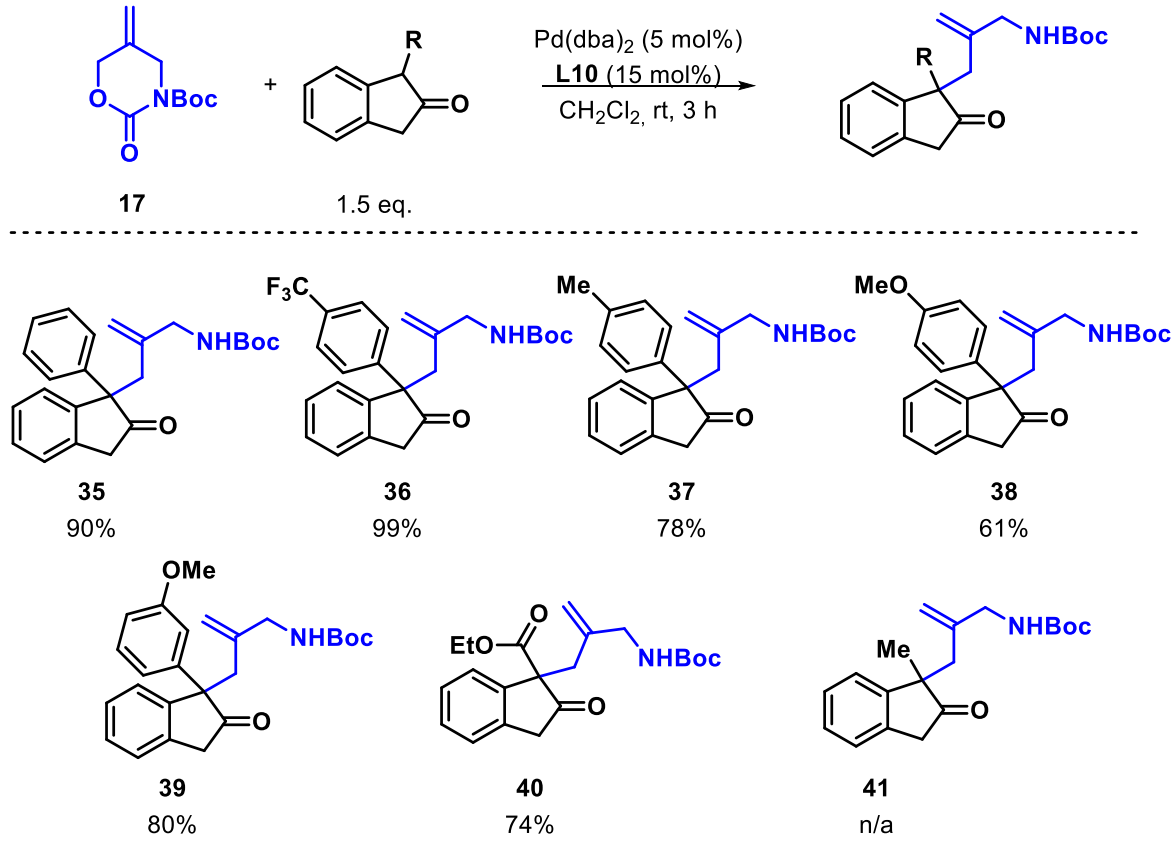

Scheme 39 *- Pd-catalysed allylation of 1-substituted-2-indanones*

This lack of selectivity suggests that both enolates, kinetic and thermodynamic, are formed and react with the Pd-stabilised zwitterion. Furthermore, allylated compound **41** could not be isolated as co-elution with regioisomer **42** occurred.

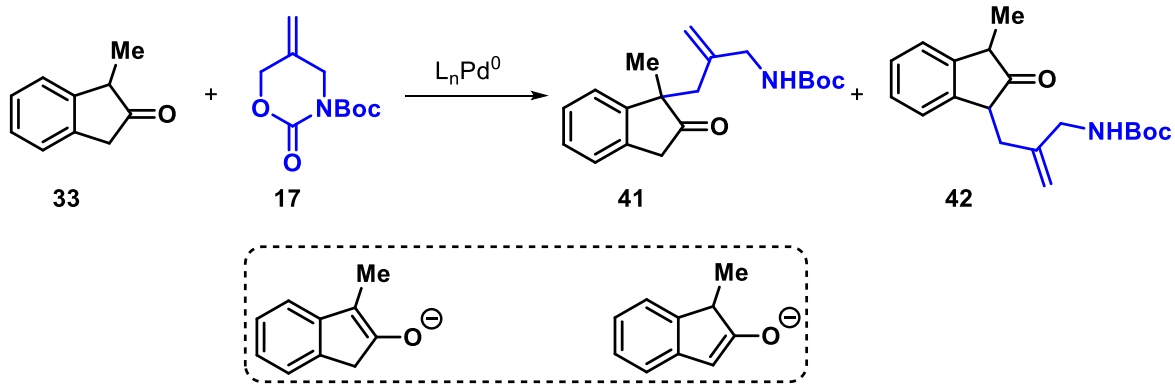

Scheme 40 *- Non-selective allylation of substrate* ***33***

After exploring the scope of the palladium-catalysed allylation with indanone substrates, attention was moved towards the conversion of the allylation products into fused 6-5-6 tricyclic piperidines. It was envisioned that a TFA-mediated deprotection-condensation sequence followed by a reduction step would allow rapid access to densely functionalised *N*-heterocycles (Scheme 41).

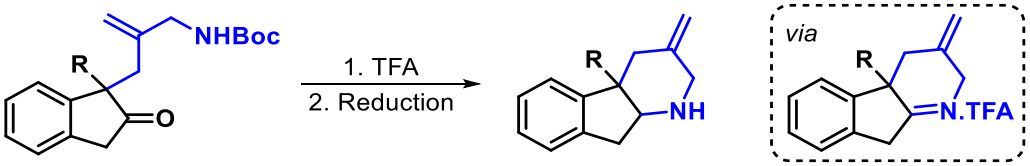

Scheme 41 *- Formation of fused 6-5-6 tricyclic core*

However, reduction of the cyclic iminium intermediate proved challenging. Initial attempts to perform the reduction with a range of hydride reducing agents were unsuccessful and resulted in complex mixtures.

It was postulated that the issue arising in this apparently simple reduction step is the formation of an unstable strained *trans*-5,6 ring system imposed by the attack of the hydride from the opposite side to the aryl group (Figure 7).

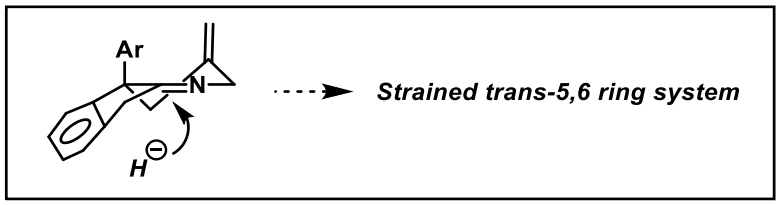

Figure 7 *- Formation of an unstable strained trans-5,6 ring system*

Based on this hypothesis, it was reasoned that reduction of the iminium salt *via* a radical pathway might ease the ring strain by either forming a free radical that could interconvert to the thermodynamically more stable conformation or by directly producing the most stable conformer (Figure 8).

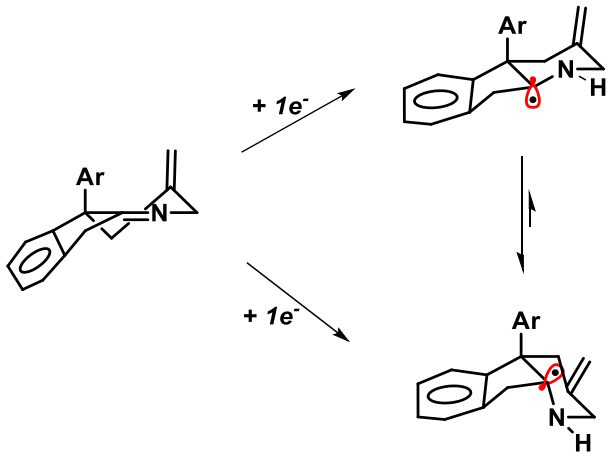

Figure 8 *- Proposed radical reduction resulting in a more stable conformation*

Therefore, iminium salts were subjected to a recent visible-light photoredox reduction reported by Wenger and co-workers.[67] Using $Ru(bpy)_3(PF_6)_2$ as a photocatalyst in the presence of 3-mercaptopropionic acid and sodium L-ascorbate in MeOH, enabled the formation of the desired tricyclic piperidines **43** to **48** as single diastereomers in acceptable yields (Scheme 42).

Analysis of the crude NMR and mass spectrometry data suggests that the moderate yields could be due to side reactions, such as radical dimerisation. Despite extensive efforts to optimise the photoredox reduction, reduced products could not be isolated in higher yields. Nevertheless, the photo-induced ruthenium-catalysed reduction

enabled the diastereoselective synthesis of highly substituted piperidines with contiguous quaternary and tertiary stereogenic centers.

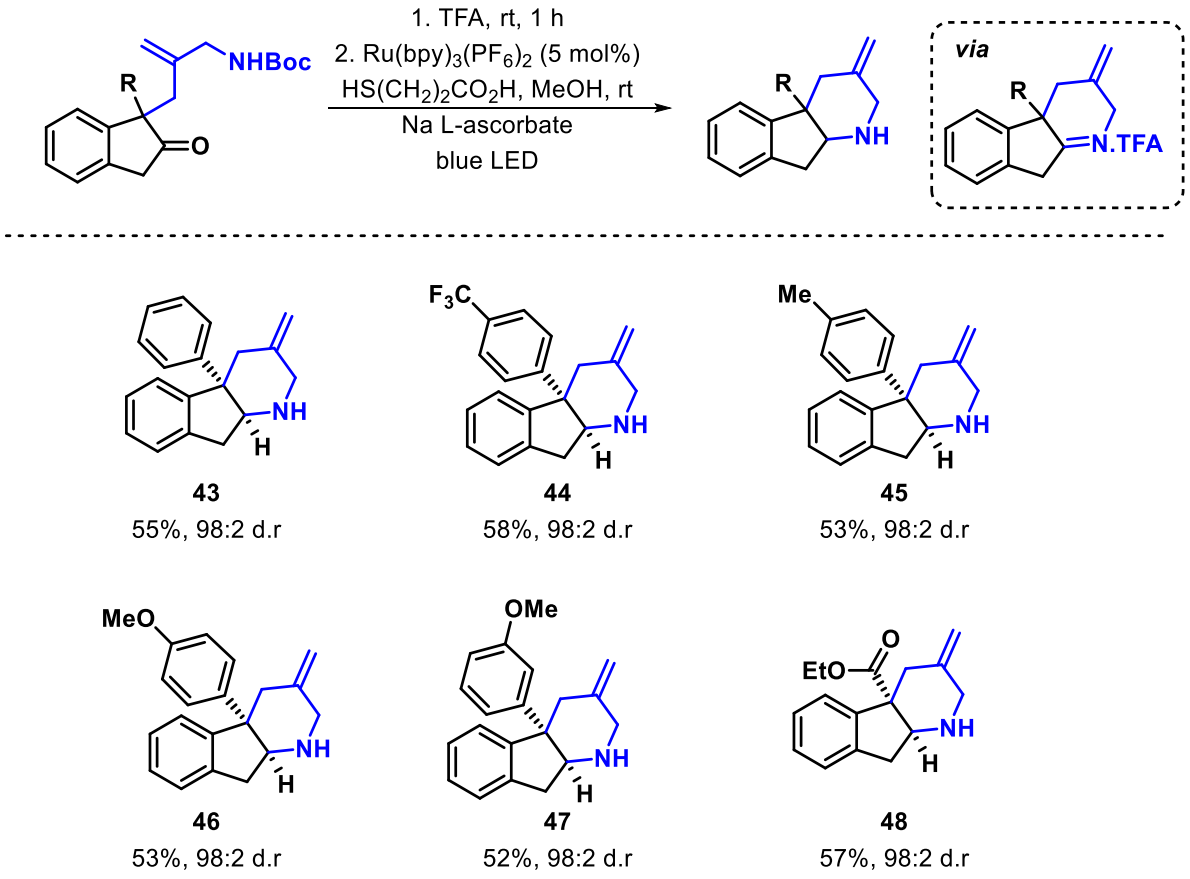

Scheme 42 - *Visible-light photoredox reduction of iminium salts*

The product stereochemistry was assigned as *cis* by analogy to compound **46**, and on the basis of a positive nOe correlation between the CH proton (adjacent to the N-atom) and the aromatic protons (Figure 9).

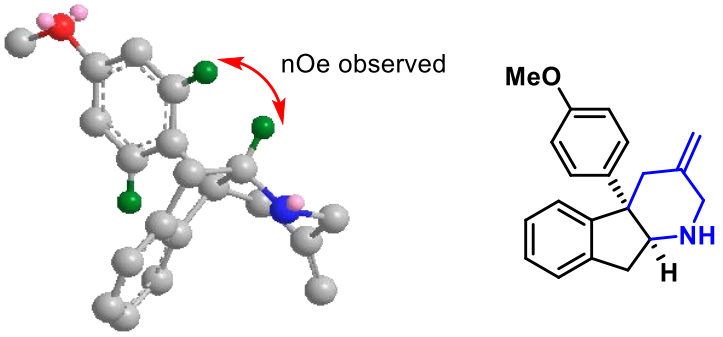

Figure 9 *- nOe correlation observed to assign the stereochemistry*

2.2.3. ***Asymmetric allylation***

Having confirmed the viability of this chemistry to access a variety of polycyclic fused piperidines, attention was turned to the investigation of an asymmetric synthesis. As previously described, earlier work in the group showed that the use of monodentate chiral phosphoramidite ligands provided promising levels of enantiocontrol.[60] Therefore, a series of chiral phosphoramidite ligands (Figure 10) with different amine substituents was prepared and investigated in the Pd-catalysed allylation process with substrate **22** (Table 1).

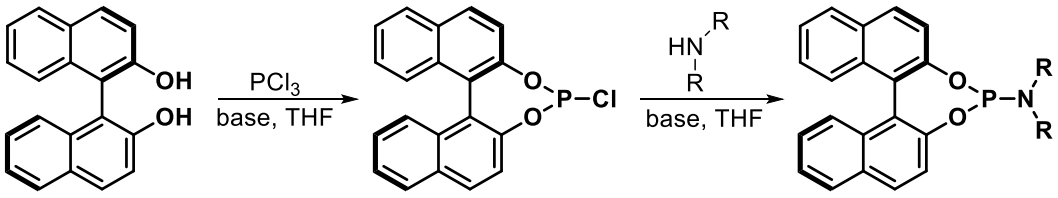

Scheme 43 *- Synthesis of chiral phosphoramidite ligands*

Phosphoramidite ligands **L11**, **L14**, **L16** and **L19** were readily prepared in a two-step sequence, by reacting first the appropriate diol with phosphorous trichloride to give the chlorophosphite, followed by addition of the commercially available amine in the presence of a base (Scheme 43).[68] The other chiral ligands were either commercially available or produced by other members of the Harrity group.

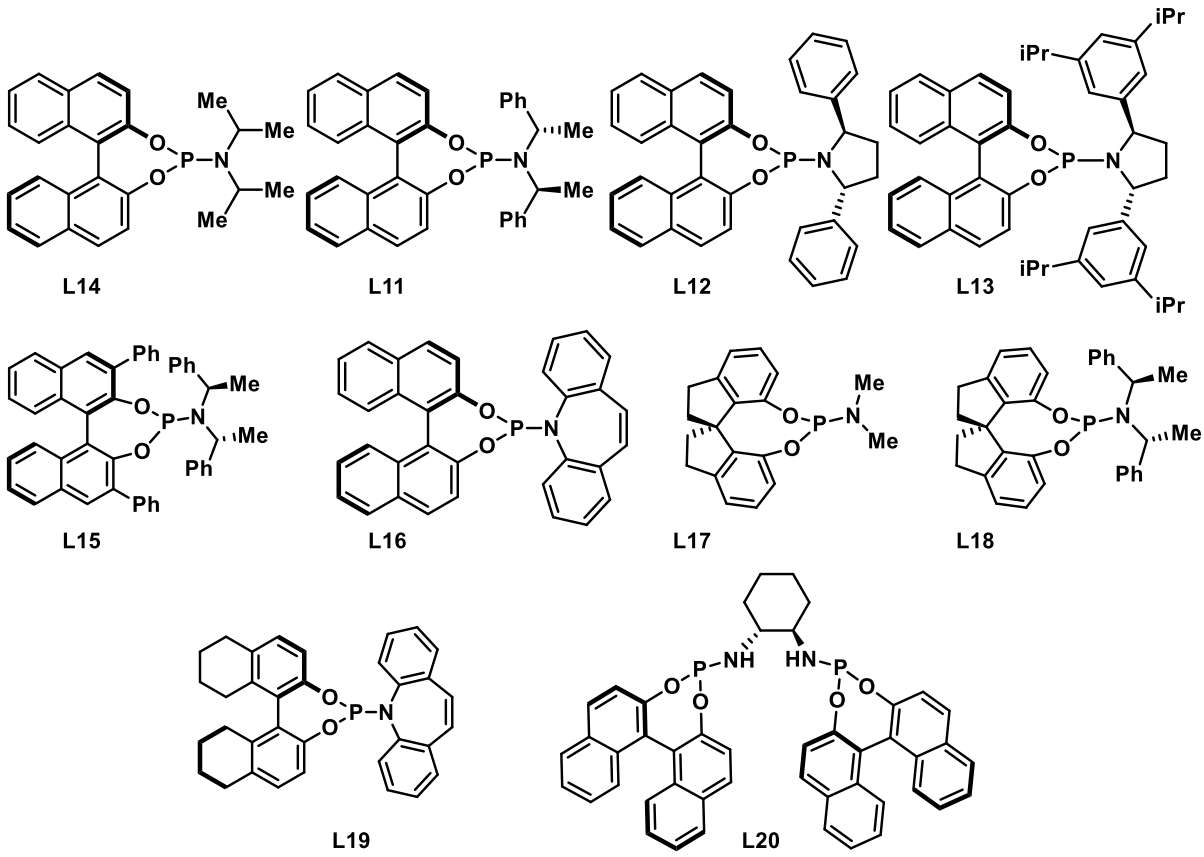

Figure 10 *- Structures of examined phosphoramidite ligands*

Subjecting ligands **L11**, **L12** and **L14** to the standard allylation conditions provided the desired allylated product, albeit with poor enantioselectivities (Table 1). Increasing the steric bulk on the BINOL or the amine moiety in order to improve the selectivity resulted in a complete lack of reactivity (**L13** and **L15**). However, the use

of ligand **L16**, bearing an achiral planar amine, improved the enantiomeric excess. Chiral phosphoramidite ligands **L17** and **L18**, which consist of a spiro backbone, were also investigated in the Pd-catalysed process. However, similar levels of enantiocontrol to the BINOL-based phosphoramidite ligands were obtained. The dibenzazepine-based ligand **L19** with an octahydro-BINOL backbone, led to a lower enantiomeric excess compared to the BINOL analogue **L16**. In the case of the bidentate phosphoramidite ligand **L20**, no reaction occurred.

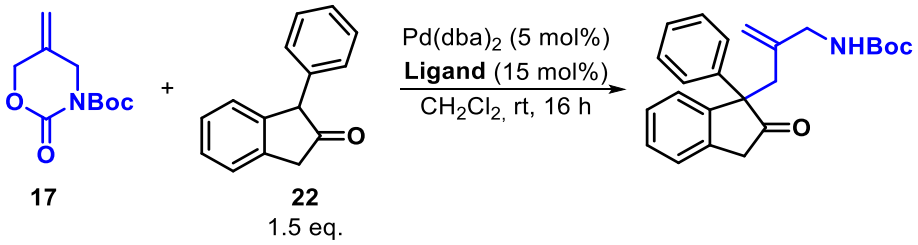

Entry	Ligand (**L**)	Conv (%)[a]	ee (%)[b]
1	**L14**	100	<5
2	**L11**	100	14
3	**L12**	100	6
4	**L13**	0	-
5	**L15**	0	-
6	**L16**	100	30
7	**L17**	100	10
8	**L18**	100	16
9	**L19**	100	22
10	**L20**	0	-

Table 1 *- Screening of chiral phosphoramidite ligands. [a] % conversion determined by* ^{1}*H NMR spectroscopy. [b] Determined by chiral HPLC*

It was thought that the “pseudo-symmetry” of the 2-aryl indanone **22** might have been responsible for the poor levels of enantiocontrol observed generally. As shown in Figure 11, the two faces of the enolate are “too similar”, which may lead to poor facial discrimination by the chiral catalyst.

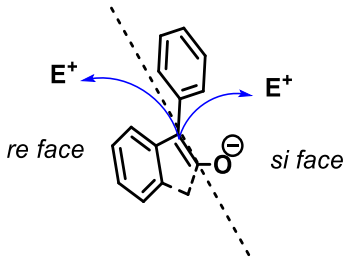

Figure 11 *- Enantiotopic faces of enolate **22***

Thus, 2-ester indanone **34** was investigated in the allylation reaction with ligands **L16** and **L12** (Table 2). However, indanone **34** gave similar selectivities to the aryl analogue.

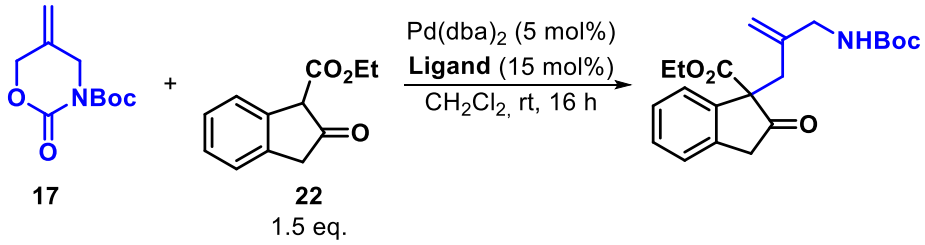

Entry	Ligand (**L**)	Conv (%)[a]	ee (%)[b]
1	**L16**	100	33
2	**L12**	100	16

Table 2 *- Investigation of **34** in the enantioselective allylation [a] % conversion determined by ^{1}H NMR spectroscopy. [b] Determined by chiral HPLC*

After screening a range of chiral phosphoramidite ligands in dichloromethane at room temperature, attention turned to the effects of changing the solvent and decreasing the temperature. Since ligand **L16** led to the most selective palladium-phosphoramidite catalyst, it was used to further optimise the reaction conditions. The allylation step was investigated in different solvents at room temperature and at −25 °C (Table 3).

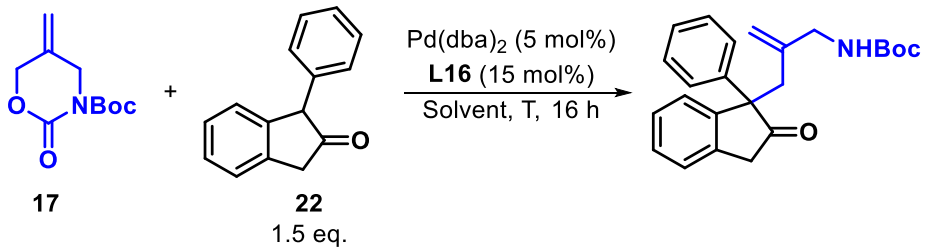

Entry	Solvent	T (°C)	Conv (%)[a]	ee (%)[b]
1	CH_2Cl_2	rt	100	30
2	THF	rt	100	36
3	PhMe	rt	100	42
4	PhMe	-25	100	58
5	CH_2Cl_2	-25	100	36

Table 3 *- Solvent and temperature optimisation study. [a] % conversion determined by* ^{1}*H NMR spectroscopy. [b] Determined by chiral HPLC*

It appeared that the selectivity increased in THF and toluene. Furthermore, decreasing the reaction temperature down to -25 °C had a beneficial effect on the enantioselectivity.

Other palladium sources were investigated and $Pd(OAc)_2$ was found to give comparable yields and enantioselectivities to $Pd(dba)_2$ in CH_2Cl_2 at room temperature, however $[PdCl(allyl)]_2$ failed to catalyse the allylation reaction (Table 4).

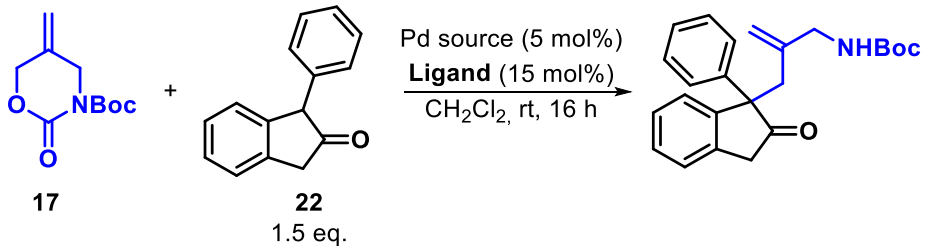

Entry	Ligand (**L**)	Catalyst	Conv (%)[a]	ee (%)[b]
1	**L16**	$Pd(dba)_2$	100	30
2	**L16**	$Pd(OAc)_2$	100	34
3	**L12**	$Pd(OAc)_2$	100	10
4	**L16**	$[PdCl(allyl)]_2$	0	-

Table 4 *- Screening of different Pd sources. [a] % of conversion determined by* ^{1}*H NMR spectroscopy. [b] Determined by chiral HPLC*

As only a moderate enantiomeric excess was obtained from the phosphoramidite ligands screening (Table 3, entry 4), the utility of chiral phosphine ligands in the allylation reaction was also probed.

Based on literature precedent,[2, 69] a range of commercial chiral phosphine ligands (Figure 12) was screened with indanone **22** in dichloromethane at room temperature (Table 5).

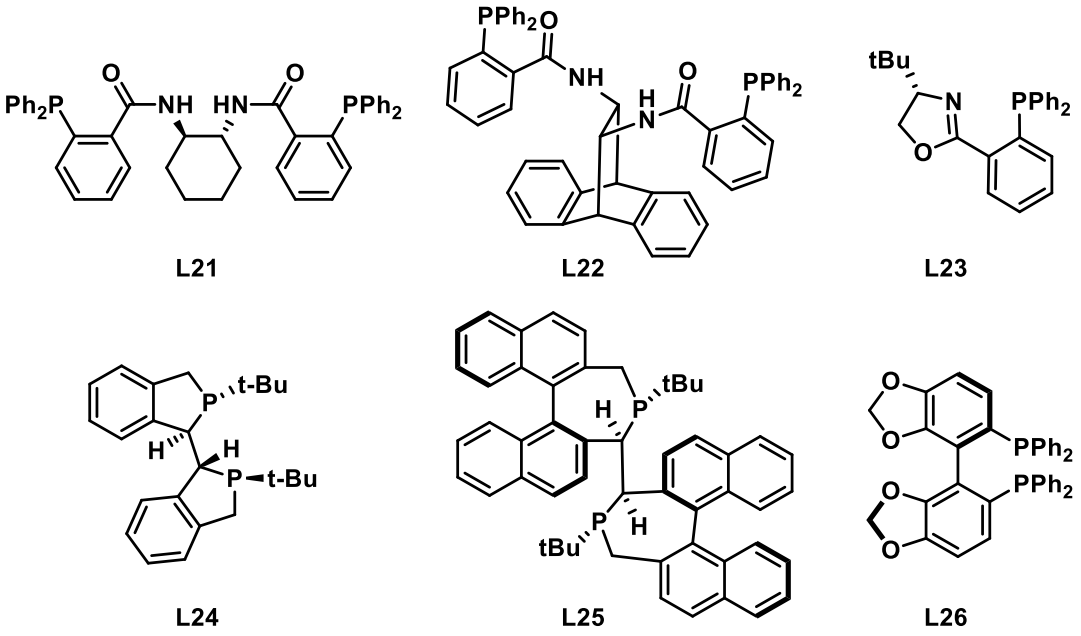

Figure 12 *- Structures of the examined chiral phosphine ligands*

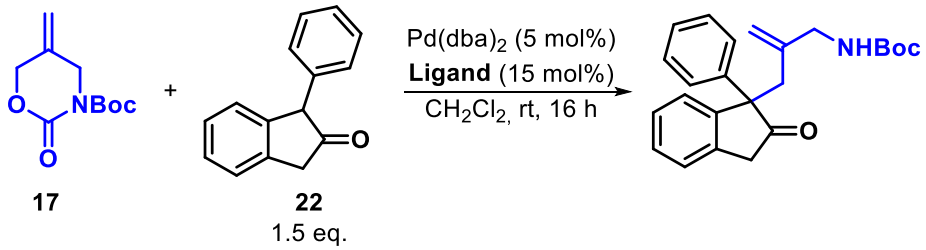

Entry	Ligand (**L**)	Conv (%)[a]	ee (%)[b]
1	**L21**	100	40
2	**L22**	56	4
3	**L23**	100	5
4	**L24**	0	-
5	**L25**	0	-
6	**L26**	0	-

Table 5 *- Screening of chiral phosphine ligands. [a] % of conversion determined by ^{1}H NMR spectroscopy. [b] Determined by chiral HPLC*

Unfortunately, higher enantioselectivities could not be obtained. The (*R*,*R*)-DACH-Ph Trost ligand **L21** was found to be the most selective phosphine ligand, resulting in an enantiomeric excess of 40%. Ligands **L22** and **L23** successfully underwent the allylation reaction, however with poor selectivities. Bulkier phosphines ligands **L24** to **L26** failed to promote the reaction.

Further asymmetric investigations in the palladium-catalysed allylation of 2-aryl indanones could not be completed within the time constraints, however other enantioselective strategies in the synthesis of 3-fluoropiperidines will be discussed in Chapter Three.

2.2.4. Product Derivatisations

Having successfully synthesised a series of polycyclic piperidines that contain orthogonal functionality, attention turned toward examining product functionalisation.

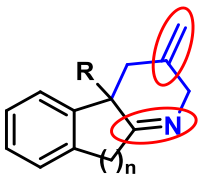

- ***Orthogonal functionality***
- ***Scope for further derivatisation***

Figure 13 - *Potential sites for derivatisations*

The oxidative cleavage of the *exo*-alkene was therefore investigated. Exposure of the reduced product **47** to OsO_4 and $NaIO_4$ failed to provide the desired product. However Boc-protection of the nitrogen followed by oxidative cleavage using $RuCl_3$ and $NaIO_4$ in the presence of 2,6-lutidine allowed the formation of **50** as a mixture of carbamate rotamers.[70] Subsequent deprotection with trifluoroacetic acid led to ketone **51** in 67% yield over three steps (Scheme 44).

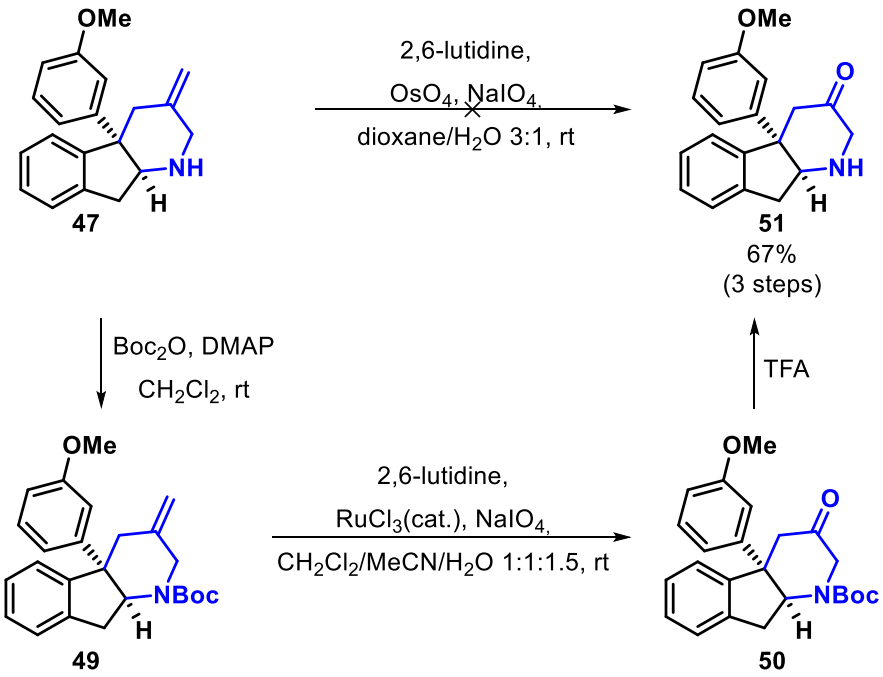

Scheme 44 - *Oxidative cleavage of the alkene*

Notably, compound **51** closely resembles an intermediate converted into haouamine A by Fürstner and co-workers (Scheme **45**).[71]

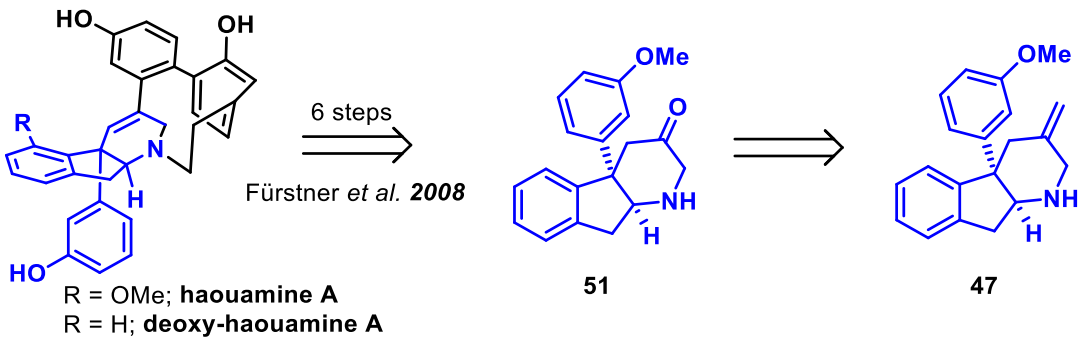

Scheme 45 *- Retrosynthetic analysis of deoxy-haouamine A*

After showing the ability of indanone-based polycyclic piperidines to undergo further derivatisation, the imine functionalisation of tetralone-based products was investigated. *N*-Alkyl ketimines exhibit a lower electrophilicity compared to imines bearing electron-withdrawing groups at nitrogen, therefore they usually require the presence of a Lewis acid or a transition metal to activate the carbon-nitrogen double bond.[72] Hence, compound **52** was treated with a range of organometallic reagents and Lewis acids, but as expected nucleophilic addition to the cyclic imine proved difficult. An iridium-catalysed addition of trimethylsilylacetylene[73] was attempted at room temperature and at 50 °C, however no traces of the propargylic amine product was observed and all starting materials were recovered (Scheme 46).

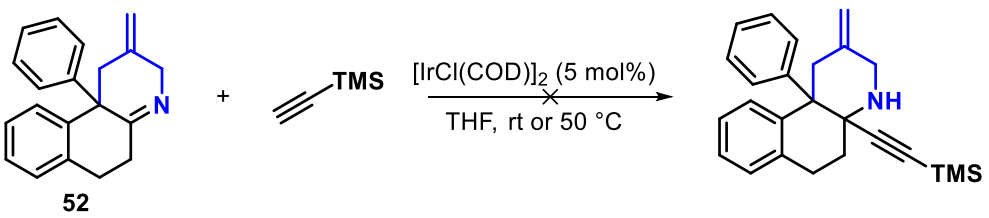

Scheme 46 *- Attempted Ir-catalysed addition of TMS-acetylene*

The 1,2 addition of organoaluminium and organomagnesium reagents, such as triethylaluminium and ethylmagnesium bromide, were also probed, however no conversion was observed (Scheme 47). The Strecker reaction using trimethylsilyl cyanide in the presence of $BF_3.OEt_2$ was unsuccessful and starting materials were recovered.

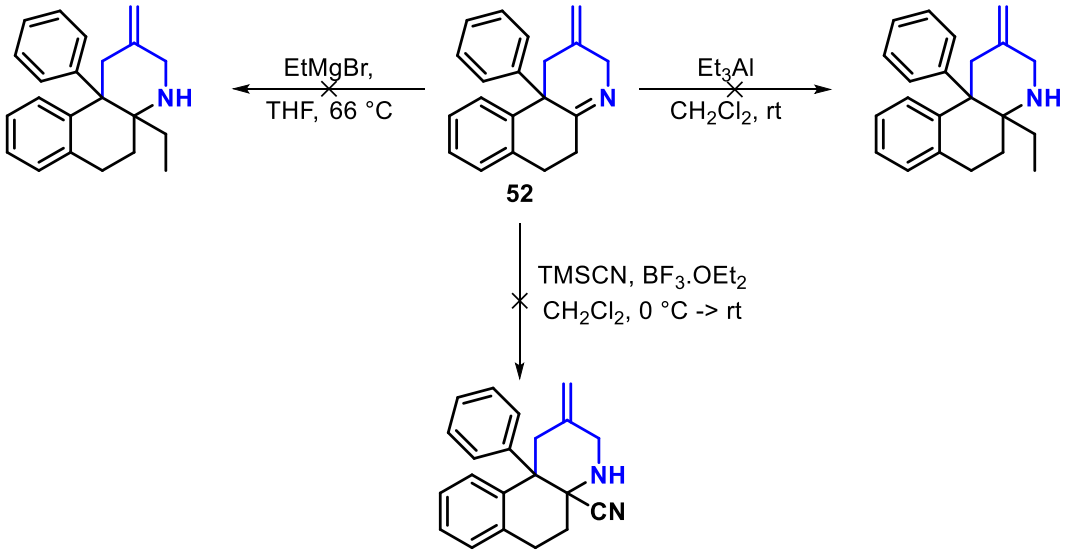

Scheme 47 *- Attempted derivatisations with organometallic species*

The Hosomi-Sakurai reaction using allyltrimethylsilane and $TiCl_4$ as a strong Lewis acid, was also performed in an attempt to form the highly functionalised product **53** (Table 6, entries 1 and 2). Unfortunately, the cyclic imine was found to be unreactive under these conditions. The use of potassium allyltrifluoroborate gave a similar outcome. However, the reaction of compound **52** with allyldiethylaluminium in CH_2Cl_2 at room temperature provided the desired homoallylic amine product **53** in a moderate yield and as a single diastereomer (Table 6, entry 4), although the relative stereochemistry could not be assigned from the spectroscopic data. Heating the

reaction mixture to reflux or using triallylaluminium as the allyl source did not have any significant effect on the reaction yield (entries 5 and 6).

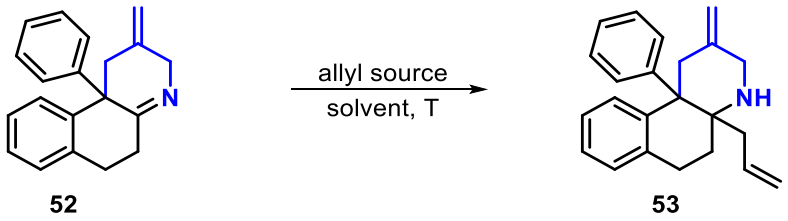

52 **53**

Entry	Allyl source	Lewis acid	Solvent	T (°C)	Yield (%)[a]	d.r.
1	Allyl-TMS	$TiCl_4$	CH_2Cl_2	rt	0	/
2	Allyl-TMS	$TiCl_4$	DCE	reflux	0	/
3	Allyl-BF_3K	-	THF	rt	0	/
4	Allyl$Al(Et)_2$	-	CH_2Cl_2	rt	57	98:2
5	Allyl$Al(Et)_2$	-	CH_2Cl_2	reflux	56	98:2
6	$(Allyl)_3Al$	-	CH_2Cl_2	rt	51	98:2

***Table 6** - Allylation of cyclic imine **52**. [a] Yield of isolated product*

2.3. Conclusions

A readily available cyclic carbamate **17** was used in the presence of a palladium catalyst to form a palladium-stabilised zwitterion, which reacts with a range of 1-substituted-2-indanone and 1-substituted-2-tetralone substrates to provide the corresponding allylated substrates. 1-Aryl-2-indanone and 1-ester-2-indanone substrates successfully underwent the allylation reaction at room temperature providing the desired products in high yields. However, 1-methyl-2-indanone **33** raised a selectivity issue and led to a mixture of regioisomers. The allylated

compounds were then converted into 6-5-6 tricyclic iminium intermediates through an acid-mediated deprotection and condensation sequence.

Further functionalisation of these nitrogen heterocycles was achieved *via* visible-light photoredox reduction of the imine and oxidative cleavage of the alkene. The simple reduction reaction using hydride sources proved a challenge and led to complex mixtures. This has been attributed to the formation of an unstable strained *trans*-5,6 ring system, which is imposed by attack of the hydride from the opposite face to the aryl group.

Oxidative cleavage of the alkene employing $RuCl_3$ and $NaIO_4$ allowed the formation of the corresponding ketone, which closely resembles an intermediate converted into haouamine A by Fürstner *et al*.

Imine derivatisation of tetralone-based product **52** with allyldiethylaluminium allowed the formation of a highly functionalised homoallylic amine product in good yield and as a single diastereomer.

The asymmetric Pd-catalysed allylation was investigated and a range of chiral phosphoramidite and phosphine ligands were examined. However, despite extensive efforts only moderate levels of enantioselectivity were obtained. Unfortunately, the development of an asymmetric variant of the Pd-catalysed allylation of 1-substituted-2-indanone and 1-substituted-2-tetralone substrates remains a key challenge.

3. Pd-catalysed Synthesis of Functionalised Fluorinated Piperidines

3.1. Introduction

In recent decades, the scientific community has shown growing interest in organofluorine compounds which has arisen from their useful properties in agrochemicals, pharmaceuticals, molecular imaging and materials science.[74-79] In particular, the incorporation of a fluorine atom or a fluorinated moiety into a biologically active molecule can have a significant impact on its pharmacokinetic and physicochemical properties, such as an improvement in metabolic stability, absorption and binding affinity.[80, 81]

As described in Chapter Two, nitrogen-containing molecules are important structures in medicinal chemistry and the majority of FDA-approved small-molecule drugs contain a nitrogen heterocycle, among which piperidine is the most prevalent motif.[56] It was demonstrated that in addition to the increased metabolic stability, incorporating a fluorine atom into the piperidine ring of bioactive compounds reduces the basicity of the amine, and thereby can lead to an improvement of the bioavailability. For instance, fluorination at the C3-position of the piperidine has been an effective strategy to enhance the pharmacological properties of a series of drugs that exhibit inhibition towards SYK,[82] CGRP [83] and MET kinase [84] (Figure 14).

Furthermore, 3-fluoropiperidine-based structures were also investigated as radiotracers for PET imaging.[85, 86]

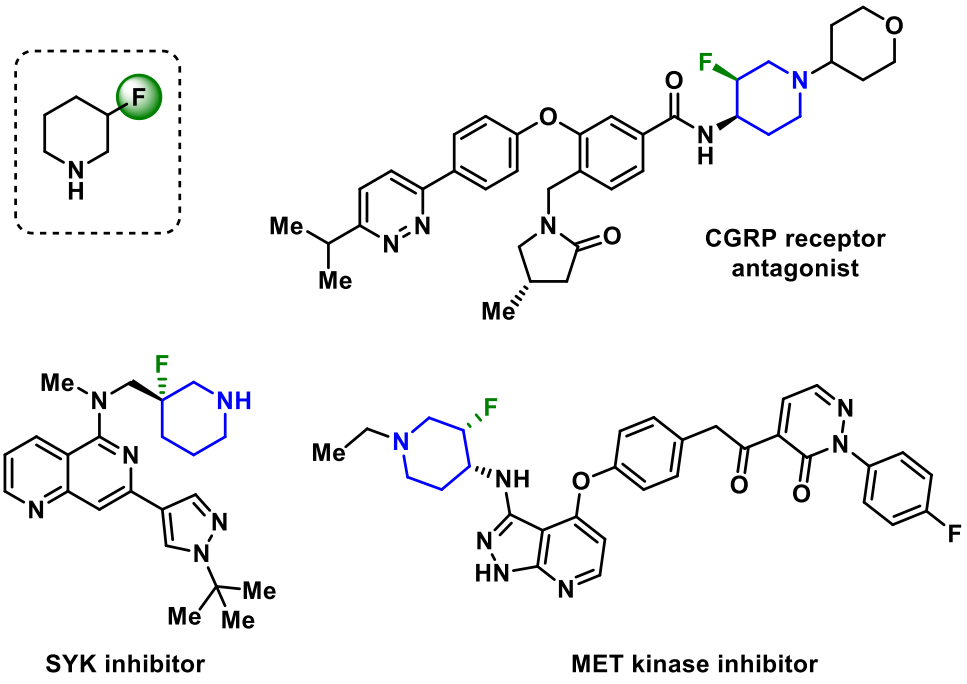

Figure 14 *- Bioactive molecules containing a 3-fluoropiperidine motif*

Despite the relevance of 3-fluoropiperidine structures, only a few synthetic approaches towards this class of fluorinated compounds are available in the literature. The electrophilic fluorination of piperidone has been reported, however this approach suffers from a lack of regioselectivity when non-symmetrical substrates are used (Scheme 48).[87-89]

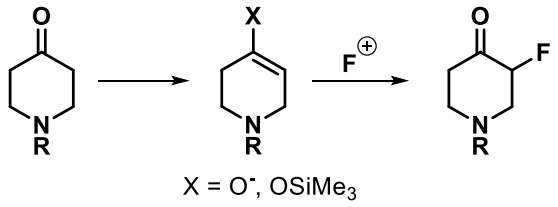

Scheme 48 *- Electrophilic fluorination of piperidone*

The deoxofluorination of 3-hydroxypiperidine derivatives has also been documented, however this process requires pre-functionalised substrates and exhibits low atom economy (Scheme 49).[90, 91]

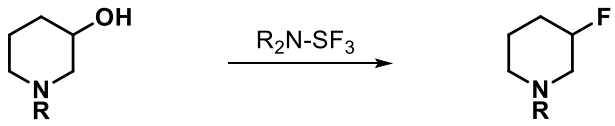

Scheme 49 *- Deoxofluorination of 3-hydroxypiperidine*

Another common synthetic route relies on the intramolecular aminofluorination of alkenes by employing hypervalent iodine reagents with or without the use of palladium-catalysis (Scheme 50).[92-95] The drawback of this method lies in the use of stoichiometric amounts of toxic or expensive reagents.

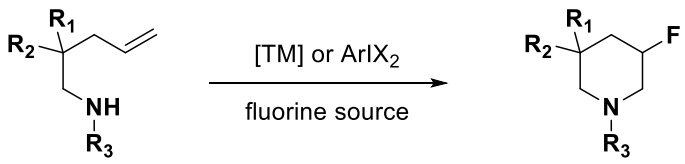

Scheme 50 *- Intramolecular aminofluorination of alkenes*

Recently, Glorius and co-workers have reported the one-pot dearomatisation-hydrogenation of fluoropyridines thus enabling the diastereoselective formation of a range of 3-fluoropiperidine compounds (Scheme 51),[96] however the required high pressure of hydrogen decreases operational simplicity.

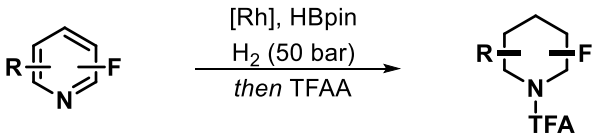

Scheme 51 *- Hydrogenation of fluoropyridines*

Based on previous results described in Chapter Two, it was envisioned that the palladium-catalysed annulation methodology would enable the formation of 3-fluoropiperidine products through allylation of α-fluoro-β-ketoester substrates followed by a chemoselective cyclisation - imine reduction sequence (Scheme 52).

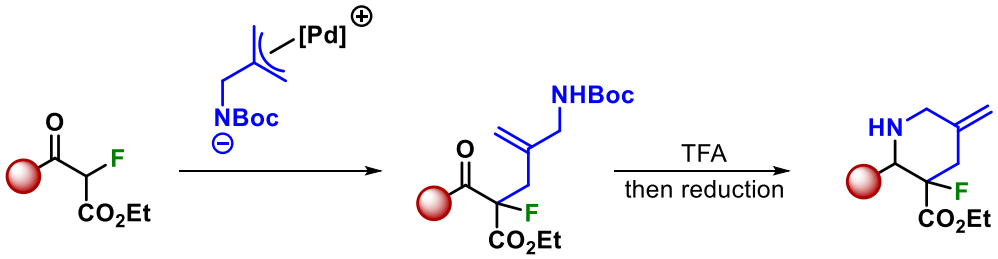

Scheme 52 *- Pd-catalysed synthesis of 3-fluoropiperidines*

Therefore, the applicability of this process to a series of readily available α-fluoro-β-ketoesters was examined. The substrate scope in this chapter was explored by other members of the Harrity group.

A number of α-fluoro-β-ketoesters were subjected to the palladium-catalysed allylation conditions with cyclic carbamate **17**. Exposure of the corresponding allylated compounds to trifluoroacetic acid allowed the deprotection of the amine followed by chemoselective cyclisation to give the desired fluorinated *N*-heterocycles (Scheme 53).

Aryl ketoesters bearing electron-donating or electron-withdrawing moieties at the *para*-position on the phenyl ring gave high yields (**55** - **59**). Substitution at the *ortho*-position with a methyl (**60**) was also well tolerated. Naphthyl and thiophenyl containing substrates (**61** - **62**) were also converted into the corresponding cyclic imines in excellent yields. In addition to α-fluoro-β-ketoesters, various fluorinated substrates such as α-fluoro-β-ketonitrile (**63**), α-fluoro-β-ketosulfone (**64**) and α-fluoro-β-ketoamide (**65**) underwent successful allylation and condensation reactions. However, the reaction with α-fluoropropiophenone failed to provide the desired product and unreacted starting materials were recovered in this case.

Furthermore, alkyl substituted α-fluoro-β-ketoesters were found to undergo regioselective allylation at the most acidic position (**66** - **71**) in agreement with the previous results described in Chapter Two. Hindered alkyl α-fluoro-β-ketoesters were tolerated and converted into the corresponding cyclic imines in excellent yields. A proline-based substrate was also examined and provided the desired product (**72**) in good yield and with moderate diastereoselectivity.

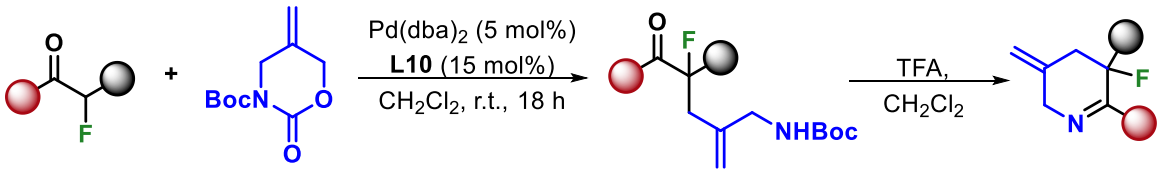

1.5 eq. **17** 1.0 eq.

■ **a) 2-Aryl 3-fluoropiperidines**

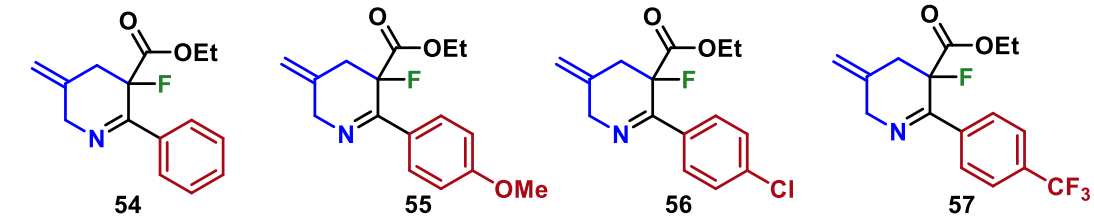

54 82% | **55** 89% | **56** 84% | **57** 80%

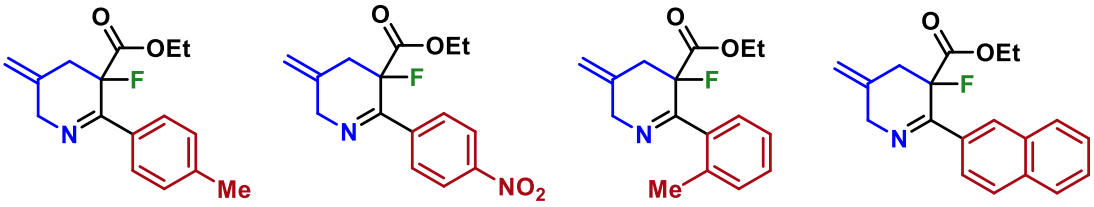

58 71% | **59** 74% | **60** 84% | **61** 98%

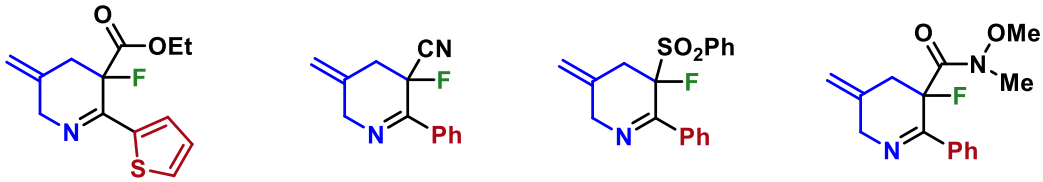

62 78% | **63** 82% | **64** 81% | **65** 87%

■ **b) 2-Alkyl 3-fluoropiperidines**

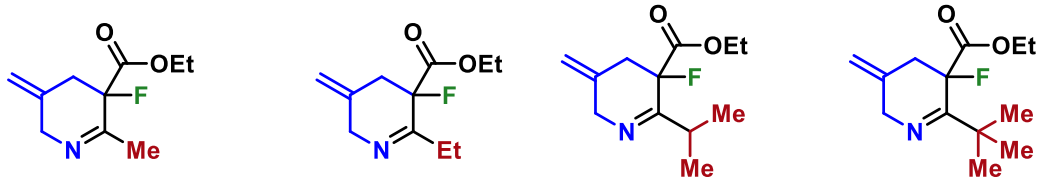

66 85% | **67** 82% | **68** 86% | **69** 76%

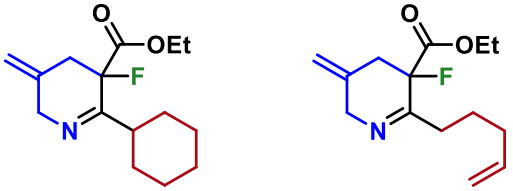

70 80% | **71** 90% | **72** 60%, 4.2:1 dr

Scheme 53 - *Synthesis of fluorinated N-heterocycles*

After the successful synthesis of a library of fluorinated and sp^3-rich *N*-heterocycles that contain orthogonal functionality, attention was focussed on showcasing the utility of these new compounds (Scheme 54).

Compound **54** was subjected to a number of selected transformations involving the ester, imine and alkene moieties. The use of $NaBH(OAc)_3$ in acetic acid allowed the chemoselective reduction of the imine to give the saturated fluoropiperidine **73** in high yield and diastereoselectivity. A subsequent Boc-protection provided compound **74** in 88% yield and its X-ray analysis allowed the determination of the relative stereochemistry of the major diastereomer (Scheme 53). Furthermore, the ester group was reduced chemoselectively with $LiAlH_4$ thus providing the alcohol derivative **75** in 50% yield. A hydrolytic decarboxylation occurred when compound **54** was heated at 100 °C in aqueous HCl. The decarboxylated compound **76** was found to undergo further transformation with $NaBH_4$ to give the reduced heterocycle **77** in good yield and as a single diastereomer. In the presence of Hoveyda-Grubbs second-generation catalyst, the exocyclic alkene was orthogonally functionalised through olefin cross-metathesis to provide compound **78** as a mixture of isomers. Furthermore, treating compound **54** with dimethyldioxirane unexpectedly provided the oxaziridine product **79** in good yield rather than the epoxide. The relative stereochemistry for compound **79** is yet to be determined.

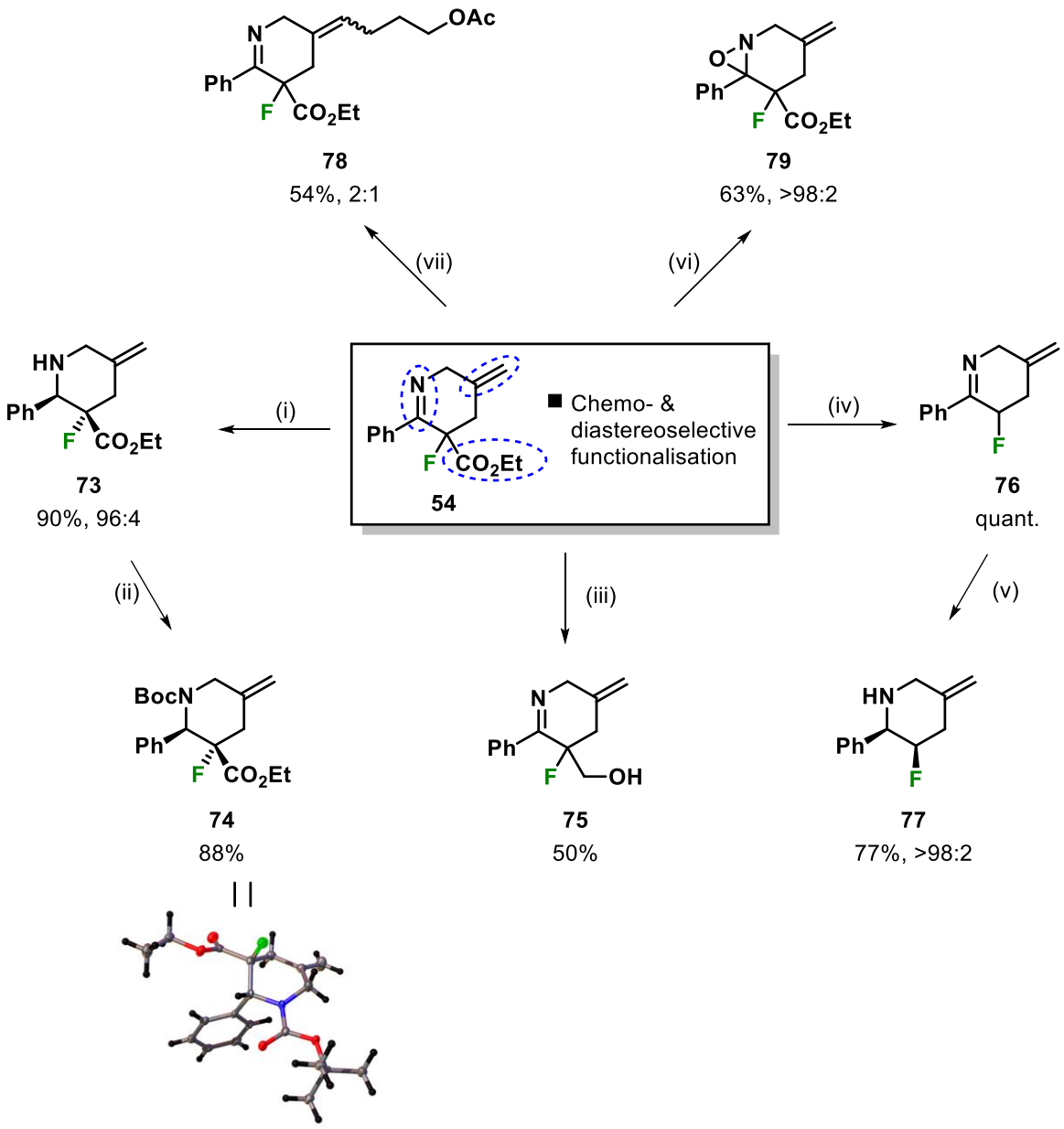

Reagents and conditions: (i) $NaBH(OAc)_3$ (1.5 eq.), AcOH, rt, 18 h; (ii) Boc_2O (2.0 eq.), Et_3N (2.0 eq.), THF, rt, 18 h; (iii) $LiAlH_4$ (2.0 eq.), THF, rt, 3.5 h; (iv) aq. HCl (15.0 eq.), 100 °C, 1 h; (v) $NaBH_4$ (2.0 eq.), MeOH, 0 °C to rt, 18 h; (vi) Oxone® (25.0 eq.), $NaHCO_3$ (125.0 eq.), acetone/H_2O, rt, 24 h; (vii) Hoveyda-Grubbs 2nd Gen. (5 mol%), pent-4-en-1-yl acetate (3.0 eq.), DCM, rt 18 h then reflux, 3 h.

Scheme 54 *- Chemoselective transformation of compound* ***54***

Having established the utility of this robust methodology, attention turned to the development of an asymmetric variant of this chemistry so that enantioenriched 3-fluoropiperidine products could be made available.

3.2. Results and Discussion

3.2.1. Asymmetric Synthesis of 3-Fluoropiperidines

For the following asymmetric investigations, compound **80** was used as a model substrate. It was synthesised in a two-step sequence from acetophenone and diethyl carbonate followed by fluorination with Selectfluor™.

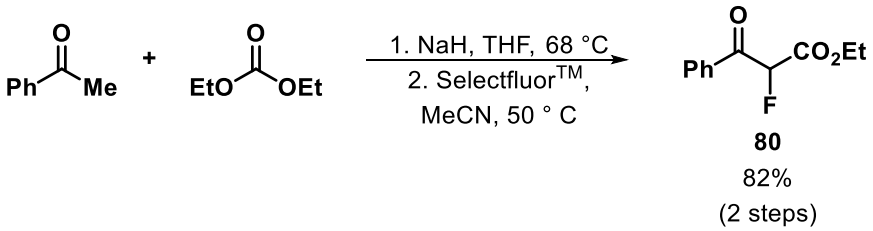

Scheme 55 - *Synthesis of substrate* ***80***

Selected chiral phosphoramidite ligands (Figure 15) were screened under the standard allylation conditions (Table 7).

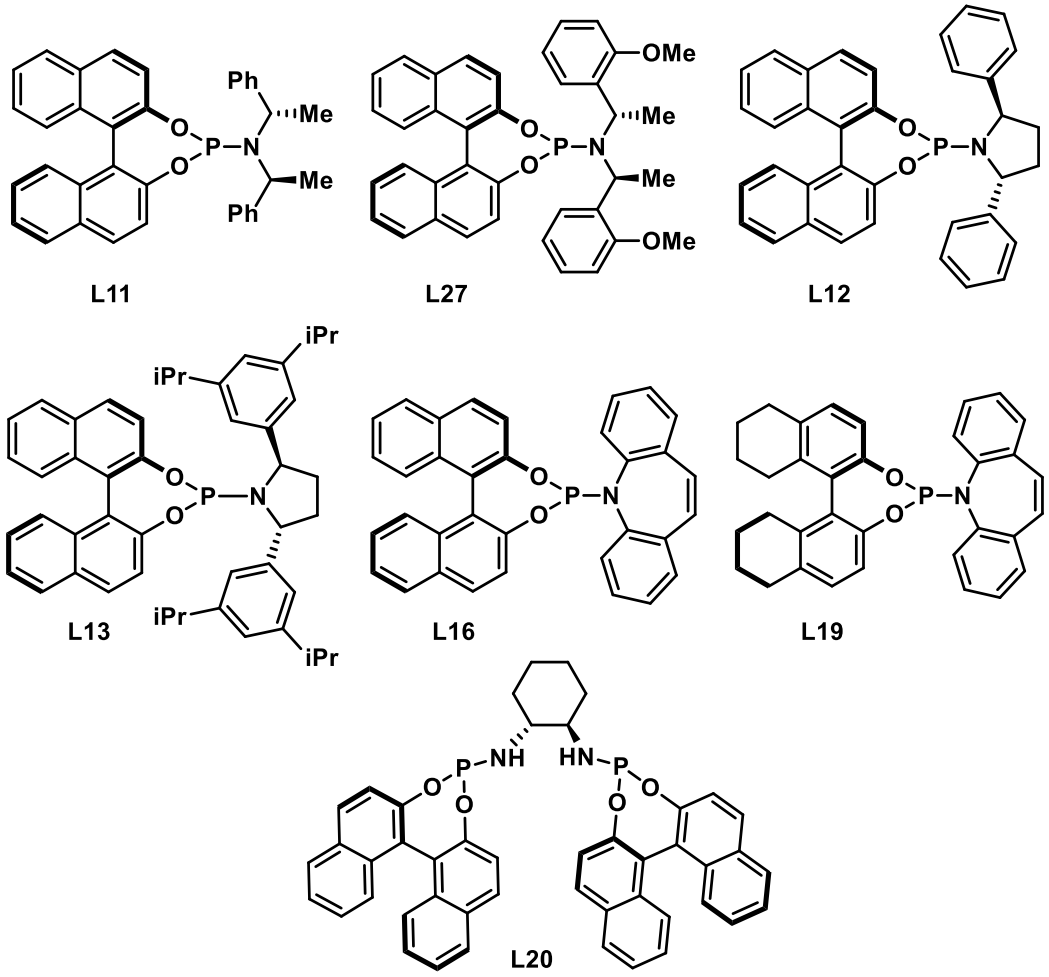

Figure 15 *- Selected phosphoramidite ligands*

Ligands **L11** and **L27** performed well in the palladium-catalysed reaction, however the product was isolated with low enantiomeric excess. Furthermore, the use of sterically demanding ligands **L12** and **L13** did not improve the enantioselectivity and chiral dibenzazepine-based ligands **L16** and **L19** led to similar levels of enantiocontrol. In the presence of the bidentate phosphoramidite ligand **L20**, substrate **80** did not undergo the allylation reaction and starting materials were recovered.

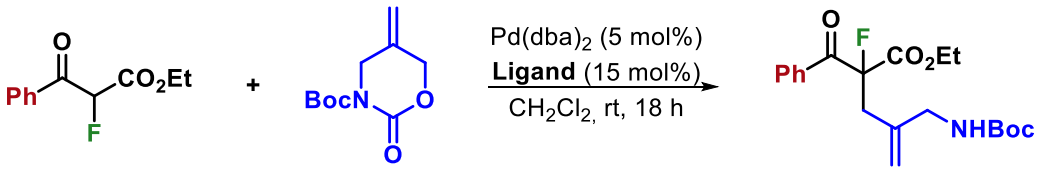

80
1.5 eq.

17
1.0 eq.

81

Entry	Ligand (**L**)	Conv (%)[a]	ee (%)[b]
1	**L11**	100	<5
2	**L27**	100	6
3	**L12**	100	<5
4	**L13**	100	<5
5	**L16**	100	8
6	**L19**	100	<5
7	**L20**	0	-

Table 7 *- Screening of chiral phosphoramidite ligands. [a] % conversion determined by* ^{1}*H NMR spectroscopy. [b] Determined by chiral HPLC*

As described in Chapter Two, preliminary asymmetric investigations have shown that cyclic 1,3-dicarbonyl compounds undergo the palladium-catalysed allylation reaction with high enantioselectivities. Furthermore, several examples from the literature show that acyclic *β*-keto esters lead to reversed or reduced enantiomeric ratios compared to the cyclic analogues.[97-101] Additionally, Goodman *et al.* highlighted the relationship between the enolate stereochemistry of acyclic *β*-keto esters and the alkylation enantioselectivity.[102]

Therefore, it was proposed that the poor selectivities obtained with the fluorinated acyclic substrates could be a result of a competition between *Z* and *E* enolates leading to opposite enantiomers (**Scheme** 56). In order to investigate this

hypothesis, it was decided to synthesize the silyl enol ether derivatives of acyclic *β*-keto esters and examine their reactivity and stereochemistry in the palladium-catalysed allylation.

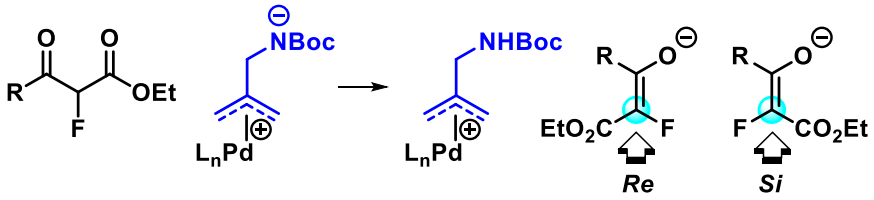

Scheme 56 - *Formation of Z and E enolates*

Accordingly, silyl enol ether **82** was prepared from compound **80**, unfortunately however, this was formed as a 2:1 mixture of *E/Z* isomers (Scheme 57).

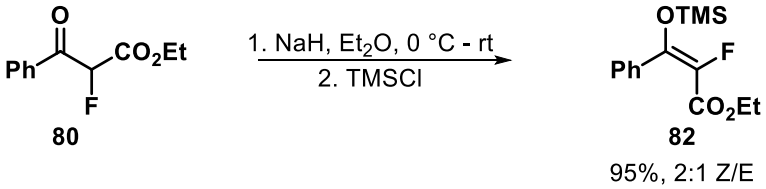

Scheme 57 - *Formation of silyl enol ether **82***

It was proposed that the introduction of a bulkier silyl group would increase the *E/Z* ratio of the silyl enol ether.[103] Compound **83** was thus synthesized in one step as a 5:1 mixture of isomers (Scheme 58), and further purification allowed the isolation of **83** in higher *E/Z* ratios. The stereochemical assignments were made on the basis of carbon-fluorine coupling constants ($^4J_{C\text{-}F}$) in agreement with the relative size of *J* values reported in the literature.[103]

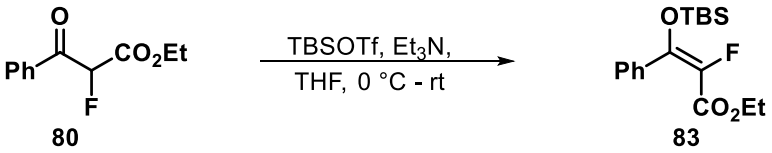

Scheme 58 *- Formation of silyl enol ether* ***83***

Silyl enol ethers **82** and **83** were then subjected to the palladium-catalysed allylation reaction with cyclic carbamate **17** and chiral ligand **L16**. TMS-enol ether **82** was readily converted into compound **81** with similar levels of enantiocontrol to that measured with substrate **80** (Table 7, entry 5). Interestingly however, TBS-enol ether **83** underwent the allylation reaction with higher selectivity. Although, increasing the *E*/*Z* ratio of silyl enol ether **83** did not translate into higher enantioselectivities.

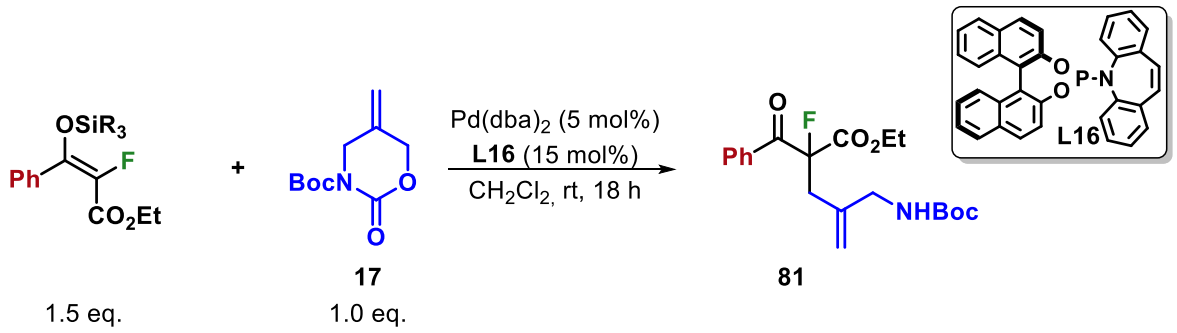

Entry	Silyl enol ether	Z/E ratio	Conv (%)[a]	ee (%)[b]
1	**82**	2:1	100	10
2	**83**	3.6:1	100	38
3	**83**	6.8:1	100	38
4	**83**	11:1	100	36

Table 8 *- Investigation of silyl enol ethers. [a] % conversion determined by* ^{1}H *NMR spectroscopy. [b] Analysed by chiral HPLC*

The data shown in Table 8 suggests that the increase in the enantiomeric excess results from the increasing steric hindrance of the silyl group (TMS to TBS) and is not, as initially hypothesised, related to a higher *E/Z* ratio.

As silyl enol ether **83** was found to give a higher enantiomeric excess than substrate **80** under the same reaction conditions, it was decided to examine its selectivity towards the allylation reaction using different chiral ligands (Figure 16).

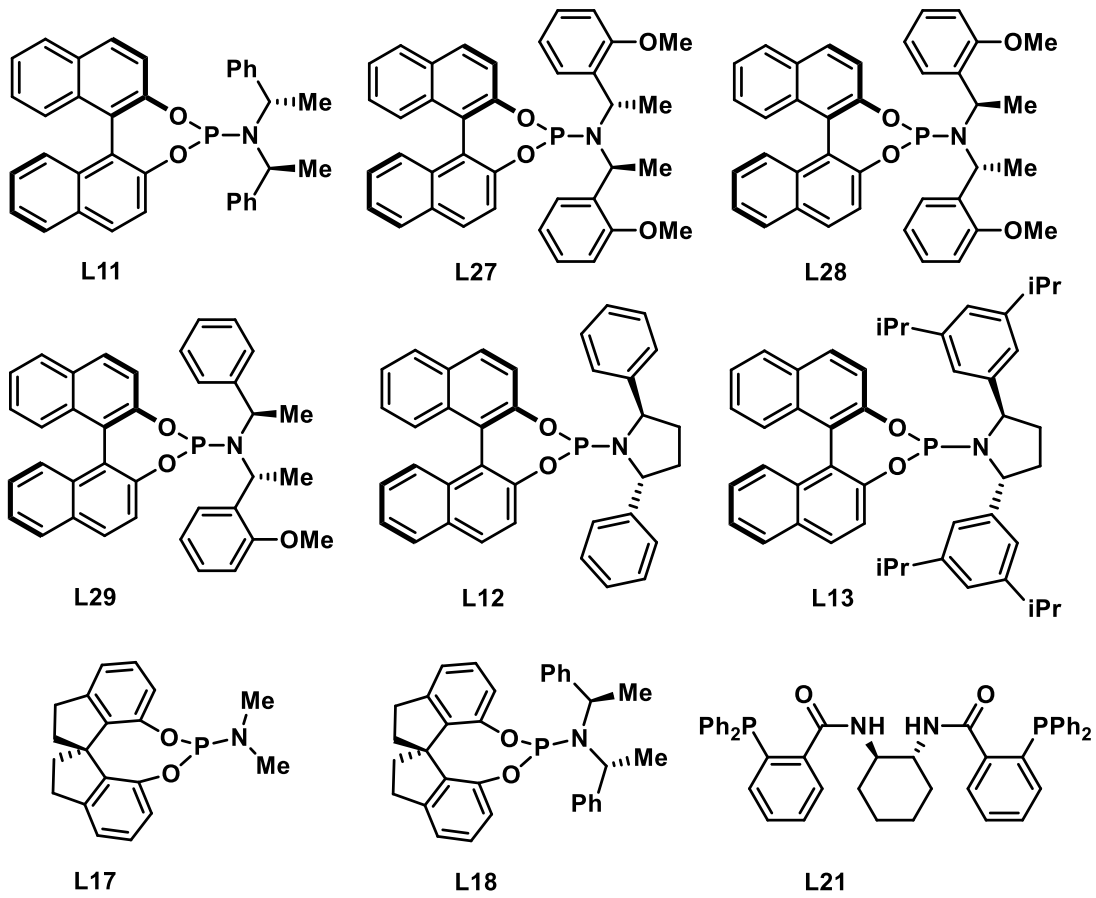

Figure 16 *- List of screened ligands with* ***83***

The chiral ligands shown in Figure 16 were screened with silyl enol ether **83** under the standard palladium-catalysed reaction conditions. All the above ligands performed well in the allylation reaction, with the exception of **L18,** where starting materials were recovered (Table 9). Regarding the enantioselectivities, unfortunately none gave a higher enantiomeric ratio than the chiral phosphoramidite ligand **L16**.

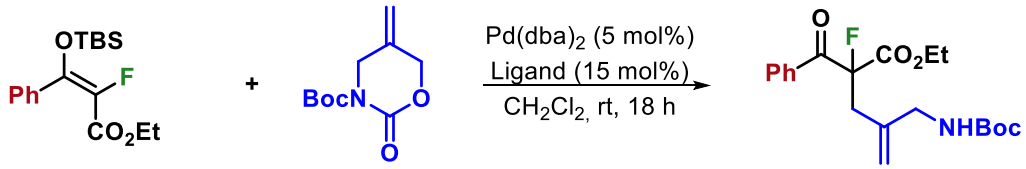

83, 3:1 Z/E
1.5 eq.

17
1.0 eq.

81

Entry	Ligand (**L**)	Conv (%)[a]	ee (%)[b]
1	**L16**	100	38
2	**L11**	100	18
3	**L27**	100	26
4	**L28**	100	10
5	**L29**	100	20
6	**L12**	100	<5
7	**L13**	100	<5
8	**L17**	100	6
9	**L18**	0	-
10	**L21**	100	23

Table 9 *- Screening with silyl enol ether* ***83****. [a] % conversion determined by* ^{1}*H NMR spectroscopy. [b] Analysed by chiral HPLC*

Given that the conventional enantioselective approach using chiral ligands failed to provide the desired products with high enantiomeric ratios, it was decided to explore alternative strategies. The following part of this chapter will focus on various approaches that were proposed and investigated to overcome the poor enantiodiscrimination in this palladium-catalysed allylation reaction.

The initial approach that was proposed involves the formation of a chiral enolate *via* coordination to a chiral Lewis acid complex, which would then allow asymmetric induction in the allylation reaction (Scheme 59).

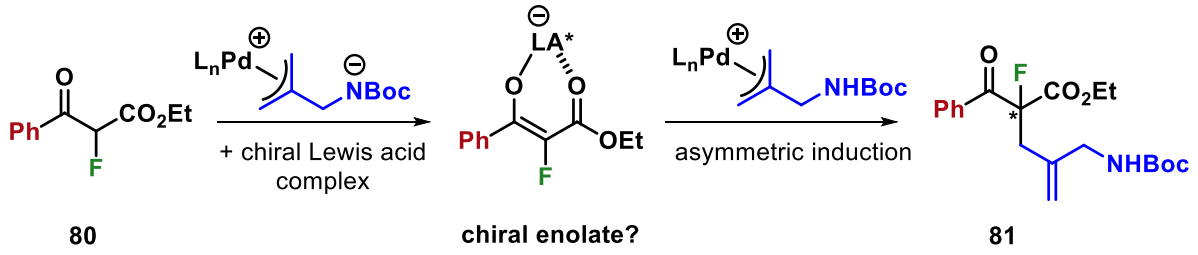

Scheme 59 *- Asymmetric induction by chiral Lewis acids*

Based on literature precedent,[104] a range of metal-based bis(oxazoline) complexes were subjected to the palladium-catalysed reaction conditions (Table 10).

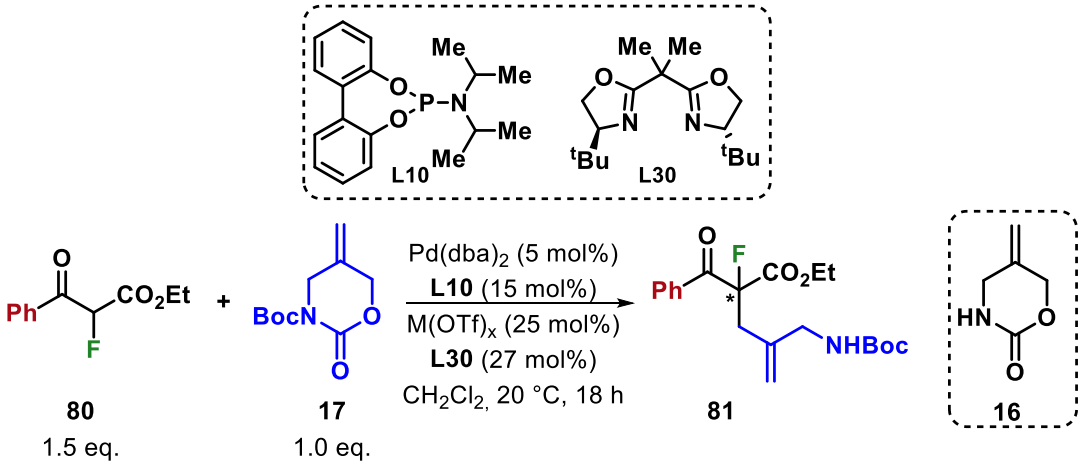

Entry	$M(OTf)_x$	Yield (%)	Outcome
1	$Cu(OTf)_2$	0	**80** + **16**
2	$Al(OTf)_3$	0	**80** + **16**
3	$Zn(OTf)_2$	0	**80** + **16**
4	$Sc(OTf)_3$	0	**80** + **16**

Table 10 *- Attempted catalytic enantioselective allylation*

However, in all cases, ^{1}H NMR analysis of the crude mixtures showed the presence of starting material **80** alongside the unprotected cyclic carbamate **16**. Furthermore, a titanium complex derived from (*R*)-BINOL was also examined; the reaction gave the desired product although as a racemic mixture.

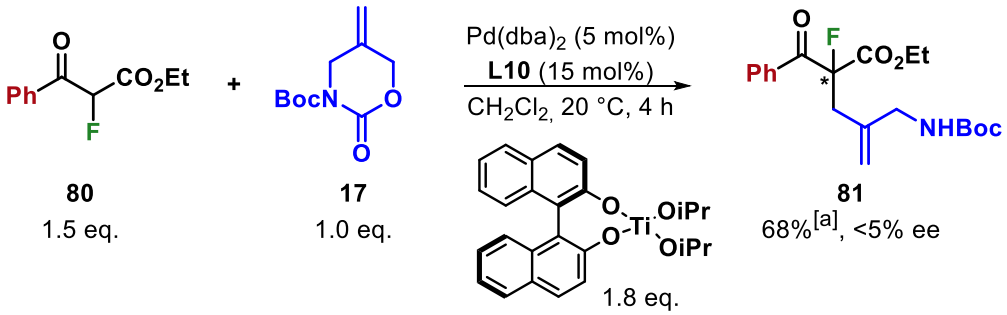

Scheme 60 *- Attempted enantioselective allylation with Ti-BINOL complex. [a] Isolated product contains traces of (R)-BINOL*

As chiral Lewis acids failed to deliver an effective asymmetric allylation reaction, attention turned to the employment of a chiral Brønsted acid promoter. In this case it was planned to use a preformed enamine, in a similar fashion to the asymmetric *α*-allylation of aldehydes reported by List and co-workers (Scheme 61).[105]

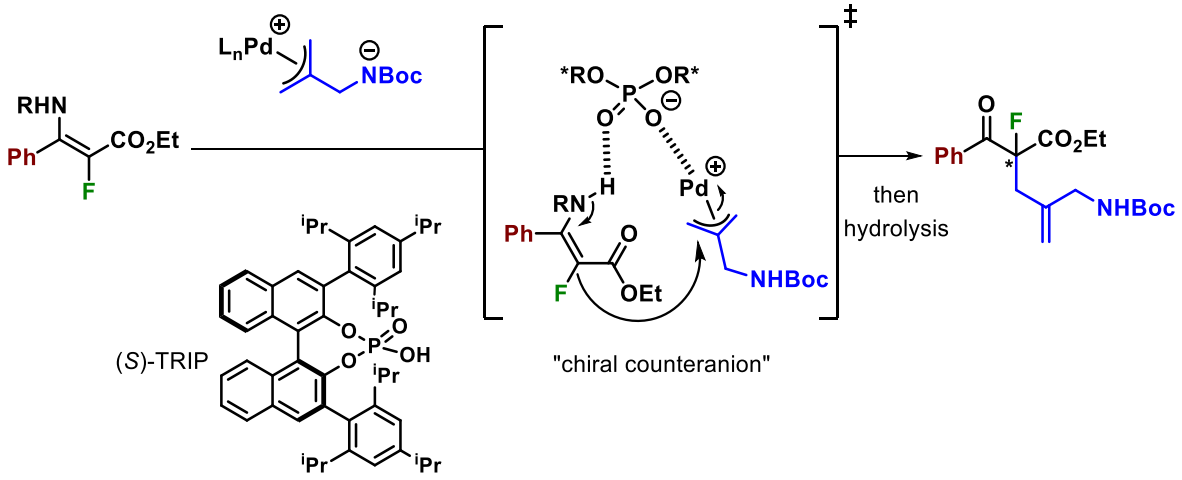

Scheme 61 *- Asymmetric induction by a chiral Brønsted acid*

Chiral phosphoric acid **86** (called (*S*)-TRIP) was synthesized in a six-step sequence from (*S*)-BINOL,[106, 107] and enamine **87** was formed by condensation of compound **80** with aniline in 64% yield (Scheme 62).[108]

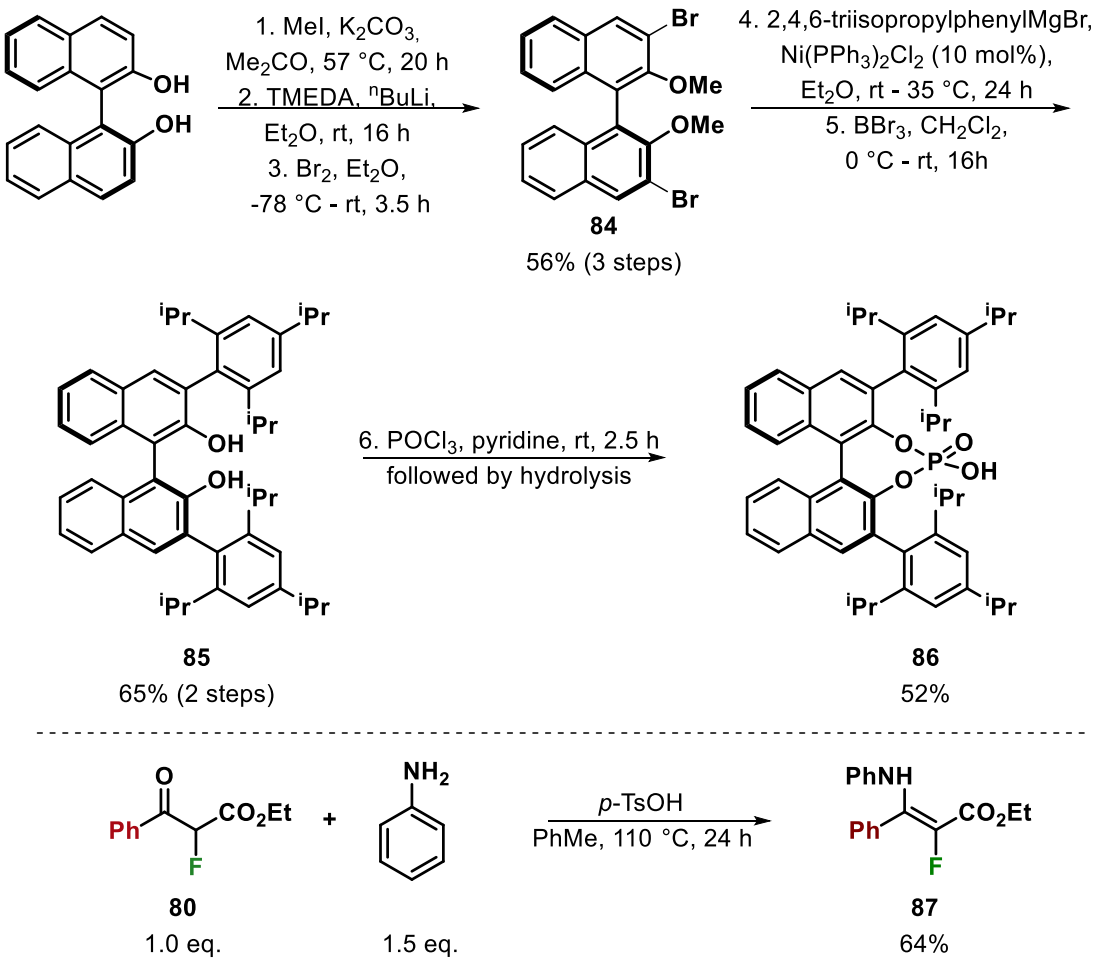

Scheme 62 *- Formation of enamine* ***87*** *and Brønsted acid* ***86***

First, the reactivity of enamine **87** was examined under the palladium-catalysed allylation reaction conditions without chiral Brønsted acid **86**. The desired allylated product was obtained in 85% yield. Enamine **87** was then subjected to the same reaction conditions in the presence of (*S*)-TRIP, however, no reaction occurred and starting materials were recovered (Scheme 63). The reason for this difference in reactivity is still unclear.

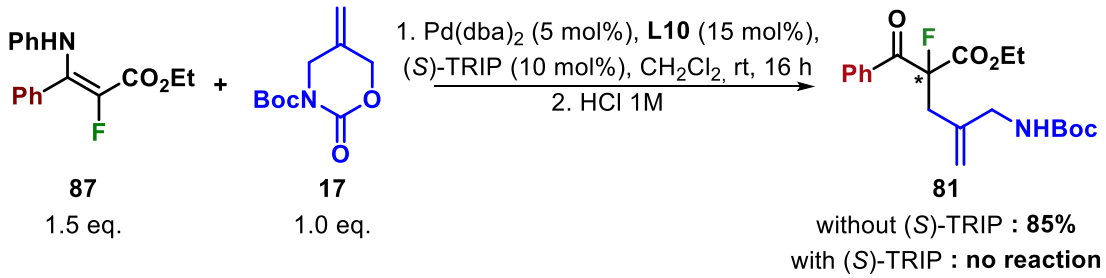

Scheme 63 *- Attempted asymmetric induction*

As previous strategies involving the use of chiral Lewis acids or Brønsted acid **86** failed to provide any enantioselectivities, an asymmetric allylation reaction mediated by a chiral phase-transfer catalyst was envisaged (Figure 17). Many examples of enantioselective alkylation reactions using cinchona-alkaloid-based phase-transfer catalysts (PTCs) are reported.[109-112] Therefore, it was proposed to examine PTC **88** in the palladium-catalysed reaction.

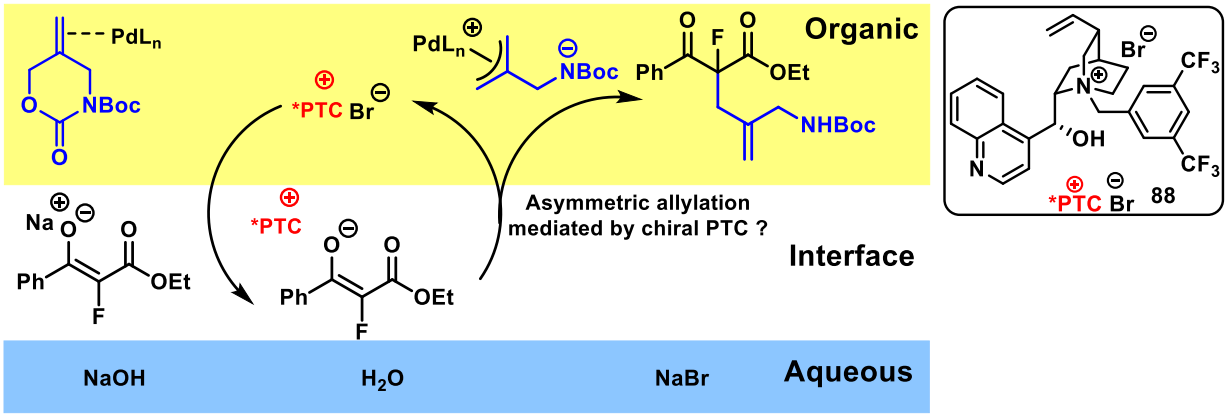

Figure 17 *- Asymmetric phase-transfer catalysis*

Compound **80** was first reacted with a base in the presence of the chiral phase-transfer catalyst, and then added to a solution containing the palladium catalyst and

cyclic carbamate **17**. However, although the desired product was obtained, these reactions resulted in no enantioselectivity.

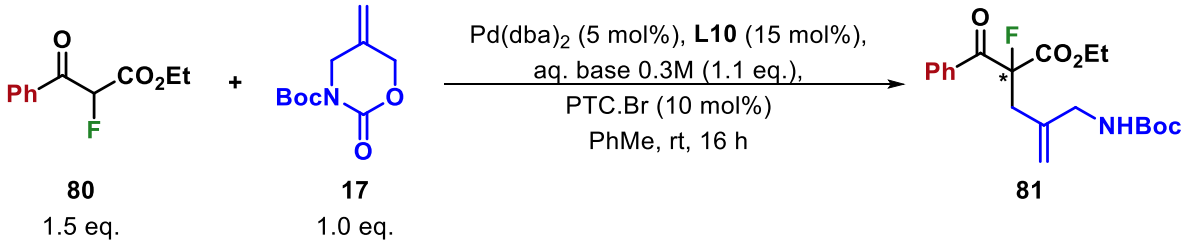

80 1.5 eq. + **17** 1.0 eq. → **81**

Entry	Base	Conversion (%)[a]	ee (%)[b]
1	-	100	0
2	NaOH	100	0
3	Na_3PO_4	81	0
4	Na_2HPO_4	53	0
5	KH_2PO_4	43	0

***Table 11** - Attempted asymmetric allylation with PTC.Br **88**. [a] % conversion determined by ^{1}H NMR spectroscopy. [b] Analysed by chiral HPLC*

In the pursuit of an enantioselective allylation, the use of chiral hydrogen-bonding catalysts was proposed. Thiourea catalysts derived from quinine alkaloids are well documented in the literature for the reaction of enolate nucleophiles (including α-fluoro-β-ketoesters) with a range of electrophiles.[113-120] These hydrogen-bonding catalysts offer multiple sites for potential substrate interactions and are readily available as well (Figure 18).

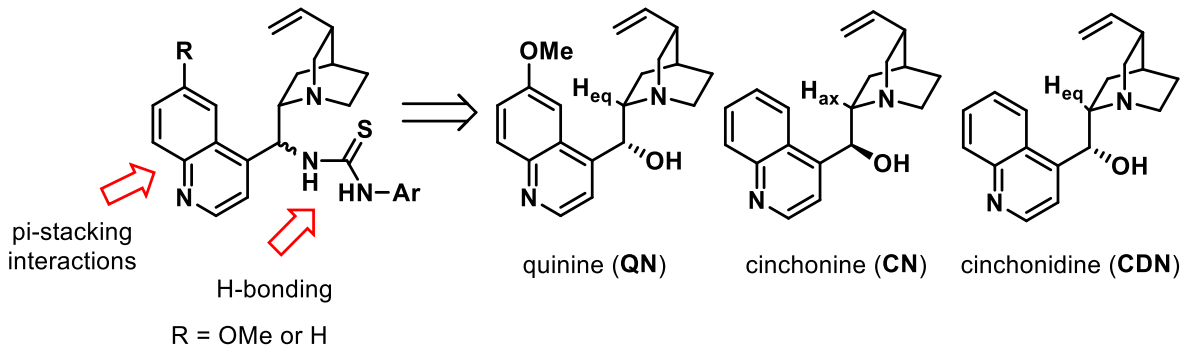

Figure 18 *- Chiral H-bonding thiourea catalysts*

It was proposed that the *in-situ* formed enolate would interact with the chiral thiourea catalyst *via* hydrogen-bonding, and thereby form a chiral nucleophile (Figure 19).

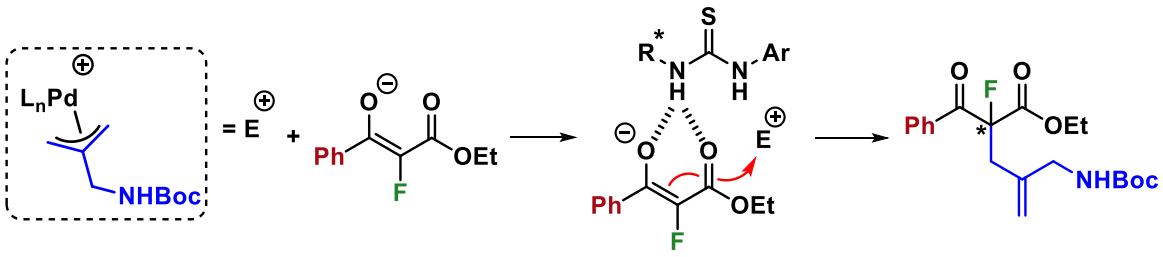

Figure 19 *- Asymmetric induction by the chiral thiourea*

Chiral hydrogen-bonding thioureas **92** - **100** were readily synthesised in a three-step sequence from the corresponding commercial hydroxy-alkaloid (Scheme 64). The synthetic sequence involves a Mitsunobu reaction to convert the alcohol to an azide, followed by selective reduction to the amine under Staudinger reaction conditions, and then nucleophilic attack to the isothiocyanate compound to give the desired thioureas.

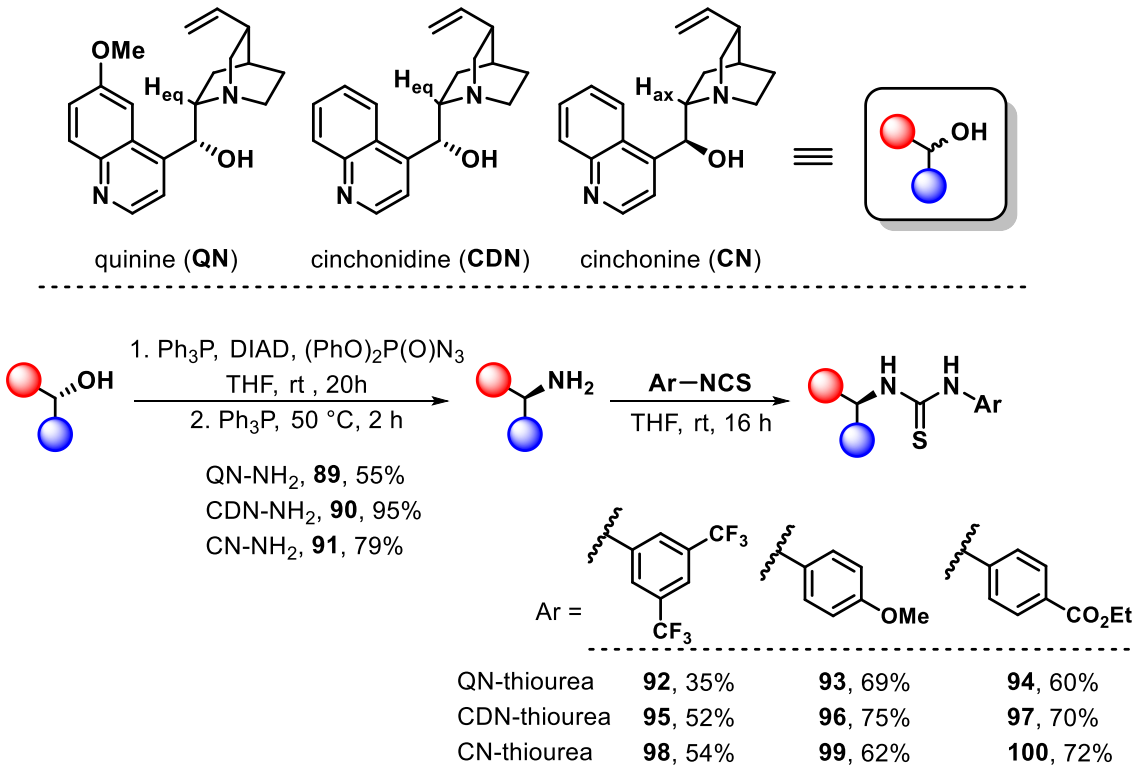

Scheme 64 *- Synthesis of various chiral H-bonding thioureas*

With a range of chiral hydrogen-bonding thioureas in hand, their utility in the palladium-catalysed allylation was investigated. However, despite the formation of the allylated product, no enantiocontrol was achieved. It is not clear whether the lack of selectivity arises from a lack of interaction between the chiral thioureas and the enolate, or the necessity for an interaction between the enolate and the π-allyl complex in the transition state, which prevents the hydrogen-bonding with the chiral thiourea catalyst.

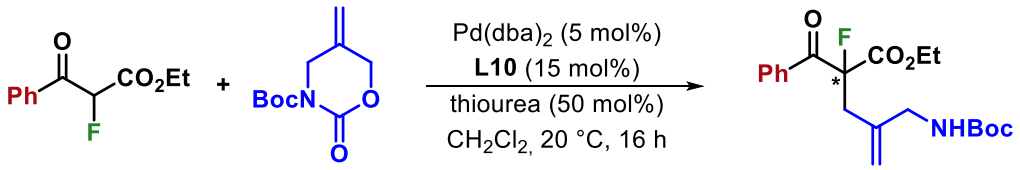

80
1.5 eq.

17
1.0 eq.

81

Entry	Thiourea	Conversion (%)[a]	ee (%)[b]
1	**92**	100	0
2	**93**	100	0
3	**94**	100	0
4	**95**	100	0
5	**96**	100	0
6	**97**	100	0
7	**98**	100	0
8	**99**	100	0
9	**100**	100	0

Table 12 *- Attempted asymmetric induction with chiral H-bonding thioureas. [a] % conversion determined by* ^{1}*H NMR spectroscopy. [b] Analysed by chiral HPLC*

In an effort to overcome the lack of enantiocontrol within the palladium-catalysed allylation reaction, a dynamic kinetic resolution of the condensed and decarboxylated product **76** was investigated. It was hypothesised that in the presence of a chiral Brønsted acid catalyst, compound **76** would rapidly interconvert between both enantiomers *via* an iminium/enamine tautomerisation. Therefore, an enantioenriched product could be obtained if reduction of one of the two iminium diastereomeric salts is faster than the other (Figure 20).[121]

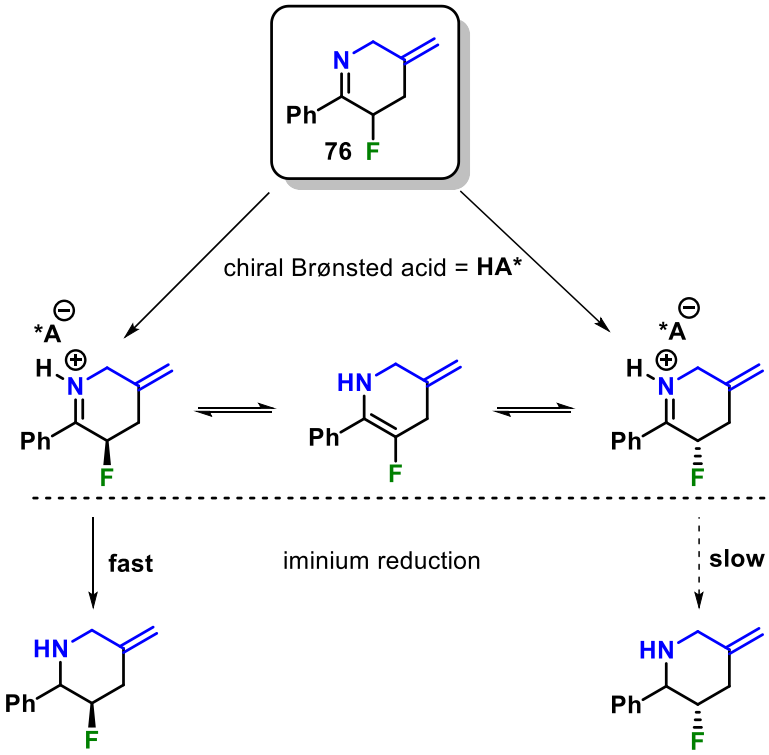

Figure 20 *- Dynamic kinetic resolution approach*

To investigate the dynamic kinetic resolution approach, compound **76** was first reacted with (*R*)-(-)-mandelic acid and L-(+)-tartaric acid. However, NMR analysis showed that the cyclic imine was not protonated (Scheme 65), and therefore a stronger chiral acid was sought.

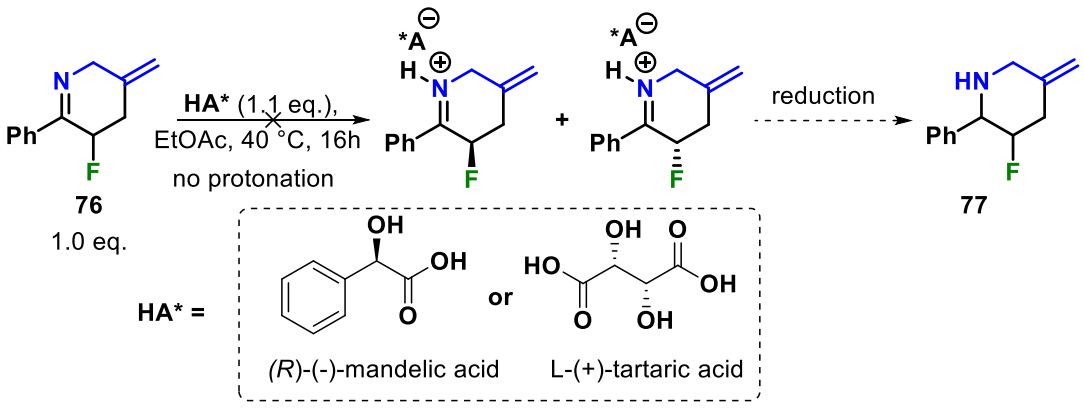

Scheme 65 *- Attempted DKR with chiral carboxylic acids*

The reaction of **76** with (1*S*)-(+)-10-camphorsulfonic acid (CSA) provided a 2:1 mixture of pseudodiastereomeric pairs, which after treatment with sodium triacetoxyborohydride gave piperidine **77** as a racemic mixture of a single diastereomer (Scheme 66). In an attempt to carry out an asymmetric protonation of an aza-enolate derived from **76**, this compound was subjected to LDA prior to addition of the chiral acid. Unfortunately, this led to the formation of pyridine **101** after fluoride elimination.

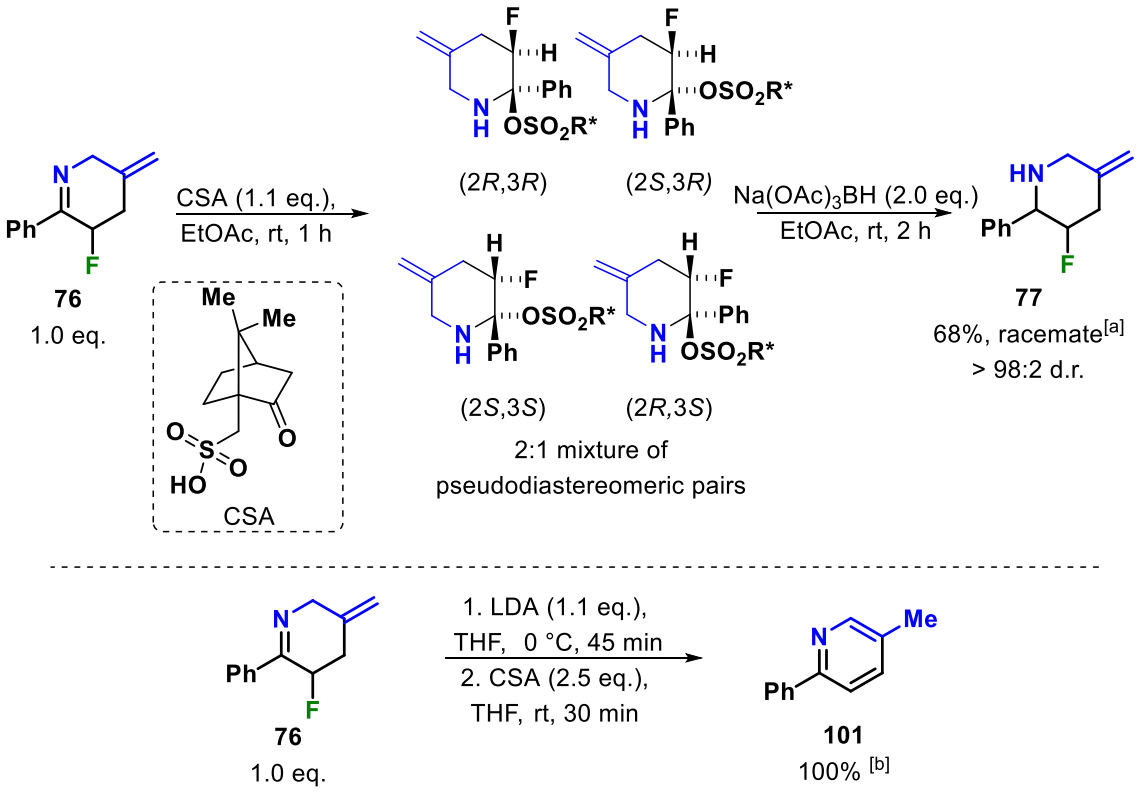

Scheme 66 *- Attempted DKR with CSA. [a] Analysed by chiral HPLC. [b] % conversion determined by* ^{1}*H NMR spectroscopy*

The use of chiral phosphoric acids **86** and **102** provided the corresponding diastereomeric salts in a 1:1 ratio, which after reduction led to a racemic mixture of piperidine **77.**

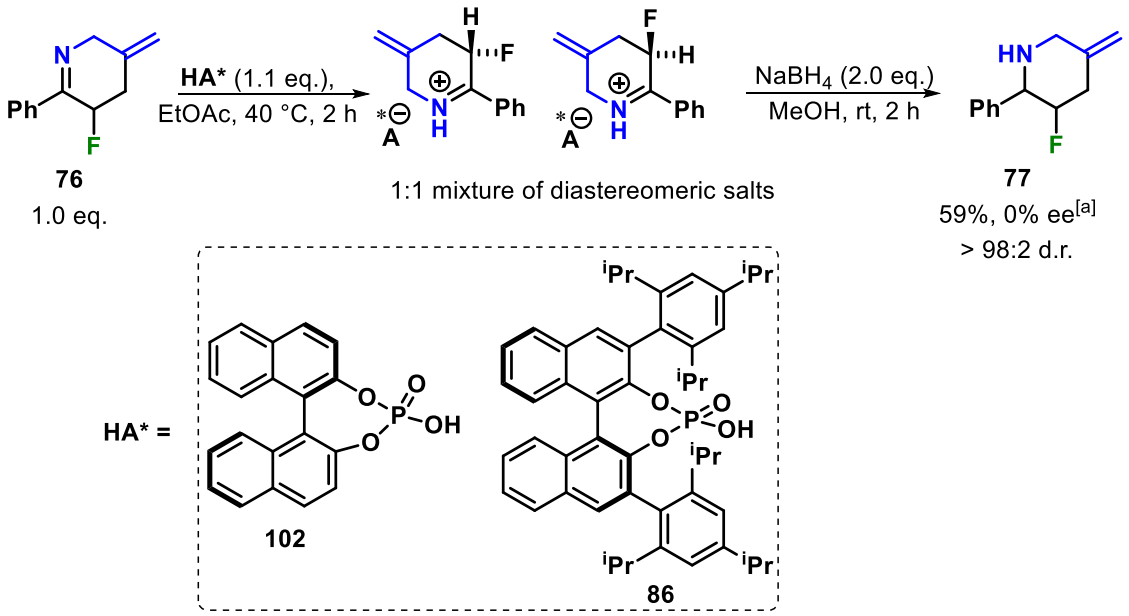

Scheme 67 *- Attempted DKR with chiral phosphoric acids* ***86*** *and* ***102****. [a] Analysed by chiral HPLC*

Furthermore, it was attempted to perform a kinetic resolution through enantioselective reduction (CBS reduction[122] or Noyori's hydrogenation[123, 124]) of the cyclic imine **76**. Therefore, (*S*)-(−)-2-methyl-CBS-oxazaborolidine **103** and RuCl(*p*-cymene)[(*R*,*R*)-Ts-DPEN] **104** were selected as suitable catalysts and investigated in the kinetic resolution approach. The reaction of compound **76** and oxazaborolidine **103** in THF led to a complex mixture of products (Scheme 68).

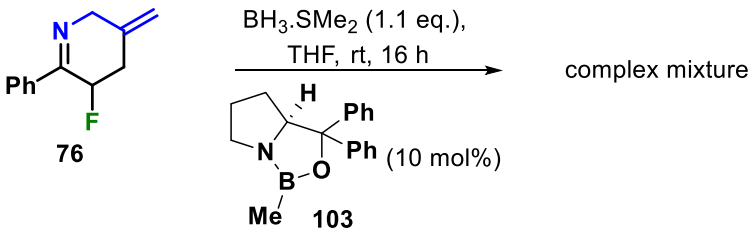

Scheme 68 *- Attempted imine CBS reduction*

Additionally, performing the reaction with Noyori-type ruthenium catalyst **104** did not improve the result, despite several different attempts (Table 13). In most cases, the cyclic imine was isolated alongside the undesired pyridine **101**.

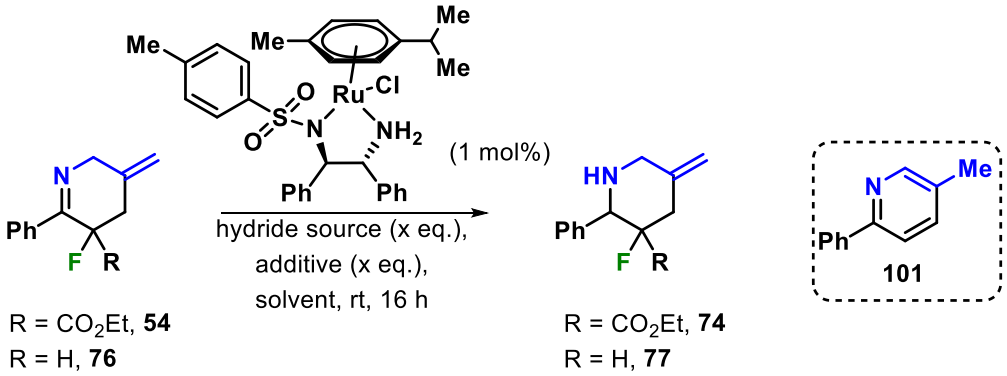

Entry	Substrate	H source (x eq.)	Additive (x eq.)	Solvent	Outcome
1	**76**	HCO_2H (4.7)	Et_3N (11.4)	-	**101** (pyridine)
2	**54**	HCO_2H (6.1)	Et_3N (14.8)	-	**54** + **101**
3	**54**	HCO_2H (6.3)	Et_3N (2.5)	MeCN	**54** + **101**
4	**54**	HCO_2H (6.3)	piperidine (2.5)	MeCN	**54** + **101**
5	**54**	H_2	TFA (1.0)	MeOH	complex mixture[a]

Table 13 *- Attempted asymmetric Noyori hydrogenation. [a] At 40 °C and 15 bar H_2 pressure*

Given the failure of the aforementioned approach and the lack of alternative options, a conventional strategy requiring the use of a chiral auxiliary was envisaged (Scheme 69). It was hypothesised that if compound **106** were to be formed, the menthol derived chiral auxiliary would perhaps induce a highly diastereoselective allylation.

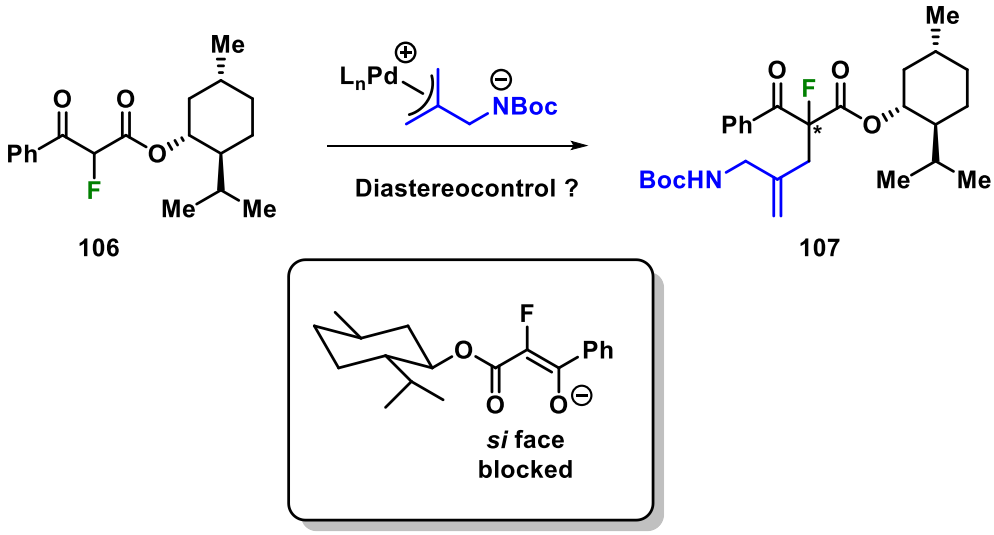

Scheme 69 *- Chiral auxiliary approach*

As ethyl fluoroacetate and L-menthol have the advantage of being readily available and inexpensive, they were chosen as starting materials for the synthesis of compound **106** in a two-step sequence (Scheme 70). First, ethyl fluoroacetate underwent a transesterification reaction with L-menthol to give ester **105** in 34% yield, and a subsequent Claisen condensation with benzoyl chloride provided the desired α-fluoro-β-ketoester **106** in 51% yield.

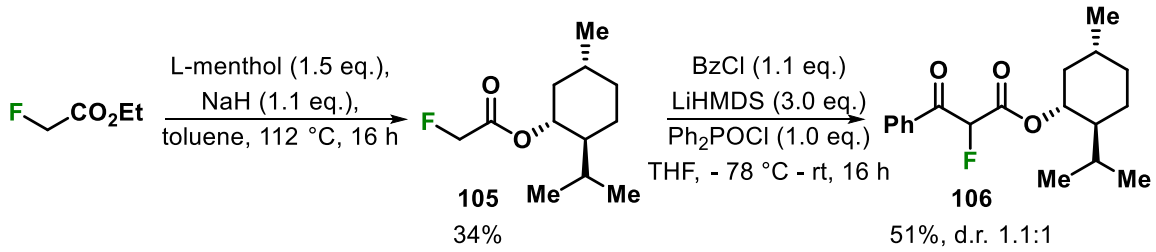

Scheme 70 *- Formation of α-fluoro-β-ketoester* ***106***

Compound **106** was then investigated in the allylation reaction. Whilst the allylated product was obtained in a good isolated yield, the diastereomeric ratio was unexpectedly very low (Scheme 71).

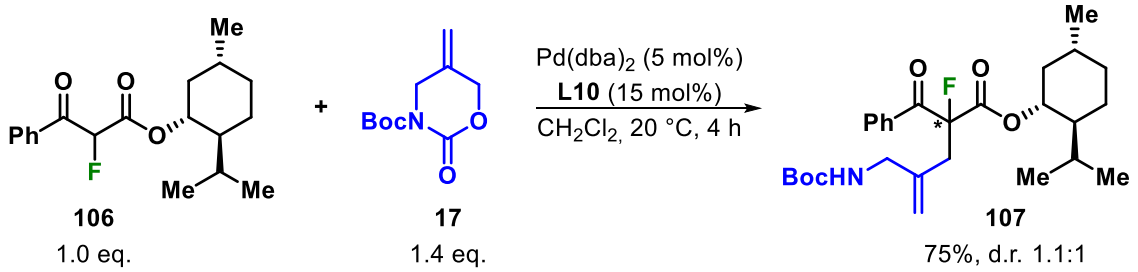

Scheme 71 *- Attempted diastereoselective allylation*

An alternative strategy was proposed involving the employment of a biocatalyst to perform an enzymatic kinetic resolution *via* asymmetric hydrolysis of lactone **108** (Scheme 72). This compound could be readily synthesised from the commercially available dimethyl fluoromalonate, using the palladium-catalysed allylation - condensation sequence.

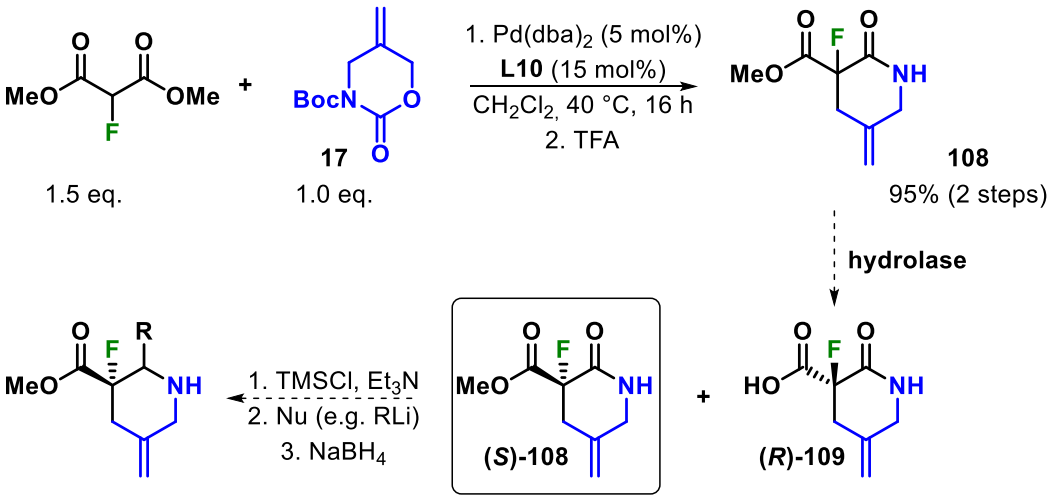

Scheme 72 *- Synthesis of* ***108*** *and enzymatic approach*

Furthermore, an enantioselective enzymatic hydrolysis of an almost identical fluorinated substrate using Candida antarctica lipase B (CAL-B) has been described in the literature.[125] Therefore, the enzymatic protocol was applied to lactone **108** (Scheme 73).

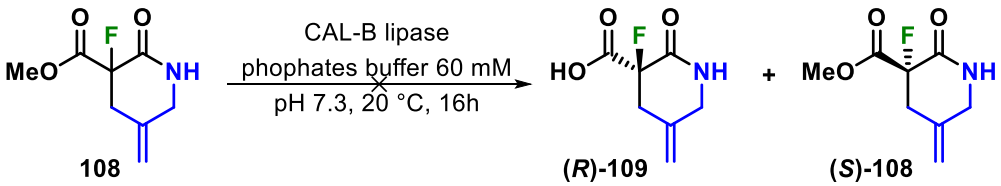

Scheme 73 *- Attempted enzymatic kinetic resolution*

However, CAL-B failed to provide any traces of the hydrolysed lactone, and the unreacted starting material was recovered. After further literature examination, it was noted that pig liver esterase (PLE) is able to enantioselectively hydrolyse prochiral malonic diesters.[126, 127] It was therefore decided to apply the desymmetrisation reaction to dimethyl fluoromalonate **110** (Scheme 74). Whilst the diester successfully

underwent hydrolysis, the product was obtained as a racemic mixture. Indeed, the addition of (*R*)-(+)-α-methylbenzylamine to the acid gave a 1:1 mixture of diastereomeric salts observable by NMR. Dimethyl fluoromalonate **110** was also examined with CAL-B, however no hydrolysis of the diester was observed.

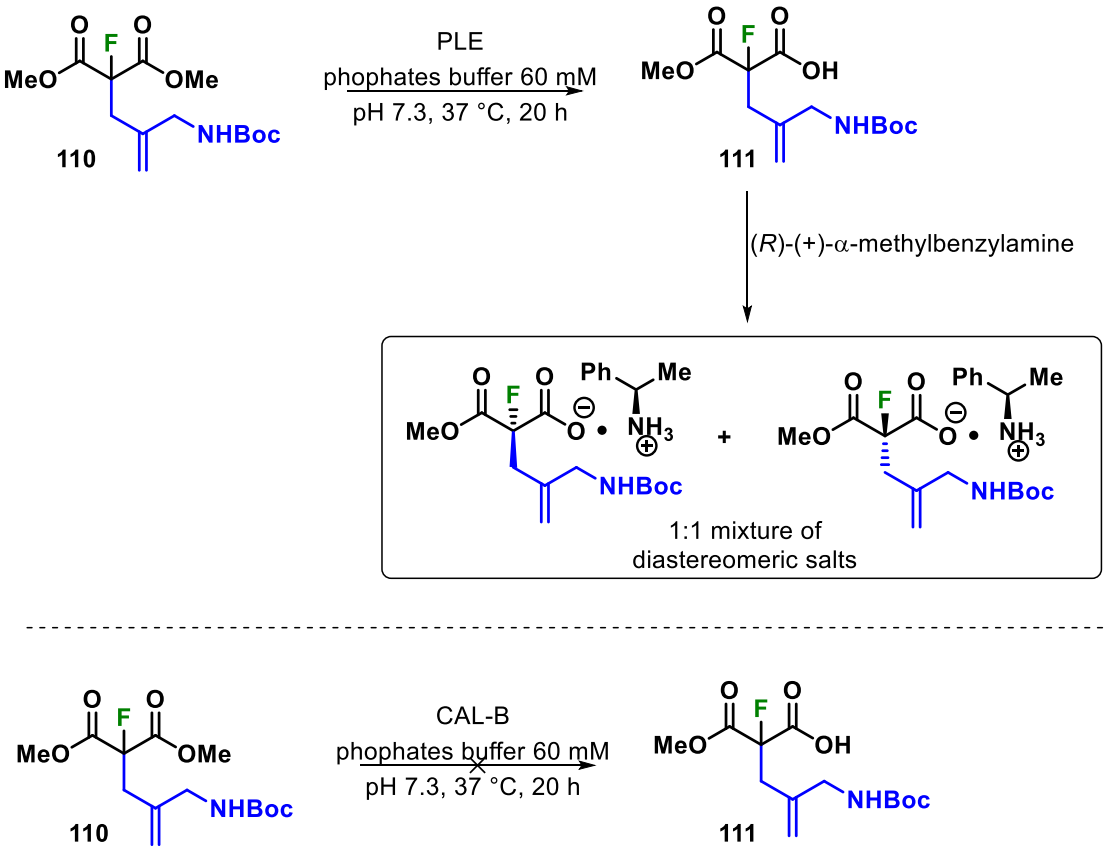

Scheme 74 *- Attempted stereoselective enzymatic hydrolysis*

3.2.2. ***Synthesis of 3-Trifluoromethylthio Piperidines***

The incorporation of trifluoromethylthio (SCF_3) groups into organic compounds has also gained considerable interest in drug and agrochemical discovery research. Due to its electron-withdrawing nature and high lipophilicity, the SCF_3 moiety can

significantly modulate the pharmacological properties of bioactive compounds.[128-132] Nevertheless, the availability of synthetic methods that deliver saturated *N*-trifluoromethylthiolated six-membered heterocycles are scarce, and those that are documented suffer from limited substrate scope.[133-137] According to the current literature on SCF_3-containing *N*-heterocycles, only two examples of 3-SCF_3-substituted piperidines have been reported.[136, 137] Therefore, the palladium-catalysed allylation-condensation methodology would be of significant value to the pharmaceutical and agrochemical sectors, and would stimulate developments in the field of fluorinated *N*-heterocycle synthesis. Based on the work previously described, it was envisioned that the palladium-catalysed annulation methodology would enable the formation of 3-trifluoromethylthiopiperidine products through allylation of α-SCF_3-ketone and α-SCF_3-β-ketoester substrates followed by a chemoselective cyclisation - imine reduction sequence (Scheme 75).

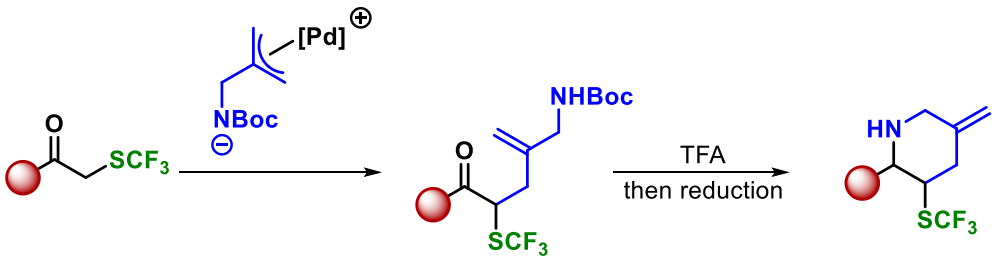

Scheme 75 *- Pd-catalysed synthesis of 3-SCF_3-piperidines*

Trifluoromethylthio-substituted starting materials **112** - **123** were readily synthesised in a single step from commercially available α-haloketones.[138] The reaction was conducted in the presence of $AgSCF_3$ and KI, which generates *in situ* an active trifluoromethylthiolate nucleophile (Scheme 76). Starting materials **125** and **126** were

produced *via* electrophilic trifluoromethylthiolation of the corresponding β-ketoester and β-ketosulfone with the readily available *N*-trifluoromethylthiosaccharin **124**.[139]

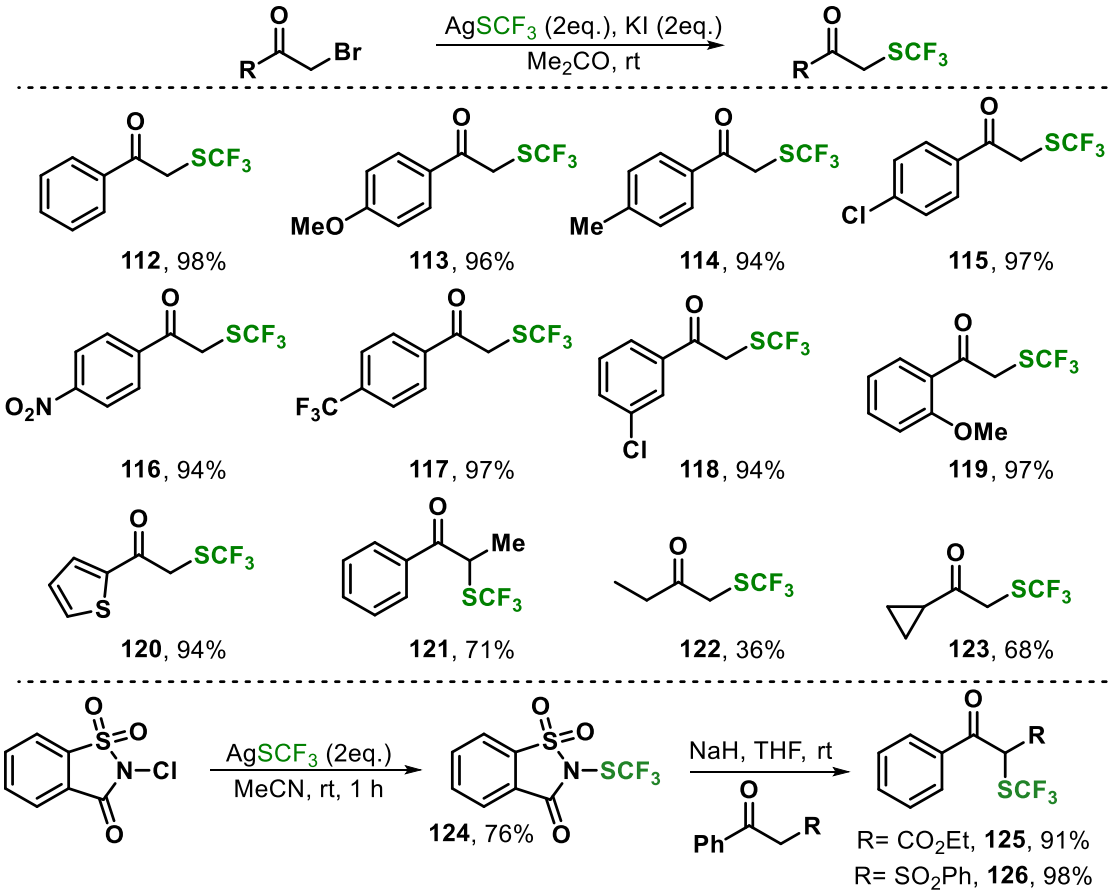

Scheme 76 *- Synthesis of SCF_3-containing starting materials*

The applicability of the palladium-catalysed process to these readily available α-SCF_3-ketones was then examined (Scheme 77). Aryl substituted ketones with either electron-withdrawing or electron-donating groups at the *para*-position on the aryl ring provided the desired allylated products in excellent yields. Substitution at other points on the aryl ring such as *meta*-chloro*, ortho*-methyl and *ortho*-methoxy were also well tolerated. The heterocyclic thiophenyl containing substrate was also converted into the corresponding allylated product in 81% yield. In addition to aryl

α-SCF_3-ketones; alkyl SCF_3-ketones, α-SCF_3-propiophenone and α-SCF_3-β-ketoesters were successfully employed in the palladium-catalysed allylation. However, α-SCF_3-ketone bearing a cyclopropyl and α-SCF_3-β-ketosulfone were found to be unreactive and starting materials were recovered in these cases.

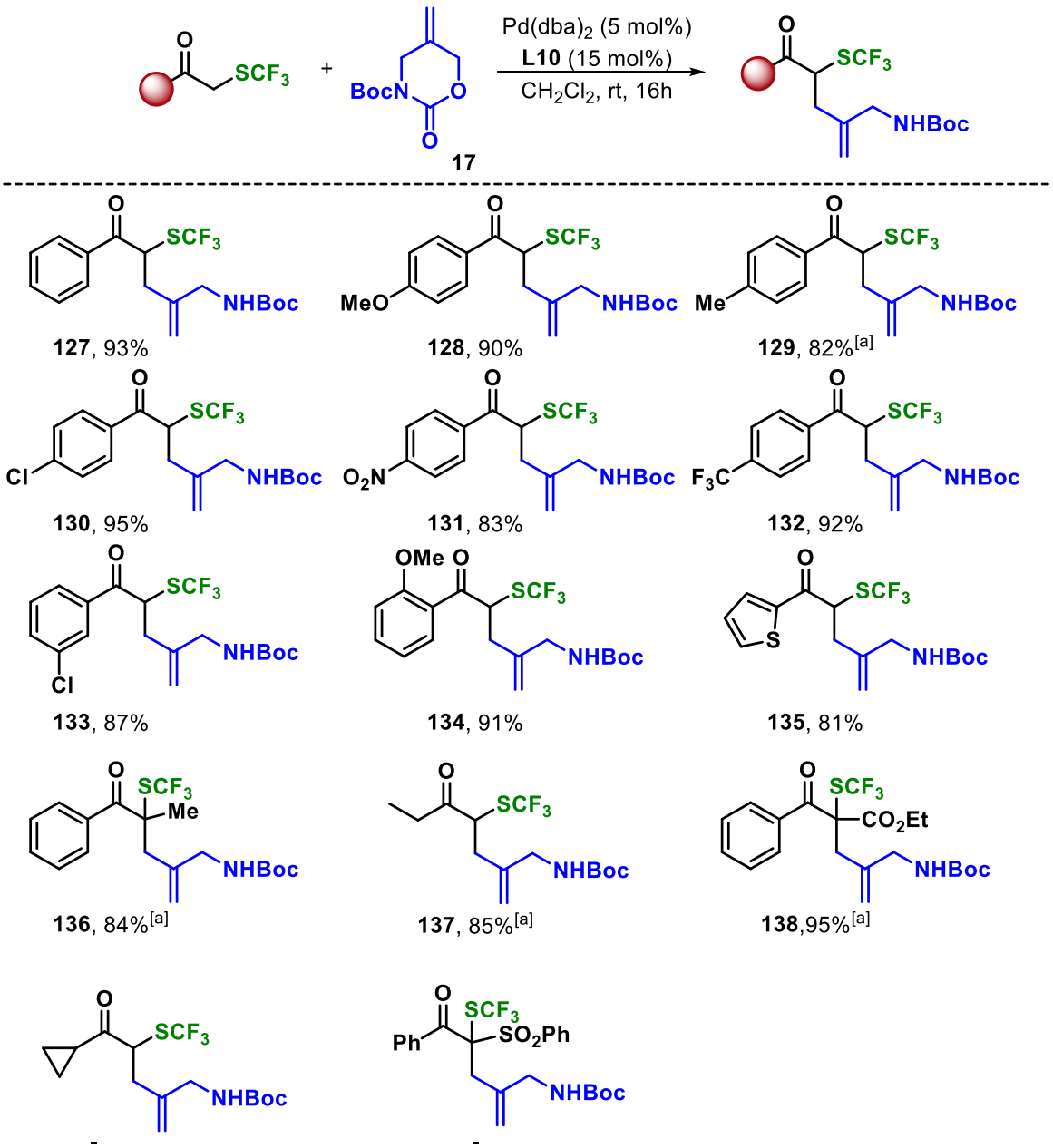

Scheme 77 *- Pd-catalysed allylation of α-SCF_3-ketones. [a] Reaction heated to 40 °C*

Exposure of the corresponding allylated compounds to trifluoroacetic acid followed by reduction of the TFA-iminium salts with sodium borohydride allowed access to a range of trifluoromethylthiolated *N*-heterocycles (Scheme 78). Aryl ketones bearing electron-neutral and electron-donating moieties at the *para*-position on the phenyl ring gave the desired saturated piperidines in good yield and high diastereoselectivity.

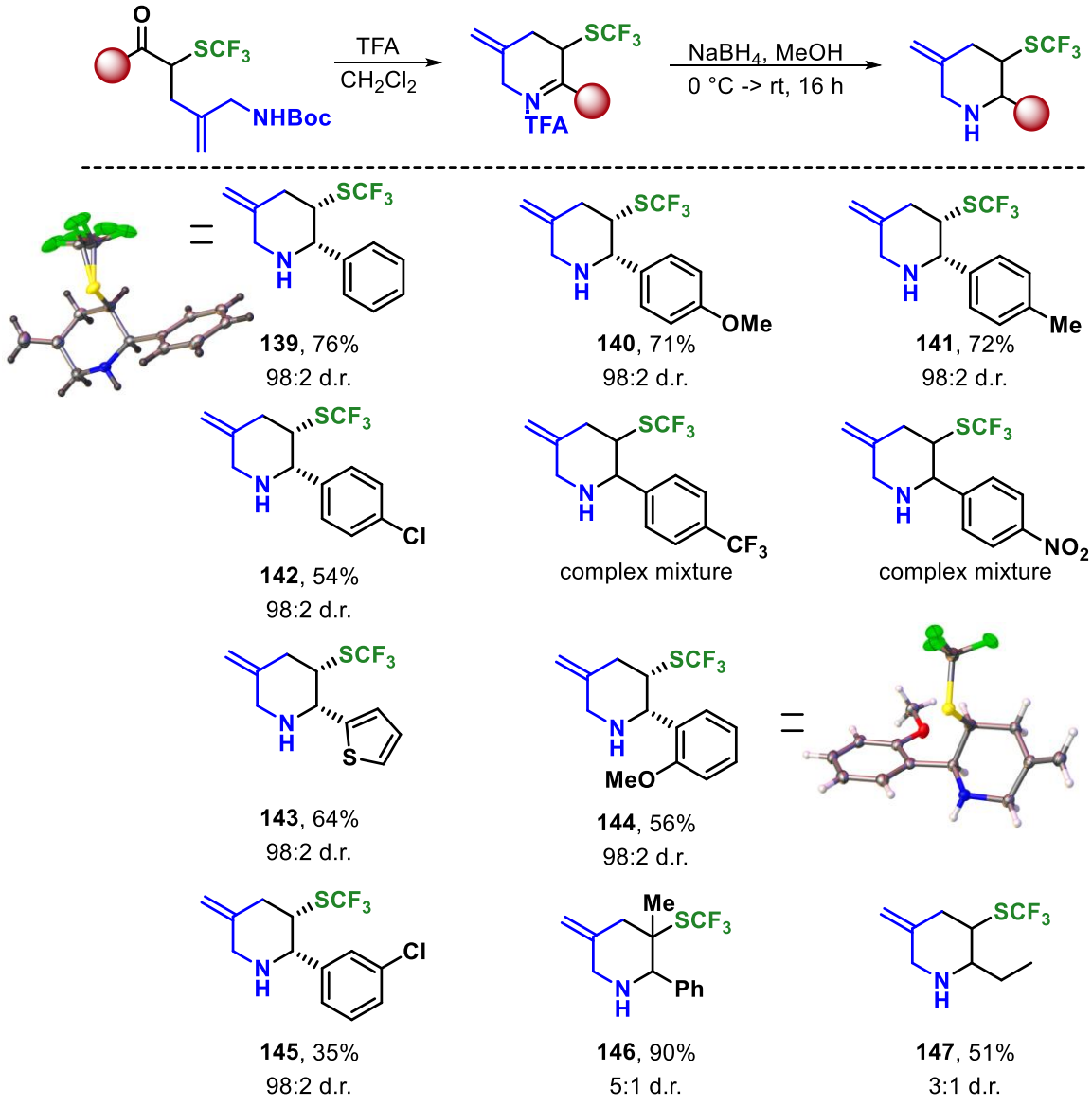

Scheme 78 - *Synthesis of 3-SCF_3 piperidines*

Furthermore, X-ray crystal structure analysis of aryl substituted products **139** and **144** confirmed the relative stereochemistry of the major diastereomer. The stereochemistry of all other aryl-substituted products has been assigned by inference. Unfortunately however, substrates containing electron-withdrawing groups were found to decompose during the TFA-mediated deprotection-condensation step, leading to a complex mixture. Substitution at the *ortho*-position with a methoxy was also tolerated. Substrate **135** bearing a thiophenyl was successfully converted into the corresponding piperidine in good yield. Compounds **136** and **137** deriving from α-trifluoromethylthio propiophenone and alkyl SCF_3-ketone were also found to undergo successful condensation-reduction, however the corresponding products were obtained as a 5:1 and 3:1 mixture of diastereoisomers, respectively (major diastereomer not determined). Surprisingly, exposing the allylated α-SCF_3-β-ketoester **138** to TFA provided a 2:1 mixture of products (Scheme 79). The major compound resulted from the intramolecular attack of the amine onto the SCF_3, whereas the minor product resulted from the desired condensation process. Despite extensive efforts to optimise the TFA-mediated cyclisation step, similar or less selective results were obtained.

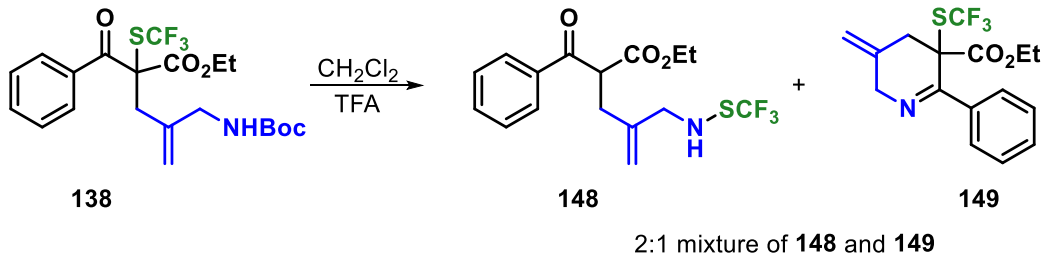

Scheme 79 *- TFA-mediated deprotection-condensation of* ***138***

3.3. Conclusions

The results presented in this chapter show that the palladium-catalysed α-allylation of fluoro- and trifluoromethylthio-containing keto-substrates followed by a condensation-reduction sequence allowed the generation of a library of novel fluorinated nitrogen-containing compounds. The current literature provides very few synthetic methods for the efficient synthesis of fluorinated six-membered *N*-heterocycles, particularly 3-fluoro- and 3-trifluoromethylthio-substituted piperidines. This methodology is therefore of great synthetic utility.

The palladium-catalysed allylation reaction proved general for a wide variety of α-fluoro- and α-trifluoromethylthio-keto substrates providing the corresponding allylated compounds in excellent yields. Whilst the TFA-mediated deprotection-condensation sequence of allylated α-fluoro-β-ketoester compounds was general, allylated aryl α-trifluoromethylthio-ketones bearing electron-withdrawing groups were found to decompose and resulted in a complex mixture.

The development of an asymmetric palladium-catalysed synthesis of 3-fluoro-piperidines was investigated and a range of chiral phosphoramidite ligands were examined. Furthermore, various enantioselective synthetic approaches employing chiral Lewis acids, Brønsted acids and chiral hydrogen bonding catalysts were studied. Dynamic kinetic resolutions, as well as enzymatic resolutions were investigated. However, despite all these different attempts to control the enantioselectivity, only low enantiomeric excesses were obtained. The

enantioselective palladium-catalysed synthesis of fluorinated *N*-heterocycles remains an ongoing challenge in the Harrity group.

.

4. Application

4.1. Studies Towards the Synthesis of Lysergic Acid

In order to showcase the potential of the Pd-catalysed process, its application towards the synthesis of lysergic acid was investigated. Lysergic acid is a fungal natural product and a precursor to a range of ergot alkaloids, which possess valuable biological activities.[140]

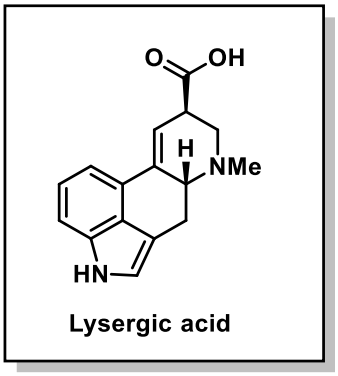

Figure 21 *- Structure of lysergic acid*

Retrosynthetically, lysergic acid **149** would be accessible in three steps from fragment **150**, which in turn could be formed from fragment **151** after a deprotection-condensation sequence followed by reduction (Scheme 80). Compound **151** would be accessed from the fused tricyclic compound **152** and cyclic carbamate **17** through the palladium-catalysed allylation process, which is the key reaction of this retrosynthetic analysis. The key synthetic intermediate **152** would arise from base-

mediated cyclisation of indole **153**, which could be traced back to indole-4-acetonitrile **154** through a C3-alkylation step. Finally, indole **154** could be accessed from the commercially available indole-4-carboxaldehyde **155** *via* functional group interconversion involving aldehyde reduction, alcohol activation and nucleophilic substitution.

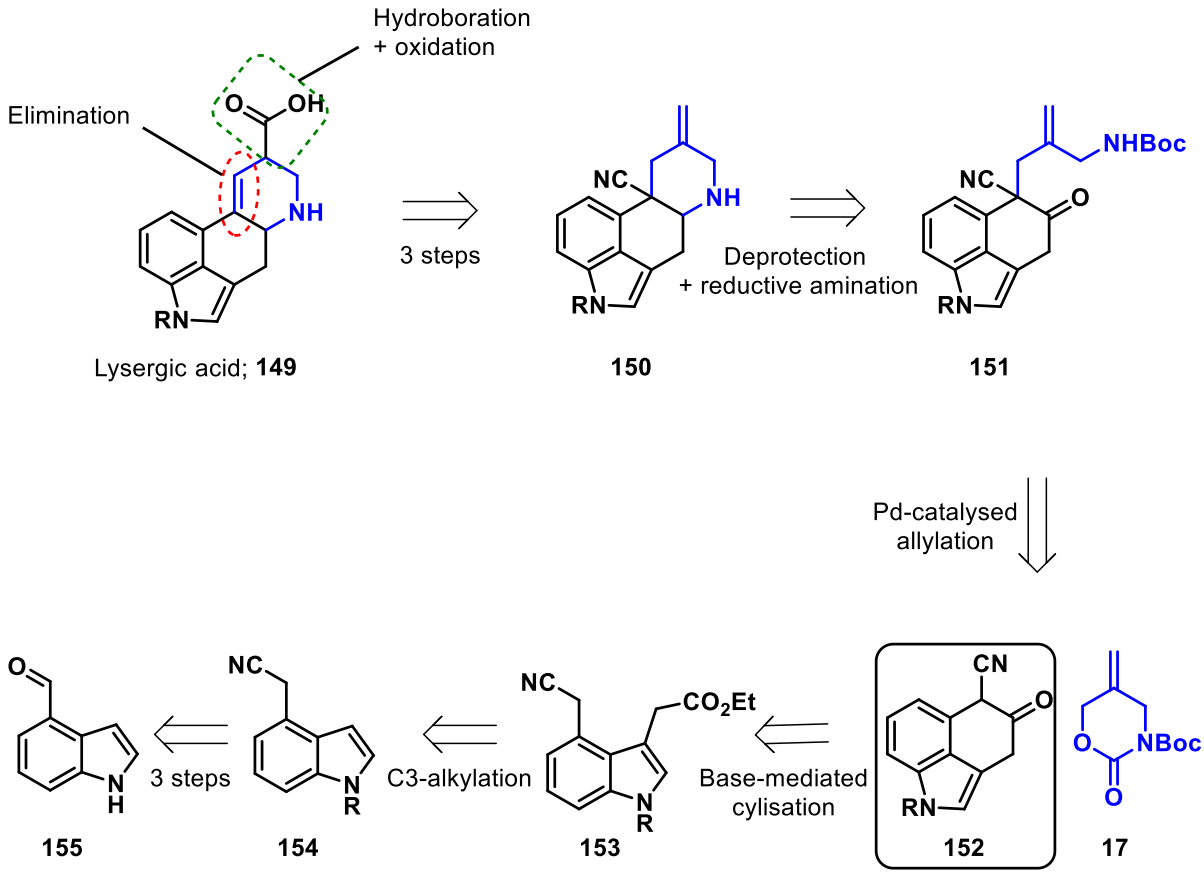

Scheme 80 *- Retrosynthetic analysis*

The synthesis began with the *N*-Cbz-protection of indole **155** followed by reduction of the aldehyde with sodium borohydride to give alcohol **157** (Scheme 81). The alcohol was then converted into the chloro-derivative **158** with thionyl chloride. Alkyl chloride

158 underwent a nucleophilic substitution with sodium cyanide in DMF to provide the nitrile compound **154** in 68% yield.

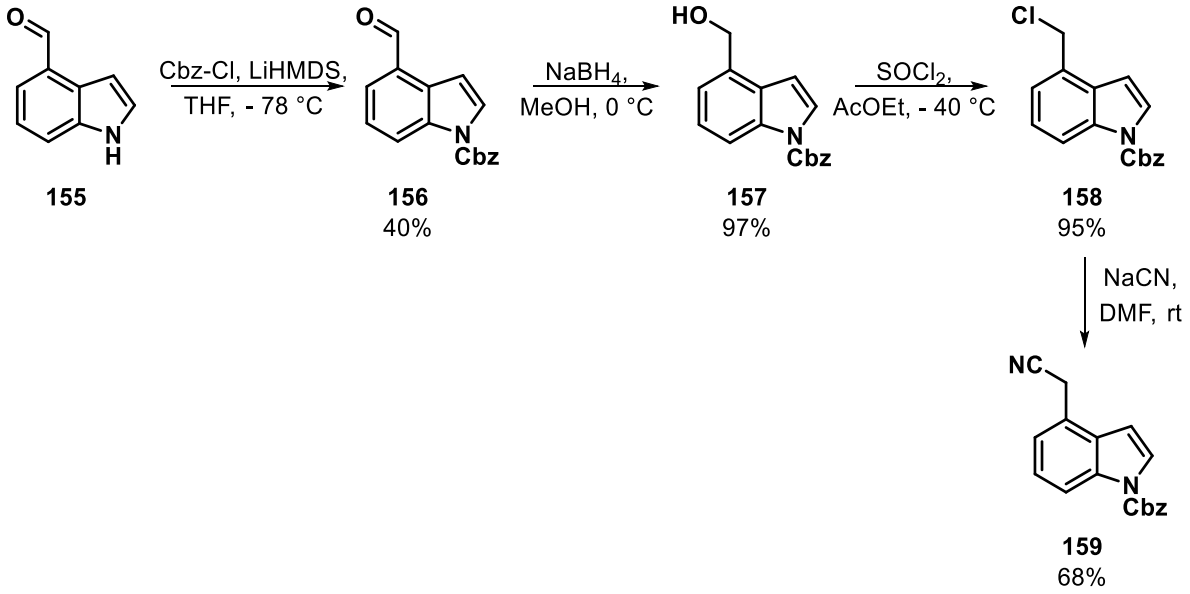

Scheme 81 *- Synthesis of indole* ***159***

Initially, formation of **160** was envisaged *via* a four-step sequence; acylation resulting from electrophilic aromatic substitution of indole **159** with oxalyl chloride, conversion of the acid chloride into the ester, thioacetal formation and then carbonyl reduction with Raney nickel (Scheme 82).

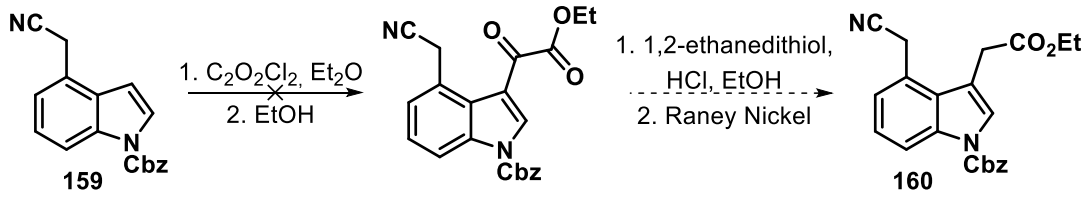

Scheme 82 *- Attempted route to compound* ***160***

However, acylation of indole **159** was unsuccessful. It was thought that the Cbz-protecting group on the nitrogen might perhaps decrease the nucleophilicity of the C3 position, thus rendering the indole unreactive towards electrophilic aromatic substitution. The acylation reaction was therefore envisaged prior to the *N*-protection step (Scheme 83).

Compound **155** underwent clean conversion to alcohol **161** with sodium borohydride. However, reaction of compound **161** with thionyl chloride was unsuccessful. The reaction led to complex mixtures, presumably due to polymerisation issues. The mass spectra obtained from the crude sample showed the presence of dimer and trimer by-products. The employment of a different chlorinating agent did not improve the outcome of the reaction.

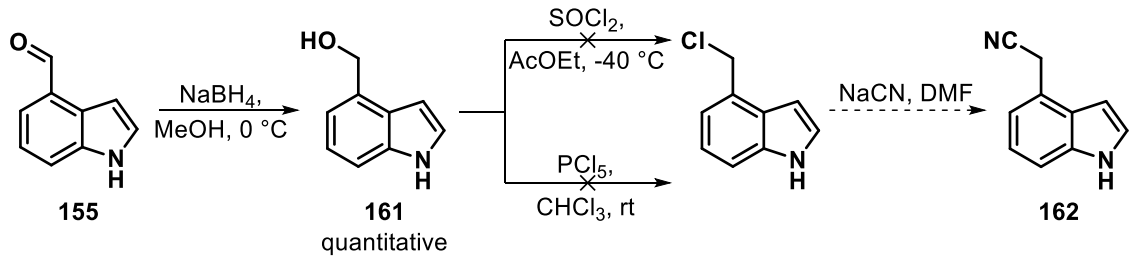

Scheme 83 *- Attempted synthesis of compound* ***162***

The one-step synthesis of indole-4-acetonitrile **162** from the readily available alcohol **161** was investigated. Attempts using trimethylsilyl cyanide and a Lewis acid or sodium cyanide in the presence of sodium iodide and trimethylsilyl chloride failed to provide the desired product. No conversion was observed and starting materials were recovered (Scheme 84).

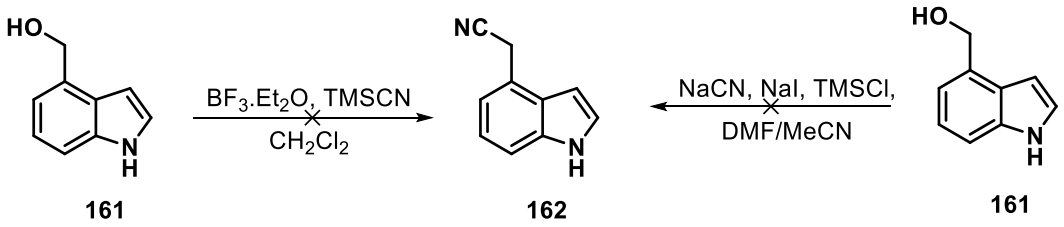

Scheme 84 *- Attempted one-step synthesis of* ***162*** *from alcohol* ***161***

A procedure reported by Somei and co-workers, which used sodium cyanide in a 1:1 mixture of methanol and formamide, described the formation of indole-3-acetonitrile from the corresponding alcohol precursor.[141] Application of this procedure to alcohol **161** led to the desired product **162** but in low yields (Scheme 85). Despite multiple attempts using different solvents mixture, product **162** could not be isolated in high yields.

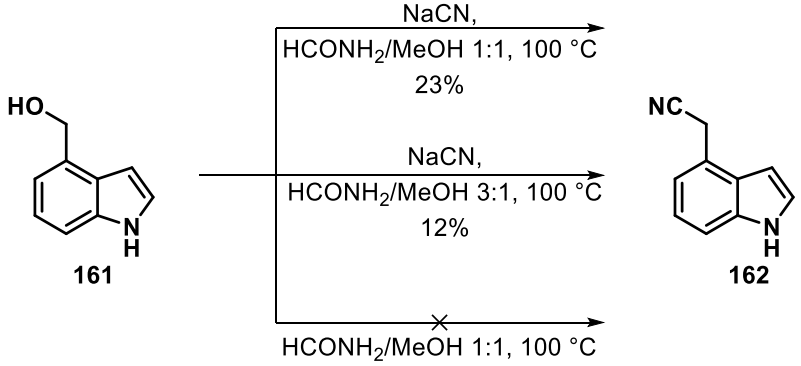

Scheme 85 *- Direct conversion of indole-4-methanol into indole-4-acetonitrile*

Asensio and co-workers described the conversion of indole-5-methanol into the corresponding acetonitrile in a two-step sequence.[142] Applying their procedure to substrate **161** allowed the synthesis of compound **163** in a very low yield (Scheme 86). The benzoylation step performed well, however substitution of the benzoyl group with potassium cyanide proved to be less effective. Analysis of the ^{1}H NMR

spectrum of the crude material showed high levels of starting material alongside the desired product. Furthermore, no traces of dimer or trimer adducts were observed, as had previously been experienced. It was reasoned that the addition of 18-crown-6 might improve the nucleophilicity of the cyanide anion by complexing the potassium cation. Indeed, treatment of indole **163** with potassium cyanide in the presence of 18-crown-6 allowed the synthesis of the desired nitrile product in 65% yield.

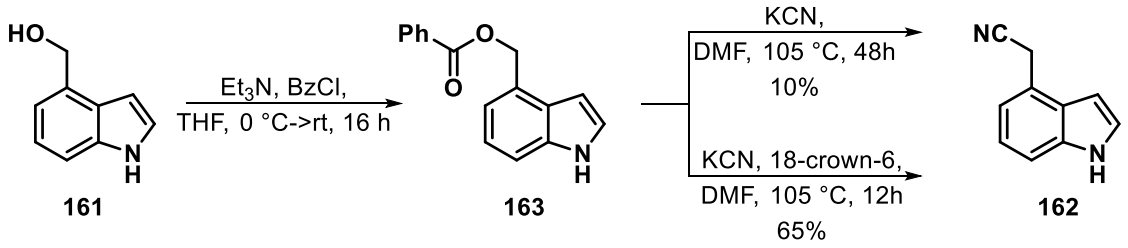

Scheme 86 - *Synthesis of indole* ***162***

Dicarbonylation of compound **162** with oxalyl chloride followed by ethanol addition to the acid chloride, provided the desired product **164** in 81% yield over two steps (Scheme 87).

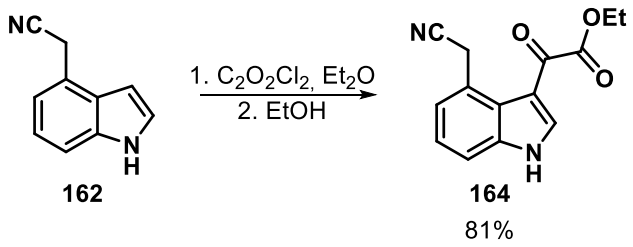

Scheme 87 - *Dicarbonylation of indole* ***162***

It was envisioned that compound **164** would be converted to indole **166** in two steps, involving dithioacetal formation followed by a desulfurisation step with Raney nickel. However, despite multiple attempts to convert the ketone into the dithioacetal, product **165** was not obtained and starting material **164** was recovered (Scheme 88).

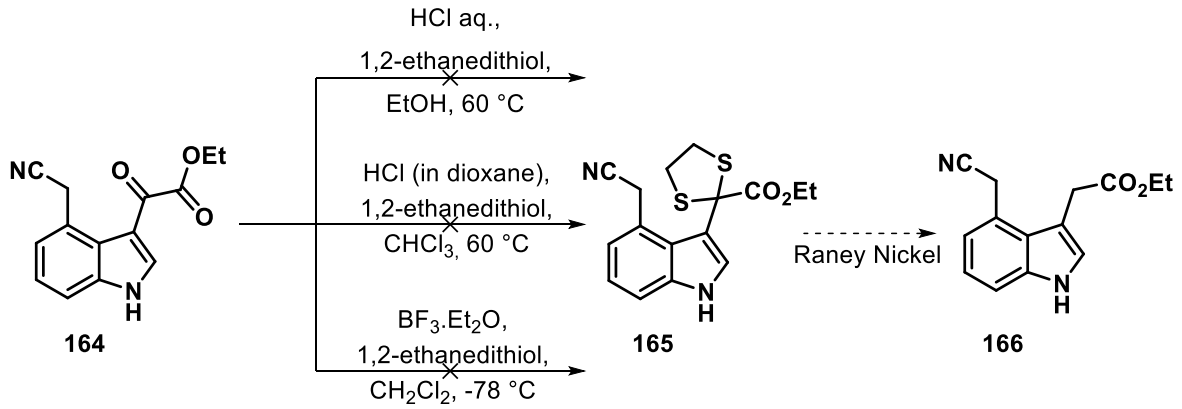

Scheme 88 - *Unsuccessful attempts for the thioacetalisation of* ***164***

Therefore, a different route was considered. The reduction of the ketone *via* ionic hydrogenation, in the presence of trifluoroacetic acid and triethylsilane, was attempted, but no reaction was observed (Scheme 89).

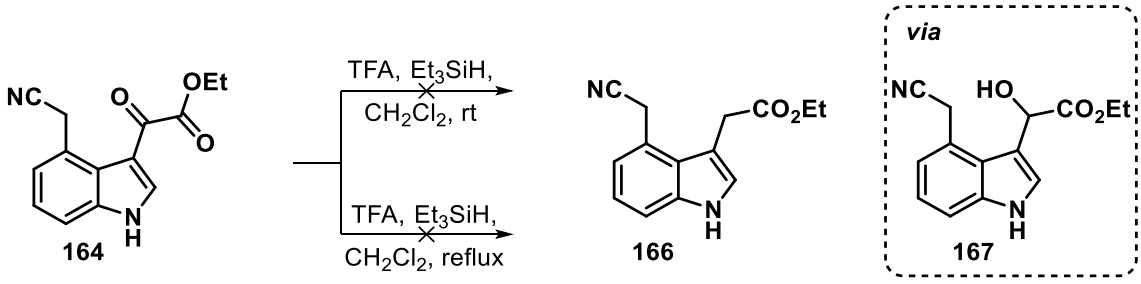

Scheme 89 - *Ionic hydrogenation of* ***164***

It was proposed that prior reduction of the ketone into the corresponding alcohol **167** would facilitate the ionic hydrogenation to indole **166**. However, reduction of compound **164** with sodium borohydride failed to give the desired product and resulted in a complex mixture. Analysis of the MS data indicated the presence of starting material and reduced indoles **168a** and **168b** alongside unidentified components (Scheme 90).

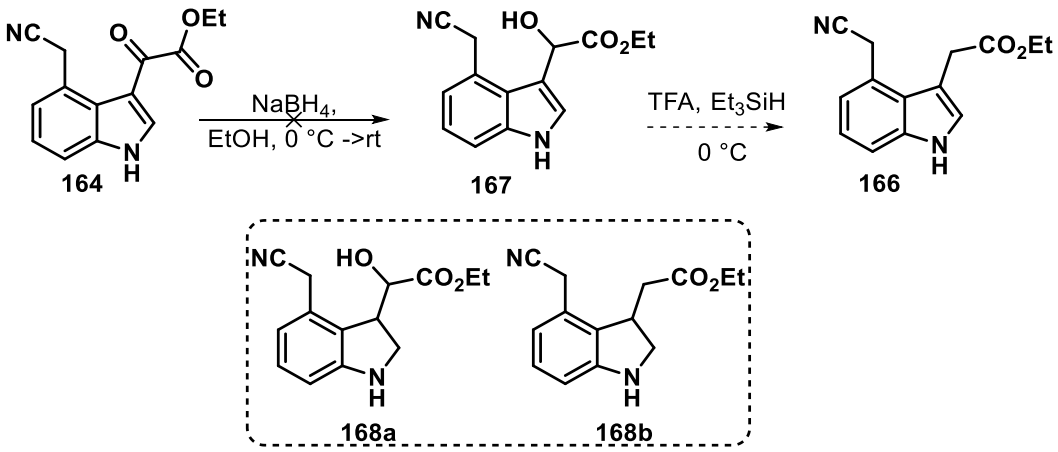

Scheme 90 *- Ketone reduction with $NaBH_4$*

As several different attempts failed to provide indole **166**, the initial strategy was re-examined. Alternative routes involving indole cross-coupling were investigated in parallel (Scheme 91). The first and second routes involve a Pd-catalysed Negishi or Kumada coupling. The third proposed strategy was inspired by the work of Ready and co-workers[143] who described the Sonogashira cross-coupling between *tert*-butoxyacetylene and aryl iodides to give ynol ethers. Further transformation into ketenes and subsequent nucleophilic attack were possible in this work, using mild conditions. The fourth strategy involves a C3-allylation under palladium catalysis followed by oxidative cleavage of the carbon-carbon double bond. Finally based on

literature precedent[144, 145], a direct oxidative coupling of the indole with *tert*-butyl acetate was also considered.

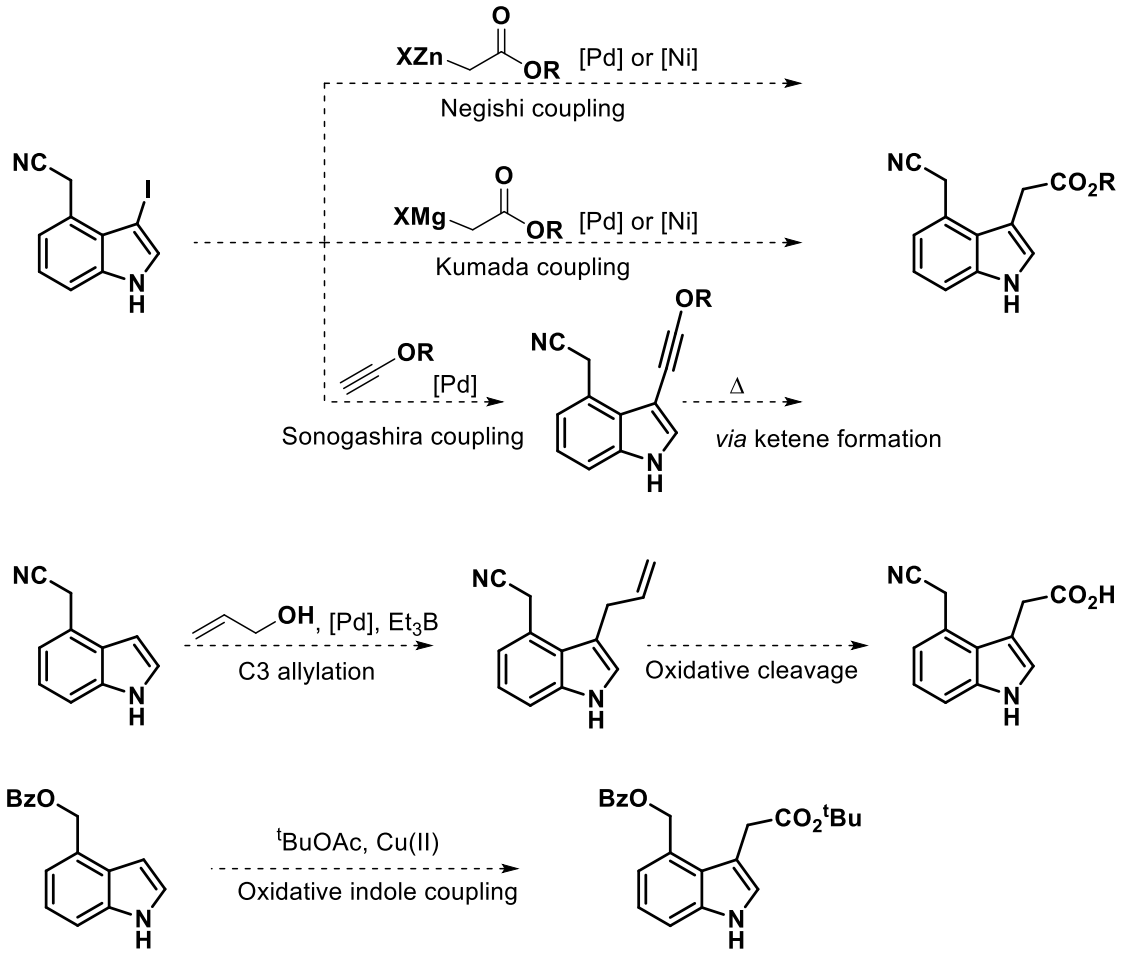

Scheme 91 *- Envisioned routes to compound* ***166***

In order to investigate the feasibility of these alternative strategies, 1*H*-indole was chosen to be used as starting material since it is commercially available and cheap.

The Pd-catalysed C3-allylation of indole **169** with allyl alcohol **170** promoted by triethylborane provided the desired allyl product in 86% yield (Scheme 92).[146]

However, oxidative cleavage of the carbon-carbon double bond proved difficult and gave a complex mixture of products.

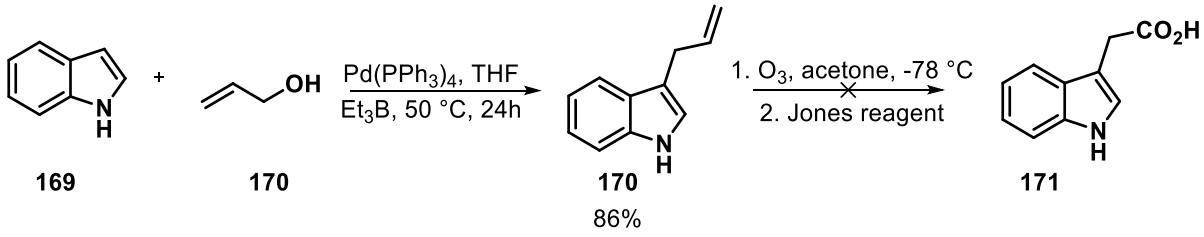

169 **170** **170** 86% **171**

Scheme 92 *- C3 allylation followed by oxidative cleavage*

The direct oxidative coupling of indole **163** with tert-butylacetate using Baran's reaction conditions was attempted, but the starting material was found to be unreactive under these conditions (Scheme 93).

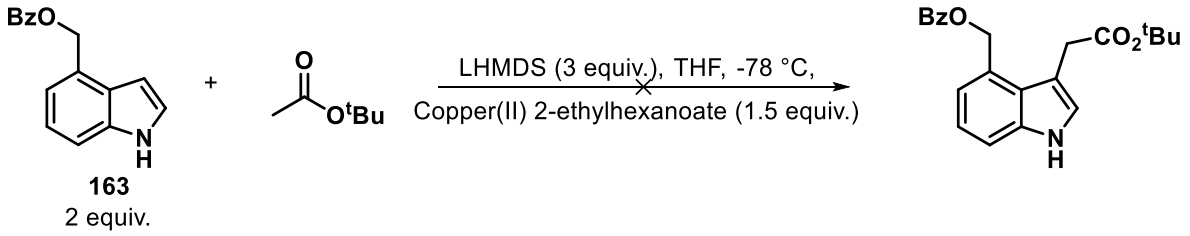

163
2 equiv.

Scheme 93 *- Unsuccessful direct oxidative coupling of* ***163***

To investigate the other proposed strategies that involve cross-coupling reactions, 3-iodoindole **172** was synthesised in a single step from **169** in 96% yield (Scheme **94**).[147] Compound **172** was then subjected to the following cross-coupling reactions; Sonogashira coupling with ethoxyacetylene, Kumada coupling with Grignard reagent **175** and Negishi coupling with several Reformatsky reagents. Attempts to

couple **172** with ethoxyacetylene and Grignard reagent **175** failed to give the desired product. The starting material was returned unchanged, no dehalogenation of the 3-iodoindole was observed.

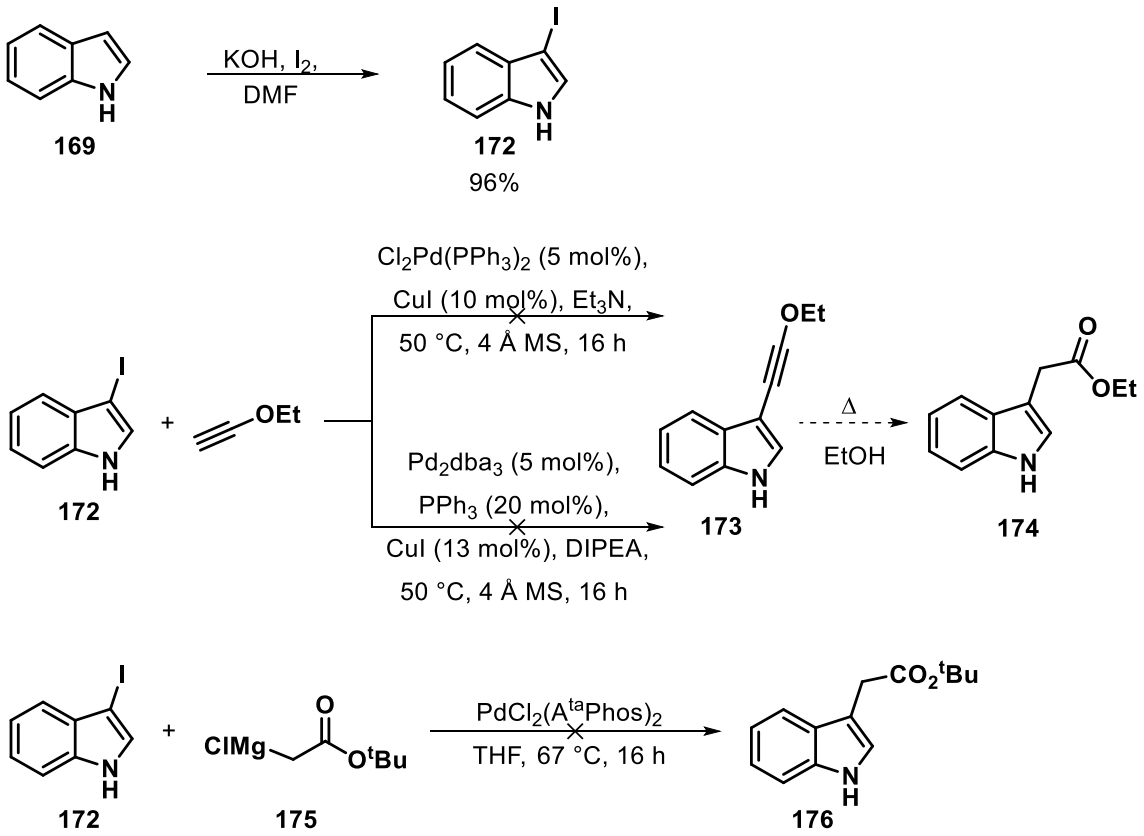

Scheme 94 *- Attempted cross-coupling reactions*

Stoltz *et al.* described a procedure that enabled a Negishi cross-coupling at the C3 position of a bromoindole-based substrate with a Reformatsky reagent. Based on that, different Negishi cross-coupling conditions were investigated (Table 14). An initial screening of catalysts and Reformatsky reagents with *N*-Boc-3-bromoindole **177** was unsuccessful and starting material was completely recovered (Table 14, entries 1-6). Attempts to couple the unprotected 3-iodoindole **172** with organozinc reagent **180** led to a mixture of starting material and dehalogenated indole

(entries 7-8). However, indole **172** performed well with the more hindered Reformatsky reagent **181** in the presence of $PdCl_2(A^{ta}Phos)_2$ at 67 °C (entry 9). Analysis of the crude NMR showed that solely the coupled product **183** was obtained.

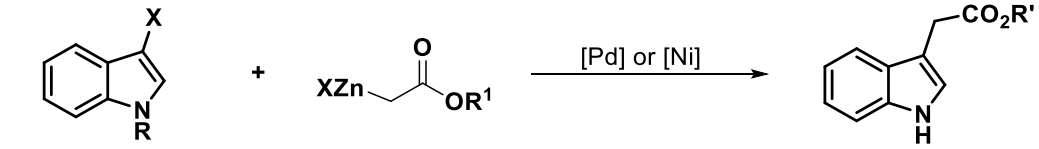

R = Boc, X = Br, **177**
R = H, X = I, **172**

X = Br, R^1 = Et, **179**
X = I, R^1 = Et, **180**
X = Br, R^1 = ^{t}Bu, **181**

R^1 = Et, **182**
R^1 = ^{t}Bu, **183**

Entry	SM	Organozinc	Catalyst	Ligand	Solvent	T (°C)	Outcome
1	**177**	**179**	Pd_2dba_3 (2.5 mol%)	SPhos (5 mol%)	DMF	rt	RSM
2	**177**	**179**	SPhosPdG1 (3 mol%)	/	THF	67	RSM
3	**177**	**179**	$Pd(OAc)_2$ (1 mol%)	SPhos (2 mol%)	THF	rt	RSM
4	**177**	**179**	$Pd(OAc)_2$ (5 mol%)	XPhos (10 mol%)	THF	67	RSM
5	**177**	**179**	$Ni(acac)_2$ (2 mol%)	2,2'-bpy (5 mol%)	THF	rt	RSM
6	**177**	**179**	XPhosPdG1 (5 mol%)	/	THF	67	RSM
7	**172**	**180**	XPhosPdG1 (10 mol%)	/	THF	67	SM + dehalogenated indole (major)
8	**172**	**180**	$PdCl_2(A^{ta}Phos)_2$ (5 mol%)	/	THF	67	SM + dehalogenated indole (major)
9	**172**	**181**	$PdCl_2(A^{ta}Phos)_2$ (5 mol%)	/	THF	67	**183** (78%)

Table 14 *- Negishi cross-coupling reaction optimisation*

The optimal Negishi conditions could not be applied to compound **184** since iodination of indole-4-acetonitrile **162** failed to provide the requisite C3 halogenated substrate.

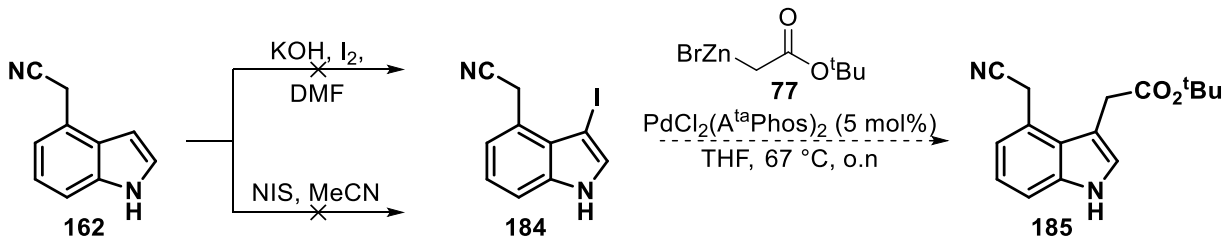

Scheme 95 *- Unsuccessful C3-iodination of compound* ***162***

It was therefore decided to perform the C3-iodination on substrate **163**, prior to the nucleophilic substitution of the benzoyl moiety with potassium cyanide. The benzoylated substrate underwent efficient iodination at the C3 position with iodine and potassium carbonate in DMF (Scheme 96). With the required halogenated substrate in hand, the Negishi reaction was attempted under the previously optimised conditions. However, no conversion was observed and compound **186** was recovered.

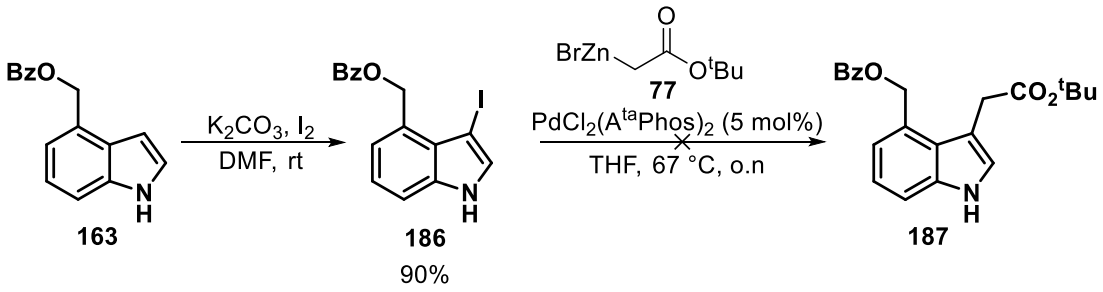

Scheme 96 *- C3-iodination of* ***163*** *followed by Negishi cross-coupling*

Unfortunately, further investigations into the synthesis of lysergic acid could not be completed within the time constraints.

4.2. Conclusions

Extensive efforts have been made towards the synthesis of lysergic acid. As the initially envisioned strategy was unable to provide the key synthetic intermediate **152**, different synthetic approaches were sought.

Initial attempts involved a palladium-catalysed C3-allylation followed by oxidative cleavage of the double bond as well as a direct oxidative coupling of the indole with *tert*-butyl acetate. Despite the successful C3-allyation of **169**, oxidative cleavage of the alkene proved difficult and led to a complex mixture. Furthermore, no conversion was observed under Baran's oxidative coupling conditions.

Compound **172** was also subjected to a range of cross-coupling reaction conditions. Sonogashira coupling with ethoxyacetylene and Kumada coupling with Grignard **175** failed to provide the desired coupled product. In both unsuccessful attempts, starting material was recovered and no dehalogenation of the 3-iodoindole was observed.

A screening of different catalyst systems, Reformatsky reagents and reaction conditions for the Negishi coupling was performed on compounds **172** and **177**. This resulted in the formation of cross-coupled product **183** in 78% yield. However, application of the optimised Negishi reaction conditions to compound **184** failed to provide the requisite precursor to the key synthetic intermediate **152**.

As formation of the required key intermediate proved to be more complicated than originally envisioned, application of the palladium-catalysed allylation methodology to the synthesis of lysergic acid could not be achieved within the project timeframe.

5. Experimental

5.1. General Experimental

All reactions were performed under argon or nitrogen atmosphere in flame-dried glassware and stirred with Teflon coated magnetic stirrer bars, unless stated otherwise. CH_2Cl_2, Et_2O, toluene, THF, MeCN and DMF were dried over alumina using a Pure Solv EN solvent purification system and transferred under nitrogen onto activated 4 Å molecular sieves. Commercial chemicals were purchased from Sigma Aldrich, Fluorochem, Acros, Alfa Aesar, Strem Chemicals and Manchester Organics and used without prior purification. Reactions were monitored using thin layer chromatography on aluminium plates coated with Merck silica gel 60 F_{254}. Visualisation was achieved using UV fluorescence (254 nm) and staining with potassium permanganate. Flash column chromatography was carried out on Sigma Aldrich silica gel 60 Å (40-63 µm) using air pressure. ^{1}H NMR experiments were recorded using Bruker AV III HD 400 (400 MHz), AV I 400 (400 MHz), AMX 400 (400 MHz) or DPX 400 (400 MHz) spectrometers at 295 - 300 K. Chemical shifts (δ) are given in ppm and are calibrated using the residual solvent peak (δ ^{1}H = 7.26 ppm). The following abbreviations were used for multiplicity: s (singlet), d (doublet), t (triplet), q (quartet), br (broad) and m (multiplet).^{13}C NMR experiments were recorded on a Bruker AV III HD 400 (101 MHz) or AV1 400 (101 MHz) and chemical shifts are given in ppm and calibrated using the residual solvent peak (δ ^{13}C = 77.16 ppm). Signals were recorded as singlets (s), doublets (d) or quartets (q). ^{19}F NMR experiments were recorded on the Bruker AV III HD 400 (377 MHz) and are

uncorrected. ^{31}P NMR spectra were recorded on the Bruker AV III HD 400 (162 MHz) and are uncorrected. All coupling constants (*J*) are quoted in Hz. Infrared spectra were recorded neat on a Perkin-Elmer Paragon 100 FTIR spectrometer. Absorption maxima (ν_{max}) are recorded in wavelengths (cm^{-1}). High-resolution mass spectra (HRMS) recorded for accurate mass analysis, were obtained on MicroMass LCT (TOF ESI+) or MicroMass Prospec operating in FAB (FAB+), EI (EI+) or CI (CI+) mode. Melting points were measured in open-ended capillaries using Gallenkamp melting apparatus and are uncorrected.

5.2. Experimental Details

5.2.1. Palladium-Stabilised Zwitterion Precursors

2-(Iodomethyl)prop-2-en-1-ol (**15**)

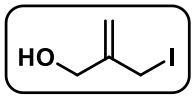

To a solution of 2-methylene-1,3-propanediol (12.0 g, 136 mmol), triphenylphosphine (39.3 g, 150 mmol) and imidazole (10.2 g, 150 mmol) in a mixture of CH_2Cl_2 (150 mL) and EtOAc (150 mL) at 0 °C under nitrogen was added iodine (34.6 g, 136 mmol) portionwise. The reaction mixture was stirred at room temperature in the dark for 24 hours before being diluted with EtOAc (150 mL) and washed with H_2O (200 mL). The aqueous layer was then extracted with EtOAc (2 × 100 mL) and the combined organic layers were dried with $MgSO_4$, filtered and concentrated under reduced pressure. The residue was purified by silica gel flash column chromatography [petroleum ether-EtOAc (80:20)] to give 2-(iodomethyl)prop-2-en-1-ol (**15**) as a colourless oil (13.7 g, 51%).

^{1}H NMR (400 MHz, $CDCl_3$) δ 5.36 - 5.34 (m, 1H), 5.21 - 5.19 (m, 1H), 4.30 (d, *J* = 5.5 Hz, 2H), 3.98 (d, *J* = 1.0 Hz, 2H), 2.11 (t, *J* = 5.5 Hz, 1H); **^{13}C NMR (101 MHz, $CDCl_3$)** δ 145.8, 114.2, 63.9, 5.8.

The data match those reported in the literature.[62]

5-Methylene-1,3-oxazinan-2-one (**16**)

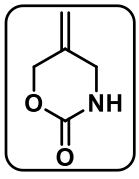

To a solution of 2-(iodomethyl)prop-2-en-1-ol **15** (11.7, 57.1 mmol) in toluene (170 mL) under nitrogen was added silver cyanate (12.8 g,

85.6 mmol) and the resulting mixture was heated to reflux for 22 h in the dark. After cooling to room temperature, the reaction mixture was filtered through a celite pad, washed with Et_2O (100 mL) and the filtrate was concentrated under reduced pressure. The product was isolated as a pure white solid without further purification (5.51 g, 85%).

m.p.: 88 - 90 °C (lit.[62] 90 - 91 °C); **^{1}H NMR (400 MHz, $CDCl_3$)** δ 5.44 (br, 1H), 5.27 (s, 1H), 5.25 (s, 1H), 4.71 (s, 2H), 4.02 - 3.98 (m, 2H); **^{13}C NMR (101 MHz, $CDCl_3$)** δ 155.2, 133.1, 113.7, 70.0, 45.2.

The data match those reported in the literature.[62]

<u>*tert*-Butyl 5-methylene-2-oxo-1,3-oxazinane-3-carboxylate (**17**)</u>

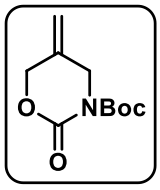

To a solution of 5-methylene-1,3-oxazinan-2-one **16** (5.49 g, 48.5 mmol) and 4-dimethylaminopyridine (1.19 g, 9.71 mmol) in CH_2Cl_2 (100 mL) was added di-*tert*-butyl dicarbonate (21.2 g, 97.1 mmol) and the reaction mixture was stirred at room temperature for 3 h. The solvent was then removed under reduced pressure and the crude material was subjected to silica gel flash column chromatography (gradient from 20-25% EtOAc in petroleum ether) to give cyclic carbamate **17** as a colourless oil which converted to a white solid upon standing in the freezer (8.40 g, 82%).

m.p.: 35 - 37 °C; **^{1}H NMR (400 MHz, $CDCl_3$)** δ 5.21 - 5.20 (m, 1H), 5.18 - 5.17 (m, 1H), 4.64 (s, 2H), 4.31 - 4.28 (m, 2H), 1.52 (s, 9H); **^{13}C NMR (100 MHz, $CDCl_3$)** δ 152.0, 150.9, 134.7, 113.0, 83.9, 69.9, 48.7, 28.0; **FTIR:** ν_{max}/cm^{-1} (neat) 1791, 1750,

1652, 1266; **HRMS (ESI$^+$):** *m/z* calcd. for $C_{10}H_{16}NO_4$: 214.1079, found: 214.1073 $[M+H]^+$.

2-(Chloromethyl)prop-2-en-1-ol (**18**)

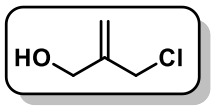

To a solution of 2-methylenepropane-1,3-diol (1.0 g, 11.3 mmol) and triethylamine (0.4 mL, 3.12 mmol) in CH_2Cl_2 (5 mL) at 0 °C was added a solution of tosyl chloride (541 mg, 2.84 mmol) in CH_2Cl_2 (5 mL) portion-wise over 30 min. The reaction mixture was stirred at 0 °C for 1 h then at r.t for 16 h. The solvent was removed under reduced pressure and the crude material was subjected to silica gel flash column chromatography [petroleum ether-EtOAc (80:20)] to give compound **18** as a colourless oil (278 mg, 92%).

^{1}H NMR (400 MHz, CDCl3) δ 5.27 - 5.26 (m, 2H), 4.29 - 4.27 (m, 2H), 4.14 (s, 2H), 1.70 (s, 1H); **^{13}C NMR (101 MHz, $CDCl_3$)** δ 144.4, 115.4, 63.5, 45.3.

The data match those reported in the literature.[148]

5.2.2. Formation of Phosphoramidite Ligands

General Procedure 1 (**GP1**)

Phosphorous trichloride (1.0 eq.) was added dropwise to a flask containing Et_3N (5.0eq.) and CH_2Cl_2 (0.15 M) at 0 °C. The reaction was stirred at 0 °C for 5 min, and then allowed to warm to r.t., followed by the slow addition of the appropriate amine (1.0 eq.). After 5 h, BINOL (1.0 eq.) was added at 0 °C then the reaction was allowed to stir at r.t. for 16 h. The resulting mixture was concentrated under reduced pressure

and the crude material was subjected to silica gel flash column chromatography to give the phosphoramidite ligand.

N,*N*-Diisopropyldibenzo[*d*,*f*][1,3,2]dioxaphosphepin-6-amine (**L10**)

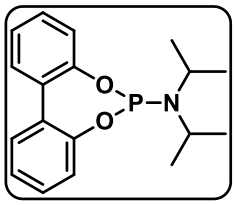

Following **GP1** using phosphorous trichloride (1.11 g, 8.06 mmol), Et_3N (4.08 g, 40.3 mmol), *N,N*-diisopropylamine (0.815 g, 8.06 mmol) and 2,2'-biphenol (1.50 g, 8.06 mmol). Following silica gel flash column chromatography [petroleum ether-CH_2Cl_2 (80:20)] ligand **L10** was isolated as a white solid (2.13 g, 84%).

^{1}H NMR (400 MHz, CDCl3) δ 7.46 (dd, *J* = 7.5, 1.5 Hz, 2H), 7.34 (td, *J* = 7.5, 1.5 Hz, 2H), 7.24 - 7.16 (m, 4H), 3.59 - 3.44 (m, 2H), 1.23 (d, *J* = 7.0 Hz, 12H); **^{13}C NMR (101 MHz, CDCl3)** δ 152.0 (d, *J* = 5.0 Hz), 131.0 (d, *J* = 3.0 Hz), 129.8, 129.0, 124.3, 122.2, 44.7 (d, *J* = 12.5 Hz), 24.6 (d, *J* = 8.0 Hz); **^{31}P NMR (162 MHz, $CDCl_3$)** δ 152.1.

The data match those reported in the literature.[149]

(11b*R*)-*N*,*N*-Diisopropyldinaphtho[2,1-*d*:1',2'-*f*][1,3,2]dioxaphosphepin-4-amine (**L14**)

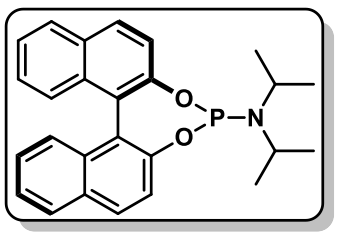

Following **GP1** using phosphorous trichloride (168 mg, 1.22 mmol), Et_3N (618 mg, 6.11 mmol), *N,N*-diisopropylamine (124 mg, 1.22 mmol) and (*R*)-BINOL (350 mg, 1.22 mmol). Following silica gel flash column chromatography [petroleum ether-CH_2Cl_2 (80:20)] ligand **L14** was isolated as a white solid (320 mg, 63%).

^{1}H NMR (400 MHz, CDCl3) δ 7.95 (d, *J* = 9.0 Hz, 1H), 7.92 - 7.87 (m, 3H), 7.50 (dd, *J* = 8.5, 1.0 Hz, 1H), 7.43 (d, *J* = 8.5 Hz, 1H), (7.42 - 7.36 (m, 3H), 7.30 (d, *J* = 8.0 Hz, 1H), 7.29 - 7.19 (m, 2H), 3.46 - 3.31 (m, 2H), 1.22 (d, *J* = 7.0 Hz, 6H), 1.18 (d, *J* = 7.0 Hz, 6H); **^{13}C NMR (101 MHz, CDCl3)** δ 150.6, 150.5, 132.9, 132.8, 131.4, 130.7, 130.3, 129.5, 128.4, 128.3, 127.3, 127.2, 126.0, 125.9, 124.7, 124.4, 124.2, 122.6, 122.5, 122.1, 44.9 (d, *J* = 12.5 Hz), 24.7 (d, *J* = 8.5 Hz); **^{31}P NMR (162 MHz, $CDCl_3$)** δ 151.8.

The data match those reported in the literature.[150]

5-((11b*R*)-Dinaphtho[2,1-*d*:1',2'-*f*][1,3,2]dioxaphosphepin-4-yl)-5*H*-dibenzo[b,f]azepine (**L16**)

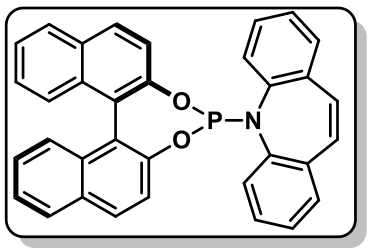

Following the procedure of Carreira,[151] a flame-dried flask was charged with (*R*)-(+)-1,1'-bi(2-naphtol) (1.14 g, 3.98 mmol), phosphorous trichloride (5.2 mL, 8.24 g, 60.0 mmol) and DMF (10 µL, 0.12 mmol), and then the reaction mixture was stirred at 50 °C for 30 min. After this time, excess phosphorous trichloride was removed under reduced pressure, followed by azeotropic distillation with toluene (3 x 2 mL) to give the phosphochloridite. Iminostilbene (0.850 g, 4.4 mmol) and THF (24 mL) were added to a separate flask and cooled to -78 °C. *n*-BuLi (2.5 M in hexane, 1.8 mL, 4.4 mmol) was then added dropwise over 10 min and the reaction was stirred at -78 °C for 1 h. The freshly prepared phosphochloridite was dissolved in THF (18 mL) and added to the iminostilbene solution dropwise over 15 min. The reaction was then gradually warmed to r.t. and stirred for 24 h. Silica gel (10 g) was added to the resulting mixture and concentrated under reduced pressure,

followed by flash column chromatography [hexane-toluene (2:1)] to give phosphoramidite ligand **L16** as a white solid (1.42 g, 70%).

^{1}H NMR (400 MHz, $CDCl_3$) δ 7.98 (d, *J* = 8.5 Hz, 1H), 7.90 (d, *J* = 8.0 Hz, 1H), 7.76 (d, *J* = 8.0 Hz, 1H), 7.61 (d, *J* = 8.5 Hz, 1H), 7.45 - 7.33 (m, 3H), 7.30 - 7.09 (m, 10H), 7.02 - 6.89 (m, 3H), 6.85 (d, *J* = 8.5 Hz, 1H), 6.53 (td, J = 8.0, 1.5 Hz, 1H); **^{13}C NMR (101 MHz, $CDCl_3$)** δ 150.0, 149.9, 148.8, 143.2, 142.6, 136.5, 135.3, 132.8, 132.3, 131.6, 131.4, 131.3, 130.4, 130.3, 129.2, 129.1, 129.1, 129.0, 129.0, 128.9, 128.6, 128.5, 128.4, 127.9, 127.2, 126.9, 126.8, 126.2, 126.1, 125.7, 124.9, 124.4, 122.2, 121.6; **^{31}P NMR (162 MHz; $CDCl_3$)** δ 137.9.

The data match those reported in the literature.[151]

5-((11b*R*)-8,9,10,11,12,13,14,15-Octahydrodinaphtho[2,1-*d*:1',2'-*f*][1,3,2] dioxaphosphepin-4-yl)-5*H*-dibenzo[*b*,*f*]azepine (**L19**)

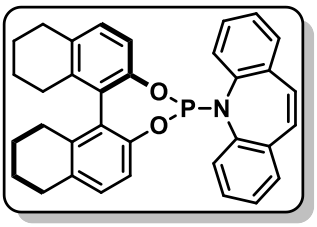

Following the procedure of Breit,[152] a flame-dried flask was charged with phosphorous trichloride (0.37 mL, 585 mg, 4.26 mmol) and THF (9.7 mL) then cooled to 0 °C. Et_3N (1.1 mL, 784 mg, 7.75 mmol) in THF (7.8 mL) was added, followed by a solution of (*R*)-(+)-5,5′,6,6′,7,7′,8,8′-octahydro-1,1′-2-naphthol (1.14 g, 3.87 mmol) in THF (7.8 mL) over 20 min. Upon complete addition, the reaction was stirred for 10 min at 0 °C, and then allowed to warm to r.t. and stirred for a further 1 h. After this time, the reaction mixture was filtered through celite with THF (30 mL) and concentrated under reduced pressure to provide the phosphochloridite. Iminostilbene (0.823 g, 4.26 mmol) and THF (10 mL) were added to a separate flask and cooled to -78 °C. *n*-BuLi (2.5 M in hexane, 1.7 mL, 4.26 mmol) was then added dropwise over

10 min and the reaction was stirred at -78 °C for 1 h. The freshly prepared phosphochloridite was dissolved in THF (7.5 mL) and added to the iminostilbene solution dropwise over 30 min. The reaction was then warmed to r.t. and stirred for 18 h. The resulting mixture was concentrated under reduced pressure and the crude material was subjected to silica gel flash column chromatography [hexane-toluene (2:1)] to give phosphoramidite ligand **L19** as a white solid (1.12 g, 56%).

^{1}H NMR (400 MHz, C_6D_6) δ 7.51 (dd, *J* = 7.5 Hz, 1.5 Hz, 1H), 7.16 - 7.10 (m, 1H), 7.05 - 6.77 (m, 9H), 6.68 (s, 2H), 6.63 (d, *J* = 8.0 Hz, 1H), 2.70 - 2.43 (m, 6H), 2.33 - 2.21 (m, 1H), 2.21 - 2.11 (m, 1H), 1.67 - 1.54 (m, 3H), 1.55 - 1.41 (m, 3H), 1.39 - 1.27 (m, 1H), 1.25 - 1.12 (m, 1H); **^{13}C NMR (101 MHz, C_6D_6)** δ 149.0, 148.6, 144.1, 143.6, 138.3, 137.3, 136.7, 136.3, 134.3, 132.6, 131.7, 129.7, 129.5, 129.2, 128.8, 128.4, 126.3, 126.0, 119.3, 119.2, 29.3, 28.0, 27.7, 22.9, 22.8, 22.6; **^{31}P NMR (162 MHz; C_6D_6)** δ 134.1.

The data match those reported in the literature.[152]

5.2.3. Synthesis of 1-Aryl-2-Indanone Substrates

General Procedure 2 (**GP2**) - Synthesis of α-Alkoxyketones

THF (1 M) was added to Weinreb amide **23** (1.0 eq.) under argon and the mixture was cooled to -78 °C. A solution of aryllithium reagent (generated from the corresponding aryl bromide (1.1 eq.) in THF (1 M) by addition of *n*-BuLi (2.5 M in hexane, 1.0 eq.)) was added dropwise and the resulting mixture was allowed to stir at -78 °C for 2 h. After this time, the reaction was warmed to 0 °C and quenched with

a saturated NH_4Cl solution (10 mL). Et_2O (3 mL) was added and the reaction was stirred at r.t. for an additional hour. The layers were separated and the aqueous layer was back-extracted with EtOAc (2 x 20 mL). The combined organic layers were dried over $MgSO_4$, filtered, and concentrated under reduced pressure. The crude material was then subjected to silica gel flash column chromatography to give the corresponding α-alkoxyketone.[64]

General Procedure 3 (**GP3**) - Enol Triflate Formation

To a solution of hexamethyldisilazane (2.5 eq.) in THF (2.5 M) at 0 °C under argon was added *n*-BuLi (2.5 M in hexane, 1.5 eq.). After 10 min at 0 °C, the mixture was cooled to -78 °C and the appropriate α-alkoxyketone (1.0 eq.) in THF (1 M) was added dropwise. Upon complete addition, the resulting mixture was stirred for 1 h at - 78 °C, then a solution of *N*-phenyl triflimide (1.5 eq.) in a 1:1 mixture of THF/DMPU (1.5 M) was added rapidly. The reaction was allowed to warm to r.t. and stirred for a further 2 h. The reaction was poured into brine and the layers were separated. The aqueous layer was back-extracted with Et_2O (2 x 50 mL). The combined organic layers were dried over $MgSO_4$, filtered, and concentrated under reduced pressure. The crude enol triflate was filtered over silica gel [petroleum ether-Et_2O-Et_3N (94:5:1)] and used immediately in the next reaction.[64]

General Procedure 4 (**GP4**) – Alkynyl Ether Formation and Sigmatropic Rearrangement/Cyclisation to 1-Aryl-2-Indanones

THF (1 M) was added to the enol triflate (1.0 eq.) under argon and the solution was cooled to -78 °C. Potassium *tert*-butoxide (3.0 eq.) in THF (1 M) was added dropwise

and the reaction was allowed to stir for 20 min. After this time, the reaction was poured into a saturated $NaHCO_3$ solution (10 mL) and the product was extracted with Et_2O (3 x 20 mL) and then dried with $MgSO_4$. After filtration and removal of solvent under reduced pressure, the crude alkynyl ether was dissolved in toluene (0.5 M) and heated to 60 °C under argon for 1 h. Solvent removal under reduced pressure followed by silica gel flash column chromatography provided the 1-aryl-2-indanone product.

3-Phenyl-1*H*-indene (**21**)

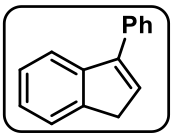

Bromobenzene (7.84 g, 49.9 mmol) was added to a flask containing flame-dried magnesium (1.21 g, 49.9 mmol), I_2 (one bead) and THF (50 mL, 1.0 M). The reaction was stirred at r.t. for 5 min, followed by heating at reflux for 1 h. Upon cooling, 1-indanone (6.0 g, 45.4 mmol) was added neat and the reaction was heated to reflux for a further 1.5 h. The reaction was then poured into an ice-water mixture and 6 M HCl was added. The product was extracted with EtOAc (3 x 60 mL) and dried with $MgSO_4$. After filtration and removal of solvent under reduced pressure, the crude material was subjected to silica gel flash column chromatography (100% petroleum ether) to give product **21** as a colourless oil (6.11 g, 70%).

^{1}H NMR (400 MHz, $CDCl_3$) δ 7.64 - 7.59 (m, 3H), 7.55 (d, *J* = 7.5 Hz, 1H), 7.47 (t, *J* = 7.5 Hz, 2H), 7.42 - 7.30 (m, 2H), 7.27 (td, *J* = 7.5, 1.0 Hz, 1H), 6.60 (t, *J* = 2.0 Hz, 1H), 3.53 (d, *J* = 2.0 Hz, 2H); **^{13}C NMR (101 MHz, $CDCl_3$)** δ 145.3, 144.9, 144.1, 136.3, 131.1, 128.7, 127.9, 127.7, 126.3, 125.0, 124.3, 120.5, 38.3.

The data match those reported in the literature.[153]

1-Phenyl-1,3-dihydro-2*H*-inden-2-one (**22**)

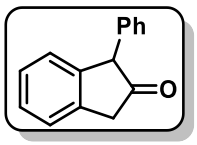

Potassium peroxymonosulfate (8.86 g, 28.8 mmol) was added portion-wise to a solution containing compound **21** (2.77 g, 28.8 mmol) and $NaHCO_3$ (14.5 g, 172.9 mmol) in acetone/H_2O/EtOAc (205 mL, 10:2:2) and then the resulting mixture was allowed to stir at r.t. for 18 h. H_2O (200 mL) was added and the product was extracted with CH_2Cl_2 (3 × 100 mL). The combined organic layers were dried with $MgSO_4$, filtered and concentrated under reduced pressure. The residue was then subjected to silica gel flash column chromatography [petroleum ether-EtOAc (90:10)] to give product **22** as a yellow oil (1.83 g, 61%).

^{1}H NMR (400 MHz, $CDCl_3$) δ 7.43 - 7.26 (m, 6H), 7.23 - 7.17 (m, 1H), 7.15 - 7.08 (m, 2H), 4.69 (s, 1H), 3.68 (s, 2H); **^{13}C NMR (101 MHz, $CDCl_3$)** δ 214.1, 141.4, 138.2, 137.4, 128.9, 128.6, 128.1, 128.0, 127.5, 126.2, 125.0, 59.9, 43.1.

The data match those reported in the literature.[154]

2-(Benzyloxy)-*N*-methoxy-*N*-methylacetamide (**23**)

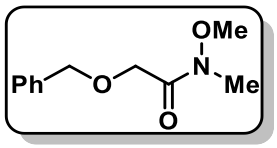

Benzyl alcohol (6.98 g, 64.5 mmol) was added to a suspension of NaH (60% dispersion in mineral oil, 7.74 g, 193.6 mmol) in THF (400 ml) under argon. The reaction was stirred at 0 °C for 15 min, then iodoacetic acid (12.0 g, 64.5 mmol) was added in one portion. The resulting mixture was stirred at reflux for 16 h, and then allowed to cool to r.t. The reaction was quenched with MeOH (30 ml) and solvents were removed under reduced pressure. Aq. NaOH (1M, 400 mL) and Et_2O (150 ml) were then added to

the residue and the layers were separated. The aqueous layer was washed twice with Et_2O (2 x 150 ml) then acidified to pH 3 with concentrated HCl. The product was extracted with Et_2O (3 × 150 ml) and the combined organic layers were washed with brine (1 x 300 ml), dried with $MgSO_4$ and concentrated under reduced pressure to provide 2-(benzyloxy)acetic acid as a pale yellow oil (9.60 g, 57.8 mmol). The aforementioned acid was then dissolved in CH_2Cl_2 (100 mL) and the solution was cooled to 0 °C. 1,1'-carbonyl diimidazole (12.2 g, 75.1 mmol) was added and the reaction was allowed to stir at r.t. for 30 min. After this time, the reaction was cooled to 0 °C, Et_3N (8.18 g, 80.9 mmol) and Weinreb amine HCl salt (7.89 g, 80.9 mmol) were added and the reaction was stirred at r.t. for 16 h. The resulting mixture was diluted with 1 M HCl (100 mL) and EtOAc (200 mL). The layers were separated and the aqueous layer was back-extracted with EtOAc (2 x 100 mL). The combined organic layers were then dried with $MgSO_4$, filtered, and concentrated under reduced pressure. Amide **23** was isolated as a pure colourless oil without further purification (12.0 g, 90%).

^{1}H NMR (400 MHz, $CDCl_3$) δ 7.40 - 7.26 (m, 5H), 4.67 (s, 2H), 4.28 (s, 2H), 3.63 (s, 3H), 3.19 (s, 3H); **^{13}C NMR (101 MHz, $CDCl_3$)** δ 171.0, 137.7, 128.6, 128.2, 127.0, 73.4, 67.2, 61.5, 32.5.

The data match those reported in the literature.[155]

2-(Benzyloxy)-1-(4-(trifluoromethyl)phenyl)ethan-1-one (**24**)

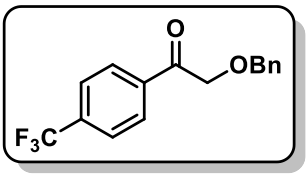

Prepared following **GP2** using Weinreb amide **23** (3.35 g, 16.0 mmol), 4-bromobenzotrifluoride (3.78 g, 16.8 mmol) and *n*-BuLi (2.5 M in hexane, 6.4 mL, 16.0 mmol). Following

silica gel flash column chromatography [petroleum ether-EtOAc (95:5)] compound **24** was isolated as a colourless oil (3.20 g, 68%).

^{1}H NMR (400 MHz, $CDCl_3$) δ 8.03 (d, *J* = 8.0 Hz, 2H), 7.72 (d, *J* = 8.0 Hz, 2H), 7.39 - 7.30 (m, 5H), 4.74 (s, 2H), 4.69 (s, 2H); **^{13}C NMR (101 MHz, $CDCl_3$)** δ 195.8, 137.8, 137.1, 134.9 (q, *J* = 33.0 Hz), 128.7, 128.6, 128.3, 128.2, 126.4 (q, *J* = 274 Hz), 125.9 (q, *J* = 4.0 Hz), 73.7, 73.0.

The data match those reported in the literature.[64]

2-(Benzyloxy)-1-(*p*-tolyl)ethan-1-one (**25**)

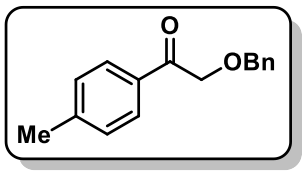

Prepared following **GP2** using Weinreb amide **23** (3.36 g, 16.1 mmol), 4-bromotoluene (3.02 g, 17.7 mmol) and *n*-BuLi (2.5 M in hexane, 6.4 mL, 16.1 mmol). Following silica gel flash column chromatography [petroleum ether-EtOAc (90:10)] compound **25** was isolated as a colourless oil (2.62 g, 67%).

^{1}H NMR (400 MHz, $CDCl_3$) δ 7.82 (d, *J* = 8.0 Hz, 2H), 7.41 - 7.24 (m, 7H), 4.74 (s, 2H), 4.69 (s, 2H), 2.41 (s, 3H); **^{13}C NMR (101 MHz, $CDCl_3$)** δ 196.0, 144.6, 137.5, 132.6, 129.5, 128.7, 128.2, 128.1, 128.0, 73.5, 72.6, 21.9.

The data match those reported in the literature.[64]

2-(Benzyloxy)-1-(4-methoxyphenyl)ethan-1-one (**26**)

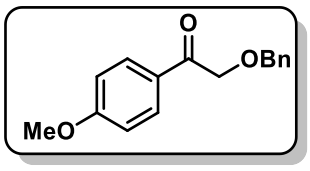

Prepared following **GP2** using Weinreb amide **23** (3.0 g, 14.3 mmol), 4-bromoanisole (2.82 g, 15.1 mmol) and *n*-BuLi

(2.5 M in hexane, 5.7 mL, 14.3 mmol). Following silica gel flash column chromatography (gradient from 10-20% EtOAc in petroleum ether) compound **26** was isolated as a colourless oil (2.37 g, 65%).

^{1}H NMR (400 MHz, $CDCl_3$) δ 7.92 (d, *J* = 9.0 Hz, 2H), 7.41 - 7.29 (m, 5H), 6.93 (d, *J* = 9.0 Hz, 2H), 4.71 (s, 2H), 4.68 (s, 2H), 3.87 (s, 3H); **^{13}C NMR (101 MHz, $CDCl_3$)** δ 194.9, 164.2, 163.9, 137.5, 130.4, 128.6, 128.2, 128.1, 114.0, 73.5, 72.6, 55.9.

The data match those reported in the literature.[64]

1-(4-(Trifluoromethyl)phenyl)-1,3-dihydro-2*H*-inden-2-one (**27**)

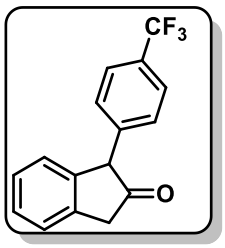

Prepared following **GP3** and **GP4** using HMDS (4.02 g, 24.9 mmol), *n*-BuLi (2.5 M in hexane, 6.0 mL, 14.9 mmol), α-alkoxyketone **24** (2.93 g, 9.96 mmol), *N*-phenyl triflimide (4.95 g, 12.5 mmol) and potassium *tert*-butoxide (3.35 g, 29.9 mmol). Following silica gel flash column chromatography [petroleum ether-CH_2Cl_2 (60:40)] compound **27** was isolated as an orange amorphous solid (1.53 g, 56%).

^{1}H NMR (400 MHz, $CDCl_3$) δ 7.59 (d, *J* = 8.0 Hz, 2H), 7.44 - 7.31 (m, 3H), 7.25 (d, *J* = 8.0 Hz, 2H), 7.18 (d, *J* = 7.5 Hz, 1H), 4.76 (s, 1H), 3.76 - 3.64 (m, 2H); **^{13}C NMR (101 MHz, $CDCl_3$)** δ 212.9, 141.9, 140.4, 137.5, 129.8 (q, *J* = 33.0 Hz), 129.0, 128.5, 128.2, 126.9 (q, *J* = 274 Hz), 126.1, 125.8 (q, *J* = 4.0 Hz), 125.2, 59.6, 43.1.

The data match those reported in the literature.[64]

1-(*p*-Tolyl)-1,3-dihydro-2*H*-inden-2-one (**28**)

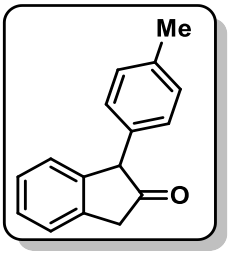

Prepared following **GP3** and **GP4** using HMDS (2.37 g, 14.7 mmol), *n*-BuLi (2.5 M in hexane, 3.5 mL, 8.80 mmol), α-alkoxyketone **25** (1.41 g, 5.87 mmol), *N*-phenyl triflimide (2.73 g, 7.63 mmol) and potassium *tert*-butoxide (1.11 g, 9.91 mmol). Following silica gel flash column chromatography [petroleum ether-EtOAc (95:5)] compound **28** was isolated as a yellow oil (424 mg, 58%).

^{1}H NMR (400 MHz, $CDCl_3$) δ 7.40 - 7.29 (m, 3H), 7.19 (d, *J* = 7.0 Hz, 1H), 7.14 (d, *J* = 8.0 Hz, 2H), 7.00 (d, *J* = 8.0 Hz, 2H), 4.65 (s, 1H), 3.67 (s, 2H), 2.33 (s, 3H); **^{13}C NMR (101 MHz, $CDCl_3$)** δ 213.9, 141.5, 137.4, 137.2, 135.3, 129.6, 128.5, 128.1, 128.0, 126.2, 125.0, 59.6, 43.1, 21.2.

The data match those reported in the literature.[64]

1-(4-Methoxyphenyl)-1,3-dihydro-2*H*-inden-2-one (**29**)

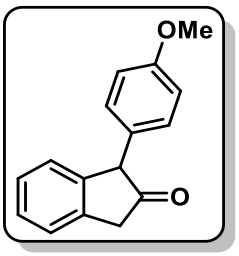

Prepared following **GP3** and **GP4** using HMDS (2.37 g, 14.7 mmol), *n*-BuLi (2.5 M in hexane, 3.5 mL, 8.81 mmol), α-alkoxyketone **26** (1.51 g, 5.88 mmol), *N*-phenyl triflimide (2.73 g, 7.64 mmol) and potassium *tert*-butoxide (1.65 g, 14.7 mmol). Following silica gel flash column chromatography [petroleum ether-EtOAc (90:10)] compound **29** was isolated as an off-white amorphous solid (659 mg, 47%).

^{1}H NMR (400 MHz, $CDCl_3$) δ 7.42 - 7.29 (m, 3H), 7.19 (d, *J* = 7.0 Hz, 1H), 7.03 (d, *J* = 8.5 Hz, 2H), 6.86 (d, *J* = 8.5 Hz, 2H), 4.63 (s, 1H), 3,79 (s, 3H), 3.66 (s, 2H);

^{13}C NMR (101 MHz, $CDCl_3$) δ 214.6, 159.0, 141.7, 137.3, 130.4, 129.6, 128.1, 128.0, 126.1, 125.0, 114.3, 59.1, 55.4, 43.0.

The data match those reported in the literature.[64]

3-(3-Methoxyphenyl)-1*H*-indene (**30**)

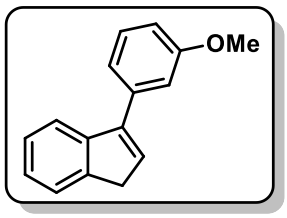

3-bromobenzene (15.6 g, 83.2 mmol) was added to a flask containing flame-dried magnesium (2.02 g, 83.2 mmol), I_2 (one bead) and THF (83 mL, 1.0 M). The reaction was stirred at r.t. for 5 min, followed by heating at reflux for 1 h. Upon cooling, 1-indanone (10.0 g, 75.7 mmol) was added neat and the reaction was heated to reflux for a further 16 h. The reaction was then poured into an ice-water mixture and aq. HCl (6.0 M) was added. The product was extracted with EtOAc (3 x 120 mL) and dried with $MgSO_4$. After filtration and removal of solvent under reduced pressure, the crude material was subjected to silica gel flash column chromatography [petroleum ether-Et_2O (95:5)] to give product **30** as a colourless oil (15.1 g, 90%).

^{1}H NMR (400 MHz, $CDCl_3$) δ 7.62 (d, *J* = 7.5 Hz, 1H), 7.55 (d, *J* = 7.5 Hz, 1H), 7.42 - 7.24 (m, 3H), 7.21 (d, *J* = 7.5, 1H), 7.17 - 7.15 (m, 1H), 6.94 (dd, *J* = 8.0 Hz, 2.0 Hz, 1H), 6.61 (t, *J* = 2.0 Hz, 1H), 3.87 (s, 3H), 3.52 (s, 2H); **^{13}C NMR (101 MHz, $CDCl_3$)** δ 159.7, 145.0, 144.7, 143.7 137.4, 131.1, 129.5, 126.3, 124.8, 124.0, 120.3, 120.1, 113.3, 113.1, 55.2, 38.3.

The data match those reported in the literature.[156]

1-(3-Methoxyphenyl)-1,3-dihydro-2*H*-inden-2-one (**31**)

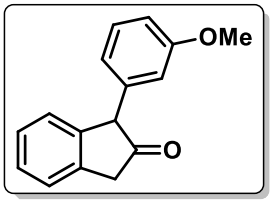

Indene **30** was dissolved in acetone (150 mL) and H_2O (20 mL) and the solution was cooled to 0 °C. NMO (9.25 g, 79.0 mmol) and OsO_4 (134 mg, 0.526 mmol) were added and the reaction was stirred at r.t. for 16 h. After this time, saturated aq. $Na_2S_2O_3$ (50 mL) was added and the resulting mixture was stirred at r.t. for 1 h. Saturated aq. $NaHCO_3$ (150 mL) was added and the product was extracted with EtOAc (3 x 150 mL). The combined organic layers were dried with $MgSO_4$, filtered and concentrated under reduced pressure. The crude diol was then dissolved in toluene (150 mL) and *p*-toluenesulfonic acid monohydrate (5.00 g, 26.3 mmol) was added. The reaction was stirred at reflux for 16 h, and then allowed to cool to r.t. The resulting mixture was diluted with EtOAc (200 mL) and saturated aq. $NaHCO_3$ (150 mL). The layers were separated and the aqueous layer was back-extracted with EtOAc (2 x 150 mL). The combined organic layers were dried with $MgSO_4$, filtered and solvents were removed under reduced pressure. The crude material was then subjected to silica gel flash column chromatography [petroleum ether-EtOAc (90:10)] to give indanone **31** as a brown oil (7.42 g, 59%).

^{1}H NMR (400 MHz, $CDCl_3$) δ 7.39 (d, *J* = 7.0 Hz, 1H), 7.37 - 7.28 (m, 2H), 7.23 (d, *J* = 8.0 Hz, 1H), 7.21 (d, *J* = 8.0 Hz, 1H), 6.81 (dd, *J* = 8.0 Hz, 2.5 Hz, 1H), 6.70 (d, *J* = 7.5 Hz, 1H), 6.68 - 6.65 (m, 1H), 4.65 (s, 1H), 3,77 (s, 3H), 3.67 (s, 2H); **^{13}C NMR (101 MHz, $CDCl_3$)** δ 211.0, 159.8, 138.5, 137.5, 134.2, 132.1, 132.0, 131.1, 129.5, 126.9, 124.1, 120.5, 114.7, 59.8, 55.3, 43.0; **FTIR:** ν_{max}/cm^{-1} (neat) 2961, 2939, 2838, 1751, 1710, 1660, 1597, 1486, 1432, 1288, 1274, 1145, 1045, 737; **HRMS (ESI$^+$):** *m/z* calcd. for $C_{16}H_{15}O_2$: 239.1067, found 239.1057 $[M+H]^+$.

3-Methyl-1*H*-indene (**32**)

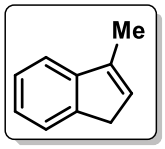

THF (40 mL) was added to methylmagnesium bromide (3 M in Et_2O, 20 mL, 60.5 mmol) and the reaction was cooled to 0 °C. 1-Indanone (4.0 g, 30.3 mmol) in THF (10 mL) was added and the reaction was stirred at r.t. for 16 h. After this time, 3M HCl (100 mL) was added and the resulting mixture was stirred for a further 5 min. The product was extracted with Et_2O (3 x 50 mL) and dried with MgSO4. After filtration and removal of solvent under reduced pressure, the crude material was subjected to silica gel flash column chromatography (100% petroleum ether) to give product **32** as a colourless oil (3.06 g, 78%).

^{1}H NMR (400 MHz, $CDCl_3$) δ 7.46 (d, *J* = 7.5 Hz, 1H), 7.37 - 7.30 (m, 2H), 7.21 (t, *J* = 7.0 Hz, 1H), 6.21 (s, 1H), 3.33 (s, 1H), 2.18 (s, 3H); **^{13}C NMR (101 MHz, $CDCl_3$)** δ 146.2, 144.2, 140.0, 128.7, 126.0, 124.5, 123.5, 118.9, 37.5, 12.9.

The data match those reported in the literature.[157]

1-Methyl-1,3-dihydro-2*H*-inden-2-one (**33**)

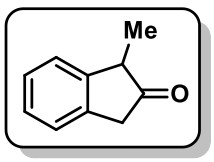

To a solution of mCPBA (77%, 4.96 g, 28.7 mmol) in CH_2Cl_2 (45 mL) and H_2O (45 mL) was added $NaHCO_3$ (2.79 g, 33.2 mmol) and the reaction was stirred at r.t. for 20 min. Indene **32** (1.44 g, 11.1 mmol) in CH_2Cl_2 (4 mL) was then added and the reaction was allowed to stir at r.t. for 2 h. After this time, the layers were separated and the aqueous layer was washed twice with CH_2Cl_2 (2 x 50 mL). The combined organic layers were dried with $MgSO_4$, filtered and concentrated under reduced pressure. The resulting epoxide was then

dissolved in CH_2Cl_2 (60 mL) and $BF_3.OEt_2$ (1.40 mL, 1.57 g, 11.1 mmol) was added dropwise. Upon complete addition, the resulting mixture was allowed to stir at r.t. for 16 h under nitrogen. The reaction mixture was poured into a saturated $NaHCO_3$ solution (60 mL) and the product was extracted with CH_2Cl_2 (2 x 60 mL) and then dried with $MgSO_4$. After filtration and solvent removal under reduced pressure, the residue was purified by silica gel flash column chromatography [petroleum ether-EtOAc (90:10)] to give indanone **33** as a yellow oil (540 mg, 33%).

^{1}H NMR (400 MHz, $CDCl_3$) δ 7.33 - 7.26 (m, 4H), 3.62 (d, *J* = 22.5 Hz, 1H), 3.58 - 3.46 (m, 2H), 1.42 (d, *J* = 7.5 Hz, 3H); **^{13}C NMR (101 MHz, $CDCl_3$)** δ 217.9, 143.3, 136.2, 127.6, 127.5, 124.8, 124.3, 47.7, 42.9, 15.6.

The data match those reported in the literature.[158]

Ethyl 2-oxo-2,3-dihydro-1*H*-indene-1-carboxylate (**34**)

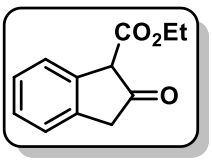

Following literature procedure[66], 2-indanone (2.0 g, 15.1 mmol) was added to a flask containing NaH (60% dispersion in mineral oil, 0.730 g, 18.2 mmol) and diethyl carbonate (19.6 mL, 161.9 mmol) under argon. The reaction was stirred at reflux for 2 h, and then allowed to cool to r.t. The resulting mixture was poured into 2M HCl (40 mL) and the product was extracted with EtOAc (3 x 40 mL). The combined organic layers were dried with $MgSO_4$, filtered and concentrated under reduced pressure. The crude material was then subjected to silica gel flash column chromatography [petroleum ether-EtOAc (97:3)] to give product **34** as a yellow solid (1.75, 57%).

^{1}H NMR (400 MHz, $CDCl_3$) δ 11.09 (s, 1H), 7.61 (d, *J* = 7.5 Hz, 1H), 7.31 - 7.25 (m, 2H), 7.11 (t, *J* = 7.5 Hz, 1H), 4.43 (q, *J* = 7.0 Hz, 2H), 3.58 (s, 2H), 1.46 (t, 7.0 Hz, 3H); **^{13}C NMR (101 MHz, $CDCl_3$)** δ 180.7, 169.0, 139.8, 133.1, 127.2, 123.8, 123.7, 120.1, 105.2, 60.7, 37.5, 14.5.

The data match those reported in the literature.[66]

5.2.4. Pd-catalysed Allylation of α-Aryl-Ketones

General Procedure 5 (**GP5**)

A flame-dried flask was charged with $Pd(dba)_2$ (5 mol%), ligand **L10** (15 mol%) and cyclic carbamate **17** (1.0 eq.) under nitrogen. CH_2Cl_2 (0.1 M) was then added and the reaction was stirred at r.t. After 5 min, a solution of the indanone (1.5 eq.) in CH_2Cl_2 (0.5 mL) was added and the resulting mixture was allowed to stir at r.t. for 3 h. The solvent was then removed under reduced pressure and the crude material was subjected to silica gel flash column chromatography to give the allylation product.

tert-Butyl (2-((2-oxo-1-phenyl-2,3-dihydro-1*H*-inden-1-yl)methyl)allyl)carbamate (**35**)

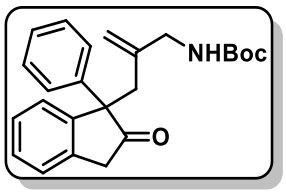

Following **GP5** using $Pd(dba)_2$ (69 mg, 0.12 mmol), ligand **L10** (114 mg, 0.360 mmol), carbamate **17** (512 mg, 2.40 mmol) and indanone **22** (1.0 g, 4.80 mmol). Following silica gel flash column chromatography (gradient from 5-10% EtOAc in petroleum ether) compound **35** was isolated as a colourless solid (820 mg, 90%)

m.p.: 95 - 97 °C; **^{1}H NMR (400 MHz, $CDCl_3$)** δ 7.41 - 7.19 (m, 9H), 4.87 (s, 1H), 4.65 (s, 1H), 4.47 (br, 1H), 3.59 (d, *J* = 22.5 Hz, 1H), 3.46 (d, *J* = 22.5 Hz, 1H), 3.41 - 3.28 (m, 2H), 3.11 (dd, *J* = 16.0, 5.5 Hz, 1H), 2.82 (d, *J* = 14.0 Hz, 1H), 1.41 (s, 9H); **^{13}C NMR (101 MHz, $CDCl_3$)** δ 216.4, 155.7, 143.4, 142.3, 141.4, 136.9, 128.7, 128.2, 127.8, 127.3, 127.1, 126.7, 125.1, 115.5, 79.3, 63.0, 46.1, 42.8, 41.6, 28.5; **FTIR:** ν_{max}/cm^{-1} (neat) 3363, 2978, 1749, 1712, 1496, 1249, 1169; **HRMS (ESI$^+$):** *m/z* calcd. for $C_{24}H_{27}NO_3Na$: 400.1883, found 400.1890 $[M+Na]^+$.

tert-Butyl(2-((2-oxo-1-(4-(trifluoromethyl)phenyl)-2,3-dihydro-1*H*-inden-1-yl) methyl)allyl)carbamate (**36**)

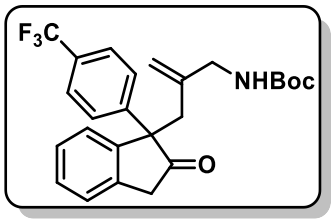

Following **GP5** using $Pd(dba)_2$ (13 mg, 0.023 mmol), ligand **L10** (22 mg, 0.070 mmol), carbamate **17** (100 mg, 0.469 mmol) and indanone **27** (194 mg, 0.703 mmol). Following silica gel flash column chromatography [petroleum ether-EtOAc (90:10)] compound **36** was isolated as a yellow oil (208 mg, 99%).

^{1}H NMR (400 MHz, $CDCl_3$) δ 7.53 (d, *J* = 8.0 Hz, 2H), 7.42 - 7.35 (m, 5H), 7.31 - 7.28 (m, 1H), 4.88 (s, 1H), 4.65 (s, 1H), 4.47 (br, 1H), 3.58 (d, *J* = 22.5 Hz, 1H), 3.49 (d, *J* = 22.5 Hz, 1H), 3.36 - 3.30 (m, 2H), 3.10 (dd, *J* = 16.0, 5.5 Hz, 1H), 2.81 (d, *J* = 14.0 Hz, 1H), 1.41 (s, 9H); **^{13}C NMR (101 MHz, $CDCl_3$)** δ 215.8, 155.8, 145.3, 142.6, 141.9, 136.9, 129.5 (q, *J* = 32.5 Hz), 128.6, 128.1, 127.7, 126.7, 125.5 (q, *J* = 3.0 Hz), 125.3, 125.2 (q, *J* = 272.5 Hz), 115.8, 79.5, 63.0, 46.1, 42.8, 41.8, 28.5; **FTIR:** ν_{max}/cm^{-1} (neat) 3384, 2979, 1752, 1704, 1511, 1325, 1249, 1167, 1124, 1070; **HRMS (ESI$^+$):** *m/z* calcd. for $C_{25}H_{26}F_3NO_3Na$: 468.1757, found 468.1770 $[M+Na]^+$.

tert-Butyl(2-((2-oxo-1-(*p*-tolyl)-2,3-dihydro-1*H*-inden-1-yl)methyl)allyl)carbamate (**37**)

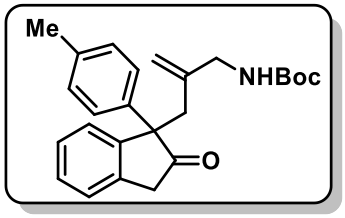

Following **GP5** using $Pd(dba)_2$ (36 mg, 0.063 mmol), ligand **L10** (60 mg, 0.19 mmol), carbamate **17** (269 mg, 1.26 mmol) and indanone **28** (420 mg, 1.89 mmol). Following silica gel flash column chromatography [petroleum ether-EtOAc (90:10)] compound **37** was isolated as an off-white amorphous solid (385 mg, 78%).

^{1}H NMR (400 MHz, $CDCl_3$) δ 7.37 - 7.28 (m, 4H), 7.12 - 7.07 (m, 4H), 4.86 (s, 1H), 4.65 (s, 1H), 4.48 (br, 1H), 3.61 (d, *J* = 22.5 Hz, 1H), 3.44 (d, *J* = 22.5 Hz, 1H), 3.36 - 3.30 (m, 2H), 3.10 (dd, *J* = 16.0, 5.5 Hz, 1H), 2.79 (d, *J* = 14.0 Hz, 1H), 2.29 (s, 3H) 1.41 (s, 9H); **^{13}C NMR (101 MHz, $CDCl_3$)** δ 216.6, 155.7, 143.5, 142.4, 138.5, 137.1, 136.9, 129.4, 128.1, 127.8, 127.0, 126.7, 125.1, 115.4, 79.4, 62.7, 46.1, 42.8, 41.6, 28.5, 21.1; **FTIR:** ν_{max}/cm^{-1} (neat) 3363, 2977, 1749, 1711, 1509, 1391, 1366, 1248, 1168; **HRMS (ESI$^+$):** *m/z* calcd. for $C_{25}H_{29}NO_3Na$: 414.2040, found 414.2044 $[M+Na]^+$.

tert-Butyl (2-((1-(4-methoxyphenyl)-2-oxo-2,3-dihydro-1*H*-inden-1-yl) methyl)allyl)carbamate (**38**)

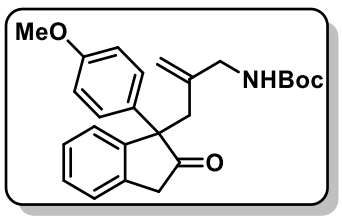

Following **GP5** using $Pd(dba)_2$ (24 mg, 0.042 mmol), ligand **L10** (40 mg, 0.13 mmol), carbamate **17** (180 mg, 0.844 mmol) and indanone **29** (300 mg, 1.26 mmol). Following silica gel flash column chromatography [petroleum ether-EtOAc (85:15)] compound **38** was isolated as a colourless oil (210 mg, 61%).

^{1}H NMR (400 MHz, $CDCl_3$) δ 7.40 - 7.27 (m, 4H), 7.14 - 7.10 (m, 2H), 6.82 - 6.78 (m, 2H), 4.85 (s, 1H), 4.64 (s, 1H), 4.48 (br, 1H), 3.76 (s, 3H), 3.58 (d, *J* = 22.5 Hz, 1H), 3.44 (d, *J* = 22.5 Hz, 1H), 3.37 - 3.30 (m, 2H), 3.10 (dd, *J* = 16.0, 5.5 Hz, 1H), 2.78 (d, *J* = 14.0 Hz, 1H), 1.41 (s, 9H); **^{13}C NMR (101 MHz, $CDCl_3$)** δ 216.6, 158.7, 155.7, 143.4, 142.2, 136.7, 133.4, 128.2, 128.0, 127.6, 126.6, 125.0, 115.3, 113.9, 79.3, 62.1, 55.3, 45.9, 42.5, 41.6, 28.4; **FTIR:** v_{max}/cm^{-1} (neat) 3385, 2976, 1747, 1709, 1508, 1391, 1366, 1251, 1168, 1034; **HRMS (ESI^+):** *m/z* calcd. for $C_{25}H_{29}NO_4Na$: 430.1989, found 430.1996 $[M+Na]^+$.

tert-Butyl (2-((1-(3-methoxyphenyl)-2-oxo-2,3-dihydro-1*H*-inden-1-yl) methyl)allyl)carbamate (**39**)

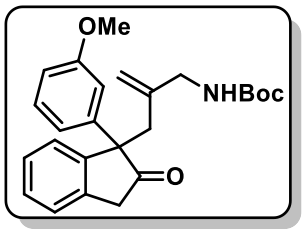

Following **GP5** using $Pd(dba)_2$ (12 mg, 0.021 mmol), ligand **L10** (20 mg, 0.064 mmol), carbamate **17** (91 mg, 0.426 mmol) and indanone **31** (152 mg, 0.639 mmol). Following silica gel flash column chromatography [petroleum ether-EtOAc (85:15)] compound **39** was isolated as a colourless oil (139 mg, 80%).

^{1}H NMR (400 MHz, $CDCl_3$) δ7.39 - 7.29 (m, 4H), 7.22 - 7.18 (m, 1H), 6.80 (d, *J* = 8.0 Hz, 1H), 6.77 - 6.75 (m, 2H), 4.86 (s, 1H), 4.65 (s, 1H), 4.47 (br, 1H), 3.74 (s, 3H), 3.60 (d, *J* = 22.5 Hz, 1H), 3.45 (d, *J* = 22.5 Hz, 1H), 3.38 - 3.31 (m, 2H), 3.10 (dd, *J* = 16.0, 5.5 Hz, 1H), 2.81 (d, *J* = 14.0 Hz, 1H), 1.41 (s, 9H); **^{13}C NMR (101 MHz, $CDCl_3$)** δ 216.0, 159.6, 155.6, 143.2, 142.9, 142.1, 136.7, 131.9, 129.5, 128.1, 127.7, 126.6, 125.0, 119.5, 115.4, 113.6, 112.0, 62.1, 55.2, 45.9, 42.7, 41.4, 28.4; **FTIR:** v_{max}/cm^{-1} (neat) 3385, 2977, 2933, 1749, 1709, 1598, 1483, 1366, 1249, 1166, 1052; **HRMS (ESI^+):** *m/z* calcd. for $C_{25}H_{29}NO_4Na$: 430.1989, found 430.1988 $[M+Na]^+$.

Ethyl 1-(2-(((*tert*-butoxycarbonyl)amino)methyl)allyl)-2-oxo-2,3-dihydro-1*H*-indene-1-carboxylate (**40**)

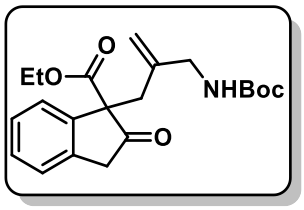

Following **GP5** using $Pd(dba)_2$ (27 mg, 0.047 mmol), ligand **L10** (44 mg, 0.14 mmol), carbamate **17** (200 mg, 0.938 mmol) and indanone **34** (287 mg, 1.41 mmol). Following silica gel flash column chromatography [petroleum ether-EtOAc (75:25)] compound **40** was isolated as a yellow oil (260 mg, 74%).

^{1}H NMR (400 MHz, $CDCl_3$) δ7.35 - 7.30 (m, 4H), 4.85 (s, 1H), 4.61 (s, 1H), 4.48 (br, 1H), 4.16 - 4.01 (m, 2H), 3.74 (d, *J* = 22.5 Hz, 1H), 3.49 (d, *J* = 22.5 Hz, 1H), 3.33 (dd, *J* = 16.0 Hz, 6.0 Hz, 1H), 3.14 (dd, *J* = 16.0, 6.0 Hz, 1H), 3.04 (d, *J* = 14.5 Hz, 1H), 2.94 (d, *J* = 14.5 Hz, 1H), 1.40 (s, 9H), 1.12 (t, *J* = 7.0 Hz, 3H); **^{13}C NMR (101 MHz, $CDCl_3$)** δ 212.4, 170.2, 155.7, 141.1, 140.5, 137.5, 128.9, 128.0, 125.3, 124.6, 115.7, 79.4, 65.5, 62.0, 46.1, 43.8, 37.5, 28.5, 14.0; **FTIR:** ν_{max}/cm^{-1} (neat) 3406, 2978, 2932, 1758, 1713, 1505, 1391, 1367, 1230, 1166, 1051, 1019; **HRMS (ESI^+):** *m/z* calcd. for $C_{21}H_{27}NO_5Na$: 396.1781, found 396.1784 $[M+Na]^+$.

tert-Butyl (2-((2-oxo-1-phenyl-1,2,3,4-tetrahydronaphthalen-1-yl) methyl)allyl)carbamate (**52a**)

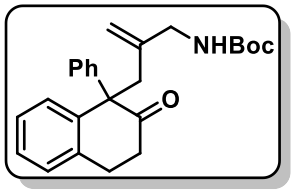

Following **GP5** using $Pd(dba)_2$ (140 mg, 0.243 mmol), ligand **L10** (231 mg, 0.732 mmol), carbamate **17** (1.03 g, 4.83 mmol) and 1-phenyl-3,4-dihydronaphthalen-2(1*H*)-one (1.62 g, 7.29 mmol). Following silica gel flash column chromatography [petroleum ether-EtOAc (85:15)] compound **52a** was isolated as an amorphous off-white solid (1.72 g, 91%).

^{1}H NMR (400 MHz, $CDCl_3$) δ7.30 - 7.15 (m, 7H), 7.12 - 7.08 (m, 2H), 4.85 (s, 1H), 4.62 (br, 1H), 4.44 (s, 1H), 3.68 (d, *J* = 15.0 Hz, 1H), 3.42 (dd, *J* = 15.5 Hz, 6.0 Hz, 1H), 3.23 (dd, 15.5 Hz, 5.5 Hz, 1H), 3.01 - 2.75 (m, 3H), 2.68 (d, *J* = 15.0 Hz, 1H), 2.56 - 2.47 (m, 1H), 1.42 (s, 9H); **^{13}C NMR (101 MHz, $CDCl_3$)** δ 210.3, 155.7, 143.0, 142.5, 139.1, 137.2, 129.7, 128.4, 128.0, 127.7, 127.0 (2C), 126.8, 114.7, 79.1, 61.0, 46.2, 41.1, 37.4, 28.3, 28.0; **FTIR:** ν_{max}/cm^{-1} (neat) 3372, 2977, 2927, 1713, 1505, 1445, 1366, 1170; **HRMS (ESI^+):** *m/z* calcd. for $C_{25}H_{29}NO_3Na$: 414.2040, found 414.2050 $[M+Na]^+$.

5.2.5. Synthesis of Functionalised Polycyclic Piperidines

General Procedure 6 (**GP6**)

TFA (75 eq.) was added to a flask containing the allylation substrate (1.0 eq.) and the reaction was stirred at r.t. for 1 h. The resulting mixture was concentrated under reduced pressure and residual TFA was removed by azeotropic distillation with toluene (3 x 1 mL). The iminium salt was then dissolved in MeOH (0.1 M) and added to a flame-dried flask containing sodium L-ascorbate (0.2 eq.), 3-mercaptopropionic acid (3 eq.), and $[Ru(bpy)_3](PF_6)_2$ (5 mmol%). The reaction mixture was degassed by three freeze-pump-thaw cycles and then irradiated with a 40 W blue LED (470 nm) photoreactor at r.t. for 16 h. After this time, the resulting mixture was diluted with a saturated solution of $NaHCO_3$ (40 mL) and extracted with CH_2Cl_2 (3 x 40 mL). The combined organic layers were dried with $MgSO_4$, filtered and concentrated under reduced pressure. The residue was then subjected to silica gel flash column chromatography to give the corresponding piperidine.

3-Methylene-4a-phenyl-2,3,4,4a,9,9a-hexahydro-1*H*-indeno[2,1-b]pyridine (**43**)

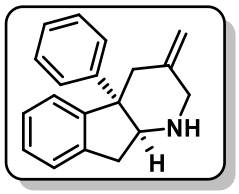

Following **GP6** using substrate **35** (156 mg, 0.413 mmol), sodium L-ascorbate (16 mg, 0.083 mmol), 3-mercaptopropionic acid (132 mg, 1.24 mmol) and $[Ru(bpy)_3](PF_6)_2$ (18 mg, 0.021 mmol). Following silica gel flash column chromatography [EtOAc-MeOH-Et_3N (94:5:1)] compound **43** was isolated as a yellow oil (59 mg, 55%).

^{1}H NMR (400 MHz, $CDCl_3$) δ 7.31 - 7.12 (m, 9H), 4.79 (s, 1H), 4.77 (s, 1H), 3.88 (dd, *J* = 5.5, 3.0 Hz, 1H), 3.40 (s, 2H), 3.03 (d, *J* = 14.5 Hz, 1H), 2.96 - 2.86 (m, 2H), 2.71 (dd, *J* = 16.0, 3.0 Hz, 1H), 2.18 (br, 1H); **^{13}C NMR (101 MHz, $CDCl_3$)** δ 146.6 (2C), 143.0, 142.0, 128.3, 127.4, 127.3, 126.9, 126.4, 125.9, 125.3, 109.9, 66.4, 57.8, 49.8, 41.8, 36.3; **FTIR:** ν_{max}/cm^{-1} (neat) 3064, 2923, 2842, 1652, 1599, 1493, 1458, 1444, 1109; **HRMS (ESI$^+$):** *m/z* calcd. for $C_{19}H_{20}N$: 262.1590, found 262.1589 $[M+H]^+$.

3-Methylene-4a-(4-(trifluoromethyl)phenyl)-2,3,4,4a,9,9a-hexahydro-1*H*-indeno[2,1-*b*] pyridine (**44**)

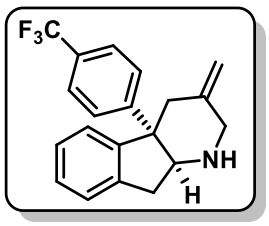

Following **GP6** using substrate **36** (192 mg, 0.431 mmol), sodium L-ascorbate (17 mg, 0.086 mmol), 3-mercaptopropionic acid (137 mg, 1.29 mmol) and $[Ru(bpy)_3](PF_6)_2$ (19 mg, 0.022 mmol). Following silica gel flash column chromatography [EtOAc-MeOH-Et_3N (94:5:1)] compound **44** was isolated as a yellow oil (82 mg, 58%).

^{1}H NMR (400 MHz, $CDCl_3$) δ 7.49 (d, *J* = 8.0 Hz, 2H), 7.33 - 7.25 (m, 5H), 7.20 - 7.17 (m, 1H), 4.82 (s, 1H), 4.80 (s, 1H), 3.85 (dd, *J* = 5.5, 3.5 Hz, 1H), 3.42 (s, 2H),

3.01 (d, *J* = 14.5 Hz, 1H), 2.96 - 2.85 (m, 2H), 2.77 (dd, *J* = 16.0, 3.5 Hz, 1H), 1.85 (br, 1H); **^{13}C NMR (101 MHz, $CDCl_3$)** δ 150.9, 146.2, 142.7, 141.9, 128.6 (q, *J* = 32.0 Hz), 127.9, 127.7, 127.1, 126.0, 125.2, 125.1 (q, *J* = 4.0 Hz), 124.3 (q, *J* = 267 Hz), 110.0, 66.6, 57.7, 49.6, 41.6, 36.2; **FTIR:** ν_{max}/cm^{-1} (neat) 3069, 2925, 1618, 1408, 1324, 1163, 1116, 1070; **HRMS (ESI$^+$):** *m/z* calcd. for $C_{20}H_{19}F_3N$: 330.1464, found 330.1466 $[M+H]^+$.

3-Methylene-4a-(*p*-tolyl)-2,3,4,4a,9,9a-hexahydro-1*H*-indeno[2,1-b]pyridine (**45**)

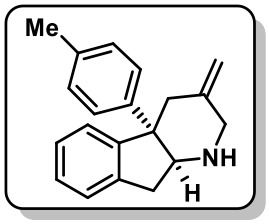

Following **GP6** using substrate **37** (180 mg, 0.460 mmol), sodium L-ascorbate (18 mg, 0.092 mmol), 3-mercaptopropionic acid (146 mg, 1.38 mmol) and $[Ru(bpy)_3](PF_6)_2$ (20 mg, 0.023 mmol). Following silica gel flash column chromatography [EtOAc-MeOH-Et_3N (94:5:1)] compound **45** was isolated as a yellow oil (68 mg, 53%).

^{1}H NMR (400 MHz, $CDCl_3$) δ 7.32 - 7.19 (m, 4H), 7.08 - 7.01 (m, 4H), 4.78 (s, 1H), 4.76 (s, 1H), 3.85 (dd, *J* = 5.5, 3.0 Hz, 1H), 3.39 (s, 2H), 3.01 (d, *J* = 14.5 Hz, 1H), 2.96 - 2.85 (m, 2H), 2.70 (dd, *J* = 16.0, 3.0 Hz, 1H), 2.30 (s, 3H), 2.24 (br, 1H); **^{13}C NMR (101 MHz, $CDCl_3$)** δ 146.8, 143.6, 143.3, 142.0, 135.9, 128.9, 127.3, 127.2, 126.8, 125.9, 125.3, 109.6, 66.4, 57.5, 49.8, 41.8, 36.3, 21.0; **FTIR:** ν_{max}/cm^{-1} (neat) 3067, 2921, 1651, 1510, 1457, 1432; **HRMS (ESI$^+$):** *m/z* calcd. for $C_{20}H_{22}N$: 276.1747, found 276.1750 $[M+H]^+$.

4a-(4-Methoxyphenyl)-3-methylene-2,3,4,4a,9,9a-hexahydro-1*H*-indeno[2,1-b] pyridine (**46**)

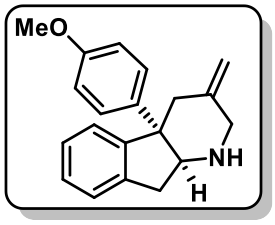

Following **GP6** using substrate **38** (194 mg, 0.476 mmol), sodium L-ascorbate (19 mg, 0.095 mmol), 3-mercaptopropionic acid (152 mg, 1.43 mmol) and $[Ru(bpy)_3](PF_6)_2$ (21 mg, 0.024 mmol). Following silica gel flash column chromatography [EtOAc-MeOH-Et_3N (94:5:1)] compound **46** was isolated as a yellow oil (73 mg, 53%).

^{1}H NMR (400 MHz, $CDCl_3$) δ 7.32 - 7.18 (m, 4H), 7.06 (d, *J* = 9.0 Hz, 2H), 6.78 (d, *J* = 9.0 Hz, 2H), 4.78 (s, 1H), 4.76 (s, 1H), 3.83 (dd, *J* = 5.5, 3.0 Hz, 1H), 3.77 (s, 3H), 3.39 (s, 2H), 3.00 (d, *J* = 14.5 Hz, 1H), 2.94 (dd, *J* = 16.0, 5.5 Hz, 1H), 2.87 (d, *J* = 14.5 Hz, 1H), 2.72 (dd, *J* = 16.0, 3.0 Hz, 1H), 1.91 (br, 1H); **^{13}C NMR (101 MHz, $CDCl_3$)** δ 158.0, 147.0, 143.3, 142.0, 138.7, 128.5, 127.2, 126.8, 125.8, 125.2, 113.5, 109.6, 66.5, 57.1, 55.3, 49.8, 41.9, 36.3; **FTIR:** ν_{max}/cm^{-1} (neat) 3066, 2929, 2835, 1607, 1508, 1458, 1294, 1247, 1182; **HRMS (ESI$^+$):** *m/z* calcd. for $C_{20}H_{22}NO$: 292.1696, found 292.1682 $[M+H]^+$.

4a-(3-Methoxyphenyl)-3-methylene-2,3,4,4a,9,9a-hexahydro-1H-indeno[2,1-b] pyridine (**47**)

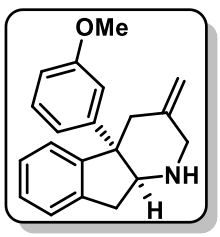

Following **GP6** using substrate **39** (129 mg, 0.316 mmol), sodium L-ascorbate (13 mg, 0.063 mmol), 3-mercaptopropionic acid (101 mg, 0.950 mmol) and $[Ru(bpy)_3](PF_6)_2$ (14 mg, 0.016 mmol). Following silica gel flash column chromatography [EtOAc-MeOH-Et_3N (94:5:1)] compound **47** was isolated as a yellow oil (48 mg, 52%).

^{1}H NMR (400 MHz, $CDCl_3$) δ 7.31 - 7.14 (m, 5H), 6.76 - 6.69 (m, 3H), 4.79 (s, 1H), 4.76 (s, 1H), 3.86 (dd, *J* = 5.5, 3.0 Hz, 1H), 3.73 (s, 3H), 3.39 (s, 2H), 3.02 (d, *J* = 14.5 Hz, 1H), 2.94 (dd, *J* = 16.0, 5.5 Hz, 1H), 2.87 (d, *J* = 14.5 Hz, 1H), 2.72 (dd, *J* = 16.0, 3.0 Hz, 1H), 1.84 (br, 1H); **^{13}C NMR (101 MHz, $CDCl_3$)** δ 159.4, 148.5, 146.6, 143.3, 142.0, 129.2, 127.3, 126.9, 125.9, 125.3, 120.0, 114.2, 110.9, 109.6, 66.5, 57.8, 55.2, 49.8, 41.8, 36.4; **FTIR:** ν_{max}/cm^{-1} (neat) 3066, 2937, 2835, 1599, 1580, 1483, 1458, 1431, 1290, 1247, 1052; **HRMS (ESI$^+$):** *m/z* calcd. for $C_{20}H_{22}NO$: 292.1696, found 292.1689 [*M*+*H*]$^+$.

Ethyl 3-methylene-1,2,3,4,9,9a-hexahydro-4a*H*-indeno[2,1-b]pyridine-4a-carboxylate (**48**)

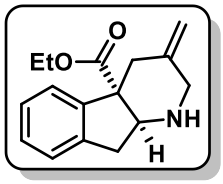

Following **GP6** using substrate **40** (98 mg, 0.278 mmol), sodium L-ascorbate (11 mg, 0.056 mmol), 3-mercaptopropionic acid (89 mg, 0.84 mmol) and $[Ru(bpy)_3](PF_6)_2$ (12 mg, 0.014 mmol). Following silica gel flash column chromatography (100% EtOAc) compound **48** was isolated as a yellow oil (41 mg, 57%).

^{1}H NMR (400 MHz, $CDCl_3$) δ 7.27 - 7.19 (m, 4H), 4.77 (s, 1H), 4.76 (s, 1H), 4.21 - 4.09 (m, 3H), 3.35 (d, *J* = 14.5 Hz, 1H), 3.29 - 3.20 (m, 2H), 2.99 (d, *J* = 14.0 Hz, 1H), 2.91 (dd, *J* = 16.0 Hz, 5.5 Hz, 1H), 2.63 (d, *J* = 14.0 Hz, 1H), 1.78 (br, 1H), 1.24 (t, *J* = 7.0 Hz, 3H); **^{13}C NMR (101 MHz, $CDCl_3$)** δ 174.0, 143.3, 142.5, 141.5, 127.9, 127.0, 125.3, 124.2, 109.9, 61.1, 60.5, 59.2, 48.5, 38.9, 36.1, 14.3; **FTIR:** ν_{max}/cm^{-1} (neat) 3067, 2981, 2930, 851, 1721, 1658, 1610, 1474, 1459, 1367, 1260, 1212, 1161, 1038, 1024, 898, 862, 748; **HRMS (ESI$^+$):** *m/z* calcd. for $C_{16}H_{20}NO_2$: 258.1489, found 258.1485 [*M*+*H*]$^+$.

5.2.6. Functionalisation of Polycyclic Piperidines

4a-(3-Methoxyphenyl)-1,2,4,4a,9,9a-hexahydro-3*H*-indeno[2,1-b]pyridin-3-one (**51**)

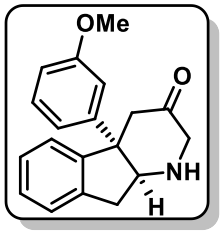

Di-*tert*-butyl dicarbonate (372 mg, 1.70 mmol) was added to a solution of piperidine **47** (248 mg, 0.851 mmol) and DMAP (21 mg, 0.170 mmol) in CH_2Cl_2 (10 mL), and the reaction was stirred at r.t. for 2 h. The reaction mixture was then diluted with CH_2Cl_2 (10 mL) and washed with 5% citric acid (3 x 15 mL) and brine (1 x 15 mL). The organic layer was dried with $MgSO_4$, filtered and concentrated under reduced pressure. The residue was then dissolved in CH_2Cl_2 (5.1 mL) and MeCN (5.1 mL), and 2,6-lutidine (182 mg, 1.70 mmol), H_2O (7.7 mL) and $NaIO_4$ (728 mg, 3.40 mmol) were added sequentially. Ruthenium(III) chloride hydrate (18 mg, 0.068 mmol, 8 mol%) was then added and the reaction was stirred vigorously for 16 h at r.t. After this time the resulting mixture was diluted with H_2O (20 mL) and the product was extracted with CH_2Cl_2 (3 x 20 mL). The combined organic layers were then washed with brine (1 x 30 mL) and dried with $MgSO_4$. After filtration and removal of solvents under reduced pressure, the residue was subjected to silica gel flash column chromatography [petroleum ether-EtOAc (85:15)]. The oxidised compound was then dissolved in CH_2Cl_2 (4 mL), and trifluoroacetic acid (4 mL) was added to the reaction mixture. The reaction was allowed to stir at r.t for 1.5 h, and then poured into a saturated $NaHCO_3$ solution (30 mL). The product was extracted with CH_2Cl_2 (3 x 30 mL), dried with $MgSO_4$ and concentrated under reduced pressure to give compound **51** as a pure yellow oil without further purification (168 mg, 67%).

^{1}H NMR (400 MHz, $CDCl_3$) δ 7.33 - 7.22 (m, 3H), 7.19 (t, *J* = 8.0 Hz, 1H), 7.07 (dd, *J* = 6.0 Hz, 2.0 Hz, 1H), 6.73 (dd, *J* = 8.0 Hz, 2.0 Hz, 1H), 6.59 (dd, *J* = 8.0 Hz, 2.0 Hz, 1H), 6.50 (t, *J* = 2.0 Hz, 1H), 3.76 (dd, *J* = 7.5 Hz, 2.0 Hz, 1H), 3.72 (s, 3H), 3.45 (dd, *J* = 17.0 Hz, 7.5 Hz, 1H), 3.36 (d, *J* = 15.5 Hz, 1H), 3.34 (s, 2H), 3.05 (d, *J* = 15.5 Hz, 1H), 2.89 (dd, *J* = 17.0 Hz, 2.0 Hz, 1H), 2.07 (br, 1H); **^{13}C NMR (101 MHz, $CDCl_3$)** δ 212.4, 159.8, 148.7, 147.4, 141.4, 129.8, 128.1, 127.8, 125.0, 124.9, 118.9, 113.1, 111.3, 66.9, 57.8, 55.3, 54.1, 48.3, 38.5; **FTIR:** ν_{max}/cm^{-1} (neat) 3061, 2917, 2849, 1674, 1599, 1581, 1486, 1458, 1432, 1290, 1256, 1174, 1049; **HRMS (ESI$^+$):** *m/z* calcd. for $C_{19}H_{20}NO_2$: 294.1489, found 294.1496 $[M+H]^+$.

4a-Allyl-2-methylene-10b-phenyl-1,2,3,4,4a,5,6,10b-octahydrobenzo[f]quinoline (**53**)

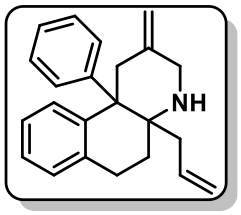

TFA (3 mL) was added to a flask containing a solution of compound **52a** (186 mg, 0.475 mmol) in CH_2Cl_2 (3 mL). The reaction was stirred at r.t. for 1 h, and then poured into a saturated $NaHCO_3$ solution (20 mL). The imine was extracted with CH_2Cl_2 (3 x 20 mL) and dried with $MgSO_4$. After filtration and solvent removal under reduced pressure, the residue was dissolved in CH_2Cl_2 (2.5 mL) and added to a freshly prepared solution of Al(allyl)Et_2 (0.5 M in hexane, 1.4 mL, 0.70 mmol, 1.5 eq.). The reaction was allowed to stir at r.t. for 24 h under argon, then quenched with H_2O (20 mL) and the product was extracted with EtOAc (3 x 20 mL). The combined organic layers were dried with $MgSO_4$, filtered and concentrated under reduced pressure. The resulting crude material was then purified by silica gel flash column chromatography [petroleum ether-EtOAc (60:40)] to give product **53** as a yellow oil (86 mg, 57%).

^{1}H NMR (400 MHz, $CDCl_3$) δ 7.23 - 7.06 (m, 9H), 5.84 (ddt, *J* = 17.0 Hz, 10.0 Hz, 7.0 Hz, 1H), 5.09 (d, *J* = 10.0 Hz, 1H), 5.01 (d, 17.0 Hz, 1H), 4.71 (s, 1H), 4.64 (s, 1H), 3.51 (d, 14.5 Hz, 2H), 3.29 (d, 14.5 Hz, 1H), 3.02 - 2.94 (m, 3H), 2.61 (br, 1H), 2.00 - 1.91 (m, 1H), 1.83 - 1.68 (m, 3H); **^{13}C NMR (101 MHz, $CDCl_3$)** δ 146.5, 144.2, 142.2, 136.0, 134.5, 130.0, 129.4, 129.1, 127.3, 126.5, 126.1, 126.0, 117.8, 109.3, 55.8, 52.5, 47.1, 40.3, 38.5, 26.6, 25.4; **FTIR:** ν_{max}/cm^{-1} (neat) 3065, 3016, 2937, 2850, 1637, 1597, 1493, 1443, 1265, 1079, 1038; **HRMS (ESI^+):** *m/z* calcd. for $C_{23}H_{26}N$: 316.2060, found 316.2068 $[M+H]^+$.

5.2.7. 3-Fluoropiperidines: Asymmetric Investigations

Ethyl 2-fluoro-3-oxo-3-phenylpropanoate (**80**)[108]

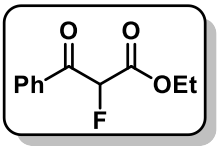

To a suspension of NaH (60% dispersion in mineral oil, 2.08 g, 52.0 mmol) in THF (42 mL) under nitrogen was added acetophenone (2.50 g, 20.8 mmol) and diethyl carbonate (6.88 g, 58.3 mmol) and the resulting mixture was heated to reflux for 16 h.The reaction was then cooled to r.t., diluted with AcOH (2.1 mL) and H_2O (80 mL) and extracted with CH_2Cl_2 (3 x 80 mL). The combined organic layers were then dried over $MgSO_4$, filtered and concentrated under reduced pressure. The residue was then dissolved in MeCN (42 mL) under nitrogen and Selectfluor^{TM} (8.84 g, 25.0 mmol) was added and the resulting mixture was heated to 50 °C for 16 h. After cooling to r.t., the reaction was diluted with H_2O (80 mL) and the product was extracted with EtOAc (3 x 80 mL) and dried with $MgSO_4$. After filtration and solvent removal under reduced pressure,

the crude residue was subjected to silica gel flash column chromatography [petroleum ether-EtOAc (90:10)] to give compound **80** as a yellow oil (3.60 g, 82%).

^{1}H NMR (400 MHz, $CDCl_3$) δ 8.05 - 8.00 (m, 2H), 7.66 - 7.59 (m, 1H), 7.52 - 7.46 (m, 2H), 5.87 (d, *J* = 49.0 Hz, 1H), 4.34 - 4.22 (m, 2H), 1.24 (t, *J* = 7.0 Hz, 3H); **^{13}C NMR (101 MHz, $CDCl_3$)** δ 189.6 (d, *J* = 20.0 Hz), 165.0 (d, *J* = 24.0 Hz), 134.6, 133.5 (d, *J* = 2.0 Hz), 129.6 (d, *J* = 3.5 Hz), 128.9, 90.1 (d, *J* = 197.5 Hz), 62.8, 14.0; **^{19}F NMR (377 MHz, $CDCl_3$)** δ -190.4 (d, *J* = 49.0 Hz); **FTIR:** v_{max}/cm^{-1} (neat) 2984, 1758, 1692, 1597, 1449, 1241, 1096, 1014.

The data match those reported in the literature.[159]

Ethyl 2-benzoyl-4-(((tert-butoxycarbonyl)amino)methyl)-2-fluoropent-4-enoate (**81**)

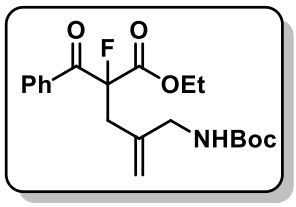

A flame-dried flask was charged with $Pd(dba)_2$ (6 mg, 0.01 mmol), ligand **L10** (10 mg, 0.03 mmol) and cyclic carbamate **17** (43 mg, 0.20 mmol) under nitrogen. CH_2Cl_2 (3 mL) was then added and the reaction was stirred at r.t. After 5 min, substrate **80** (63 mg, 0.30 mmol) was added in CH_2Cl_2 (0.5 mL) and the resulting mixture was allowed to stir at r.t. for 16 h. The solvent was then removed under reduced pressure and the crude material was subjected to silica gel flash chromatography [petroleum ether-EtOAc (80:20)] to give the allylation product **81** as a yellow oil (74 mg, 97%).

^{1}H NMR (400 MHz, $CDCl_3$) δ 8.02 (d, *J* = 8.0 Hz, 2H), 7.58 (t, *J* = 7.5 Hz, 1H), 7.45 (t, *J* = 8.0 Hz, 2H), 5.14 (s, 1H), 5.03 (s, 1H), 4.77 (br, 1H), 4.35 - 4.16 (m, 2H), 3.76 (d, *J* = 4.0 Hz, 2H), 3.14 (dd, *J* = 33.0, 15.0 Hz, 1H), 2.97 (dd, *J* = 18.5, 15.5 Hz, 1H), 1.43 (s, 9H), 1.20 (t, *J* = 7.0 Hz, 3H); **^{13}C NMR (101 MHz, $CDCl_3$)** δ 191.3 (d, *J* =

26.0 Hz), 167.1 (d, *J* = 26.0 Hz), 155.9, 139.8, 134.1, 133.8 (d, *J* = 3.0 Hz), 129.9 (d, *J* = 5.5 Hz), 128.8, 116.2, 100.0 (d, *J* = 200.0 Hz), 79.5, 62.9, 45.8, 38.2 (d, *J* = 20.5 Hz), 28.5, 14.1; **^{19}F NMR (377 MHz, $CDCl_3$)** δ -157.6 (dd, *J* = 33.0, 18.5 Hz); **FTIR:** ν_{max}/cm^{-1} (neat) 2981, 2931, 1755, 1697, 1509, 1449, 1267, 1240, 1168, 908, 729, 694; **HRMS (ESI$^+$):** *m/z* calcd. for $C_{20}H_{26}FNO_5Na$: 402.1687, found 402.1701 $[M+Na]^+$.

Ethyl 2-fluoro-3-phenyl-3-((trimethylsilyl)oxy)acrylate (**82**)

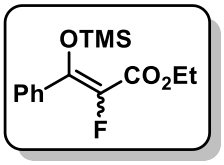

A flame-dried flask was charged with NaH (60% dispersion in mineral oil, 171 mg, 7.14 mmol) and Et_2O (2 mL) under nitrogen. The suspension was cooled to 0 °C and a solution of α-fluoro-β-ketoester **80** (450 mg, 2.14 mmol) in Et_2O (2 mL) was added and the reaction was stirred at r.t. After 30 min, the reaction mixture was cooled to 0 °C and chlorotrimethylsilane (0.54 mL, 465 mg, 4.28 mmol) was added. The reaction was then warmed to r.t. and stirred for 16 h. After this time, the reaction was filtered and concentrated under reduced pressure to give silyl enol ether **82** as a yellow oil without further purification (2:1 mixture of isomers, 571 mg, 95%). This compound was tentatively characterised by ^{1}H and ^{19}F NMR.

Major isomer:

^{1}H NMR (400 MHz, $CDCl_3$) δ 7.48 - 7.32 (m, 5H), 4.10 (q, *J* = 7.0 Hz, 2H), 1.10 (t, *J* = 7.0 Hz, 3H), 0.18 (s, 9H); **^{19}F NMR (377 MHz, $CDCl_3$)** δ -148.3.

Minor isomer:

^{1}H NMR (400 MHz, $CDCl_3$) δ 7.63 - 7.55 (m, 2H), 7.48 - 7.32 (m, 3H), 4.35 (q, *J* = 7.0 Hz, 2H), 1.38 (t, *J* = 7.0 Hz, 3H), 0.13 (s, 9H); **^{19}F NMR (377 MHz, $CDCl_3$)** δ -158.9.

Ethyl 3-((*tert*-butyldimethylsilyl)oxy)-2-fluoro-3-phenylacrylate (**83**)

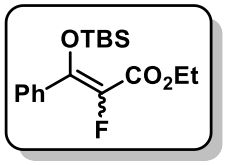

α-Fluoro-β-ketoester **80** (1.31 g, 6.23 mmol) was dissolved in CH_2Cl_2 (10 mL) and cooled to 0 °C. *tert*-Butyldimethylsilyl trifluoromethanesulfonate (2.9 mL, 3.29 g, 12.5 mmol) followed by Et_3N (2.2 mL, 1.58 g, 15.6 mmol) were each added dropwise and the reaction was allowed to warm to r.t. and stirred under nitrogen for 16 h. After solvent removal under reduced pressure, the crude material was subjected to silica gel flash column chromatography [petroleum ether-EtOAc (95:5)] to give silyl enol ether **83** as a colourless oil (5:1 mixture of isomers, 1.98 g, 98%).

Major isomer:

^{1}H NMR (400 MHz, $CDCl_3$) δ 7.42 - 7.33 (m, 5H), 4.09 (q, *J* = 7.0 Hz, 2H), 1.10 (t, *J* = 7.0 Hz, 3H), 0.89 (s, 9H), 0.06 (s, 6H); **^{13}C NMR (101 MHz, $CDCl_3$)** δ 161.9 (d, *J* = 30.0 Hz), 149.8 (d, *J* = 14.5 Hz), 138.2 (d, *J* = 241.5 Hz), 134.9, 129.6, 129.2 (d, *J* = 2.5 Hz), 127.9, 60.9, 25.5, 18.5, 14.0, -4.3; **^{19}F NMR (377 MHz, $CDCl_3$)** δ -148.3; **HRMS (ESI$^+$):** *m/z* calcd. for $C_{17}H_{26}FO_3Si$: 325.1630, found 325.1642 $[M+H]^+$.

Minor isomer:

^{1}H NMR (400 MHz, $CDCl_3$) δ 7.56 - 7.51 (m, 2H), 7.42 - 7.33 (m, 3H), 4.34 (q, *J* = 7.0 Hz, 2H), 1.37 (t, *J* = 7.0 Hz, 3H), 0.92 (s, 9H), -0.05 (s, 6H); **^{13}C NMR (101 MHz, $CDCl_3$)** δ 161.9 (d, *J* = 30.0 Hz), 149.8 (d, *J* = 14.5 Hz), 139.8 (d, *J* = 237.0 Hz), 134.7, 129.9, 128.5 (d, *J* = 5.5 Hz), 128.2, 61.0, 25.8, 18.6, 14.6, -4.2; **^{19}F NMR (377 MHz, $CDCl_3$)** δ -158.7; **HRMS (ESI$^+$):** *m/z* calcd. for $C_{17}H_{26}FO_3Si$: 325.1630, found 325.1642 $[M+H]^+$.

Ethyl (*E*)-2-fluoro-3-phenyl-3-(phenylamino)acrylate (**87**)[108]

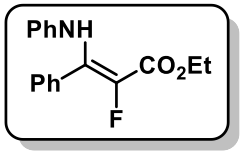

α-Fluoro-β-ketoester **80** (353 mg, 1.68 mmol) was added to a flask containing aniline (0.23 mL, 235 mg, 2.52 mmol), *p*-toluenesulfonic acid monohydrate (32 mg, 0.17 mmol) and toluene (8 mL). The reaction was stirred at reflux for 24 h, and then concentrated under reduced pressure. The crude residue was purified by silica gel flash column chromatography [petroleum ether-EtOAc (98:2)] to give enamine **87** as a yellow solid (305 mg, 64%, 98:2 E/Z). The crystallographic data of this compound is reported in the literature.[108]

^{1}H NMR (400 MHz, $CDCl_3$) δ 9.11 (br, 1H), 7.46 - 7.41 (m, 2H), 7.38 - 7.32 (m, 3H), 7.05 (t, *J* = 8.0 Hz, 2H), 6.86 (t, *J* = 7.5 Hz, 1H), 6.61 (d, *J* = 8.0 Hz, 2H), 4.36 (q, *J* = 7.0 Hz, 2H), 1.40 (t, *J* = 7.0 Hz, 3H); **^{19}F NMR (377 MHz, $CDCl_3$)** δ -170.8.

(*S*)-2,2'-Dimethoxy-1,1'-binaphthalene (**84a**)[107]

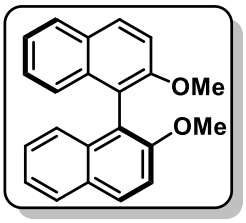

A flame-dried flask was charged with (*S*)-BINOL (4.64 g, 16.2 mmol), K_2CO_3 (7.61 g, 55.1 mmol) and acetone (150 mL) under nitrogen. Methyl iodide (5.0 mL, 11.5 g, 81.0 mmol) was then added to the suspension and the reaction was stirred at reflux for 20 h. The resulting mixture was cooled to r.t. and the solvent was removed under reduced pressure. The white solid was diluted with CH_2Cl_2 (200 mL) and H_2O (200 mL), then the layers were separated and the aqueous layer was further extracted with CH_2Cl_2 (2 x 100 mL). The combined organic layers were dried with $MgSO_4$, filtered and concentrated under reduced pressure to give (*S*)-2,2'-

dimethoxy-1,1'-binaphthalene as a white solid without further purification (5.09 g, quant.).

^{1}H NMR (400 MHz, $CDCl_3$) δ 7.99 (d, *J* = 9.0 Hz, 2H), 7.87 (d, *J* = 8.0 Hz, 2H), 7.47 (d, *J* = 9.0 Hz, 2H), 7.35 - 7.31 (m, 2H), 7.26 - 7.20 (m, 2H), 7.11 (d, *J* = 8.5 Hz, 2H), 3.77 (s, 6H); **^{13}C NMR (101 MHz, $CDCl_3$)** δ 155.0, 134.0, 129.4, 129.3, 128.0, 126.3, 125.3, 123.5, 119.5, 114.3, 56.9.

The data match those reported in the literature.[107]

(*S*)-3,3'-Dibromo-2,2'-dimethoxy-1,1'-binaphthalene (**84b**)[107]

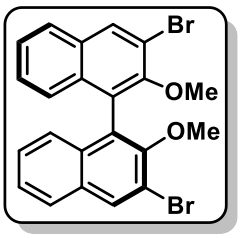

n-Buli (2.5 M in hexane, 15.8 mL, 39.4 mmol) and TMEDA (5.4 mL, 4.22 g, 36.3 mmol) were added to a flask containing Et_2O (250 mL) and the reaction was stirred at r.t. for 15 min. (*S)*-2,2'-dimethoxy-1,1'-binaphtyl (4.96 g, 15,8 mmol) was then added neat and the reaction was stirred at r.t. for 16 h. After this time, the reaction mixture was cooled to -78 °C and Br_2 (1.70 mL, 33.1 mmol) was added dropwise over 10 min. Upon complete addition, the reaction was allowed to warm to r.t. and stirred for a further 3.5 h. The resulting mixture was diluted with a saturated $Na_2S_2O_3$ solution (100 mL), stirred for an additional hour and then poured into H_2O (100 mL). The product was extracted with Et_2O (3 x 100 mL) and the combined organic layers were washed with brine (1 x 100 mL) and then dried with $MgSO_4$. After filtration and solvent removal under reduced pressure, the crude material was subjected to silica gel flash column chromatography [petroleum ether-EtOAc (90:10)] to give compound **84b** as an off-white solid (4.20 g, 56%).

^{1}H NMR (400 MHz, $CDCl_3$) δ 8.27 (s, 2H), 7.82 (d, *J* = 8.0 Hz, 2H), 7.43 (t, *J* = 7.5 Hz, 2H), 7.30 - 7.26 (m, 2H), 7.07 (d, *J* = 8.5 Hz, 2H), 3.50 (s, 6H); **^{13}C NMR (101 MHz, $CDCl_3$)** δ 152.6, 133.2, 133.1, 131.5, 127.3, 127.0, 126.6, 126.0, 125.9, 117.6, 61.3.

The data match those reported in the literature.[107]

(*S*)-3,3'-Bis(2,4,6-triisopropylphenyl)-[1,1'-binaphthalene]-2,2'-diol (**85**)[106]

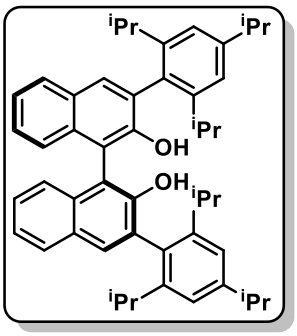

(2, 4, 6-Triisopropylphenyl)magnesium bromide (1.39 M in Et_2O, 25 mL) was added dropwise to a flame-dried flask containing compound **84b** (4.05 g, 8.58 mmol), $Ni(PPh_3)_2Cl_2$ (561 mg, 0.858 mmol) and Et_2O (90 mL). The reaction was then stirred at reflux for 24 h. Once allowed to cool, the reaction mixture was quenched with 1M HCl (50 mL) and extracted with Et_2O (3 x 50 mL). The combined organic layers were dried with $MgSO_4$, filtered and concentrated under reduced pressure. The crude material was then dissolved in CH_2Cl_2 (150 mL) and the solution was cooled on ice. Boron tribromide (1 M in CH_2Cl_2, 39 mL, 38.7 mmol) was added slowly, and the reaction was allowed to warm to r.t. and stirred for 16 h. The resulting mixture was then cooled to 0 °C, quenched with H_2O (60 mL) and extracted with CH_2Cl_2 (3 x 60 mL). The combined organic layers were dried over $MgSO_4$, filtered and concentrated under reduced pressure to give compound **85** as an off-white solid (3.86 g, 65%).

^{1}H NMR (400 MHz, $CDCl_3$) δ 7.87 (d, *J* = 8.0 Hz, 2H), 7.77 (s, 2H), 7.41 - 7.35 (m, 2H), 7.34 - 7.28 (m, 4H), 7.15 - 7.11 (m, 4H), 4.92 (s, 2H), 3.01 - 2.91 (m, 2H), 2.89 - 2.79 (m, 2H), 2.73 - 2.63 (m, 2H), 1.31 (d, *J* = 7.0 Hz, 12H), 1.20 (d, *J* = 7.0 Hz, 6H),

1.12 - 1.07 (m, 12H), 1.03 (d, *J* = 7.0 Hz, 6H); **^{13}C NMR (101 MHz, $CDCl_3$)** δ 150.8, 149.3, 148.0, 147.6, 133.6, 130.9, 130.6, 129.3, 129.2, 128.4, 126.8, 124.7, 124.0, 121.4, 121.4, 113.3, 34.6, 31.1, 31.1, 24.5, 24.5, 24.3, 24.2, 24.1, 23.9.

The data match those reported in the literature.[106]

(11b*S*)-4-Hydroxy-2,6-bis(2,4,6-triisopropylphenyl)dinaphtho[2,1-*d*:1',2'-*f*][1,3,2] dioxaphosphepine 4-oxide (**86**)

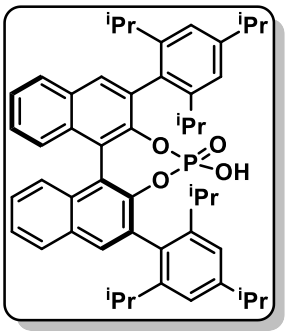

$POCl_3$ (0.47 mL, 772 mg, 5.04 mmol) was added to a flask containing compound **85** (1.16 g, 1.68 mmol) and anhydrous pyridine (3.5 mL, 3.45 g, 43.7 mmol), and then the reaction was stirred at reflux for 16 h. Once allowed to cool, H_2O (4 mL) was added and the resulting slurry was stirred at reflux for a further 3 h. After this time, the reaction was allowed to cool to r.t. and then diluted with CH_2Cl_2 (30 mL). The organic layer was washed with 1 M HCl (3 x 20 mL), brine (1 x 30 mL) and then dried with $MgSO_4$. After filtration and solvent removal under reduced pressure, the crude material was recrystallised from MeCN to give compound **86** as an off-white solid (654 mg, 52%).

^{1}H NMR (400 MHz, CD_2Cl_2) δ 7.87 (d, *J* = 8.0 Hz, 2H), 7.75 (s, 2H), 7.50 - 7.45 (m, 2H), 7.32 - 7.22 (m, 4H), 6.93 (s, 2H), 6.91 (s, 2H), 5.91 (br, 1H), 2.85 - 2.80 (m, 2H), 2.60 - 2.54 (m, 2H), 2.46 - 2.51 (m, 2H), 1.20 (d, *J* = 7.0 Hz, 12H), 1.01 (d, *J* = 7.0 Hz, 6H), 0.93 (d, *J* = 7.0 Hz, 6H), 0.86 (d, *J* = 7.0 Hz, 6H), 0.68 (d, *J* = 7.0 Hz, 6H); **^{13}C NMR (101 MHz, CD_2Cl_2)** δ 148.5, 147.8, 147.4, 145.8, 145.7, 132.6, 132.3, 132.0, 131.9, 131.3, 131.0, 128.1, 127.1, 126.2, 125.7, 121.9, 121.1, 120.2, 34.1, 31.0, 30.7, 26.0, 24.6, 23.8, 23.7, 22.8, 22.7; **^{31}P NMR (162 MHz; CD_2Cl_2)** δ 3.21.

The data match those reported in the literature.[160]

Ethyl 3-fluoro-5-methylene-2-phenyl-3,4,5,6-tetrahydropyridine-3-carboxylate (**54**)

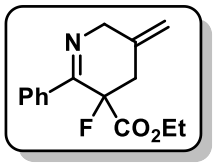

To a solution of compound **81** (74 mg, 0.195 mmol) in CH_2Cl_2 (2 mL) was added TFA (1.1 mL, 1.67 g, 14.6 mmol) and the reaction was stirred at r.t. for 1 h. The resulting mixture was then basified to pH 8 using a saturated $NaHCO_3$ solution and stirred for a further 20 min. The product was extracted with CH_2Cl_2 (3 x 25 mL), dried with $MgSO_4$ and concentrated under reduced pressure to give compound **54** as a yellow oil (43 mg, 87%).

^{1}H NMR (400 MHz, $CDCl_3$) δ 7.72 - 7.66 (m, 2H), 7.39 - 7.31 (m, 3H), 5.09 (s, 1H), 5.02 (s, 1H), 4.64 (dd, *J* = 20.5, 5.5 Hz, 1H), 4.53 (dd, *J* = 20.5, 5.5 Hz, 1H), 4.19 - 4.06 (m, 2H), 3.00 - 2.83 (m, 2H), 1.03 (t, *J* = 7.0 Hz, 3H); **^{13}C NMR (101 MHz, $CDCl_3$)** δ 169.1 (d, *J* = 26.5 Hz), 160.3 (d, *J* = 18.5 Hz), 136.9, 136.3 (d, *J* = 3.5 Hz), 130.0, 128.4, 127.2 (d, *J* = 2.5 Hz), 112.6, 90.8 (d, *J* = 196.0 Hz), 62.3, 56.0, 39.5 (d, *J* = 24.0 Hz), 13.9; **^{19}F NMR (377 MHz, $CDCl_3$):** δ -146.5 - -146.7 (m); **FTIR:** ν_{max}/cm^{-1} (neat) 2983, 1754, 1635, 1447, 1322, 1262, 1076, 1061, 856, 694; **HRMS (ESI$^+$):** *m/z* calcd. for $C_{15}H_{17}FNO_2$: 262.1238, found 262.1240 $[M+H]^+$.

5-Fluoro-3-methylene-6-phenyl-2,3,4,5-tetrahydropyridine (**76**)

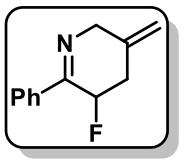

Aqueous HCl (6 M, 0.48 mL) was added to a flask containing compound **54** (50 mg, 0.191 mmol) and the reaction was stirred at 100 °C for 1.5 h. Once allowed to cool, the resulting mixture was basified to pH 8 with a saturated $NaHCO_3$ solution and the product was extracted with EtOAc (3 x 25 mL). The combined organic layers were then dried with $MgSO_4$, filtered and concentrated under reduced pressure to give the decarboxylated product **76** as a yellow oil (0.38 g, quant.).

^{1}H NMR (400 MHz, $CDCl_3$) δ 7.86 - 7.79 (m, 2H), 7.45 - 7.39 (m, 3H), 5.53 (dt, *J* = 48.5, 5.0 Hz, 1H), 5.07 (s, 1H), 5.03 (s, 1H), 4.55 (dd, *J* = 20.5, 5.5 Hz, 1H), 4.45 (dd, *J* = 20.5, 5.5 Hz, 1H), 2.90 - 2.70 (m, 2H); **^{13}C NMR (101 MHz, $CDCl_3$)** δ 162.7 (d, *J* = 16.5 Hz), 137.7 (d, *J* = 4.0 Hz), 137.3, 130.3, 128.5, 127.0 (d, *J* = 1.5 Hz), 112.0, 84.5 (d, *J* = 177.5 Hz), 56.3 (d, *J* = 2.0 Hz), 35.7 (d, *J* = 22.0 Hz); **^{19}F NMR (376 MHz, $CDCl_3$)** δ -170.5 - -170.9 (m); **FTIR:** ν_{max}/cm^{-1} (neat) 3061, 2923, 1632, 1447, 1319, 1015, 899; **HRMS (ESI^+):** *m/z* calcd. for $C_{12}H_{13}FN$: 190.1027, found 190.1034 $[M+H]^+$.

3-Fluoro-5-methylene-2-phenylpiperidine (**77**)

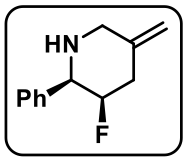

To a solution of compound **76** (50 mg, 0.264 mmol) in MeOH (0.52 mL) at 0 °C was added $NaBH_4$ (20 mg, 0.529 mmol) and the reaction was warmed to r.t. and stirred for 16 h. The resulting mixture was then diluted with a saturated $NaHCO_3$ solution (10 mL) and extracted with EtOAc (5 x 10 mL). The combined organic layers were dried with $MgSO_4$, filtered and concentrated under reduced pressure. The crude material was then purified by silica gel flash column chromatography [petroleum ether-EtOAc (60:40)] to give piperidine **77** as a white solid (39 mg, 77%).

^{1}H NMR (400 MHz, $CDCl_3$) δ 7.39 - 7.21 (m, 5H), 4.97 - 4.79 (m, 3H), 3.87 (d, *J* = 30.0 Hz, 1H), 3.63 (dd, *J* = 14.0, 1.5 Hz, 1H), 3.46 (d, *J* = 14.0 Hz, 1H), 2.84 - 2.75 (m, 1H), 2.56 (dd, *J* = 45.0, 15.0 Hz, 1H), 1.93 (s, 1H); **^{13}C NMR (101 MHz, $CDCl_3$)** δ 140.3, 140.0 128.5, 127.6, 127.2, 112.1, 90.4 (d, *J* = 178.5 Hz), 62.7 (d, *J* = 19.0 Hz), 53.1, 38.9 (d, *J* = 23.5 Hz); **^{19}F NMR (377 MHz, $CDCl_3$)** δ -197.5 (dddd, *J* = 48.5 Hz, 45.0 Hz, 30.0 Hz, 11.0 Hz); **FTIR:** ν_{max}/cm^{-1} (neat) 3291, 2937, 1656, 1467,

1261, 1100, 1022; **HRMS (ESI$^+$):** *m/z* calcd. for$C_{12}H_{15}FN$: 192.1183, found 192.1186 $[M+H]^+$.

(1*R*,2*S*,5*R*)-2-Isopropyl-5-methylcyclohexyl 2-fluoroacetate (**105**)

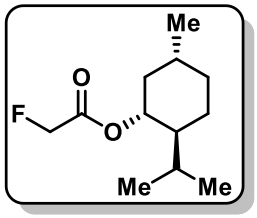

L-Menthol (483 mg, 3.09 mmol) was added to a suspension of NaH (60% dispersion in mineral oil, 91 mg, 2.27 mmol) in toluene (8 mL) at 0 °C. The reaction was allowed to cool to r.t. and ethyl fluoroacetate (0.219 mg, 2.06 mmol) was added, and then the resulting mixture was stirred at reflux under nitrogen for 16 h. The reaction was quenched with a saturated $NaHCO_3$ solution (30 mL) and the product was extracted with EtOAc (3 x 30 mL). The combined organic layers were dried with $MgSO_4$, filtered and concentrated under reduced pressure. The crude residue was then subjected to silica gel flash column chromatography [petroleum ether-EtOAc (90:10)] to give menthol ester **105** as a yellow oil (153 mg, 34%). This substrate was tentatively characterised by ^{1}H and ^{19}F NMR and then used in the next reaction.

^{1}H NMR (400 MHz, $CDCl_3$) δ 4.89 - 4.87 (m, 1H), 4.87 - 4.80 (m, 1H), 4.77 - 4.75 (m, 1H), 2.06 - 1.99 (m, 1H), 1.88 - 1.78 (m, 1H), 1.72 - 1.65 (m, 2H), 1.55 - 1.47 (m, 1H), 1.47 - 1.37 (m, 1H), 1.09 - 1.00 (m, 2H), 0.93 - 0.87 (m, 7H), 0.77 (d, *J* = 7.0 Hz, 3H); **^{19}F NMR (377 MHz, $CDCl_3$)** δ -229.2 (t, *J* = 47.2 Hz).

(1*R*,2*S*,5*R*)-2-Isopropyl-5-methylcyclohexyl 2-fluoro-3-oxo-3-phenylpropanoate (**106**)

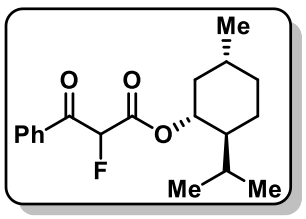

Compound **105** (135 mg, 0.624 mmol) dissolved in THF (5mL) was added to a flask containing diphenylphosphinic

chloride (148 mg, 0.624 mmol) under nitrogen. The reaction mixture was cooled to -78 °C and lithium bis(trimethylsilyl)amide (1.0 M in hexane, 1.9 mL, 1.87 mmol) was added dropwise. After 15 min, benzoyl chloride (97 mg, 0.687 mmol) was added and the reaction was allowed to stir at r.t. for 16 h. The resulting mixture was then diluted with a saturated NH_4Cl solution (25 mL) and stirred for a further 30 min. The product was extracted with EtOAc (1 x 30 mL) and the organic layer was washed with 1 M NaOH (2 x 25mL) and then dried with $MgSO_4$. After filtration and solvent removal under reduced pressure, the crude material was purified by silica gel flash column chromatography [petroleum ether-EtOAc (90:10)] to give the fluorinated ketoester **106** as a yellow oil (101 mg, 51%, 1.1:1 d.r.).

Major diastereoisomer

^{1}H NMR (400 MHz, $CDCl_3$) δ 8.04 - 8.00 (m, 2H), 7.60 - 7.64 (m, 1H), 7.51 - 7.45 (m, 2H), 5.89 (d, *J* = 18.5 Hz, 1H), 4.94 - 4.74 (m, 1H), 1.88 - 0.35 (m, 18H); **^{19}F NMR (377 MHz, $CDCl_3$)** δ -189.8; **LCMS (ESI^+):** *m/z* calcd. for $C_{19}H_{25}FO_3Na$: 343.17, found 343.20 $[M+Na]^+$.

Minor diastereoisomer

^{1}H NMR (400 MHz, $CDCl_3$) δ 8.04 - 8.00 (m, 2H), 7.60 - 7.64 (m, 1H), 7.51 - 7.45 (m, 2H), 5.76 (d, *J* = 18.5 Hz, 1H), 4.94 - 4.74 (m, 1H), 1.88 - 0.35 (m, 18H); **^{19}F NMR (377 MHz, $CDCl_3$)** δ -190.4; **LCMS (ESI^+):** *m/z* calcd. for $C_{19}H_{25}FO_3Na$: 343.17, found 343.20 $[M+Na]^+$.

The data match those reported in the literature.[161]

(1*R*,2*S*,5*R*)-2-Isopropyl-5-methylcyclohexyl 2-benzoyl-4-(((*tert*-butoxycarbonyl)amino)methyl)-2-fluoropent-4-enoate (**107**)

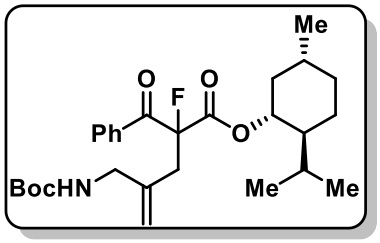

A flame-dried flask was charged with $Pd(dba)_2$ (4 mg, 0.01 mmol), ligand **L10** (7 mg, 0.02 mmol) and cyclic carbamate **17** (30 mg, 0.14 mmol) under nitrogen. CH_2Cl_2 (1.4 mL) was then added and the reaction was stirred at r.t. After 5 min, compound **106** (26 mg, 0.08 mmol) was added as a solution in CH_2Cl_2 (0.5 mL) and the resulting mixture was allowed to stir at r.t. for 4 h. The solvent was then removed under reduced pressure and the crude material was subjected to silica gel flash chromatography [petroleum ether-EtOAc (90:10)] to give the allylation product **107** as a yellow oil (30 mg, 75%, 1.1:1 d.r.).

Major diastereoisomer

^{1}H NMR (400 MHz, $CDCl_3$) δ 8.06 (d, *J* = 8.0 Hz, 2H), 7.58 (t, *J* = 7.5 Hz, 1H), 7.44 (t, *J* = 8.0 Hz, 2H), 5.15 (s, 1H), 5.05 (s, 1H), 4.78 (br, 1H), 4.73 (dd, *J* = 11.0 Hz, 4.0 Hz, 1H), 3.85 - 3.70 (m, 2H), 3.18 - 2.93 (m, 2H), 1.95 - 0.82 (m, 21H), 0.79 (d, *J* = 7.0 Hz, 3 H), 0.68 (d, *J* = 7.0 Hz, 3 H); **^{13}C NMR (101 MHz, $CDCl_3$)** δ 191.5 (d, *J* = 25.5 Hz), 166.8 (d, *J* = 25.5 Hz), 155.9, 139.7, 134.2, 133.9 (d, *J* = 3.5 Hz), 130.0 (d, *J* = 5.5 Hz), 128.8, 116.2, 99.8 (d, *J* = 200.7 Hz), 79.5, 77.7, 46.8, 45.9, 40.6, 38.1 (d, *J* = 20.5 Hz), 34.1, 31.5, 28.5, 25.9, 22.9, 22.0, 20.9, 15.8 **^{19}F NMR (377 MHz, $CDCl_3$)** δ -157.4; **HRMS (ESI^+):** *m/z* calcd. for $C_{28}H_{40}FNO_5Na$: 512.2783, found 512.2799 $[M+Na]^+$.

Minor diastereoisomer

^{1}H NMR (400 MHz, $CDCl_3$) δ 8.02 (d, *J* = 8.0 Hz, 1H), 7.58 (t, *J* = 7.5 Hz, 1H), 7.44 (t, *J* = 8.0 Hz, 2H), 5.15 (s, 1H), 5.05 (s, 1H), 4.78 (br, 1H), 4.68 (dd, *J* = 11.0 Hz,

4.0 Hz, 1H), 3.85 - 3.70 (m, 2H), 3.18 - 2.93 (m, 2H), 1.95 - 0.82 (m, 21H), 0.59 (d, *J* = 7.0 Hz, 3 H), 0.30 (d, *J* = 7.0 Hz, 3 H); **^{13}C NMR (101 MHz, $CDCl_3$)** δ 190.5 (d, *J* = 25.5 Hz), 166.7 (d, *J* = 25.5 Hz), 155.9, 139.6, 134.0, 133.7 (d, *J* = 3.5 Hz), 129.9 (d, *J* = 5.5 Hz), 128.7, 116.1, 99.6 (d, *J* = 199.0 Hz), 79.5, 77.7, 46.6, 45.8, 40.0, 38.0 (d, *J* = 20.5 Hz), 34.0, 31.4, 28.5, 25.5, 22.9, 21.9, 20.6, 15.3; **^{19}F NMR (377 MHz, $CDCl_3$)** δ -156.8; **HRMS (ESI$^+$):** *m/z* calcd. for $C_{28}H_{40}FNO_5Na$: 512.2783, found 512.2799 [*M*+*Na*]$^+$.

Dimethyl 2-(2-(((*tert*-butoxycarbonyl)amino)methyl)allyl)-2-fluoromalonate (**110**)

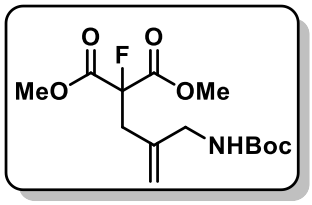

A flame-dried flask was charged with $Pd(dba)_2$ (94 mg, 0.164 mmol), ligand **L10** (155 mg, 0.492 mmol) and cyclic carbamate **17** (700 mg, 3.28 mmol) under nitrogen. CH_2Cl_2 (32 mL) was then added and the reaction was stirred at r.t. After 5 min, dimethyl fluoromalonate (641 mg, 4.27 mmol) was added neat and the resulting mixture was allowed to stir at reflux for 16 h. The solvent was then removed under reduced pressure and the crude material was subjected to silica gel flash chromatography [petroleum ether-EtOAc (85:15)] to give compound **110** as a colourless oil (998 mg, 95%).

^{1}H NMR (400 MHz, $CDCl_3$) δ 5.13 (s, 1H), 5.02 (s, 1H), 4.72 (br, 1H), 3.83 (s, 6H), 3.72 (d, *J* = 5.5 Hz, 2H), 2.93 (d, 25.5 Hz, 2H), 1.44 (s, 9H); **^{13}C NMR (101 MHz, $CDCl_3$)** δ 166.2 (d, *J* = 25.5 Hz), 155.9, 139.4, 116.1, 95.3 (d, *J* = 201.5 Hz), 79.6, 53.6, 45.7, 38.2 (d, *J* = 20.5 Hz), 28.5; **^{19}F NMR (377 MHz, $CDCl_3$):** δ -163.6 (t, *J* = 25.5 Hz); **HRMS (ESI$^+$):** *m/z* calcd. for $C_{14}H_{22}FNO_6Na$: 342.1323, found 342.1337 [*M*+*Na*]$^+$.

4-(((*Tert*-butoxycarbonyl)amino)methyl)-2-fluoro-2-(methoxycarbonyl)pent-4-enoic acid (**111**)

Basic hydrolysis:

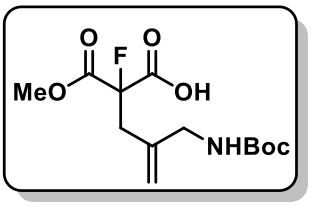

A flask was charged with compound **110** (79 mg, 0.247 mmol), THF (0.4 mL) and H_2O (3.6 mL). The reaction mixture was cooled to 0 °C and KOH (0.26 M, 1 mL, 0.260 mmol) was added dropwise. The reaction was stirred at 0 °C for 2 h, then acidified to pH 1 with concentrated HCl. Brine (15 mL) was added and the product was extracted with EtOAc (3 x 15mL) then dried with $MgSO_4$. After filtration and solvent removal under reduced pressure, compound **111** was isolated as a yellow oil without further purification (76 mg, quant.).

^{1}H NMR (400 MHz, DMSO) δ 4.96 (s, 1H), 4.89 (s, 1H), 3.74 (s, 3H), 3.49 - 3.46 (m, 2H), 2.90 - 2.70 (m, 2H), 1.37 (s, 9H); **^{13}C NMR (101 MHz, DMSO)** δ 166.7 (d, *J* = 25.0 Hz), 166.4 (d, *J* = 21.5 Hz), 155.6, 140.1, 113.5, 94.6 (d, *J* = 198.0 Hz), 77.7, 53.2, 45.0, 37.5 (d, *J* = 20.5 Hz), 28.3; **^{19}F NMR (377 MHz, $CDCl_3$):** δ -161.8; **HRMS (ESI$^+$):** *m/z* calcd. for $C_{13}H_{20}FNO_6$: 328.1167, found 328.1177 $[M+Na]^+$.

Enzymatic hydrolysis:

A flask was charged with compound **110** (114 mg, 0.357 mmol), phosphate buffer (10 mL, 3:1 0.06 M Na_2HPO_4: 0.06 M KH_2PO_4, pH 7.3) and PLE (200 mg). The reaction mixture was stirred at 37 °C for 16 h, then another portion of PLE was added (50 mg) and the reaction was stirred for a further 4 h. The resulting mixture was concentrated under reduced pressure and the residue was diluted with EtOAC (20 mL). After filtration, the organic layer was dried with $MgSO_4$ and the solvent was

removed under reduced pressure to give compound **111** as a yellow oil (36 mg, 33%).

Methyl 3-fluoro-5-methylene-2-oxopiperidine-3-carboxylate (**108**)

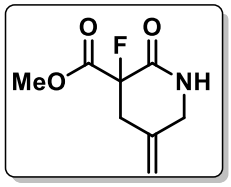

To a solution of compound **110** (980 mg, 3.07 mmol) in CH_2Cl_2 (30 mL) was added TFA (2.4 mL, 3.50 g, 30.7 mmol) and the reaction was stirred at r.t. for 1 h. The resulting mixture was then basified to pH 8 using a saturated $NaHCO_3$ solution and the product was extracted with CH_2Cl_2 (3 x 40 mL). The combined organic layers were washed with brine (1 x 50mL), dried with $MgSO_4$ and concentrated under reduced pressure to give lactam **108** as an off-white solid (580 mg, quant.).

^{1}H NMR (400 MHz, $CDCl_3$) δ 6.77 (br, 1H), 5.15 (s, 1H), 5.11 (s,1H), 4.06 (s, 2H), 3.85 (s, 3H), 3.12 (dd, *J* = 22.0 Hz, 14.5 Hz, 1H), 2.93 (t, *J* = 14.5 Hz, 1H); **^{13}C NMR (101 MHz, $CDCl_3$)** δ 167.7 (d, *J* = 26.0 Hz), 165.5 (d, *J* = 22.0 Hz), 132.7 (d, *J* = 5.5 Hz), 115.9, 90.7 (d, *J* = 194.5 Hz), 53.3, 47.3, 39.0 (d, *J* = 23.5 Hz); **^{19}F NMR (377 MHz, $CDCl_3$):** δ -158.4 (dd, *J* = 22.0 Hz, 14.5 Hz); **HRMS (ESI$^+$):** *m/z* calcd. for $C_8H_{10}FNO_3Na$: 210.0537, found 210.0545 $[M+Na]^+$.

5.2.8. Synthesis of α-Trifluoromethylthioketo Substrates

General Procedure 7 (**GP7**)

Following literature procedure,[138] $AgSCF_3$ (2.0 eq.) was added to a suspension of α-haloketone (1 eq.) and KI (2 eq.) in acetone (0.12 M) and the reaction was stirred

at r.t. under nitrogen for 1h. After rotary evaporation, the residue was diluted in Et_2O (30 mL), filtered and concentrated under reduced pressure. The crude material was then subjected to silica gel flash column chromatography to give the desired α-SCF_3-ketone.

General Procedure 8 (**GP8**)

Following the procedure of Shen,[139] α-ketoester (1.0 eq.) or α-ketosulfone (1.0 eq.) was dissolved in THF (0.3 M) and added to a suspension of NaH (60% dispersion in mineral oil, 1.1 eq.) in THF (0.3 M) under nitrogen. The reaction was stirred at r.t. for 30 min, then cooled to 0 °C and a solution of *N*-SCF_3-saccharin **124** (1.3 eq.) in THF (0.4 M) was added. The reaction mixture was allowed to stir at r.t. for 45 min, and then the solvent was removed under reduced pressure. The crude material was purified by silica gel flash column chromatography to give the corresponding α-SCF_3-ketoester or α-SCF_3-ketosulfone respectively.

2-((Trifluoromethyl)thio)benzo[*d*]isothiazol-3(2*H*)-one 1,1-dioxide (**124**)

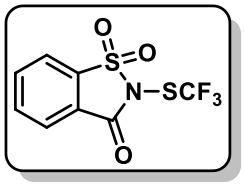

Following the procedure of Shen,[139] a flask was charged with *N*-chlorosaccharin (1.0 g, 4.59 mmol), $AgSCF_3$ (1.15 g, 5.51 mmol) and MeCN (7 mL). The reaction was vigorously stirred at r.t. under nitrogen for 1 h. After rotary evaporation, the residue was diluted in CH_2Cl_2 (20 mL) and filtered through celite. The solvent was then removed under reduced pressure to give *N*-SCF_3-saccharin **124** as a white solid (991 mg, 76%).

^{1}H NMR (400 MHz, $CDCl_3$) δ 8.19 (d, *J* = 7.5 Hz, 1H), 8.07 - 7.97 (m, 2H), 7.96 - 7.89 (m, 2H); **^{13}C NMR (101 MHz, $CDCl_3$)** δ 158.5, 138.1, 136.5, 135.1, 127.4 (q, *J* = 316.0 Hz), 126.7, 126.3, 122.1; **^{19}F NMR (377 MHz, $CDCl_3$):** δ -47.3.

The data match those reported in the literature.[139]

1-Phenyl-2-((trifluoromethyl)thio)ethan-1-one (**112**)

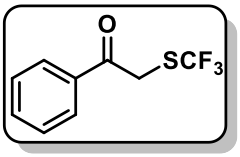

Following **GP7** using 2-bromoacetophenone (800 mg, 4.02 mmol), $AgSCF_3$ (1.68 g, 8.04 mmol) and KI (1.33 g, 8.04 mmol). Following silica gel flash column chromatography [petroleum ether-CH_2Cl_2 (70:30)] compound **112** was isolated as a yellow oil (872 mg, 98%).

^{1}H NMR (400 MHz, $CDCl_3$) δ 7.96 (d, *J* = 8.0 Hz, 2H), 7.64 (t, *J* = 7.5 Hz, 1H), 7.52 (t, *J* = 8.0 Hz, 2H), 4.53 (s, 2H); **^{13}C NMR (101 MHz, $CDCl_3$)** δ 192.1, 134.8, 134.4, 130.8 (q, *J* = 306.0 Hz), 129.1, 128.6, 38.6; **^{19}F NMR (377 MHz, $CDCl_3$):** δ -41.4.

The data match those reported in the literature.[139]

1-(4-Methoxyphenyl)-2-((trifluoromethyl)thio)ethan-1-one (**113**)

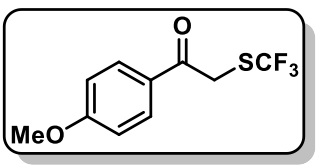

Following **GP7** using 2-bromo-4′-methoxyacetophenone (311 mg, 1.36 mmol), $AgSCF_3$ (568 mg, 2.72 mmol) and KI (452 mg, 2.72 mmol). Following silica gel flash column chromatography [petroleum ether-CH_2Cl_2 (70:30)] compound **113** was isolated as a yellow oil (328 mg, 96%).

^{1}H NMR (400 MHz, $CDCl_3$) δ 7.93 (d, *J* = 9.0 Hz, 2H), 6.97 (d, *J* = 9.0 Hz, 2H), 4.48 (s, 2H), 3.89 (s, 3H); **^{13}C NMR (101 MHz, $CDCl_3$)** δ 190.6, 164.5, 131.0, 130.9 (q, *J* = 306.0 Hz), 127.9, 114.3, 55.6, 38.4; **^{19}F NMR (377 MHz, $CDCl_3$):** δ -41.4.

The data match those reported in the literature.[162]

1-(*p*-Tolyl)-2-((trifluoromethyl)thio)ethan-1-one (**114**)

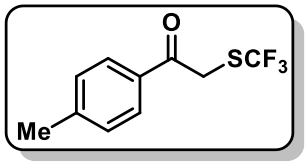

Following **GP7** using 2-bromo-4′-methylacetophenone (290 mg, 1.36 mmol), $AgSCF_3$ (568 mg, 2.72 mmol) and KI (452 mg, 2.72 mmol). Following silica gel flash column chromatography [petroleum ether-CH_2Cl_2 (70:30)] compound **114** was isolated as a yellow solid (301 mg, 94%).

^{1}H NMR (400 MHz, $CDCl_3$) δ 7.85 (d, *J* = 8.0 Hz, 2H), 7.30 (d, *J* = 8.0 Hz, 2H), 4.50 (s, 2H), 2.44 (s, 3H); **^{13}C NMR (101 MHz, $CDCl_3$)** δ 191.7, 145.5, 132.4, 130.9 (q, *J* = 306.0 Hz), 129.8, 128.7, 38.6, 21.9; **^{19}F NMR (377 MHz, $CDCl_3$):** δ -41.4.

The data match those reported in the literature.[162]

1-(4-Chlorophenyl)-2-((trifluoromethyl)thio)ethan-1-one (**115**)

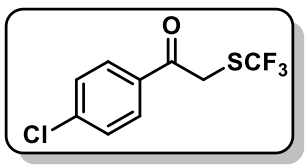

Following **GP7** using 2-bromo-4′-chloroacetophenone (317 mg, 1.36 mmol), $AgSCF_3$ (568 mg, 2.72 mmol) and KI (452 mg, 2.72 mmol). Following silica gel flash column chromatography [petroleum ether-CH_2Cl_2 (70:30)] compound **115** was isolated as a yellow oil (335 mg, 97%).

^{1}H NMR (400 MHz, $CDCl_3$) δ 7.90 (d, *J* = 8.5 Hz, 2H), 7.49 (d, *J* = 8.5 Hz, 2H), 4.47 (s, 2H); **^{13}C NMR (101 MHz, $CDCl_3$)** δ 191.0, 141.1, 133.1, 130.7 (q, *J* = 307.0 Hz), 129.9, 129.5, 38.3; **^{19}F NMR (377 MHz, $CDCl_3$):** δ -41.4.

The data match those reported in the literature.[162]

1-(4-nitrophenyl)-2-((trifluoromethyl)thio)ethan-1-one (**116**)

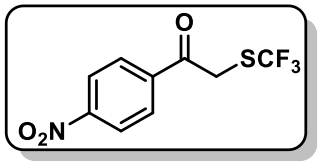

Following **GP7** using 2-bromo-4′-nitroacetophenone (332 mg, 1.36 mmol), $AgSCF_3$ (568 mg, 2.72 mmol) and KI (452 mg, 2.72 mmol). Following silica gel flash column chromatography [petroleum ether-CH_2Cl_2 (70:30)] compound **116** was isolated as a yellow solid (340 mg, 94%).

^{1}H NMR (400 MHz, $CDCl_3$) δ 8.37 (d, *J* = 9.0 Hz, 2H), 8.13 (d, *J* = 9.0 Hz, 2H), 4.51 (s, 2H); **^{13}C NMR (101 MHz, $CDCl_3$)** δ 190.9, 151.1, 139.1, 130.4 (q, *J* = 307.0 Hz), 129.7, 124.4, 38.3; **^{19}F NMR (377 MHz, $CDCl_3$):** δ -41.4.

The data match those reported in the literature.[163]

1-(4-(Trifluoromethyl)phenyl)-2-((trifluoromethyl)thio)ethan-1-one (**117**)

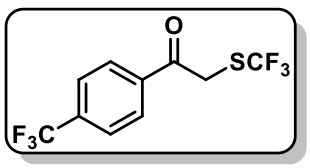

Following **GP7** using 2-bromo-4′-(trifluoromethyl) acetophenone (363 mg, 1.36 mmol), $AgSCF_3$ (568 mg, 2.72 mmol) and KI (452 mg, 2.72 mmol). Following silica gel flash column chromatography [petroleum ether-CH_2Cl_2 (70:30)] compound **117** was isolated as a yellow solid (381 mg, 97%).

^{1}H NMR (400 MHz, $CDCl_3$) δ 8.07 (d, *J* = 8.0 Hz, 2H), 7.79 (d, *J* = 8.0 Hz, 2H), 4.50 (s, 2H); **^{13}C NMR (101 MHz, $CDCl_3$)** δ 191.4, 137.4, 135.6 (q, *J* = 33.0 Hz), 130.6 (q, *J* = 306.0 Hz), 129.0, 126.2 (q, *J* = 3.0 Hz), 123.5 (q, *J* = 273.0 Hz), 38.3; **^{19}F NMR (377 MHz, $CDCl_3$):** δ -41.4, 63.3.

The data match those reported in the literature.[162]

1-(3-Chlorophenyl)-2-((trifluoromethyl)thio)ethan-1-one (**118**)

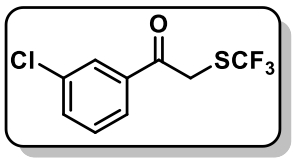

Following **GP7** using 2-bromo-3′-chloroacetophenone (317 mg, 1.36 mmol), $AgSCF_3$ (568 mg, 2.72 mmol) and KI (452 mg, 2.72 mmol). Following silica gel flash column chromatography [petroleum ether-CH_2Cl_2 (70:30)] compound **118** was isolated as a yellow oil (326 mg, 94%).

^{1}H NMR (400 MHz, $CDCl_3$) δ 7.93 (t, *J* = 2.0 Hz, 1H), 7.83 (ddd, *J* = 8.0 Hz, 2.0 Hz, 1.0 Hz, 1H), 7.62 (ddd, *J* = 8.0 Hz, 2.0 Hz, 1.0 Hz, 1H), 7.47 (t, *J* = 8.0 Hz, 1H), 4.47 (s, 2H); **^{13}C NMR (101 MHz, $CDCl_3$)** δ 191.0, 136.3, 135.6, 134.4, 130.7 (q, *J* = 307 Hz), 130.5, 128.6, 126.6, 38.4; **^{19}F NMR (377 MHz, $CDCl_3$):** δ -41.4.

The data match those reported in the literature.[164]

1-(2-Methoxyphenyl)-2-((trifluoromethyl)thio)ethan-1-one (**119**)

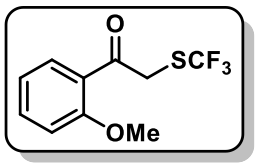

Following **GP7** using 2-bromo-2′-methoxyacetophenone (311 mg, 1.36 mmol), $AgSCF_3$ (568 mg, 2.72 mmol) and KI (452 mg, 2.72 mmol). Following silica gel flash column chromatography

[petroleum ether-CH_2Cl_2 (70:30)] compound **119** was isolated as a pale yellow solid (331 mg, 97%).

^{1}H NMR (400 MHz, $CDCl_3$) δ 7.87 (dd, *J* = 8.0 Hz, 2.0 Hz, 1H), 7.55 (ddd, *J* = 8.5 Hz, 7.5 Hz, 2.0 Hz, 1H), 7.06 (t, *J* = 8.0 Hz, 1H), 7.01 (d, *J* = 8.5 Hz, 1H), 4.43 (s, 2H), 3.95 (s, 3H); **^{13}C NMR (101 MHz, $CDCl_3$)** δ 193.4, 159.2, 135.3, 131.5, 131.0 (q, *J* = 306 Hz), 124.9, 121.3, 111.7, 55.8, 42.7; **^{19}F NMR (377 MHz, $CDCl_3$):** δ -41.6.

The data match those reported in the literature.[165]

1-(Thiophen-2-yl)-2-((trifluoromethyl)thio)ethan-1-one (**120**)

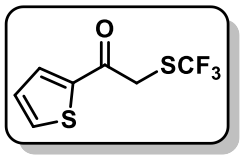

Following **GP7** using 2-bromo-1-(thiophen-2-yl)ethan-1-one (279 mg, 1.36 mmol), $AgSCF_3$ (568 mg, 2.72 mmol) and KI (452 mg, 2.72 mmol). Following silica gel flash column chromatography [petroleum ether-CH_2Cl_2 (70:30)] compound **120** was isolated as a yellow solid (289 mg, 94%).

^{1}H NMR (400 MHz, $CDCl_3$) δ 7.78 (dd, *J* = 4.0 Hz, 1.0 Hz, 1H), 7.55 (dd, *J* = 5.0 Hz, 1.0 Hz, 1H), 7.19 (dd, *J* = 5.0 Hz, 4.0 Hz, 1H), 4.36 (s, 2H); **^{13}C NMR (101 MHz, $CDCl_3$)** δ 184.9, 141.5, 135.5, 133.3, 130.6 (q, *J* = 307 Hz), 128.6, 37.7; **^{19}F NMR (377 MHz, $CDCl_3$):** δ -41.5.

The data match those reported in the literature.[162]

1-Phenyl-2-((trifluoromethyl)thio)propan-1-one (**121**)

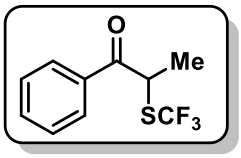

Following an adapted **GP7** using 2-bromopropiophenone (290 mg, 1.36 mmol), $AgSCF_3$ (852 mg, 4.08 mmol) and KI (677 mg, 4.08 mmol) for 16 h. Following silica gel flash column chromatography [petroleum ether-CH_2Cl_2 (75:25)] compound **121** was isolated as a brown oil (225 mg, 71%).

^{1}H NMR (400 MHz, $CDCl_3$) δ 7.98 (d, *J* = 8.0 Hz, 2H), 7.64 (t, *J* = 7.5 Hz, 1H), 7.52 (t, *J* = 8.0 Hz, 2H), 4.98 (q, *J* = 7.0 Hz, 1H), 1.73 (d, *J* = 7.0 Hz, 3H); **^{13}C NMR (101 MHz, $CDCl_3$)** δ 196.4, 134.2, 134.1, 130.8 (q, *J* = 307 Hz), 129.2, 128.9, 44.6, 19.9; **^{19}F NMR (377 MHz, $CDCl_3$):** δ -39.8.

The data match those reported in the literature.[165]

1-((Trifluoromethyl)thio)butan-2-one (**122**)

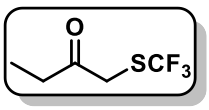

Following **GP7** using 1-bromo-2-butanone (618 mg, 4.09 mmol), $AgSCF_3$ (1.54 g, 7.36 mmol) and KI (1.22 g, 7.36 mmol). Following silica gel flash column chromatography [petroleum ether-CH_2Cl_2 (75:25)] compound **122** was isolated as a brown oil (226 mg, 36%).

^{1}H NMR (400 MHz, $CDCl_3$) 3.81 (s, 2H), 2.62 (q, *J* = 7.0 Hz, 2H), 1.13 (t, *J* = 7.0 Hz, 3H); **^{13}C NMR (101 MHz, $CDCl_3$)** δ 203.7, 130.5 (q, *J* = 307 Hz), 39.8, 34.7, 7.9; **^{19}F NMR (377 MHz, $CDCl_3$):** δ -41.7.

1-Cyclopropyl-2-((trifluoromethyl)thio)ethan-1-one (**123**)

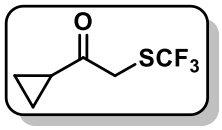

Following **GP7** using 2-bromo-1-cyclopropylethanone (667 mg, 4.09 mmol), $AgSCF_3$ (1.54 g, 7.36 mmol) and KI (1.22g, 7.36 mmol). Following silica gel flash column chromatography [petroleum ether-CH_2Cl_2 (75:25)] compound **123** was isolated as a brown oil (462 mg, 68%).

^{1}H NMR (400 MHz, $CDCl_3$) δ 3.96 (s, 2H), 2.16 - 2.08 (m, 1H), 1.18 - 1.13 (m, 2H), 1.06 - 1.00 (m, 2H); **^{13}C NMR (101 MHz, $CDCl_3$)** δ 202.8, 130.4 (q, *J* = 307 Hz), 40.7, 19.6, 12.3; **^{19}F NMR (377 MHz, $CDCl_3$):** δ -41.7.

The data match those reported in the literature.[138]

Ethyl 3-oxo-3-phenyl-2-((trifluoromethyl)thio)propanoate (**125**)

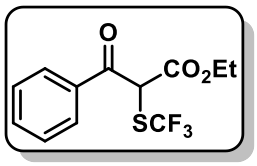

Following **GP8** using ethyl benzoylacetate (500 mg, 2.60 mmol), NaH (60% dispersion in mineral oil, 114 mg, 2.86 mmol) and *N*-SCF_3-saccharin **124** (956 mg, 3.38 mmol). Following silica gel flash column chromatography [petroleum ether-EtOAc (95:5)] compound **125** was isolated as a pale yellow oil (692 mg, 91%, 2:1 enol:keto).

Enol:

^{1}H NMR (400 MHz, $CDCl_3$) δ 14.5 (s, 1H), 7.60 (d, *J* = 8.0 Hz, 2H), 7.55 - 7.43 (m, 3H), 4.39 (q, *J* = 7.0 Hz, 2H), 1.39 (t, *J* = 7.0 Hz, 3H); **^{13}C NMR (101 MHz, $CDCl_3$)** δ 184.5, 173.2, 133.9, 129.2 (q, *J* = 311 Hz), 131.0, 128.9, 127.9, 62.5, 14.0; **^{19}F NMR (377 MHz, $CDCl_3$):** δ -45.2.

Ketone:

^{1}H NMR (400 MHz, $CDCl_3$) δ 8.03 (d, *J* = 8.0 Hz, 2H), 7.66 (t, J = 7.5 Hz, 1H), 7.55 - 7.41 (m, 2H), 5.62 (s, 1H), 4.30 - 4.17 (m, 2H), 1.21 (t, *J* = 7.0 Hz, 3H); **^{13}C NMR (101 MHz, $CDCl_3$)** δ 188.5, 165.9, 134.7, 133.8, 130.0 (q, *J* = 308 Hz), 129.1, 129.0, 63.3, 55.0, 13.7; **^{19}F NMR (377 MHz, $CDCl_3$):** δ -40.5.

The data match those reported in the literature.[139]

Ethyl 3-oxo-3-phenyl-2-((trifluoromethyl)thio)propanoate (**126**)

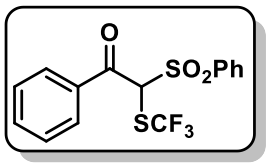

Following **GP8** using 1-phenyl-2-(phenylsulfonyl)ethanone (200 mg, 0.768 mmol), NaH (60% dispersion in mineral oil, 34 mg, 0.845 mmol) and *N*-SCF_3-saccharin **124** (283 mg, 0.999 mmol). Following silica gel flash column chromatography [petroleum ether-EtOAc (80:20] compound **126** was isolated as a yellow oil (273 mg, 98%).

^{1}H NMR (400 MHz, $CDCl_3$) δ 7.99 (d, *J* = 8.0 Hz, 2H), 7.90 (d, *J* = 8.0 Hz, 2H), 7.76 - 7.66 (m, 2H), 7.61 - 7.52 (m, 4H), 6.03 (s, 1H); **^{13}C NMR (101 MHz, $CDCl_3$)** δ 188.7, 135.4, 135.2, 134.9, 134.7, 130.8, 129.7, 129.3, 129.2, 129.1 (q, *J* = 310 Hz), 68.9; **^{19}F NMR (377 MHz, $CDCl_3$):** δ -40.0.

The data match those reported in the literature.[166]

5.2.9. Pd-catalysed Allylation of α-Trifluoromethylthioketones

General Procedure 9 (**GP9**)

A flame-dried flask was charged with $Pd(dba)_2$ (5 mol%), ligand **L10** (15 mol%) and cyclic carbamate **17** (1.0 eq.) under nitrogen. CH_2Cl_2 (0.1 M) was then added and the reaction was stirred at r.t. After 5 min, a solution of the α-SCF_3-ketone (1.5 eq.) in CH_2Cl_2 (0.5 mL) was added and the resulting mixture was allowed to stir at r.t. for 16 h. The solvent was then removed under reduced pressure and the crude material was subjected to silica gel flash column chromatography to give the allylation product.

tert-Butyl (2-methylene-5-oxo-5-phenyl-4-((trifluoromethyl)thio)pentyl)carbamate (**127**)

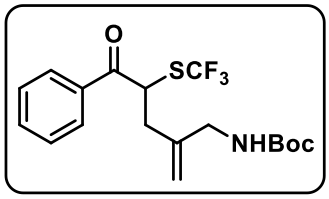

Following **GP9** using $Pd(dba)_2$ (13 mg, 0.02 mmol), ligand **L10** (22 mg, 0.07 mmol), carbamate **17** (100 mg, 0.469 mmol) and α-SCF_3-ketone **112** (155 mg, 0.703 mmol). Following silica gel flash column chromatography [petroleum ether-CH_2Cl_2-EtOAc (65:30:5)] compound **127** was isolated as yellow oil (171 mg, 93%).

^{1}H NMR (400 MHz, $CDCl_3$): δ 8.02 (d, *J* = 7.5 Hz, 2H), 7.62 (t, *J* = 7.5 Hz, 1H), 7.51 (t, *J* = 7.5 Hz, 2H), 5.15 (t, *J* = 7.0 Hz, 1H), 5.01 (s, 1H), 4.91 (s, 1H), 4.63 (br, 1H), 3.80 - 3.69 (m, 2H), 2.96 (dd, *J* = 14.5 Hz, 8.0 Hz, 1H), 2.66 (dd, *J* = 14.5 Hz, 7.0 Hz, 1H), 1.43 (s, 9H); **^{13}C NMR (101 MHz, $CDCl_3$)** δ 194.3, 155.8, 141.7, 137.6, 133.8, 133.2 (q, *J* = 309 Hz), 128.8, 128.6, 115.5, 79.7, 44.9, 44.6, 36.1, 28.2 ; **^{19}F NMR (377 MHz, $CDCl_3$)**: δ -39.4; **FTIR:** ν_{max}/cm^{-1} (neat) 3375, 2982, 2932, 1687, 1510,

1449, 1367, 1275, 1260, 1156, 1107, 750, 688; **HRMS (ESI$^+$):** *m/z* calcd. for $C_{18}H_{22}F_3NO_3SNa$: 412.1165, found: 412.1177 $[M+Na]^+$.

tert-Butyl (5-(4-methoxyphenyl)-2-methylene-5-oxo-4-((trifluoromethyl)thio)pentyl) carbamate (**128**)

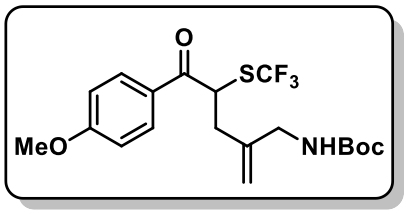

Following **GP9** using $Pd(dba)_2$ (13 mg, 0.02 mmol), ligand **L10** (22 mg, 0.07 mmol), carbamate **17** (100 mg, 0.469 mmol) and α-SCF_3-ketone **113** (176 mg, 0.703 mmol). Following silica gel flash column chromatography [petroleum ether-CH_2Cl_2-EtOAc (65:30:5)] compound **128** was isolated as yellow oil (178 mg, 90%).

^{1}H NMR (400 MHz, $CDCl_3$): δ 8.01 (d, *J* = 9.0 Hz, 2H), 6.97 (d, *J* = 9.0 Hz, 2H), 5.10 (t, *J* = 7.0 Hz, 1H), 4.99 (s, 1H), 4.90 (s, 1H), 4.63 (br, 1H), 3.89 (s, 3H), 3.80 - 3.69 (m, 2H), 2.94 (dd, *J* = 14.5 Hz, 8.5 Hz, 1H), 2.64 (dd, *J* = 14.5 Hz, 7.0 Hz, 1H), 1.43 (s, 9H); **^{13}C NMR (101 MHz, $CDCl_3$)** δ 194.4, 164.3, 155.9, 141.9, 131.2, 130.5 (q, *J* = 308 Hz), 127.8, 115.6, 114.2, 79.7, 55.6, 44.8, 44.7, 36.6, 28.3; **^{19}F NMR (377 MHz, $CDCl_3$)**: δ -39.5; **FTIR:** ν_{max}/cm^{-1} (neat) 3386, 2983, 2939, 1676, 1600, 1575, 1512, 1417, 1367, 1257, 1156, 1106, 1027, 759, 601; **HRMS (ESI$^+$):** *m/z* calcd. for $C_{19}H_{24}F_3NO_4SNa$: 442.1270, found: 442.1290 $[M+Na]^+$.

tert-Butyl (2-methylene-5-oxo-5-(p-tolyl)-4-((trifluoromethyl)thio)pentyl) carbamate (**129**)

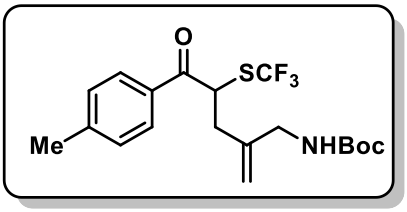

Following an adapted **GP9** using $Pd(dba)_2$ (13 mg, 0.02 mmol), ligand **L10** (22 mg, 0.07 mmol), carbamate **17** (100 mg, 0.469 mmol) and α-SCF_3-ketone **114** (165 mg, 0.703 mmol). Reaction mixture was stirred at reflux for 18 h. Following silica gel flash column chromatography [petroleum ether-CH_2Cl_2-EtOAc (65:30:5)] compound **129** was isolated as yellow oil (155 mg, 82%).

^{1}H NMR (400 MHz, $CDCl_3$): δ 7.91 (d, *J* = 8.0 Hz, 2H), 7.30 (d, *J* = 8.0 Hz, 2H), 5.09 - 5.13 (m, 1H), 5.00 (s, 1H), 4.90 (s, 1H), 4.62 (br, 1H), 3.80 - 3.69 (m, 2H), 2.94 (dd, *J* = 14.5 Hz, 8.5 Hz, 1H), 2.65 (dd, *J* = 14.5 Hz, 7.0 Hz, 1H), 2.43 (s, 3H), 1.43 (s, 9H); **^{13}C NMR (101 MHz, $CDCl_3$)** δ 195.5, 155.9, 145.2, 141.9, 132.4, 130.4 (q, *J* = 308 Hz), 129.7, 128.9, 115.6, 79.7, 45.0, 44.8, 36.5, 28.3, 21.8; **^{19}F NMR (377 MHz, $CDCl_3$)**: δ -39.4; **FTIR:** ν_{max}/cm^{-1} (neat) 3367, 2983, 2926, 1681, 1606, 1509, 1367, 1272, 1257, 1153, 1109, 1046, 762, 750, 595; **HRMS (ESI$^+$):** *m/z* calcd. for $C_{19}H_{24}F_3NO_3SNa$: 426.1321, found: 426.1333 $[M+Na]^+$.

tert-Butyl (5-(4-chlorophenyl)-2-methylene-5-oxo-4-((trifluoromethyl)thio)pentyl) carbamate (**130**)

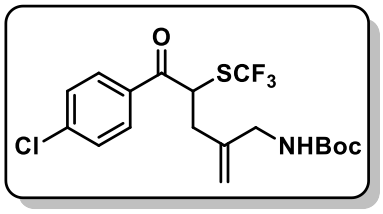

Following **GP9** using $Pd(dba)_2$ (13 mg, 0.02 mmol), ligand **L10** (22 mg, 0.07 mmol), carbamate **17** (100 mg, 0.469 mmol) and α-SCF_3-ketone **115** (179 mg,

0.703 mmol). Following silica gel flash column chromatography [petroleum ether-CH_2Cl_2-EtOAc (65:30:5)] compound **130** was isolated as yellow oil (189 mg, 95%).

^{1}H NMR (400 MHz, $CDCl_3$): δ 7.97 (d, *J* = 8.5 Hz, 2H), 7.48 (d, *J* = 8.5 Hz, 2H), 5.12 (t, *J* = 7.0 Hz, 1H), 5.01 (s, 1H), 4.90 (s, 1H), 4.64 (br, 1H), 3.80 (dd, *J* = 16.0 Hz, 6.0 Hz, 1H), 3.70 (dd, *J* = 16.0 Hz, 6.0 Hz, 1H), 2.93 (dd, *J* = 14.5 Hz, 8.0 Hz, 1H), 2.64 (dd, *J* = 14.5 Hz, 7.0 Hz, 1H), 1.42 (s, 9H); **^{13}C NMR (101 MHz, $CDCl_3$)** δ 194.9, 155.9, 141.8, 140.6, 133.3, 130.3 (q, *J* = 308 Hz), 130.2, 129.3, 116.1, 79.8, 44.8, 44.7, 36.2, 28.3; **^{19}F NMR (377 MHz, $CDCl_3$)**: δ -39.3; **FTIR:** ν_{max}/cm^{-1} (neat) 3363, 2981, 2930, 1688, 1590, 1508, 1367, 1275, 1260, 1157, 1108, 1050, 764, 751, 532; **HRMS (ESI$^+$):** *m/z* calcd. for $C_{18}H_{21}{}^{35}ClF_3NO_3SNa$: 446.0775, found: 446.0790 $[M+Na]^+$.

tert-Butyl (2-methylene-5-(4-nitrophenyl)-5-oxo-4-((trifluoromethyl)thio)pentyl) carbamate (**131**)

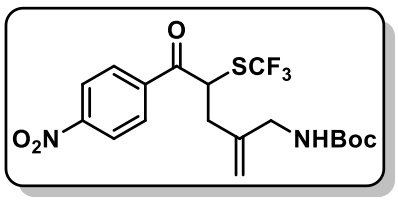

Following **GP9** using $Pd(dba)_2$ (13 mg, 0.02 mmol), ligand **L10** (22 mg, 0.07 mmol), carbamate **17** (100 mg, 0.469 mmol) and α-SCF_3-ketone **116** (186 mg, 0.703 mmol). Following silica gel flash column chromatography [petroleum ether-CH_2Cl_2-EtOAc (65:30:5)] compound **131** was isolated as yellow oil (170 mg, 83%).

^{1}H NMR (400 MHz, $CDCl_3$): δ 8.34 (d, *J* = 8.5 Hz, 2H), 8.20 (d, *J* = 8.5 Hz, 2H), 5.22 (t, *J* = 7.0 Hz, 1H), 5.03 (s, 1H), 4.93 (s, 1H), 4.70 (br, 1H), 3.85 (dd, *J* = 16.0 Hz, 6.0 Hz, 1H), 3.69 (dd, *J* = 16.0 Hz, 6.0 Hz, 1H), 2.95 (dd, *J* = 14.5 Hz, 8.0 Hz, 1H), 2.67 (dd, *J* = 14.5 Hz, 7.0 Hz, 1H), 1.41 (s, 9H); **^{13}C NMR (101 MHz, $CDCl_3$)** δ 195.2,

156.3, 150.8, 141.8, 140.0, 130.3 (q, *J* = 308 Hz), 130.0, 124.2, 116.8, 80.1 45.3, 44.6, 35.9, 28.4; **^{19}F NMR (377 MHz, $CDCl_3$)**: δ -38.9; **FTIR:** ν_{max}/cm^{-1} (neat) 3417, 2983, 2930 1694, 1605, 1528, 1367, 1346, 1275, 1260, 1157, 1104, 854, 764, 750, 699; **HRMS (ESI$^+$):** *m/z* calcd. for $C_{18}H_{21}F_3N_2O_5SNa$ 457.1015, found: 457.1037 $[M+Na]^+$.

tert-Butyl (2-methylene-5-oxo-5-(4-(trifluoromethyl)phenyl)-4-((trifluoromethyl)thio)pentyl)carbamate (**132**)

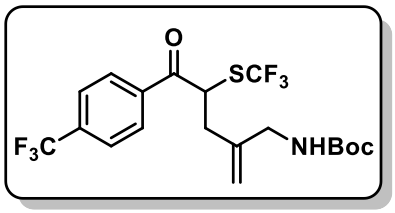

Following **GP9** using $Pd(dba)_2$ (13 mg, 0.02 mmol), ligand **L10** (22 mg, 0.07 mmol), carbamate **17** (100 mg, 0.469 mmol) and α-SCF_3-ketone **117** (203 mg, 0.703 mmol). Following silica gel flash column chromatography [petroleum ether-CH_2Cl_2-EtOAc (65:30:5)] compound **132** was isolated as yellow oil (197 mg, 92%).

^{1}H NMR (400 MHz, $CDCl_3$): δ 8.14 (d, *J* = 8.0 Hz, 2H), 7.77 (d, *J* = 8.0 Hz, 2H), 5.19 (t, *J* = 7.0 Hz, 1H), 5.02 (s, 1H), 4.92 (s, 1H), 4.66 (br, 1H), 3.83 (dd, *J* = 16.0 Hz, 6.0 Hz, 1H), 3.70 (dd, *J* = 16.0 Hz, 6.0 Hz, 1H), 2.95 (dd, *J* = 14.5 Hz, 8.0 Hz, 1H), 2.65 (dd, *J* = 14.5 Hz, 7.0 Hz, 1H), 1.41 (s, 9H); **^{13}C NMR (101 MHz, $CDCl_3$)** δ 195.4, 156.2, 141.9, 138.0, 135.5 (q, *J* = 33.0 Hz), 130.3 (q, *J* = 308 Hz), 129.3 ,126.1 (q, *J* = 3.0 Hz),), 123.5 (q, *J* = 273.0 Hz), 116.4, 80.0, 45.2, 44.7, 36.1, 28.4; **^{19}F NMR (377 MHz, $CDCl_3$)**: δ -63.3, -39.1; **FTIR:** ν_{max}/cm^{-1} (neat) 3375, 2985, 2932, 1693, 1512, 1411, 1368, 1323, 1276, 1261, 1160, 1105, 1067, 1016, 858, 765, 750, 699; **HRMS (ESI$^+$):** *m/z* calcd. for $C_{19}H_{21}F_6NO_3SNa$ 480.1039, found: 480.1060 $[M+Na]^+$.

tert-Butyl (5-(3-chlorophenyl)-2-methylene-5-oxo-4-((trifluoromethyl)thio)pentyl) carbamate (**133**)

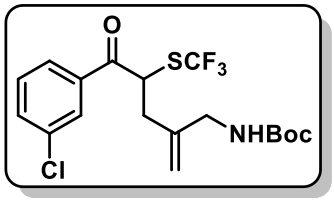

Following **GP9** using $Pd(dba)_2$ (13 mg, 0.02 mmol), ligand **L10** (22 mg, 0.07 mmol), carbamate **17** (100 mg, 0.469 mmol) and α-SCF_3-ketone **118** (179 mg, 0.703 mmol). Following silica gel flash column chromatography [petroleum ether-CH_2Cl_2-EtOAc (65:30:5)] compound **133** was isolated as yellow oil (174 mg, 87%).

^{1}H NMR (400 MHz, $CDCl_3$): δ 8.00 (s, 1H), 7.91 (d, *J* = 7.5 Hz, 1H), 7.59 (d, *J* = 8.0 Hz, 1H), 7.45 (t, *J* = 8.0 Hz, 1H), 5.10 (t, *J* = 7.0 Hz, 1H), 5.02 (s, 1H), 4.91 (s, 1H), 4.66 (br, 1H), 3.81 (dd, *J* = 16.0 Hz, 6.0 Hz, 1H), 3.70 (dd, *J* = 16.0 Hz, 6.0 Hz, 1H), 2.94 (dd, *J* = 14.5 Hz, 8.0 Hz, 1H), 2.65 (dd, *J* = 14.5 Hz, 7.0 Hz, 1H), 1.42 (s, 9H); **^{13}C NMR (101 MHz, $CDCl_3$)** δ 194.9, 156.0, 141.8, 136.6, 135.4, 133.9, 130.2, 130.1 (q, *J* = 308 Hz), 128.8, 126.8, 116.0, 79.8, 45.0, 44.7, 36.1, 28.3; **^{19}F NMR (377 MHz, $CDCl_3$)**: δ -39.2; **FTIR:** ν_{max}/cm^{-1} (neat) 3385, 2984, 2937, 1693, 1512, 1341, 1276, 1261, 1159, 1112, 1049, 764, 750; **HRMS (ESI$^+$):** *m/z* calcd. for $C_{18}H_{21}{}^{35}ClF_3NO_3SNa$: 446.0775, found: 446.0791 $[M+Na]^+$.

tert-Butyl (5-(2-methoxyphenyl)-2-methylene-5-oxo-4-((trifluoromethyl)thio)pentyl) carbamate (**134**)

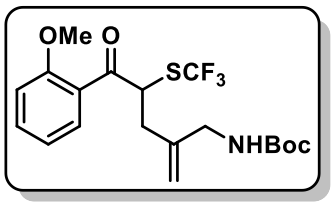

Following **GP9** using $Pd(dba)_2$ (13 mg, 0.02 mmol), ligand **L10** (22 mg, 0.07 mmol), carbamate **17** (100 mg, 0.469 mmol) and α-SCF_3-ketone **119** (176 mg, 0.703 mmol).

Following silica gel flash column chromatography [petroleum ether-CH_2Cl_2-EtOAc (65:30:5)] compound **134** was isolated as yellow oil (179 mg, 91%).

^{1}H NMR (400 MHz, $CDCl_3$): δ 7.70 (dd, *J* = 8.0 Hz, 2.0 Hz, 1H), 7.54 - 7.48 (m, 1H), 7.03 (t, *J* = 7.0 Hz, 1H), 6.99 (d, *J* = 8.0 Hz, 1H), 5.27 (t, *J* = 7.0 Hz, 1H), 5.04 (s, 1H), 4.95 (s, 1H), 4.62 (br, 1H), 3.95 (s, 3H), 3.80 - 3.69 (m, 2H), 2.96 (dd, *J* = 15.0 Hz, 8.0 Hz, 1H), 2.59 (dd, *J* = 15.0 Hz, 7.0 Hz, 1H), 1.43 (s, 9H); **^{13}C NMR (101 MHz, $CDCl_3$)** δ 197.3, 158.3, 155.8, 142.1, 134.5, 131.8, 130.5 (q, *J* = 308 Hz), 125.8, 121.1, 114.4, 111.6, 79.5, 55.6, 49.9, 44.9, 36.6, 28.3; **^{19}F NMR (377 MHz, $CDCl_3$)**: δ -39.5; **FTIR:** ν_{max}/cm^{-1} (neat) 3384, 2981, 2929, 1692, 1598, 1506, 1486, 1438, 1367, 1276, 1260 1162, 1108, 1021, 764, 751, 643; **HRMS (ESI$^+$):** *m/z* calcd. for $C_{19}H_{24}F_3NO_4SNa$: 442.1270, found: 442.1290 $[M+Na]^+$.

tert-Butyl (2-methylene-5-oxo-5-(thiophen-2-yl)-4-((trifluoromethyl)thio)pentyl) carbamate (**135**)

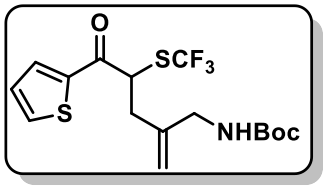

Following **GP9** using $Pd(dba)_2$ (13 mg, 0.02 mmol), ligand **L10** (22 mg, 0.07 mmol), carbamate **17** (100 mg, 0.469 mmol) and α-SCF_3-ketone **120** (159 mg, 0.703 mmol). Following silica gel flash column chromatography [petroleum ether-CH_2Cl_2-EtOAc (65:30:5)] compound **135** was isolated as yellow oil (150 mg, 81%).

^{1}H NMR (400 MHz, $CDCl_3$): δ 7.98 - 7.95 (m, 1H), 7.75 (d, *J* = 5.0 Hz, 1H), 7.18 (t, *J* = 5.0 Hz, 1H), 5.02 (s, 1H), 5.01 - 4.97 (m, 1H), 4.94 (s, 1H), 4.65 (br, 1H), 3.83 - 3.72 (m, 2H), 2.92 (dd, *J* = 14.5 Hz, 8.5 Hz, 1H), 2.63 (dd, *J* = 14.5 Hz, 7.0 Hz, 1H), 1.43 (s, 9H); **^{13}C NMR (101 MHz, $CDCl_3$)** δ 188.8, 156.0, 142.0, 141.6, 136.0, 133.7, 130.3 (q, *J* = 308 Hz), 128.6, 116.2, 79.8, 46.3, 44.6, 36.4, 28.3; **^{19}F NMR (377 MHz,**

$CDCl_3$): δ -39.7; **FTIR:** ν_{max}/cm^{-1} (neat) 3384, 2982, 2931, 1697, 1662, 1516, 1413, 1367, 1356, 1275, 1260 1157, 1112, 916, 857, 764, 750; **HRMS (ESI^+):** *m/z* calcd. for $C_{16}H_{20}F_3NO_3S_2Na$: 418.0729, found: 418.0743 $[M+Na]^+$.

tert-Butyl (4-methyl-2-methylene-5-oxo-5-phenyl-4-((trifluoromethyl)thio)pentyl) carbamate (**136**)

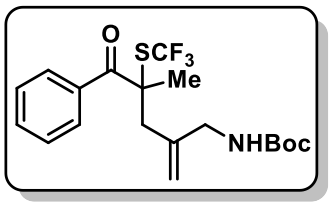

Following an adapted **GP9** using $Pd(dba)_2$ (13 mg, 0.02 mmol), ligand **L10** (22 mg, 0.07 mmol), carbamate **17** (100 mg, 0.469 mmol) and α-SCF_3-ketone **121** (165 mg, 0.703 mmol). Reaction mixture was stirred at reflux for 18 h. Following silica gel flash column chromatography [petroleum ether-CH_2Cl_2-EtOAc (65:30:5)] compound **136** was isolated as yellow oil (159 mg, 84%).

^{1}H NMR (400 MHz, $CDCl_3$): δ 8.08 (d, *J* = 7.5 Hz, 2H), 7.54 (t, *J* = 7.5 Hz, 1H), 7.44 (t, *J* = 7.5 Hz, 2H), 5.13 (s, 1H), 4.90 (s, 1H), 4.63 (br, 1H), 3.65 (dd, *J* = 16.0 Hz, 6.0 Hz, 1H), 3.56 (dd, *J* = 16.0 Hz, 6.0 Hz, 1H), 3.08 (d, *J* = 14.5 Hz, 1H), 2.72 (d, *J* = 14.5 Hz , 1H), 1.75 (s, 3H), 1.43 (s, 9H); **^{13}C NMR (101 MHz, $CDCl_3$)** δ 198.7, 155.7, 140.5, 135.9, 132.5, 129.5, 129.4 (q, *J* = 308 Hz), 128.4, 117.0, 79.6, 58.2, 46.2, 42.3, 28.4, 24.5; **^{19}F NMR (377 MHz, $CDCl_3$)**: δ -35.8; **FTIR:** ν_{max}/cm^{-1} (neat) 3356, 2980, 2934, 1682, 1597, 1512, 1448, 1392, 1367, 1275, 1250, 1161, 1109, 1071, 971, 912, 757, 696; **HRMS (ESI^+):** *m/z* calcd. for $C_{19}H_{24}F_3NO_3SNa$: 426.1321, found: 426.1337 $[M+Na]^+$.

tert-Butyl (2-methylene-5-oxo-4-((trifluoromethyl)thio)heptyl)carbamate (**137**)

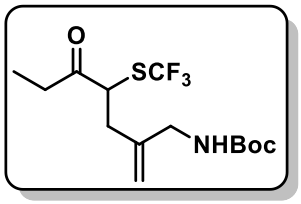

Following an adapted **GP9** using $Pd(dba)_2$ (13 mg, 0.02 mmol), ligand **L10** (22 mg, 0.07 mmol), carbamate **17** (100 mg, 0.469 mmol) and α-SCF_3-ketone **122** (121 mg, 0.703 mmol). Reaction mixture was stirred at reflux for 18 h. Following silica gel flash column chromatography [petroleum ether-CH_2Cl_2-EtOAc (65:30:5)] compound **137** was isolated as yellow oil (136 mg, 85%).

^{1}H NMR (400 MHz, $CDCl_3$): δ 5.05 (s, 1H), 4.89 (s, 1H), 4.68 (br, 1H), 4.11 (t, *J* = 7.5 Hz, 1H), 3.78 (dd, *J* = 16.0 Hz, 6.5 Hz, 1H), 3.66 (dd, *J* = 16.0 Hz, 6.0 Hz, 1H), 2.80 - 2.57 (m, 3H), 2.44 (dd, *J* = 14.5 Hz, 7.0 Hz, 1H), 1.44 (s, 9H), 1.08 (t, *J* = 7.0 Hz, 3H); **^{13}C NMR (101 MHz, $CDCl_3$)** δ 206.6, 156.0, 141.8, 130.2 (q, *J* = 308 Hz), 115.3, 79.4, 49.6, 44.6, 35.2, 34.0, 28.3, 7.69; **^{19}F NMR (377 MHz, $CDCl_3$)**: δ -39.7; **FTIR:** ν_{max}/cm^{-1} (neat) 3363, 2981, 2935, 1702, 1513, 1457, 1392, 1367, 1275, 1254, 1158, 1116, 1048, 915, 757; **HRMS (ESI$^+$):** *m/z* calcd. for $C_{14}H_{22}F_3NO_3SNa$: 364.1165, found: 364.1181 $[M+Na]^+$.

Ethyl 2-benzoyl-4-(((*tert*-butoxycarbonyl)amino)methyl)-2-((trifluoromethyl)thio) pent-4-enoate (**138**)

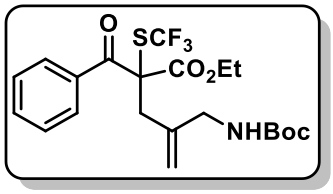

Following an adapted **GP9** using $Pd(dba)_2$ (20 mg, 0.035 mmol), ligand **L10** (33 mg, 0.11 mmol), carbamate **17** (150 mg, 0.703 mmol) and α-SCF_3-ketone **125** (308 mg, 1.05 mmol). Reaction mixture was stirred at reflux for 18 h. Following silica gel flash column chromatography [petroleum ether-CH_2Cl_2-EtOAc (65:30:5)] compound **138** was isolated as yellow oil (309 mg, 95%).

^{1}H NMR (400 MHz, $CDCl_3$): δ 8.00 (d, *J* = 8.0 Hz, 2H), 7.57 (t, *J* = 7.5 Hz, 1H), 7.44 (t, *J* = 8.0 Hz, 2H), 5.16 (s, 1H), 4.94 (s, 1H), 4.68 (br, 1H), 4.23 - 4.06 (m, 2H), 3.74 (d, *J* = 6.0 Hz, 2H), 3.29 (d, *J* = 15.5 Hz, 1H), 3.24 (d, *J* = 15.5 Hz , 1H), 1.43 (s, 9H), 1.03 (t, *J* = 7.0 Hz, 3H); **^{13}C NMR (101 MHz, $CDCl_3$)** δ 190.5, 168.5, 155.8, 140.3, 134.3, 133.8, 129.5 (q, *J* = 309 Hz), 129.3, 128.8, 117.3, 79.5, 63.5, 60.6, 45.9, 39.2, 28.5, 13.6; **^{19}F NMR (377 MHz, $CDCl_3$)**: δ -36.4; **HRMS (ESI^+):** *m/z* calcd. for $C_{21}H_{26}F_3NO_5SNa$: 484.1376, found: 484.1394 $[M+Na]^+$.

5.2.10. Synthesis of 3-Trifluoromethylthiopiperidines

General Procedure 10 (**GP10**)

To a solution of the allylated product (1 eq.) in CH_2Cl_2 (0.1 M) was added TFA (75 eq.) and the resulting mixture was stirred at r.t. for 1 h. The reaction mixture was concentrated under reduced pressure and residual TFA was removed by azeotropic distillation with toluene (3 x 1 mL). The iminium salt was dissolved in MeOH (0.2 M) and cooled to 0 °C. $NaBH_4$ (4 eq.) was added and the reaction was then allowed to warm to r.t. and stirred for 16 h under nitrogen. The reaction mixture was diluted with a saturated $NaHCO_3$ solution (15 mL) and extracted with EtOAc (4 x 15 mL). The combined organic layers were dried with $MgSO_4$, filtered and concentrated under reduced pressure. The residue was then subjected to silica gel flash column chromatography to give the corresponding 3-SCF_3-piperidine.

5-Methylene-2-phenyl-3-((trifluoromethyl)thio)piperidine (**139**)

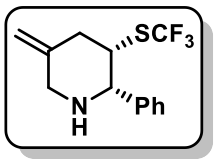

Following **GP10** using compound **127** (312 mg, 0.801 mmol), TFA (6.8 g, 60.1 mmol) and $NaBH_4$ (121 mg, 3.20 mmol). Purification by flash column chromatography [petroleum ether-EtOAc (80:20)] gave piperidine **139** as a white solid (166 mg, 76%).

^{1}H NMR (400 MHz, $CDCl_3$): δ 7.40 - 7.27 (m, 5H), 5.07 (s, 1H), 4.96 (s, 1H), 4.25 (s, 1H), 3.70 - 3.63 (m, 2H), 3.49 (d, *J* = 12.5 Hz, 1H), 2.90 (d, *J* = 14.0 Hz, 1H), 2.81 (d, *J* = 14.0 Hz, 1H), 2.12 (br, 1H); **^{13}C NMR (101 MHz, $CDCl_3$)** δ 140.2, 138.3, 131.3 (q, *J* = 306 Hz), 128.3, 127.8, 126.8, 113.8, 63.7, 53.2, 50.6, 41.6; **^{19}F NMR (377 MHz, $CDCl_3$)**: δ -40.3; **FTIR:** ν_{max}/cm^{-1} (neat) 3311, 2991, 2956, 2786, 1662, 1493, 1452, 1347, 1275, 1261, 1104, 1030, 954, 907, 764, 750, 699; **HRMS (ESI$^+$):** *m/z* calcd. for $C_{13}H_{14}F_3NS$: 273.0794, found: 273.0788 $[M]^+$.

2-(4-Methoxyphenyl)-5-methylene-3-((trifluoromethyl)thio)piperidine (**140**)

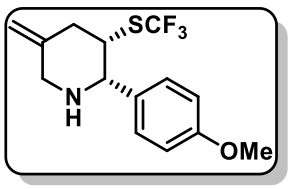

Following **GP10** using compound **128** (153 mg, 0.365 mmol), TFA (3.1 g, 27.4 mmol) and $NaBH_4$ (55 mg, 1.46 mmol). Purification by flash column chromatography [petroleum ether-EtOAc (80:20)] gave piperidine **140** as an amorphous white solid (79 mg, 71%).

^{1}H NMR (400 MHz, $CDCl_3$): δ 7.26 (d, *J* = 8.5 Hz, 2H), 6.88 (d, *J* = 8.5 Hz, 2H), 5.05 (s, 1H), 4.94 (s, 1H), 4.18 (s, 1H), 3.80 (s, 3H), 3.65 (d, *J* = 12.5 Hz, 1H), 3.62 - 3.59 (m, 1H), 3.48 (d, *J* = 12.5 Hz, 1H), 2.88 (d, *J* = 13.5 Hz, 1H), 2.79 (d, *J* = 13.5 Hz, 1H), 2.11 (br, 1H); **^{13}C NMR (101 MHz, $CDCl_3$)** δ 159.1, 138.6, 132.6, 131.4 (q, *J* = 306 Hz), 127.9, 113.6, 113.5, 63.3, 55.2, 53.4, 50.8, 41.5; **^{19}F NMR (377 MHz,**

$CDCl_3$): δ -40.2; **FTIR:** ν_{max}/cm^{-1} (neat) 3006, 2984, 2958, 2838, 2777, 1661, 1613, 1514, 1443, 1347, 1276, 1254, 1108, 1033, 905, 822, 764, 750; **HRMS (ESI^+):** *m/z* calcd. for $C_{14}H_{17}F_3NOS$: 304.0977, found: 304.0993 $[M+H]^+$.

5-Methylene-2-(*p*-tolyl)-3-((trifluoromethyl)thio)piperidine (**141**)

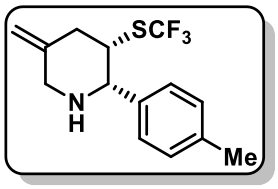

Following **GP10** using compound **129** (125 mg, 0.310 mmol), TFA (2.6 g, 23.2 mmol) and $NaBH_4$ (47 mg, 1.24 mmol). Purification by flash column chromatography [petroleum ether-EtOAc (80:20)] gave piperidine **141** as an amorphous white solid (64 mg, 72%).

^{1}H NMR (400 MHz, $CDCl_3$): δ 7.22 (d, *J* = 8.0 Hz, 2H), 7.16 (d, *J* = 8.0 Hz, 2H), 5.05 (s, 1H), 4.94 (s, 1H), 4.20 (s, 1H), 3.68 - 3.61 (m, 2H), 3.48 (d, *J* = 12.5 Hz, 1H), 2.88 (d, *J* = 14.0 Hz, 1H), 2.80 (d, *J* = 14.0 Hz, 1H), 2.12 (br, 1H); **^{13}C NMR (101 MHz, $CDCl_3$)** δ 138.6, 137.4, 137.3, 131.4 (q, *J* = 306 Hz), 128.9, 126.6, 113.5, 63.5, 53.3, 50.7, 41.5, 21.1; **^{19}F NMR (377 MHz, $CDCl_3$)**: δ -40.2; **FTIR:** ν_{max}/cm^{-1} (neat) 3006, 2958, 2838, 2777, 1661, 1613, 1514, 1443, 1347, 1276, 1254, 1108, 1033, 905, 822, 764, 750; **HRMS (ESI^+):** *m/z* calcd. for $C_{14}H_{17}F_3NS$: 288.1028, found: 288.1042 $[M+H]^+$.

2-(4-Chlorophenyl)-5-methylene-3-((trifluoromethyl)thio)piperidine (**142**)

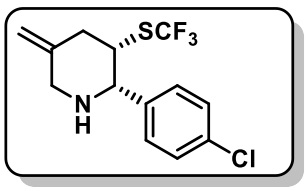

Following **GP10** using compound **130** (174 mg, 0.410 mmol), TFA (3.5 g, 30.8 mmol) and $NaBH_4$ (62 mg, 1.64 mmol). Purification by flash column chromatography [petroleum ether-EtOAc (80:20)] gave piperidine **142** as a colourless oil (68 mg, 54%).

^{1}H NMR (400 MHz, $CDCl_3$): δ 7.35 - 7.27 (m, 4H), 5.06 (s, 1H), 4.95 (s, 1H), 4.20 (s, 1H), 3.64 (d, *J* = 12.5 Hz, 1H), 3.61 - 3.58 (m, 1H), 3.47 (d, *J* = 12.5 Hz, 1H), 2.88 (d, *J* = 14.0 Hz, 1H), 2.80 (d, *J* = 14.0 Hz, 1H), 2.12 (br, 1H); **^{13}C NMR (101 MHz, $CDCl_3$)** δ 139.0, 138.2, 133.5, 131.3 (q, *J* = 306 Hz), 128.4, 128.2, 113.8, 63.2, 53.2, 50.5, 41.6; **^{19}F NMR (377 MHz, $CDCl_3$)**: δ -40.4; **FTIR:** ν_{max}/cm^{-1} (neat) 3008, 2989, 2954, 2794, 1661, 1493, 1447, 1276, 1261, 1110, 1014, 906, 812, 764, 750; **HRMS (ESI$^+$):** *m/z* calcd. for $C_{13}H_{14}{}^{35}ClF_3NS$: 308.0482, found: 308.0497 $[M+H]^+$.

5-Methylene-2-(thiophen-2-yl)-3-((trifluoromethyl)thio)piperidine (**143**)

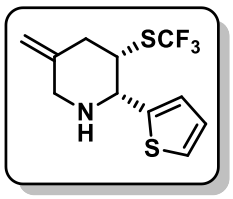

Following **GP10** using compound **135** (124 mg, 0.313 mmol), TFA (2.7 g, 23.5 mmol) and $NaBH_4$ (47 mg, 1.25 mmol). Purification by flash column chromatography [petroleum ether-EtOAc (80:20)] gave piperidine **143** as an amorphous white solid (56 mg, 64%).

^{1}H NMR (400 MHz, $CDCl_3$): δ 7.26 - 7.25 (m, 1H), 7.06 - 6.98 (m, 2H), 5.04 (s, 1H), 4.95 (s, 1H), 4.52 (s, 1H), 3.71 (dd, *J* = 6.0 Hz, 3.0 Hz, 1H), 3.61 (d, *J* = 13.0 Hz, 1H), 3.48 (d, *J* = 13.0 Hz, 1H), 2.86 (d, *J* = 14.0 Hz, 1H), 2.80 (dd, *J* = 14.0 Hz, 3.0 Hz, 1H), 1.89 (br, 1H); **^{13}C NMR (101 MHz, $CDCl_3$)** δ 143.5, 138.4, 131.4 (q, *J* = 306 Hz), 126.6, 124.7, 124.6, 113.8, 60.0, 52.9, 50.5, 41.0; **^{19}F NMR (377 MHz, $CDCl_3$)**: δ -40.1; **FTIR:** ν_{max}/cm^{-1} (neat) 3306, 3008, 2991, 2961, 2798, 1664, 1435, 1311, 1276, 1261, 1121, 1103, 949, 906, 764, 750, 702; **HRMS (ESI$^+$):** *m/z* calcd. for $C_{11}H_{13}F_3NS_2$: 280.0436, found: 280.0439 $[M+H]^+$.

2-(2-Methoxyphenyl)-5-methylene-3-((trifluoromethyl)thio)piperidine (**144**)

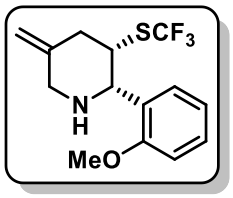

Following **GP10** using compound **134** (162 mg, 0.386 mmol), TFA (3.3 g, 29.0 mmol) and $NaBH_4$ (58 mg, 1.54 mmol). Purification by flash column chromatography [petroleum ether-EtOAc (80:20)] gave piperidine **144** as a white solid (66 mg, 56%).

^{1}H NMR (400 MHz, $CDCl_3$): δ 7.32 (d, *J* = 7.5 Hz, 1H), 7.27 (t, *J* = 8.0 Hz, 1H), 6.97 (t, *J* = 7.5 Hz, 1H), 6.87 (d, *J* = 8.0 Hz, 1H), 5.03 (s, 1H), 4.92 (s, 1H), 4.48 (s, 1H), 3.96 - 3.91 (m, 1H), 3.86 (s, 3H), 3.65 (d, *J* = 12.5 Hz, 1H), 3.49 (d, *J* = 12.5 Hz, 1H), 2.91 (d, *J* = 14.0 Hz, 1H), 2.75 (d, *J* = 14.0 Hz, 1H), 1.67 (br, 1H); **^{13}C NMR (101 MHz, $CDCl_3$)** δ 156.1, 139.6, 131.5 (q, *J* = 307 Hz), 128.8, 128.4, 127.3, 120.4, 112.9, 109.9, 57.9, 55.3, 53.7, 47.9, 41.5; **^{19}F NMR (377 MHz, $CDCl_3$)**: δ -40.4; **FTIR:** ν_{max}/cm^{-1} (neat) 3008, 2989, 2957, 2839, 2777, 1661, 1603, 1493, 1466, 1348, 1276, 1260, 1108, 1028, 903, 764, 750; **HRMS (ESI$^+$):** *m/z* calcd. for $C_{14}H_{17}F_3NOS$: 304.0977, found: 304.0976 $[M+H]^+$.

2-(3-Chlorophenyl)-5-methylene-3-((trifluoromethyl)thio)piperidine (**145**)

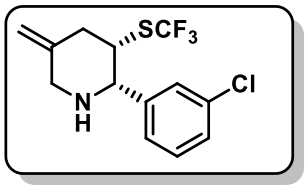

Following **GP10** using compound **133** (184 mg, 0.434 mmol), TFA (3.7 g, 32.6 mmol) and $NaBH_4$ (66 mg, 1.74 mmol). Purification by flash column chromatography [petroleum ether-EtOAc (80:20)] gave piperidine **145** as a yellow oil (47 mg, 35%).

^{1}H NMR (400 MHz, $CDCl_3$): δ 7.36 - 7.20 (m, 4H), 5.06 (s, 1H), 4.94 (s, 1H), 4.19 (s, 1H), 3.67 - 3.60 (m, 2H), 3.46 (d, *J* = 12.5 Hz, 1H), 2.88 (d, *J* = 14.0 Hz, 1H), 2.79 (d, *J* = 14.0 Hz, 1H), 1.70 (br, 1H); **^{13}C NMR (101 MHz, $CDCl_3$)** δ 142.7, 138.4, 134.2,

131.3 (q, *J* = 306 Hz), 129.8, 127.9, 127.1, 125.0, 113.6, 63.3, 53.2, 50.4, 41.6; **^{19}F NMR (377 MHz, $CDCl_3$)**: δ -40.4; **FTIR:** ν_{max}/cm^{-1} (neat) 3008, 2989, 2954, 2803, 1661, 1478, 1447, 1276, 1261, 1100, 1035, 907, 848, 764, 750; **HRMS (ESI$^+$):** *m/z* calcd. for $C_{13}H_{14}{}^{35}ClF_3NS$: 308.0482, found: 308.0477 $[M+H]^+$.

3-Methyl-5-methylene-2-phenyl-3-((trifluoromethyl)thio)piperidine (**146**)

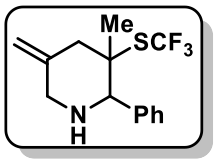

Following **GP10** using compound **136** (122 mg, 0.302 mmol), TFA (2.6 g, 22.7 mmol) and $NaBH_4$ (46 mg, 1.21 mmol). Purification by flash column chromatography [petroleum ether-EtOAc (80:20)] gave piperidine **146** as a yellow oil (78 mg, 90%, 5:1 d.r.). Data reported for major diastereomer only.

^{1}H NMR (400 MHz, $CDCl_3$): δ 7.42 - 7.31 (m, 5H), 5.05 (s, 1H), 4.91 (s, 1H), 3.72 - 3.67 (m, 2H), 3.48 (d, *J* = 12.0 Hz, 1H), 2.89 (d, *J* = 14.0 Hz, 1H), 2.45 (d, *J* = 14.0 Hz, 1H), 1.78 (br, 1H), 1.43 (s, 3H); **^{13}C NMR (101 MHz, $CDCl_3$)** δ 140.0, 138.4, 131.6 (q, *J* = 307.5 Hz), 129.0, 128.3, 127.9, 112.7, 72.4, 56.8, 53.6, 48.3, 26.5; **^{19}F NMR (377 MHz, $CDCl_3$)**: δ -33.5; **FTIR:** ν_{max}/cm^{-1} (neat) 3033, 3005, 2988, 2785, 1661, 1494, 1455, 1340, 1275, 1261, 1096, 1074, 1032, 899, 764, 750, 700; **HRMS (ESI$^+$):** *m/z* calcd. for $C_{14}H_{17}F_3NS$: 288.1028, found: 288.1015 $[M+H]^+$.

2-Ethyl-5-methylene-3-((trifluoromethyl)thio)piperidine (**147**)

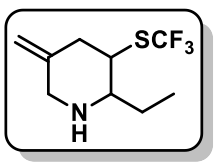

Following **GP10** using compound **137** (119 mg, 0.349 mmol), TFA (3.0 g, 26.1 mmol) and $NaBH_4$ (53 mg, 1.39 mmol). Purification by flash column chromatography [petroleum ether-EtOAc (80:20)]

gave piperidine **147** as a yellow oil (40 mg, 51%, 3:1 d.r.). Data reported for major diastereomer only.

^{1}H NMR (400 MHz, $CDCl_3$): δ 4.94 (s, 1H), 4.85 (s, 1H), 3.54 - 3.51 (m, 1H), 3.45 (d, *J* = 12.5 Hz, 1H), 3.30 (d, *J* = 12.5 Hz, 1H), 2.81 (t, *J* = 7.0 Hz, 1H), 2.72 - 2.63 (m, 2H), 1.74 (br, 1H), 1.64 - 1.48 (m, 2H) 0.97 (t, *J* = 7.5 Hz, 3H); **^{13}C NMR (101 MHz, $CDCl_3$)** δ 140.0, 131.9 (q, *J* = 306 Hz), 112.6, 61.4, 52.9, 48.1, 41.4, 26.6, 10.1; **^{19}F NMR (377 MHz, $CDCl_3$)**: δ -39.4; **FTIR:** ν_{max}/cm^{-1} (neat) 2966, 2939, 2880, 2791, 1661, 1437, 1275, 1261, 1141, 1099, 1004, 899, 764, 750, 704, 659; **HRMS (ESI^{+}):** *m/z* calcd. for $C_9H_{15}F_3NS$: 226.0872, found: 226.0876 $[M+H]^+$.

5.2.11. Investigations Towards the Synthesis of Lysergic Acid

Benzyl 4-formyl-1*H*-indole-1-carboxylate (**156**)[167]

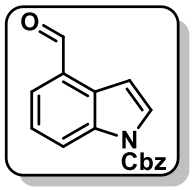

THF (28 mL) was added to indole-4-carboxaldehyde (1.0 g, 6.89 mmol) and the mixture was cooled to -78 °C. Lithium bis(trimethylsilyl)amide (1.0 M in THF, 13.8 mL, 13.8 mmol) was added dropwise followed by the addition of a solution of benzyl chloroformate (1.76 g, 10.3 mmol) in THF (2 mL) over 1 h. Upon complete addition, the reaction was stirred for a further 2 h at -78 °C, and then diluted with H_2O (40 mL) and extracted with EtOAc (3 x 40 mL). The combined organic layers were dried with $MgSO_4$, filtered and concentrated under reduced pressure. The crude material was then subjected to silica gel flash column chromatography [petroleum ether-EtOAc (95:5)] to give compound **156** as a colourless oil (769 mg, 40%).

^{1}H NMR (400 MHz, $CDCl_3$): δ 10.2 (s, 1H), 8.50 (d, *J* = 7.5 Hz, 1H), 7.82 (d, *J* = 3.5 Hz, 1H), 7.74 (d, *J* = 7.5 Hz, 1H), 7.52 - 7.37 (m, 7H), 5.48 (s, 2H).

The data match those reported in the literature.[167]

Benzyl 4-(hydroxymethyl)-1*H*-indole-1-carboxylate (**157**)[167]

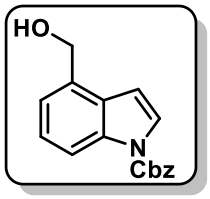

MeOH (5 mL) was added to indole **156** (500 mg, 1.79 mmol) and the solution was cooled to 0 °C. $NaBH_4$ (271 mg, 7.16 mmol) was added portion wise over 30 min, and then the reaction was stirred at 0 °C for a further 1 h. After this time, the resulting mixture was diluted with a saturated NH_4Cl solution (60 mL) and the product was extracted with $CHCl_3$ (3 x 60 mL). The combined organic layers were washed brine (1 x 100 mL), dried with $MgSO_4$ and then concentrated under reduced pressure to give compound **157** as a pure colourless oil without further purification (489 mg, 97%).

^{1}H NMR (400 MHz, $CDCl_3$): δ 8.15 (d, *J* = 7.5 Hz, 1H), 7.67 (d, *J* = 3.5 Hz, 1H), 7.49 (dd, *J* = 7.5 Hz, 1.5 Hz, 2H), 7.45 - 7.23 (m, 5H), 6.76 (d, *J* = 3.5 Hz, 1H), 5.46 (s, 2H), 4.94 (s, 2H).

The data match those reported in the literature.[167]

Benzyl 4-(chloromethyl)-1*H*-indole-1-carboxylate (**158**)[167]

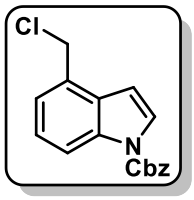

Compound **157** (489 mg, 1.74 mmol) was dissolved in EtOAc (5 mL) and the mixture was cooled to -40 °C. A solution of thionyl chloride (0.51 mL, 6.95 mmol) in EtOAc (2 mL) was then added and the reaction was stirred at this temperature for 2.5 h. After this time, the solvent was

removed under reduced pressure to give indole **158** as a pure brown oil (496 mg, 95%).

^{1}H NMR (400 MHz, $CDCl_3$): δ 8.19 (m, 1H), 7.71 (d, *J* = 3.5 Hz, 1H), 7.51 - 7.23 (m, 7H), 6.78 (d, *J* = 3.5Hz, 1H), 5.47 (s, 2H), 4.85 (s, 2H); **^{13}C NMR (101 MHz, $CDCl_3$)** δ 150.8, 135.6, 135.0, 129.5, 129.4, 128.9, 128.8, 128.6, 126.1, 124.7, 123.6, 115.9, 106.1, 68.9, 44.3.

The data match those reported in the literature.[167]

Benzyl 4-(cyanomethyl)-1H-indole-1-carboxylate (**159**)[167]

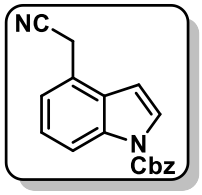

To a solution of compound **158** (496 mg, 1.65 mmol) in DMF (5 mL) was added NaCN (324 mg, 6.62 mmol) and the reaction was stirred at r.t. for 48 h. After this time, the resulting mixture was diluted with a saturated ferrous sulphate solution (40 mL), and then filtered through celite with $CHCl_3$ (40 mL). After solvent removal under reduced pressure, the residue was poured into H_2O (60 mL) and extracted with EtOAc (3 x 60 mL). The combined organic layers were washed with brine (1 x 100 mL), dried with $MgSO_4$, filtered and then concentrated under reduced pressure to give indole **159** as an amorphous white solid (326 mg, 68%).

^{1}H NMR (400 MHz, $CDCl_3$): δ 8.20 (d, *J* = 8.0 Hz, 1H), 7.69 (d, *J* = 3.5 Hz, 1H), 7.51 - 7.20 (m, 7H), 6.65 (d, *J* = 3.5 Hz, 1H), 5.47 (s, 2H), 3.98 (s, 2H); **FTIR:** ν_{max}/cm^{-1} (neat) 2928, 2855, 2248, 1739, 1490, 1434, 1335, 1277, 1128, 1051, 971, 758; **LCMS (ESI$^+$):** *m/z* calcd. for $C_{18}H_{15}N_2O_2$: 291.11, found 291.10 $[M+H]^+$.

The data match those reported in the literature.[167]

(1*H*-Indol-4-yl)methanol (**161**)

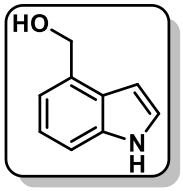

THF (20 mL) was added to indole-4-carboxaldehyde (2.0 g, 13.8 mmol) and the reaction was cooled on ice. $NaBH_4$ (678 mg, 17.9 mmol) was added and the reaction was stirred at 0 °C for 2 h. After this time, the resulting mixture was diluted with a saturated NH_4Cl solution (50 mL) and the product was extracted with EtOAc (3 x 50 mL). The combined organic layers were dried with $MgSO_4$, filtered and concentrated under reduced pressure to give indole **161** as a pure brown solid without further purification (2.03 g, quant.).

^{1}H NMR (400 MHz, $CDCl_3$): δ 8.31 (br, 1H), 7.37 (d, *J* = 8.0 Hz, 1H), 7.26 - 7.23 (m, 1H), 7.23 - 7.17 (m, 1H), 7.14 (d, *J* = 7.0 Hz, 1H), 6.71 - 6.68 (m, 1H), 5.0 (s, 2H), 1.75 (br, 1H).

The data match those reported in the literature.[168]

(1*H*-Indol-4-yl)methyl benzoate (**163**)[142]

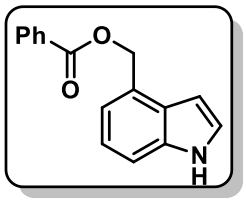

Benzoyl chloride (3.4 mL, 28.9 mmol) was added to a flask containing indole **161** (3.55 g, 24.1 mmol), Et_3N (10.1 mL, 72.4 mmol) and THF (130 mL) at 0 °C. The reaction was allowed to stir at r.t. for 16 h then the solvent was removed under reduced pressure. The residue was diluted with EtOAc (150 mL) and washed with 5% citric acid (2 x 100 mL), a saturated $NaHCO_3$ solution (2 x 100 mL) and brine (1 x 100 mL). The organic layer was then dried with $MgSO_4$, filtered and concentrated under

reduced pressure to give compound **163** as a pure off-white amorphous solid (6.06 g, quant.).

^{1}H NMR (400 MHz, $CDCl_3$): δ 8.31 (br, 1H), 8.09 (d, *J* = 8.0 Hz, 2H), 7.54 (t, *J* = 8.0 Hz, 1H), 7.45 - 7.39 (3H), 7.27 - 7.19 (m, 3H), 6.73 - 6.70 (m, 1H), 5.69 (s, 2H); **^{13}C NMR (101 MHz, $CDCl_3$)** δ 166.8, 136.1, 133.0, 130.5, 129.9, 128.5, 127.8, 127.0, 124.7, 122.0, 120.1, 111.6, 101.2, 65.8.

The data match those reported in the literature.[142]

2-(1*H*-Indol-4-yl)acetonitrile (**162**)

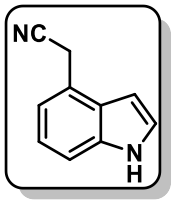

Potassium cyanide (4.24 g, 65.2 mmol) and [18]-crown-6 (3.45 g, 13.3 mmol) were added to a solution of compound **163** (3.28 g, 13.0 mmol) in DMF (50 mL). The reaction was stirred at 100 °C for 18 h, and then poured into brine (200 mL). The product was extracted with Et_2O (4 x 100 mL) and then the combined organic layers were dried with $MgSO_4$. After filtration and solvent removal under reduced pressure, the crude material was purified by flash column chromatography [petroleum ether-EtOAc (75:25)] to give indole **162** as an off-white amorphous solid (1.33 g, 65%).

^{1}H NMR (400 MHz, $CDCl_3$): δ 8.41 (br, 1H), 7.40 (d, *J* = 8.0 Hz, 1H), 7.29 - 7.26 (m, 1H), 7.20 (t, *J* = 7.5 Hz, 1H), 7.14 (d, *J* = 7.0 Hz, 1H), 6.61 - 6.57 (m, 1H), 3.98 (s, 2H); **^{13}C NMR (101 MHz, $CDCl_3$)** δ 135.9, 126.5, 125.0, 122.3, 121.5, 119.5, 118.1, 111.3, 100.1, 21.8; **HRMS (ESI^+):** *m/z* calcd. for $C_{10}H_9N_2$: 157.0760, found: 157.0757 $[M+H]^+$.

The data match those reported in the literature.[169]

Ethyl 2-(4-(cyanomethyl)-1*H*-indol-3-yl)-2-oxoacetate (**164**)

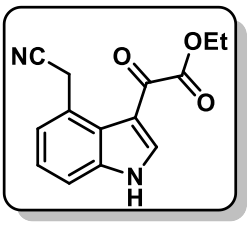

Oxalyl chloride (1 mL, 11.3 mmol) was added dropwise to a flask containing indole **162** and Et_2O (20 mL) under argon. The reaction was stirred at r.t. for 3 h, then cooled on ice and filtered off. The solid was then dissolved in EtOH (20 mL) and the reaction mixture was stirred at r.t. for 16 h. The resulting mixture was concentrated under reduced pressure leading to an off-white solid which was then recrystallised from EtOH (5 mL) and H_2O (15 mL) to give compound **164** as a white solid (781 mg, 81%).

m.p.: 128 - 130 °C; **^{1}H NMR (400 MHz, $CDCl_3$)**: δ 9.66 (br, 1H), 8.40 (d, *J* = 3.5 Hz, 1H), 7.42 (d, *J* = 7.0 Hz, 1H), 7.35 - 7.27 (m, 2H), 4.62 (s, 2H), 4.40 (q, *J* = 7.0 Hz, 2H), 1.40 (t, *J* = 7.0 Hz, 3H); **^{13}C NMR (101 MHz, $CDCl_3$)** δ 179.1, 163.9, 139.2, 137.7, 125.1, 124.7, 124.6, 123.6, 119.3, 114.5, 112.3, 62.5, 24.6, 14.1; **HRMS (ESI$^+$):** *m/z* calcd. for $C_{14}H_{13}N_2O_3$: 257.0921, found: 257.0921 $[M+H]^+$.

3-Allyl-1*H*-indole (**170**)

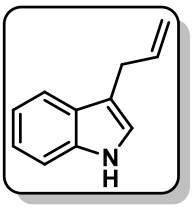

To a solution of indole (500 mg, 4.27 mmol) in THF (11 mL) was added $Pd(PPh_3)_4$ (247 mg, 0.213 mmol), allyl alcohol (273 mg, 4.69 mmol) and triethylborane (1 M in hexane, 1.3 mL, 1.28 mmol). The reaction was stirred at 50 °C for 24 h, then diluted with EtOAc (100 mL) and washed with a saturated $NaHCO_3$ solution (1 x 100 mL) and brine (1 x100 mL). The organic layer was dried with $MgSO_4$, filtered off and concentrated under reduced pressure. The crude material was then subjected to silica gel column chromatography [petroleum ether-EtOAc (90:10)] to give indole **170** as pale yellow oil (578 mg, 86 %).

^{1}H NMR (400 MHz, $CDCl_3$): δ 7.95 (br, 1H), 7.62 (d, *J* = 8.0 Hz, 1H), 7.37 (d, *J* = 8.0 Hz, 1H), 7.21 (t, *J* = 7.5 Hz, 1H), 7.13 (t, *J* = 7.5 Hz, 1H), 7.00 - 6.98 (m, 1H), 6.15 - 6.03 (m, 1H), 5.22 - 5.14 (m, 1 H), 5.11 - 5.06 (m, 1H), 3.54 (dd, *J* = 6.5 Hz, 1.0 Hz, 2H); **^{13}C NMR (101 MHz, $CDCl_3$)** δ 137.3, 136.3, 127.4, 121.9, 121.7, 119.2, 119.1, 115.2, 114.3, 111.1, 29.8.

The data match those reported in the literature.[170]

3-Iodo-1*H*-indole (**172**)

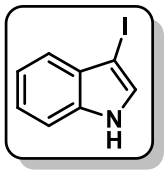

KOH (1.20 g, 21.3 mmol) was added to a solution of indole (1.0 g, 8.54 mmol) in DMF (15 mL) and the resulting mixture was stirred at r.t. for 20 min. After this time, a solution of I_2 (2.17 g, 8.54 mmol) in DMF (2.5 mL) was added and the reaction was stirred at r.t. for a further 1 h. The reaction was then poured into an ice/H_2O mixture (200 mL) and the product was collected by filtration and washed with H_2O (50 mL). After residual H_2O removal by azeotropic distillation with toluene (3 x 3 mL), the product was isolated as a pure off-white solid (1.99 g, 96%).

^{1}H NMR (400 MHz, $CDCl_3$): δ 8.34 (br, 1H), 7.47 (d, *J* = 8.0 Hz, 1H), 7.38 (d, *J* = 8.0 Hz, 1H), 7.31 - 7.19 (m, 3H); **^{13}C NMR (101 MHz, $CDCl_3$)** δ 135.7, 129.9, 128.6, 123.3, 121.1, 121.0, 111.6, 57.6.

The data match those reported in the literature.[147]

tert-Butyl 2-(1*H*-indol-3-yl)acetate (**183)**

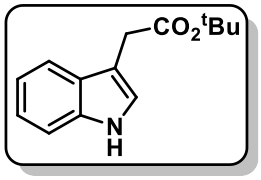

Indole **172** (102 mg, 0.420 mmol) and $PdCl_2(A^{ta}Phos)_2$ (15 mg, 0.02 mmol) were added to a flame-dried flask which was then exposed to 3 vacuum/argon purge cycles. THF (2 mL) was added followed by 2-*tert*-butoxy-2-oxoethylzinc bromide-THF adduct (279 mg, 0.839 mmol) and the reaction was stirred at 65 °C for 18 h. After this time, the reaction was allowed to cool to r.t. and then quenched with MeOH (1 mL). The solvents were removed under reduced pressure and the residue was subjected to silica gel flash column chromatography [petroleum ether-EtOAc (90:10)] to give the cross-coupled product **183** as a colourless oil.

^{1}H NMR (400 MHz, $CDCl_3$): δ 8.11 (br, 1H), 7.63 (d, *J* = 8.0 Hz, 1H), 7.35 (d, *J* = 8.0 Hz, 1H), 7.19 (t, *J* = 8.0 Hz, 1H), 7.16 - 7.10 (m, 2H), 3.69 (s, 2H), 1.46 (s. 9H); **^{13}C NMR (101 MHz, $CDCl_3$)** δ 171.6, 136.3, 127.5, 123.0, 122.2, 119.6, 119.1, 111.2, 109.3, 80.8, 32.8, 28.2; ; **HRMS (ESI$^+$):** *m/z* calcd. for $C_{14}H_{17}NO_2Na$: 254.1151, found: 254.1146 $[M+Na]^+$

(3-Iodo-1*H*-indol-4-yl)methyl benzoate (**186**)

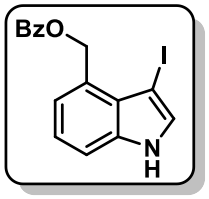

Compound **163** (1.0 g, 3.97 mmol) was added to a suspension of K_2CO_3 (1.54 g, 11.1 mmol) in DMF (15 mL) and the reaction mixture was stirred at r.t. for 15 min. A solution of I_2 (1.01 g, 3.97 mmol) in DMF (7.4 mL) was then added dropwise and the reaction was stirred at r.t. for 16 h. After this time, the reaction was poured into a mixture of a saturated NH_4Cl solution (100 mL) and sat. $Na_2S_2O_5$ (15 mL), and then the product was extracted with Et_2O (200 mL). The organic layer was washed with brine (5 x 100

mL), dried with $MgSO_4$ and concentrated under reduced pressure to give indole **186** as an off-white amorphous solid without further purification (1.35 g, 90%).

^{1}H NMR (400 MHz, $CDCl_3$): δ 8.60 (br, 1H), 8.12 (d, *J* = 8.0 Hz, 2H), 7.54 (t, *J* = 7.5 Hz, 1H), *7*.46 - 7.39 (m, 3H), 7.35 (d, *J* = 2.5 Hz, 1H), 7.28 - 7.20 (m, 2H), 5.93 (s, 2H); **^{13}C NMR (101 MHz, $CDCl_3$)** δ 166.7, 136.5, 133.0, 130.6, 130.4 130.0, 128.4, 123.1, 127.9, 126.2, 122.81 112.7, 63.7, 52.5; **HRMS (ESI$^+$):** *m/z* calcd. for $C_6H_{12}INO_2Na$: 399.9805, found 399.9824 $[M+Na]^+$.

Appendix 1: Crystal data of compound **139**

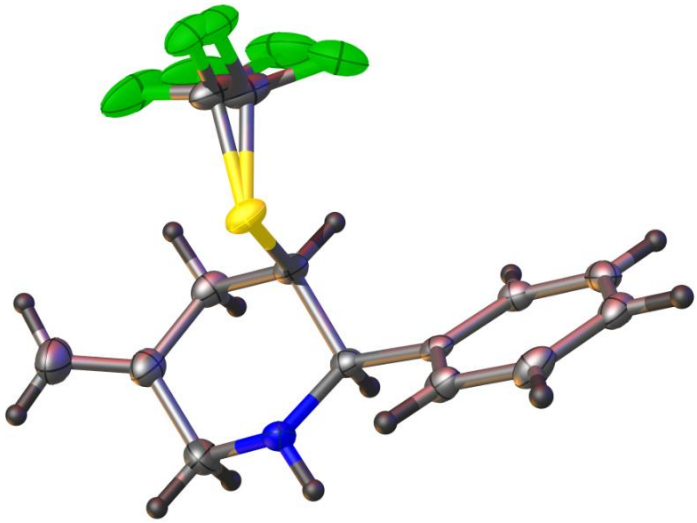

Table 1 Crystal data and structure refinement for ojh390v_0m.

Identification code	ojh390v_0m
Empirical formula	$C_{13}H_{14}F_3NS$
Formula weight	273.31
Temperature/K	100.0
Crystal system	monoclinic
Space group	$P2_1/n$
a/Å	14.7081(9)
b/Å	5.3695(3)
c/Å	18.0831(11)
α/°	90
β/°	113.266(2)
γ/°	90
Volume/Å^3	1311.98(14)
Z	4
ρ_{calc}g/cm^3	1.384
μ/mm^{-1}	2.383
F(000)	568.0
Crystal size/mm^3	0.33 × 0.172 × 0.076
Radiation	CuKα (λ = 1.54178)
2Θ range for data collection/°	6.604 to 133.054
Index ranges	-17 ≤ h ≤ 17, -6 ≤ k ≤ 6, -21 ≤ l ≤ 20
Reflections collected	17305
Independent reflections	2317 [R_{int} = 0.0375, R_{sigma} = 0.0238]
Data/restraints/parameters	2317/182/198
Goodness-of-fit on F^2	1.115
Final R indexes [I>=2σ (I)]	R_1 = 0.0343, wR_2 = 0.0845
Final R indexes [all data]	R_1 = 0.0360, wR_2 = 0.0855
Largest diff. peak/hole / e Å^{-3}	0.32/-0.21

Table 2 Fractional Atomic Coordinates (×10^4) and Equivalent Isotropic Displacement Parameters (Å^2×10^3) for ojh390v_0m. U_{eq} is defined as 1/3 of of the trace of the orthogonalised U_{IJ} tensor.

Atom	*x*	*y*	*z*	U(eq)
S1	3132.6(3)	8600.6(7)	5503.2(2)	24.92(14)
F1A	4848(4)	8395(19)	5417(6)	63(2)
F1B	4944.2(16)	7069(10)	5802(3)	61.1(16)
F2A	4820(5)	6615(9)	6462(6)	70(3)
F2B	4484(3)	6594(5)	6772.6(18)	50.7(10)
F3A	4749(15)	10740(20)	6326(10)	35(2)
F3B	4816(9)	10204(15)	6479(6)	42.8(16)
N1	1141.0(10)	6616(3)	4294.3(8)	25.2(3)
C1	1708.4(11)	4992(3)	4969.8(9)	20.4(3)
C2	2818.7(11)	5369(3)	5163.2(10)	21.0(3)
C3	3042.1(12)	4809(3)	4421.2(10)	27.6(4)
C4	2375.1(13)	6300(3)	3713.0(10)	30.4(4)
C5	1299.6(13)	6002(4)	3557.8(10)	32.9(4)
C6	1450.4(10)	5472(3)	5691.4(9)	18.6(3)
C7	1772.5(11)	3807(3)	6336.4(9)	21.2(3)
C8	1575.9(11)	4228(3)	7016.3(10)	24.0(3)
C9	1044.6(11)	6315(3)	7058.7(10)	24.8(4)
C10	712.1(12)	7970(3)	6418.4(11)	25.8(4)
C11	920.4(11)	7566(3)	5744.7(10)	23.6(3)
C12A	4452(7)	8530(20)	5968(7)	34.4(10)
C12B	4378(4)	8089(13)	6140(4)	34.4(10)
C13	2690.3(16)	7747(4)	3273.5(12)	43.8(5)

Table 3 Anisotropic Displacement Parameters (Å^2×10^3) for ojh390v_0m. The Anisotropic displacement factor exponent takes the form: -2π^2[h^{2}a*^{2}U$_{11}$+2hka*b*U$_{12}$+…].

Atom	U_{11}	U_{22}	U_{33}	U_{23}	U_{13}	U_{12}
S1	18.7(2)	19.1(2)	37.4(3)	-4.46(16)	11.59(17)	-2.26(14)
F1A	34(2)	96(5)	73(4)	-47(4)	37(3)	-25(3)
F1B	16.8(9)	101(3)	64(3)	-45(2)	13.6(12)	1.5(12)
F2A	37(3)	54(3)	79(6)	8(3)	-19(3)	2(2)
F2B	38.6(16)	60.9(14)	34.4(13)	-6.9(10)	-5.0(10)	1.9(11)
F3A	31(3)	31(3)	46(6)	-15(3)	17(4)	-13(3)
F3B	32(2)	55(4)	42(3)	-20(2)	16(2)	-22(3)
N1	16.9(7)	32.1(8)	24.3(7)	6.2(6)	5.8(6)	1.1(6)
C1	17.4(7)	18.3(8)	23.9(8)	-0.1(6)	6.3(6)	-1.7(6)
C2	18.1(7)	17.6(7)	26.5(8)	-1.2(6)	7.8(6)	1.1(6)
C3	25.3(8)	27.0(9)	33.4(9)	-7.3(7)	14.7(7)	-1.7(7)
C4	31.1(9)	35.3(10)	27.6(9)	-5.6(7)	14.4(7)	-4.6(7)
C5	29.3(9)	42.8(11)	24.6(9)	3.3(8)	8.5(7)	-3.7(8)
C6	12.3(7)	17.1(7)	24.2(8)	-0.8(6)	4.8(6)	-3.1(6)
C7	17.7(7)	16.6(7)	26.9(8)	0.2(6)	6.1(6)	0.1(6)
C8	20.4(8)	24.4(8)	23.5(8)	2.6(7)	4.6(6)	-2.3(6)
C9	21.3(8)	27.0(9)	28.0(8)	-6.1(7)	11.9(7)	-7.0(6)

Table 3 Anisotropic Displacement Parameters ($Å^2×10^3$) for ojh390v_0m. The Anisotropic displacement factor exponent takes the form: $-2π^2[h^2a^{*2}U_{11}+2hka^*b^*U_{12}+…]$.

Atom	U_{11}	U_{22}	U_{33}	U_{23}	U_{13}	U_{12}
C10	22.5(8)	18.2(8)	41.1(10)	-2.7(7)	17.1(7)	0.1(6)
C11	19.0(7)	18.0(8)	33.6(9)	5.3(7)	10.1(7)	1.3(6)
C12A	21.8(12)	42(2)	40(2)	-19.4(17)	12.9(13)	-6.7(14)
C12B	21.8(12)	42(2)	40(2)	-19.4(17)	12.9(13)	-6.7(14)
C13	44.5(11)	57.3(13)	35.4(10)	0.9(10)	22.0(9)	-9.9(10)

Table 4 Bond Lengths for ojh390v_0m.

Atom	Atom	Length/Å	Atom	Atom	Length/Å
S1	C2	1.8380(16)	C1	C6	1.518(2)
S1	C12A	1.785(10)	C2	C3	1.532(2)
S1	C12B	1.758(5)	C3	C4	1.501(2)
F1A	C12A	1.341(9)	C4	C5	1.502(2)
F1B	C12B	1.332(6)	C4	C13	1.320(3)
F2A	C12A	1.328(10)	C6	C7	1.396(2)
F2B	C12B	1.354(5)	C6	C11	1.393(2)
F3A	C12A	1.341(11)	C7	C8	1.388(2)
F3B	C12B	1.330(7)	C8	C9	1.385(2)
N1	C1	1.464(2)	C9	C10	1.386(2)
N1	C5	1.477(2)	C10	C11	1.385(2)
C1	C2	1.543(2)			

Table 5 Bond Angles for ojh390v_0m.

Atom	Atom	Atom	Angle/˚	Atom	Atom	Atom	Angle/˚
C12A	S1	C2	102.7(4)	C8	C7	C6	121.00(14)
C12B	S1	C2	97.5(2)	C9	C8	C7	120.01(15)
C1	N1	C5	112.22(13)	C8	C9	C10	119.53(15)
N1	C1	C2	108.32(12)	C11	C10	C9	120.44(15)
N1	C1	C6	111.23(13)	C10	C11	C6	120.73(15)
C6	C1	C2	112.61(12)	F1A	C12A	S1	111.2(7)
C1	C2	S1	107.66(10)	F2A	C12A	S1	114.3(7)
C3	C2	S1	111.47(11)	F2A	C12A	F1A	106.1(8)
C3	C2	C1	110.48(13)	F2A	C12A	F3A	113.1(10)
C4	C3	C2	110.40(13)	F3A	C12A	S1	107.1(11)
C3	C4	C5	112.82(15)	F3A	C12A	F1A	104.6(11)
C13	C4	C3	124.16(17)	F1B	C12B	S1	116.2(4)
C13	C4	C5	123.01(18)	F1B	C12B	F2B	105.0(4)
N1	C5	C4	109.72(14)	F2B	C12B	S1	112.9(3)
C7	C6	C1	119.46(14)	F3B	C12B	S1	111.0(6)
C11	C6	C1	122.24(14)	F3B	C12B	F1B	106.6(7)
C11	C6	C7	118.29(14)	F3B	C12B	F2B	104.1(5)

Table 6 Torsion Angles for ojh390v_0m.

A	B	C	D	Angle/˚	A	B	C	D	Angle/˚
S1	C2	C3	C4	-66.14(15)	C2	C3	C4	C13	126.75(19)
N1	C1	C2	S1	64.20(14)	C3	C4	C5	N1	54.9(2)

Table 6 Torsion Angles for ojh390v_0m.

A	B	C	D	Angle/˚	A	B	C	D	Angle/˚
N1	C1	C2	C3	-57.73(17)	C5	N1	C1	C2	61.80(17)
N1	C1	C6	C7	168.11(13)	C5	N1	C1	C6	-173.92(13)
N1	C1	C6	C11	-13.6(2)	C6	C1	C2	S1	-59.25(15)
C1	N1	C5	C4	-60.35(19)	C6	C1	C2	C3	178.82(13)
C1	C2	C3	C4	53.52(18)	C6	C7	C8	C9	0.6(2)
C1	C6	C7	C8	178.03(14)	C7	C6	C11	C10	-0.5(2)
C1	C6	C11	C10	-178.89(14)	C7	C8	C9	C10	0.0(2)
C2	S1	C12A	F1A	73.8(7)	C8	C9	C10	C11	-1.0(2)
C2	S1	C12A	F2A	-46.3(8)	C9	C10	C11	C6	1.2(2)
C2	S1	C12A	F3A	-172.5(8)	C11	C6	C7	C8	-0.4(2)
C2	S1	C12B	F1B	57.3(4)	C12A	S1	C2	C1	164.1(4)
C2	S1	C12B	F2B	-64.1(4)	C12A	S1	C2	C3	-74.6(4)
C2	S1	C12B	F3B	179.4(6)	C12B	S1	C2	C1	150.7(2)
C2	C1	C6	C7	-70.08(18)	C12B	S1	C2	C3	-88.0(2)
C2	C1	C6	C11	108.25(16)	C13	C4	C5	N1	-124.4(2)
C2	C3	C4	C5	-52.58(19)					

Table 7 Hydrogen Atom Coordinates (Å×10^4) and Isotropic Displacement Parameters (Å^2×10^3) for ojh390v_0m.

Atom	*x*	*y*	*z*	U(eq)
H1	520(16)	6390(40)	4207(12)	37(6)
H1A	1534.59	3225.46	4795.86	25
H2	3213.14	4214.45	5608.45	25
H3A	3741.13	5221.88	4536.93	33
H3B	2944.23	3010.66	4292.98	33
H5A	895.67	7119.34	3114.09	39
H5B	1089.71	4265.43	3394.51	39
H7	2131.68	2363.1	6309.8	25
H8	1805.64	3085.25	7452.57	29
H9	909.1	6609.63	7523.14	30
H10	338.96	9389.41	6441.68	31
H11	699.36	8730.96	5314.34	28
H13A	3379.1	7892.01	3398.63	53
H13B	2228.42	8644.4	2831.98	53

Table 8 Atomic Occupancy for ojh390v_0m.

Atom	*Occupancy*	Atom	*Occupancy*	Atom	*Occupancy*
F1A	0.361(11)	F1B	0.639(11)	F2A	0.361(11)
F2B	0.639(11)	F3A	0.361(11)	F3B	0.639(11)
C12A	0.361(11)	C12B	0.639(11)		

Crystal structure determination of ojh390v_0m

Crystal Data for $C_{13}H_{14}F_3NS$ (*M* =273.31 g/mol): monoclinic, space group $P2_1/n$ (no. 14), *a* = 14.7081(9) Å, *b* = 5.3695(3) Å, *c* = 18.0831(11) Å, *β* = 113.266(2)°, *V* = 1311.98(14) Å^3, *Z* = 4, *T* = 100.0 K, μ(CuKα) = 2.383 mm^{-1}, *Dcalc* = 1.384 g/cm^3, 17305 reflections measured (6.604° ≤ 2Θ ≤ 133.054°), 2317 unique (R_{int} = 0.0375, R_{sigma} = 0.0238) which were used in all calculations. The final R_1 was 0.0343 (I > 2σ(I)) and wR_2 was 0.0855 (all data).

Appendix 2: Crystal data of compound **144**

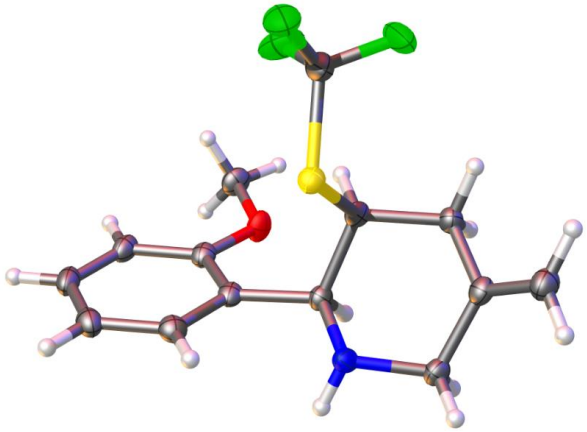

Table 1 Crystal data and structure refinement for OJH392v_0m.

Identification code	OJH392v_0m
Empirical formula	$C_{14}H_{16}F_3NOS$
Formula weight	303.34
Temperature/K	100.0
Crystal system	monoclinic
Space group	C2/c
a/Å	27.4272(12)
b/Å	10.8556(5)
c/Å	10.1597(4)
α/°	90
β/°	107.448(2)
γ/°	90
Volume/Å^3	2885.8(2)
Z	8
ρ_{calc}g/cm^3	1.396
μ/mm^{-1}	2.276
F(000)	1264.0
Crystal size/mm^3	0.31 × 0.256 × 0.22
Radiation	CuKα (λ = 1.54178)
2Θ range for data collection/°	6.756 to 133.228
Index ranges	-32 ≤ h ≤ 32, -12 ≤ k ≤ 12, -12 ≤ l ≤ 11
Reflections collected	24510
Independent reflections	2550 [R_{int} = 0.0476, R_{sigma} = 0.0195]
Data/restraints/parameters	2550/0/186
Goodness-of-fit on F^2	1.034
Final R indexes [I>=2σ (I)]	R_1 = 0.0289, wR_2 = 0.0705
Final R indexes [all data]	R_1 = 0.0320, wR_2 = 0.0726
Largest diff. peak/hole / e Å^{-3}	0.35/-0.23

Table 2 Fractional Atomic Coordinates (×10^4) and Equivalent Isotropic Displacement Parameters (Å^2×10^3) for OJH392v_0m. U_{eq} is defined as 1/3 of of the trace of the orthogonalised U_{IJ} tensor.

Atom	*x*	*y*	*z*	U(eq)
S1	3984.5(2)	6816.8(3)	3716.5(3)	19.88(11)
F1	4719.4(4)	7582.9(9)	5746.3(9)	36.6(2)
F2	4759.6(4)	8273.5(10)	3797.2(11)	43.4(3)
F3	4974.6(4)	6416.3(12)	4373.9(13)	55.2(4)
O1	3798.0(4)	8731.2(9)	-136.2(11)	24.3(2)
N1	3099.6(5)	5876.6(11)	1335.4(13)	20.0(3)
C1	3431.2(5)	6800.6(12)	989.0(14)	18.2(3)
C2	3981.2(5)	6585.8(13)	1920.8(14)	18.3(3)
C3	4158.0(5)	5285.8(13)	1690.7(15)	20.3(3)
C4	3779.5(6)	4334.2(13)	1832.6(14)	20.4(3)
C5	3240.2(5)	4624.3(13)	1005.5(15)	21.8(3)
C6	3246.5(5)	8103.0(13)	1105.4(14)	19.1(3)
C7	3452.6(5)	9073.7(13)	524.4(14)	20.4(3)
C8	3306.1(6)	10291.0(14)	638.5(15)	23.9(3)
C9	2951.5(6)	10537.7(14)	1331.1(16)	26.3(3)
C10	2742.3(6)	9597.9(14)	1904.7(15)	25.7(3)
C11	2893.1(6)	8385.5(14)	1790.3(15)	22.5(3)
C12	4069.7(6)	9683.1(14)	-589.9(16)	26.5(3)
C13	4633.7(6)	7282.4(15)	4419.0(17)	29.3(4)
C14	3906.2(6)	3334.3(14)	2602.3(16)	26.3(3)

Table 3 Anisotropic Displacement Parameters (Å^2×10^3) for OJH392v_0m. The Anisotropic displacement factor exponent takes the form: -2π^2[h^{2}a*^{2}U_{11}+2hka*b*U_{12}+…].

Atom	U_{11}	U_{22}	U_{33}	U_{23}	U_{13}	U_{12}
S1	21.31(19)	19.43(19)	17.97(18)	0.24(12)	4.49(14)	0.25(13)
F1	33.1(5)	43.1(6)	26.1(5)	-10.7(4)	-2.5(4)	3.1(4)
F2	36.5(6)	52.6(7)	42.8(6)	-13.4(5)	14.3(5)	-22.9(5)
F3	25.7(5)	62.2(8)	63.7(7)	-34.1(6)	-8.0(5)	19.1(5)
O1	32.8(6)	16.2(5)	27.8(5)	2.0(4)	15.1(5)	-1.5(4)
N1	17.6(6)	16.9(6)	24.5(6)	1.3(5)	4.8(5)	-0.6(5)
C1	20.7(7)	16.3(7)	18.0(7)	0.5(5)	6.1(6)	-0.6(5)
C2	20.4(7)	17.2(7)	17.8(7)	0.3(5)	6.5(6)	-1.1(5)
C3	19.9(7)	18.5(7)	22.8(7)	-1.6(5)	6.7(6)	0.4(5)
C4	24.6(7)	17.6(7)	19.3(7)	-3.1(5)	7.1(6)	-0.7(6)
C5	23.2(7)	16.9(7)	25.0(8)	-0.7(6)	6.6(6)	-2.6(6)
C6	20.5(7)	18.7(7)	14.9(7)	-0.2(5)	0.5(5)	1.7(5)
C7	23.2(7)	20.0(7)	15.5(7)	-0.9(5)	2.1(6)	0.9(6)
C8	29.0(8)	16.3(7)	22.2(7)	0.0(6)	1.4(6)	0.2(6)
C9	28.5(8)	18.8(7)	26.5(8)	-4.6(6)	0.4(6)	5.2(6)
C10	23.6(8)	28.2(8)	23.8(8)	-4.5(6)	4.9(6)	5.2(6)
C11	21.8(7)	24.4(8)	19.5(7)	0.2(6)	3.5(6)	1.6(6)
C12	30.7(8)	21.1(8)	28.6(8)	3.8(6)	10.5(7)	-4.6(6)
C13	24.3(8)	31.2(9)	29.4(8)	-10.3(7)	3.3(6)	3.8(7)
C14	30.1(8)	19.8(8)	26.7(8)	0.1(6)	5.0(6)	-0.5(6)

Table 4 Bond Lengths for OJH392v_0m.

Atom	Atom	Length/Å	Atom	Atom	Length/Å
S1	C2	1.8389(14)	C2	C3	1.5328(19)
S1	C13	1.7813(16)	C3	C4	1.502(2)
F1	C13	1.3380(18)	C4	C5	1.499(2)
F2	C13	1.344(2)	C4	C14	1.322(2)
F3	C13	1.3363(19)	C6	C7	1.407(2)
O1	C7	1.3665(18)	C6	C11	1.387(2)
O1	C12	1.4289(18)	C7	C8	1.396(2)
N1	C1	1.4660(18)	C8	C9	1.387(2)
N1	C5	1.4788(19)	C9	C10	1.382(2)
C1	C2	1.539(2)	C10	C11	1.395(2)
C1	C6	1.5184(19)			

Table 5 Bond Angles for OJH392v_0m.

Atom	Atom	Atom	Angle/˚	Atom	Atom	Atom	Angle/˚
C13	S1	C2	98.23(7)	C11	C6	C1	123.01(13)
C7	O1	C12	117.85(11)	C11	C6	C7	118.31(13)
C1	N1	C5	110.59(11)	O1	C7	C6	115.29(12)
N1	C1	C2	108.23(11)	O1	C7	C8	123.88(13)
N1	C1	C6	111.90(11)	C8	C7	C6	120.83(14)
C6	C1	C2	112.42(11)	C9	C8	C7	119.21(14)
C1	C2	S1	107.57(9)	C10	C9	C8	120.95(14)
C3	C2	S1	111.67(10)	C9	C10	C11	119.38(14)
C3	C2	C1	110.01(11)	C6	C11	C10	121.32(14)
C4	C3	C2	111.05(11)	F1	C13	S1	108.99(11)
C5	C4	C3	113.32(12)	F1	C13	F2	106.63(13)
C14	C4	C3	123.71(14)	F2	C13	S1	113.93(11)
C14	C4	C5	122.97(14)	F3	C13	S1	114.34(11)
N1	C5	C4	110.28(12)	F3	C13	F1	107.03(13)
C7	C6	C1	118.65(12)	F3	C13	F2	105.43(14)

Table 6 Torsion Angles for OJH392v_0m.

A	B	C	D	Angle/˚	A	B	C	D	Angle/˚
S1	C2	C3	C4	67.20(13)	C3	C4	C5	N1	-53.45(15)
O1	C7	C8	C9	179.93(13)	C5	N1	C1	C2	-64.41(14)
N1	C1	C2	S1	-62.33(12)	C5	N1	C1	C6	171.18(11)
N1	C1	C2	C3	59.50(14)	C6	C1	C2	S1	61.77(13)
N1	C1	C6	C7	-166.23(12)	C6	C1	C2	C3	-176.40(11)
N1	C1	C6	C11	15.49(19)	C6	C7	C8	C9	-0.2(2)
C1	N1	C5	C4	61.24(15)	C7	C6	C11	C10	0.1(2)
C1	C2	C3	C4	-52.17(15)	C7	C8	C9	C10	-0.1(2)
C1	C6	C7	O1	1.71(18)	C8	C9	C10	C11	0.4(2)
C1	C6	C7	C8	-178.16(13)	C9	C10	C11	C6	-0.4(2)
C1	C6	C11	C10	178.38(13)	C11	C6	C7	O1	-179.93(12)
C2	S1	C13	F1	176.17(11)	C11	C6	C7	C8	0.2(2)
C2	S1	C13	F2	57.23(12)	C12	O1	C7	C6	-172.02(12)
C2	S1	C13	F3	-64.12(14)	C12	O1	C7	C8	7.8(2)

Table 6 Torsion Angles for OJH392v_0m.

A	B	C	D	Angle/˚	A	B	C	D	Angle/˚
C2	C1	C6	C7	71.73(16)	C13	S1	C2	C1	-152.60(10)
C2	C1	C6	C11	-106.55(15)	C13	S1	C2	C3	86.60(11)
C2	C3	C4	C5	49.71(16)	C14	C4	C5	N1	126.88(15)
C2	C3	C4	C14	-130.62(15)					

Table 7 Hydrogen Atom Coordinates (Å×10^4) and Isotropic Displacement Parameters (Å^2×10^3) for OJH392v_0m.

Atom	*x*	*y*	*z*	U(eq)
H1	2787(7)	6041(16)	822(18)	25(4)
H1A	3425.12	6663.11	10.91	22
H2	4213.11	7203.5	1688.26	22
H3A	4199.39	5232.18	757.23	24
H3B	4494.25	5118.95	2372.68	24
H5A	3206.15	4569.97	9.13	26
H5B	3005.35	4014.44	1214.16	26
H8	3447.65	10942.61	246.4	29
H9	2850.86	11364.67	1412.33	32
H10	2498.19	9776.04	2372.51	31
H11	2750.71	7740.34	2189.64	27
H12A	3827.44	10199.69	-1272.2	40
H12B	4313.38	9312.83	-1009.26	40
H12C	4254.75	10189.49	200.63	40
H14A	3650.07	2761.14	2648.52	32
H14B	4253.28	3188.93	3109.15	32

sCrystal structure determination of OJH392v_0m

Crystal Data for $C_{14}H_{16}F_3NOS$ (*M* =303.34 g/mol): monoclinic, space group C2/c (no. 15), *a* = 27.4272(12) Å, *b* = 10.8556(5) Å, *c* = 10.1597(4) Å, *β* = 107.448(2)°, *V* = 2885.8(2) Å^3, *Z* = 8, *T* = 100.0 K, μ(CuKα) = 2.276 mm^{-1}, *Dcalc* = 1.396 g/cm^3, 24510 reflections measured (6.756° ≤ 2Θ ≤ 133.228°), 2550 unique (R_{int} = 0.0476, R_{sigma} = 0.0195) which were used in all calculations. The final R_1 was 0.0289 (I > 2σ(I)) and wR_2 was 0.0726 (all data).

6. References

1. F. A. Carey and R. J. Sundberg, *Advanced organic chemistry*, Springer, New York, 5th edn., 2007.
2. B. M. Trost and M. L. Crawley, *Chem. Rev.*, 2003, **103**, 2921-2944.
3. B. M. Trost, *J. Org. Chem.*, 2004, **69**, 5813-5837.
4. B. M. Trost and D. A. Thaisrivongs, *J. Am. Chem. Soc.*, 2008, **130**, 14092-14093.
5. J. Clayden, N. Greeves and S. G. Warren, *Organic chemistry*, Oxford University Press, Oxford ; New YorK, 2nd edn., 2012.
6. S.-C. Sha, J. Zhang, P. J. Carroll and P. J. Walsh, *J. Am. Chem. Soc.*, 2013, **135**, 17602-17609.
7. B. M. Trost and D. L. Van Vranken, *Chem. Rev.*, 1996, **96**, 395-422.
8. B. D. W. Allen, C. P. Lakeland and J. P. A. Harrity, *Chem. Eur. J.*, 2017, **23**, 13830-13857.
9. B. M. Trost and D. M. T. Chan, *J. Am. Chem. Soc.*, 1979, **101**, 6429-6432.
10. B. M. Trost and P. J. Bonk, *J. Am. Chem. Soc.*, 1985, **107**, 8277-8279.
11. B. M. Trost, S. M. Mignani and T. N. Nanninga, *J. Am. Chem. Soc.*, 1986, **108**, 6051-6053.
12. B. M. Trost, S. M. Mignani and T. N. Nanninga, *J. Am. Chem. Soc.*, 1988, **110**, 1602-1608.
13. B. M. Trost, S. A. King and T. Schmidt, *J. Am. Chem. Soc.*, 1989, **111**, 5902-5915.
14. B. M. Trost, P. Seoane, S. Mignani and M. Acemoglu, *J. Am. Chem. Soc.*, 1989, **111**, 7487-7500.
15. B. M. Trost and S. A. King, *J. Am. Chem. Soc.*, 1990, **112**, 408-422.
16. B. M. Trost and T. A. Grese, *J. Am. Chem. Soc.*, 1991, **113**, 7363-7372.
17. B. M. Trost, T. A. Grese and D. M. T. Chan, *J. Am. Chem. Soc.*, 1991, **113**, 7350-7362.
18. B. M. Trost and M. C. Matelich, *J. Am. Chem. Soc.*, 1991, **113**, 9007-9009.
19. B. M. Trost and T. A. Grese, *J. Org. Chem.*, 1992, **57**, 686-697.
20. L.-L. Shiu, T.-I. Lin, S.-M. Peng, G.-R. Her, D. D. Ju, S.-K. Lin, J.-H. Hwang, C. Y. Mou and T.-Y. Luh, *J. Chem. Soc., Chem. Commun.*, 1994, 647-648.
21. B. M. Trost and J. R. Parquette, *J. Org. Chem.*, 1994, **59**, 7568-7569.
22. B. M. Trost, J. R. Parquette and C. Nübling, *Tetrahedron Lett.*, 1995, **36**, 2917-2920.
23. C. W. Holzapfel and T. L. van der Merwe, *Tetrahedron Lett.*, 1996, **37**, 2307-2310.
24. B. M. Trost and R. I. Higuchi, *J. Am. Chem. Soc.*, 1996, **118**, 10094-10105.
25. M. D. Jones and R. D. W. Kemmitt, *J. Chem. Soc., Chem. Commun.*, 1986, DOI: 10.1039/C39860001201, 1201-1203.
26. B. M. Trost and P. J. Bonk, *J. Am. Chem. Soc.*, 1985, **107**, 1778-1781.
27. B. M. Trost and C. M. Marrs, *J. Am. Chem. Soc.*, 1993, **115**, 6636-6645.
28. B. M. Trost, S. M. Silverman and J. P. Stambuli, *J. Am. Chem. Soc.*, 2007, **129**, 12398-12399.
29. B. M. Trost and S. M. Silverman, *J. Am. Chem. Soc.*, 2010, **132**, 8238-8240.
30. R. Shintani and T. Hayashi, *J. Am. Chem. Soc.*, 2006, **128**, 6330-6331.
31. R. Shintani, S. Park, W.-L. Duan and T. Hayashi, *Angew. Chem. Int. Ed.*, 2007, **46**, 5901-5903.
32. R. Shintani, T. Ito, M. Nagamoto, H. Otomo and T. Hayashi, *Chem. Commun.*, 2012, **48**, 9936-9938.
33. R. B. Bambal and R. D. W. Kemmitt, *J. Organomet. Chem.*, 1989, **362**, C18-C20.
34. S. J. Hedley, W. J. Moran, A. H. G. P. Prenzel, D. A. Price and J. P. A. Harrity, *Synlett*, 2001, **2001**, 1596-1598.
35. S. J. Hedley, W. J. Moran, D. A. Price and J. P. A. Harrity, *J. Org. Chem.*, 2003, **68**, 4286-4292.
36. Y. Keiji, I. Toru and T. Jiro, *Chem. Lett.*, 1987, **16**, 1157-1158.
37. L.-Y. Mei, X.-Y. Tang and M. Shi *Chem. Eur. J.*, 2014, **20**, 13136-13142.
38. B. Cao, L.-Y. Mei, X.-G. Li and M. Shi, *RSC Advances*, 2015, **5**, 92545-92548.
39. R. Shintani, M. Murakami and T. Hayashi, *J. Am. Chem. Soc.*, 2007, **129**, 12356-12357.
40. R. Shintani, S. Park, F. Shirozu, M. Murakami and T. Hayashi, *J. Am. Chem. Soc.*, 2008, **130**, 16174-16175.

41. R. Shintani, M. Murakami and T. Hayashi, *Org. Lett.*, 2009, **11**, 457-459.
42. R. Shintani, K. Ikehata and T. Hayashi, *J. Org. Chem.*, 2011, **76**, 4776-4780.
43. D. C. D. Butler, G. A. Inman and H. Alper, *J. Org. Chem.*, 2000, **65**, 5887-5890.
44. G. A. Inman, D. C. D. Butler and H. Alper, *Synlett*, 2001, **2001**, 0914-0919.
45. A. Martorell, G. A. Inman and H. Alper, *J. Mol. Catal. A: Chem.*, 2003, **204-205**, 91-96.
46. H.-B. Zhou and H. Alper, *J. Org. Chem.*, 2003, **68**, 3439-3445.
47. H.-B. Zhou and H. Alper, *Tetrahedron*, 2004, **60**, 73-79.
48. B. M. Trost and D. R. Fandrick, *J. Am. Chem. Soc.*, 2003, **125**, 11836-11837.
49. K. Aoyagi, H. Nakamura and Y. Yamamoto, *J. Org. Chem.*, 2002, **67**, 5977-5980.
50. J. G. Knight, K. Tchabanenko, P. A. Stoker and S. J. Harwood, *Tetrahedron Lett.*, 2005, **46**, 6261-6264.
51. T. Ibuka, N. Mimura, H. Aoyama, M. Akaji, H. Ohno, Y. Miwa, T. Taga, K. Nakai, H. Tamamura, N. Fujii and Y. Yamamoto, *J. Org. Chem.*, 1997, **62**, 999-1015.
52. J. G. Knight, P. A. Stoker, K. Tchabanenko, S. J. Harwood and Kenneth W. M. Lawrie, *Tetrahedron*, 2008, **64**, 3744-3750.
53. M. A. Lowe, M. Ostovar, S. Ferrini, C. C. Chen, P. G. Lawrence, F. Fontana, A. A. Calabrese and V. K. Aggarwal, *Angew. Chem. Int. Ed.*, 2011, **50**, 6370-6374.
54. C. Wang and J. A. Tunge, *Org. Lett.*, 2006, **8**, 3211-3214.
55. C. Wang and J. A. Tunge, *J. Am. Chem. Soc.*, 2008, **130**, 8118-8119.
56. E. Vitaku, D. T. Smith and J. T. Njardarson, *J. Med. Chem.*, 2014, **57**, 10257-10274.
57. F. Lovering, J. Bikker and C. Humblet, *J. Med. Chem.*, 2009, **52**, 6752-6756.
58. T. J. Ritchie, S. J. F. Macdonald, R. J. Young and S. D. Pickett, *Drug Discovery Today*, 2011, **16**, 164-171.
59. B. D. W. Allen, PhD, University of Sheffield, 2017.
60. B. D. W. Allen, M. J. Connolly and J. P. A. Harrity, *Chem. Eur. J.*, 2016, **22**, 13000-13003.
61. B. M. Trost, J. P. Stambuli, S. M. Silverman and U. Schwörer, *J. Am. Chem. Soc.*, 2006, **128**, 13328-13329.
62. M. Suzuki, S. Yoshida, K. Shiraga and T. Saegusa, *Macromolecules*, 1998, **31**, 1716-1719.
63. R. S. Phatake and C. V. Ramana, *Tetrahedron Lett.*, 2015, **56**, 3868-3871.
64. A. A. Tudjarian and T. G. Minehan, *J. Org. Chem.*, 2011, **76**, 3576-3581.
65. P. S. Baran and N. Z. Burns, *J. Am. Chem. Soc.*, 2006, **128**, 3908-3909.
66. A. Ros, A. Magriz, H. Dietrich, J. M. Lassaletta and R. Fernández, *Tetrahedron*, 2007, **63**, 7532-7537.
67. X. Guo and O. S. Wenger, *Angew. Chem. Int. Ed.*, 2018, **57**, 2469-2473.
68. J. F. Teichert and B. L. Feringa, *Angew. Chem. Int. Ed.*, 2010, **49**, 2486-2528.
69. B. M. Trost and J. E. Schultz, *Synthesis*, 2019, **51**, 1-30.
70. D. W. Watson, M. Gill, P. Kemmitt, S. G. Lamont, M. V. Popescu and I. Simpson, *Tetrahedron Lett.*, 2018, **59**, 4479-4482.
71. A. Fürstner and J. Ackerstaff, *Chem. Commun.*, 2008, 2870-2872.
72. V. N. G. Lindsay and A. B. Charette, in *Comprehensive Organic Synthesis*, eds. P. Knochel and G. A. Molander, Elsevier, Amsterdam, 2nd edn., 2014, vol. 1, ch. 1, pp. 367-368.
73. C. Fischer and E. M. Carreira, *Org. Lett.*, 2001, **3**, 4319-4321.
74. P. A. Champagne, J. Desroches, J.-D. Hamel, M. Vandamme and J.-F. Paquin, *Chem. Rev.*, 2015, **115**, 9073-9174.
75. S. Fustero, D. M. Sedgwick, R. Román and P. Barrio, *Chem. Commun.*, 2018, **54**, 9706-9725.
76. C. N. Neumann and T. Ritter, *Angew. Chem. Int. Ed.*, 2015, **54**, 3216-3221.
77. S. Purser, P. R. Moore, S. Swallow and V. Gouverneur, *Chem. Soc. Rev.*, 2008, **37**, 320-330.
78. E. P. Gillis, K. J. Eastman, M. D. Hill, D. J. Donnelly and N. A. Meanwell, *J. Med. Chem.*, 2015, **58**, 8315-8359.
79. R. Berger, G. Resnati, P. Metrangolo, E. Weber and J. Hulliger, *Chem. Soc. Rev.*, 2011, **40**, 3496-3508.

80. K. Müller, C. Faeh and F. Diederich, *Science*, 2007, **317**, 1881-1886.
81. P. Shah and A. D. Westwell, *J. Enzyme Inhib. Med. Chem.*, 2007, **22**, 527-540.
82. N. R. Curtis, S. H. Davies, M. Gray, S. G. Leach, R. A. McKie, L. E. Vernon and A. J. Walkington, *Org. Process Res. Dev.*, 2015, **19**, 865-871.
83. C. Molinaro, E. M. Phillips, B. Xiang, E. Milczek, M. Shevlin, J. Balsells, S. Ceglia, J. Chen, L. Chen, Q. Chen, Z. Fei, S. Hoerrner, J. Qi, M. de Lera Ruiz, L. Tan, B. Wan and J. Yin, *J. Org. Chem.*, 2019, **84**, 8006-8018.
84. B. M. Liederer, L. M. Berezhkovskiy, B. J. Dean, V. Dinkel, J. Peng, M. Merchant, E. G. Plise, H. Wong and X. Liu, *Xenobiotica*, 2011, **41**, 327-339.
85. R. Koudih, G. Gilbert, M. Dhilly, A. Abbas, L. Barré, D. Debruyne and F. Sobrio, *Eur. J. Med. Chem.*, 2012, **53**, 408-415.
86. R. Koudih, G. Gilbert, M. Dhilly, A. Abbas, L. Barré, D. Debruyne and F. Sobrio, *Org. Biomol. Chem.*, 2012, **10**, 8493-8500.
87. A. Sun, D. C. Lankin, K. Hardcastle and J. P. Snyder, *Chem. Eur. J.*, 2005, **11**, 1579-1591.
88. S. J. Shaw, D. A. Goff, L. A. Boralsky, M. Irving and R. Singh, *J. Org. Chem.*, 2013, **78**, 8892-8897.
89. C. Walpole, Z. Liu, E. E. Lee, H. Yang, F. Zhou, N. Mackintosh, M. Sjogren, D. Taylor, J. Shen and R. A. Batey, *Tetrahedron Lett.*, 2012, **53**, 2942-2947.
90. N. W. Goldberg, X. Shen, J. Li and T. Ritter, *Org. Lett.*, 2016, **18**, 6102-6104.
91. X. Li, R. K. Russell, J. Spink, S. Ballentine, C. Teleha, S. Branum, K. Wells, D. Beauchamp, R. Patch, H. Huang, M. Player and W. Murray, *Org. Process Res. Dev.*, 2014, **18**, 321-330.
92. T. Wu, G. Yin and G. Liu, *J. Am. Chem. Soc.*, 2009, **131**, 16354-16355.
93. Y. A. Serguchev, M. V. Ponomarenko and N. V. Ignat'ev, *J. Fluorine Chem.*, 2016, **185**, 1-16.
94. E. Vardelle, A. Martin-Mingot, M.-P. Jouannetaud, C. Bachmann, J. Marrot and S. Thibaudeau, *J. Org. Chem.*, 2009, **74**, 6025-6034.
95. W. Kong, P. Feige, T. de Haro and C. Nevado, *Angew. Chem. Int. Ed.*, 2013, **52**, 2469-2473.
96. Z. Nairoukh, M. Wollenburg, C. Schlepphorst, K. Bergander and F. Glorius, *Nature Chemistry*, 2019, **11**, 264-270.
97. T. Okino, Y. Hoashi, T. Furukawa, X. Xu and Y. Takemoto, *J. Am. Chem. Soc.*, 2005, **127**, 119-125.
98. Z.-H. Zhang, X.-Q. Dong, D. Chen and C.-J. Wang, *Chem. Eur. J.*, 2008, **14**, 8780-8783.
99. Y. K. Kang and D. Y. Kim, *J. Org. Chem.*, 2009, **74**, 5734-5737.
100. S. H. Jung and D. Y. Kim, *Tetrahedron Lett.*, 2008, **49**, 5527-5530.
101. Z.-H. Zhang, X.-Q. Dong, H.-Y. Tao and C.-J. Wang, *Arch. Org. Chem.*, 2011, **(ii)**, 137.
102. L. Simón and J. M. Goodman, *J. Am. Chem. Soc.*, 2012, **134**, 16869-16876.
103. F.-M. Liao, Z.-Y. Cao, J.-S. Yu and J. Zhou, *Angew. Chem. Int. Ed.*, 2017, **56**, 2459-2463.
104. G. Desimoni, G. Faita and K. A. Jørgensen, *Chem. Rev.*, 2006, **106**, 3561-3651.
105. G. Jiang and B. List, *Angew. Chem. Int. Ed.*, 2011, **50**, 9471-9474.
106. S. S. Zhu, D. R. Cefalo, D. S. La, J. Y. Jamieson, W. M. Davis, A. H. Hoveyda and R. R. Schrock, *J. Am. Chem. Soc.*, 1999, **121**, 8251-8259.
107. B. Mechsner, B. Henßen and J. Pietruszka, *Org. Biomol. Chem.*, 2018, **16**, 7674-7681.
108. Z. Han, Y.-Q. Guan, G. Liu, R. Wang, X. Yin, Q. Zhao, H. Cong, X.-Q. Dong and X. Zhang, *Org. Lett.*, 2018, **20**, 6349-6353.
109. C. Ding and K. Maruoka, *Synlett*, 2009, **2009**, 664-666.
110. X. Huang, W.-B. Yi, D. Ahad and W. Zhang, *Tetrahedron Lett.*, 2013, **54**, 6064-6066.
111. H. Wang, *Catalysts*, 2019, **9**, 244.
112. B. Xiang, K. M. Belyk, R. A. Reamer and N. Yasuda, *Angew. Chem. Int. Ed.*, 2014, **53**, 8375-8378.
113. X. Han, J. Luo, C. Liu and Y. Lu, *Chem. Commun.*, 2009, DOI: 10.1039/B823184B, 2044-2046.
114. H. Li, S. Zhang, C. Yu, X. Song and W. Wang, *Chem. Commun.*, 2009, DOI: 10.1039/B900777F, 2136-2138.

115. X. Han, J. Kwiatkowski, F. Xue, K.-W. Huang and Y. Lu, *Angew. Chem. Int. Ed.*, 2009, **48**, 7604-7607.
116. S. J. Yoon, Y. K. Kang and D. Y. Kim, *Synlett*, 2011, **2011**, 420-424.
117. Y. Oh, S. M. Kim and D. Y. Kim, *Tetrahedron Lett.*, 2009, **50**, 4674-4676.
118. J. Xu, Y. Hu, D. Huang, K.-H. Wang, C. Xu and T. Niu, *Adv. Synth. Catal.*, 2012, **354**, 515-526.
119. W.-B. Yi, Z. Zhang, X. Huang, A. Tanner, C. Cai and W. Zhang, *RSC Advances*, 2013, **3**, 18267-18270.
120. R. Ding and C. Wolf, *Org. Lett.*, 2018, **20**, 892-895.
121. S. Hoffmann, M. Nicoletti and B. List, *J. Am. Chem. Soc.*, 2006, **128**, 13074-13075.
122. E. H. M. Kirton, G. Tughan, R. E. Morris and R. A. Field, *Tetrahedron Lett.*, 2004, **45**, 853-855.
123. J. Pecháček, J. Václavík, J. Přech, P. Šot, J. Januščák, B. Vilhanová, J. Vavřík, M. Kuzma and P. Kačer, *Tetrahedron: Asymmetry*, 2013, **24**, 233-239.
124. B. Vilhanová, J. Václavík, P. Šot, J. Pecháček, J. Zápal, R. Pažout, J. Maixner, M. Kuzma and P. Kačer, *Chem. Commun.*, 2016, **52**, 362-365.
125. N. J. Willis, C. A. Fisher, C. M. Alder, A. Harsanyi, L. Shukla, J. P. Adams and G. Sandford, *Green Chemistry*, 2016, **18**, 1313-1318.
126. P. E. Maligres, M. M. Chartrain, V. Upadhyay, D. Cohen, R. A. Reamer, D. Askin, R. P. Volante and P. J. Reider, *J. Org. Chem.*, 1998, **63**, 9548-9551.
127. T. Kitazume and T. Yamazaki, in *Organofluorine Chemistry: Techniques and Synthons*, ed. R. D. Chambers, Springer, Berlin, 1997, pp. 91-130.
128. B. Manteau, S. Pazenok, J.-P. Vors and F. R. Leroux, *J. Fluorine Chem.*, 2010, **131**, 140-158.
129. F. Pertusati, M. Serpi and E. Pileggi, in *Fluorine in Life Sciences: Pharmaceuticals, Medicinal Diagnostics, and Agrochemicals*, Elsevier, 2019, pp. 141-180.
130. L. Gregory, P. Armen and R. L. Frederic, *Curr. Top. Med. Chem.*, 2014, **14**, 941-951.
131. S. Barata-Vallejo, S. Bonesi and A. Postigo, *Org. Biomol. Chem.*, 2016, **14**, 7150-7182.
132. X.-H. Xu, K. Matsuzaki and N. Shibata, *Chem. Rev.*, 2015, **115**, 731-764.
133. F. Hu, X. Shao, D. Zhu, L. Lu and Q. Shen, *Angew. Chem. Int. Ed.*, 2014, **53**, 6105-6109.
134. L. Candish, L. Pitzer, A. Gómez-Suárez and F. Glorius, *Chem. Eur. J.*, 2016, **22**, 4753-4756.
135. X. Shao, T. Liu, L. Lu and Q. Shen, *Org. Lett.*, 2014, **16**, 4738-4741.
136. J. Luo, Y. Liu and X. Zhao, *Org. Lett.*, 2017, **19**, 3434-3437.
137. C. Zhang, Y. Wang, Y. Song, H. Gao, Y. Sun, X. Sun, Y. Yang, M. He, Z. Yang, L. Zhan, Z.-X. Yu and Y. Rao, *CCS Chemistry*, 2019, **1**, 352-364.
138. M. Jiang, F. Zhu, H. Xiang, X. Xu, L. Deng and C. Yang, *Org. Biomol. Chem.*, 2015, **13**, 6935-6939.
139. C. Xu, B. Ma and Q. Shen, *Angew. Chem. Int. Ed.*, 2014, **53**, 9316-9320.
140. C. Wallwey and S.-M. Li, *Natural Product Reports*, 2011, **28**, 496-510.
141. F. Yamada, T. Hashizume and M. Somei, *Heterocycles*, 1998, **47**, 509-516.
142. E. Jiménez-Moreno, G. Jiménez-Osés, A. M. Gómez, A. G. Santana, F. Corzana, A. Bastida, J. Jiménez-Barbero and J. L. Asensio, *Chem. Sci.*, 2015, **6**, 6076-6085.
143. W. Zhang and J. M. Ready, *Angew. Chem.*, 2014, **126**, 9126-9130.
144. P. S. Baran and J. M. Richter, *J. Am. Chem. Soc.*, 2004, **126**, 7450-7451.
145. J. M. Richter, B. W. Whitefield, T. J. Maimone, D. W. Lin, M. P. Castroviejo and P. S. Baran, *J. Am. Chem. Soc.*, 2007, **129**, 12857-12869.
146. M. Kimura, M. Futamata, R. Mukai and Y. Tamaru, *J. Am. Chem. Soc.*, 2005, **127**, 4592-4593.
147. J. S. Oakdale and D. L. Boger, *Org. Lett.*, 2010, **12**, 1132-1134.
148. M. K. Eberle, P. Hiestand, A.-M. Jutzi-Eme, F. Nuninger and H. R. Zihlmann, *J. Med. Chem.*, 1995, **38**, 1853-1864.
149. J. Durán, M. Gulías, L. Castedo and J. L. Mascareñas, *Org. Lett.*, 2006, **8**, 2899-2899.
150. L. A. Arnold, R. Imbos, A. Mandoli, A. H. M. de Vries, R. Naasz and B. L. Feringa, *Tetrahedron*, 2000, **56**, 2865-2878.
151. J. Y. Hamilton, D. Sarlah and E. M. Carreira, *J. Am. Chem. Soc.*, 2013, **135**, 994-997.

152. T. M. Beck and B. Breit, *Angew. Chem. Int. Ed.*, 2017, **56**, 1903-1907.
153. L. Ma, W. Li, H. Xi, X. Bai, E. Ma, X. Yan and Z. Li, *Angew. Chem. Int. Ed.*, 2016, **55**, 10410-10413.
154. G. Zhang, X. Hu, C.-W. Chiang, H. Yi, P. Pei, A. K. Singh and A. Lei, *J. Am. Chem. Soc.*, 2016, **138**, 12037-12040.
155. G. L. Beutner, J. T. Kuethe, M. M. Kim and N. Yasuda, *J. Org. Chem.*, 2009, **74**, 789-794.
156. C. Vila, M. Giannerini, V. Hornillos, M. Fañanás-Mastral and B. L. Feringa, *Chem. Sci.*, 2014, **5**, 1361-1367.
157. N. G. Léonard and P. J. Chirik, *ACS Catalysis*, 2018, **8**, 342-348.
158. G. Henrion, T. E. J. Chavas, X. Le Goff and F. Gagosz, *Angew. Chem. Int. Ed.*, 2013, **52**, 6277-6282.
159. S. Suzuki, T. Kamo, K. Fukushi, T. Hiramatsu, E. Tokunaga, T. Dohi, Y. Kita and N. Shibata, *Chem. Sci.*, 2014, **5**, 2754-2760.
160. F. Romanov-Michailidis, L. Guénée and A. Alexakis, *Angew. Chem. Int. Ed.*, 2013, **52**, 9266-9270.
161. J. L. Howard, Y. Sagatov and D. L. Browne, *Tetrahedron*, 2018, **74**, 3118-3123.
162. H. Guyon, H. Chachignon, V. Tognetti, L. Joubert and D. Cahard, *Eur. J. Org. Chem.*, 2018, **2018**, 3756-3763.
163. Y. Huang, X. He, H. Li and Z. Weng, *Eur. J. Org. Chem.*, 2014, **2014**, 7324-7328.
164. S. Alazet, E. Ismalaj, Q. Glenadel, D. Le Bars and T. Billard, *Eur. J. Org. Chem.*, 2015, **2015**, 4607-4610.
165. Y. Huang, X. He, X. Lin, M. Rong and Z. Weng, *Org. Lett.*, 2014, **16**, 3284-3287.
166. I. Saidalimu, S. Suzuki, T. Yoshioka, E. Tokunaga and N. Shibata, *Org. Lett.*, 2016, **18**, 6404-6407.
167. PCT Int. Appl., WO2009115874A2, 2009.
168. P. Madsen, A. Ling, M. Plewe, C. K. Sams, L. B. Knudsen, U. G. Sidelmann, L. Ynddal, C. L. Brand, B. Andersen, D. Murphy, M. Teng, L. Truesdale, D. Kiel, J. May, A. Kuki, S. Shi, M. D. Johnson, K. A. Teston, J. Feng, J. Lakis, K. Anderes, V. Gregor and J. Lau, *J. Med. Chem.*, 2002, **45**, 5755-5775.
169. M. Matsumoto and N. Watanabe, *Heterocycles*, 1986, **24**, 2611-2618.
170. Y. Zhang, D. Stephens, G. Hernandez, R. Mendoza and O. V. Larionov, *Chem. Eur. J.*, 2012, **18**, 16612-16615.